# A *Dictyostelium* Model for Tauopathies

Submitted by

Katelyn H Mroczek BBioSc (Hons)

A thesis submitted in the total fulfilment of the requirements

for the degree of

Doctor of Philosophy

Department of Microbiology, Anatomy, Physiology, Pharmacology and Psychology

School of Agriculture, Biomedicine and Environment

La Trobe University

Victoria, Australia

**February 2022**

# Table of Contents

# List of Figures

# List of Tables

# List of Abbreviations

| | |
|---|---|
| A | amps |
| ATP | adenosine triphosphate |
| AD | Alzheimer's disease |
| Amp | ampicillin |
| Aβ | amyloid beta |
| APP | amyloid precursor protein |
| bp | base pairs |
| BSA | bovine serum albumin |
| BCYE | buffered charcoal yeast extract |
| cAMP | 3',5' cyclic adenosine monophosphate |
| cm | centimetres |
| cfu | colony forming units |
| CBD | corticobasal degeneration |
| d | day(s) |
| dNTP | deoxynucleotide triphosphate |
| $dH_2O$ | distilled water |
| DMSO | dimethyl sulfoxide |
| DS | Down's syndrome |
| EDTA | ethylene diamine tetracetic acid |
| FITC | fluorescein isothiocyanate |
| FTDP-17 | frontotemporal dementia with parkinsonism linked to chromosome 17 |
| gDNA | genomic DNA |
| G418 | geneticin |
| GSK-3b | glycogen synthase kinase 3 beta |
| g | gram |
| g | relative centrifugal force |
| HBS | HEPES-saline buffer |
| HEPES | N-hydroxyethylpiperazine-N-2-ethanesulphonic acid |
| hr | hour(s) |
| IPTG | b-D-isopropyl-thiogalactopyranoside |
| Kan | kanamycin |
| Kb | kilobases |

| | |
|---|---|
| kDa | kilodalton |
| KO | knockout |
| L | litre(s) |
| LBs | Lewy bodies |
| LB | luria broth |
| MT | microtubule(s) |
| MAPT | microtubule associated protein tau |
| µg | microgram |
| µl | microliter |
| µM | micromolar |
| mg | milligram |
| ml | millilitre |
| mM | millimolar |
| min | minute(s) |
| M | molar |
| MPP+ | 1-methyl-4-phenylpyridinium ion |
| MPTP | 1-methyl-4-phenyl-1,2,3,4-tetrahydopyridine |
| ng | nanogram |
| nm | nanometres |
| NFT | neurofibrillary tangles |
| nM | nanomolar |
| OD | optical density |
| PD | Parkinson's disease |
| PHF | paired helical filaments |
| PBS | phosphate buffered saline |
| PiD | Pick's disease |
| pg | picograms |
| Pmol | picomoles |
| PCR | Polymerase chain reaction |
| PVC | polyvinyl chloride |
| PrP | prion protein |
| PSP | progressive supranuclear palsy |
| rpm | revolutions per minute |

| | |
|---|---|
| RT | room temperature |
| SBE | sucrose/bromophenol blue/EDTA loading |
| sec | second |
| SDS | sodium dodecyl sulphate |
| SF | straight filaments |
| SM | standard medium |
| SS | sterile saline |
| SOC | super optimal broth with catabolite repression |
| TE | tris EDTA buffer |
| TBE | tris-borate-EDTA buffer |
| TBS | tris buffered saline |
| TBST | tris buffered saline-tween |
| TF | twisted filaments |
| TGS | tris-glycine-SDS |
| UV | ultraviolet |
| V | volts |
| v/v | volume per volume |
| w/v | weight per volume |
| X-gal | 5-bromo-4-chloro-3-indolyl-beta-d glucopyranoside |
| 3R | 3 repeat |
| 4R | 4 repeat |

## Summary

The abnormal accumulation of the tau protein into aggregates is a hallmark in neurodegenerative diseases collectively known as tauopathies. In normal conditions, tau binds off and on microtubules aiding in their assembly and stability dependent on the phosphorylation state of the protein. In disease-affected neurons, hyperphosphorylation leads to the accumulation of the tau protein into aggregates, mainly neurofibrillary tangles (NFT) which have been seen to colocalise with other protein aggregates in neurodegeneration. One such protein is α-synuclein, the main constituent of Lewy bodies (LB), a hallmark of Parkinson's disease (PD). In many neurodegenerative diseases, including PD, the colocalisation of tau and α-synuclein has been observed, suggesting possible interactions between the two proteins. To explore the cytotoxicity and interactions between these two proteins, I expressed full length human tau and α-synuclein in *Dictyostelium discoideum* alone, and in combination. Western blot analysis showed that tau is phosphorylated in *D. discoideum,* and immunofluorescence microscopy indicated that tau colocalises closely (within 40 nm) with tubulin throughout the cytoplasm of the cell as well as with α-synuclein at the cortex. Previously, expression of α-synuclein alone inhibited growth on bacterial lawns, phagocytosis and intracellular *Legionella* proliferation rates, but activated mitochondrial respiration and non-mitochondrial oxygen consumption. The expression of tau alone impaired multicellular morphogenesis, axenic growth and phototaxis, while enhancing intracellular *Legionella* proliferation. Direct respirometric assays showed that tau impairs mitochondrial ATP synthesis and increased the "proton leak", while having no impact on respiratory Complex I or II function. In most cases depending on the phenotype, the coexpression of tau and α-synuclein exacerbated (phototaxis, fruiting body morphology), or reversed (phagocytosis, growth on plates, mitochondrial respiratory function, *Legionella* proliferation) the defects caused by either tau or α-synuclein expressed individually. Proteomics data revealed distinct patterns of dysregulation in strains ectopically expressing tau or α-synuclein or both, but down regulation of expression of cytoskeletal proteins was apparent in all three groups and most evident in the strains expressing both proteins. These results indicate that tau and α-synuclein exhibit different but overlapping patterns of intracellular localization, that they individually exert distinct but overlapping patterns of cytotoxic effects and that they interact, probably physically in the cell cortex as well as directly or indirectly in affecting some phenotypes. The results show the efficacy of using *D. discoideum* as a model to study the interaction of proteins involved in neurodegeneration.

# Statement of Authorship

Except where reference is made in the text of the thesis, this thesis contains no material published elsewhere or extracted in whole or in part from a thesis submitted for the award of any other degree or diploma. No other person's work has been used without due acknowledgment in the main text of the thesis. This thesis has not been submitted for the award of any degree or diploma in any other tertiary institution.

The research undertaken in connection with this thesis was approved by the Institutional Biosafety Committee (IBC20020).

This work was supported by an Australian Postgraduate Award Scholarship and an Australian Government Research Training Program Scholarship.

Katelyn Mroczek

Date 23/02/2022

# Acknowledgements

This thesis has been a long time coming and there are many people that have helped me get to this point. Firstly, I would like to thank my supervisors, Dr Sarah Annesley and Prof. Paul Fisher for giving me the chance to compete this work. It has been a long road and without your support and guidance I wouldn't be where I am.

Sarah, thank you so much for your technical support in the lab and with the help of reading and drafting my writing so many times. You were always there to provide encouragement and motivation when I lacked it. Also, for the laughs and kindness along the way.

Thank you to Paul for taking me into the lab all those years ago and for helping with your wealth of knowledge and with the statistical analysis and direction of the project. You have always been there when I needed a chat about the project or life.

I really appreciate all the support from both of you.

To all the past and present members of the Fisher/Annesley lab. Thank you for your friendship and camaraderie over the years, for being there during the good days and the bad and making it so enjoyable to come into the lab. Special thanks to Oana Sanislav and Sui Lay for the early technical help, your knowledge was much appreciated, and to Xavier Pearce, my friend and coffee buddy who was always there to lend a hand or an ear and provided me with much comic relief.

I have met so many colleagues at La Trobe University that have been supportive along the way, particularly in the microbiology discipline. To them I want to say thank you so much for your kind words and positivity over the journey. Especially to Anna Morris who has been a great motivator and mentor and was always there to boost my morale and provide positive reassurance. Also, to A/Prof. Karla Helbig who came in and gave me the boost I needed to finish my writing. You have helped me immensely.

On a personal note, I want to thank my parents Jerzy and Karen who have continually supported me through the years. This endeavour has taken longer than expected but you never doubted me, and I know I have made you proud. To my brother Dale, you boosted me up when you didn't know I needed it. Thank you for the confidence you always had in me.

To my partner and best friend Liam, you have provided more support to me than I think you know. Thanks for being my biggest fan and for providing the belief that I could do this since we met, even when I felt defeated.

Lastly to my wonderful friends that have supported me with kind words and encouragement along the way, my sincerest gratitude. You all knew that I could do this, even when I didn't. Your friendship has been a blessing.

# Publications

## Book chapter:

The following publication has been used and adapted to form part of the introduction to this thesis. The full paper has been attached in Appendix 8.

**Mroczek, K.H.,** S.J. Annesley, and P.R. Fisher. **2020**. Chapter 28 - Tau and its interactions with other proteins in neurodegenerative diseases. In Genetics, Neurology, Behavior, and Diet in Parkinson's Disease. C.R. Martin and V.R. Preedy, editors. Academic Press. 447-462.

## Journal Publications:

The following publication has been used and adapted to form part of the introduction, results and discussion sections of this thesis. The full paper has been attached in appendix 9.

**Mroczek, K.,** S. Fernando, P.R. Fisher, and S.J. Annesley**. 2021.** Interactions and Cytotoxicity of Human Neurodegeneration- Associated Proteins Tau and α-Synuclein in the Simple Model *Dictyostelium discoideum*. Front Cell Dev Biol. 9:741662

The following publications include work described herein or work to which I contributed during the period of my candidature:

Fernando, S., C.Y. Allan, **Mroczek, K.,** Pearce, X., Sanislav, O., Fisher, P.R., and Annesley, S.J**. 2020.** Cytotoxicity and Mitochondrial Dysregulation Caused by α-Synuclein in *Dictyostelium discoideum*. Cells. 9:2289

Ugalde, C.L., Annesley, S.J., Gordon, S.E., **Mroczek, K.,** Perugini,M.A., Lawson, V.R., Fisher, P.R., Finkelstein, D.I., and Hill, A.F. **2020.** Misfolded α-synuclein causes hyperactive respiration without functional deficit in live neuroblastoma cells. Disease models & mechanisms : DMM. 13 (1): dmm040899

## Oral presentations

**Mroczek, K.H.,** P.R. Fisher, and S.J. Annesley**. 2022.** A *Dictyostelium discoideum* model for Alzheimer's disease and other Tauopathies. Abstract 120. 43rd Annual Lorne Genome Conference 13$^{th}$ – 16$^{th}$ February, 2022. Victoria, Australia.

**Mroczek, K.H.,** S.J. Annesley, and P.R. Fisher **2017.** A *Dictyostelium discoideum* model for Alzheimer's disease and other Tauopathies. Dicty2017. Annual International *Dictyostelium* Conference. August 20-24, Geneva, Switzerland, Talk 25

## Poster Presentation

**Mroczek, K.H.,** S.J. Annesley, and P.R. Fisher. **2017.** A *Dictyostelium discoideum* model for Alzheimer's disease and other Tauopathies. ComBio Conference, October 2nd -5th, 2017. Adelaide, Australia.

Annesley, S.J., Allan, C., **Mroczek, K.H.,** Sanislav, O., Lay, S.T., Jasim, R.A.F., Chen, S., Ugalde, C., Hill, A., Fisher, P.R. **2017.** Does Parkinson's Disease really involve pathologically impaired mitochondrial function? LIMS Fellows Research Symposium. 17th November 2017, Austin Hospital, Heidelberg, Victoria, Australia.

# 1.0 INTRODUCTION

## 1.1 Neurodegeneration and protein accumulation

Neurodegenerative diseases are the leading cause of disability worldwide and as the population ages they are expected to increase in their prevalence. The WHO estimates that by 2040 neurological disorders will collectively eclipse cancer as the second leading cause of death worldwide (Gammon, 2014). The most common neurodegenerative disease is Alzheimer's disease (AD) in which the hallmarks like other neurodegenerative diseases are the accumulation of aggregated proteins. The accumulation of the tau protein is present as the dominant aggregate in a group of neurodegenerative diseases known as tauopathies (Table 1.1) with AD being the most common tauopathy. However, tau aggregation is also implicated in other diseases including Pick's disease, Cortico-basal degeneration, Progressive supranuclear palsy and Fronto-temporal dementia with Parkinsonism linked to chromosome 17 (Goedert and Spillantini, 2011; Lee et al., 2001; Spillantini and Goedert, 1998). Other proteins implicated in neurodegeneration and protein aggregation include α-synuclein, the hallmark of synucleinopathies (Galpern and Lang, 2006), amyloid beta, one of the main proteins involved in Alzheimer's disease (Glenner and Wong, 1984a) and the abnormal isoform of prion protein involved in disorders known as prion diseases (Prusiner, 1991). Tau and its abnormal aggregation is implicated in many disorders and has been associated with these aforementioned proteins in different diseases (Figure 1.1). In many of these disorders more than one of these proteins are detected with an overlap of symptoms and pathologies between diseases. This may indicate an interaction and a possible synergistic relationship of these proteins leading to neurodegeneration.

**Table 1.1 Neurodegenerative tauopathies. Neurodegenerative diseases with predominant tau pathology are classified as tauopathies.**

| |
|---|
| Alzheimer's disease |
| Down's syndrome |
| Dementia pugilistica |
| Corticobasal degeneration |
| Frontotemporal dementia with parkinsonism linked to chromosome 17 |
| Progressive supranuclear palsy |
| Argyrophilic grain disease |
| Pick's disease |
| Dementia with tangles |
| Diffuse neurofibrillary tangles with calcification |
| Myotonic dystrophy |

Tau accumulates into aggregates that are the hallmarks of these diseases (Ferrer et al., 2014; Goedert and Spillantini, 2011; Iqbal et al., 2005; Lee et al., 2001; Spillantini and Goedert, 1998).

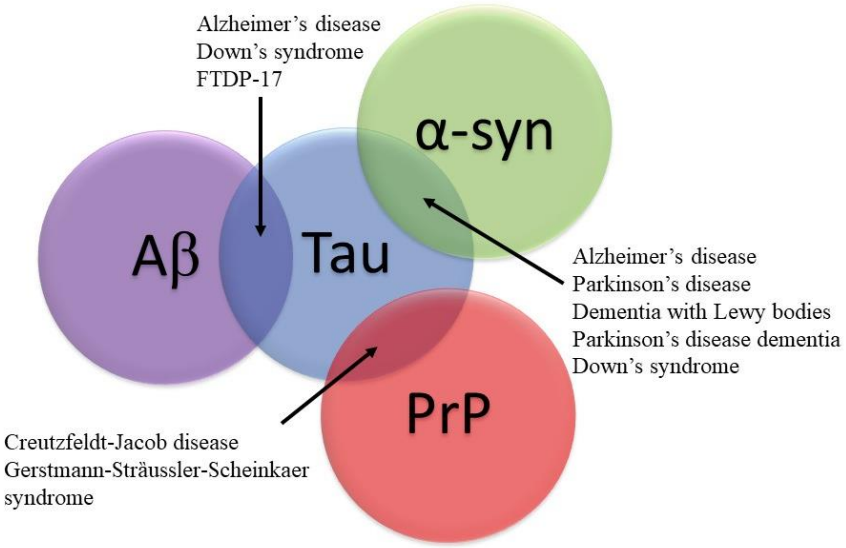


**Figure 1.1 Protein deposits in neurodegenerative diseases.** Illustration of the disorders in which neurotoxic protein aggregates of amyloid beta (Ab), α-synuclein (α-syn), and prion protein (PrP) are found together with tau protein aggregates.

## 1.2 Tau

Tau is encoded by the MAPT gene, which is located on chromosome 17q21, contains 16 exons and is 100 kb in size. The protein binds to tubulin, promoting the assembly and stability of microtubules (MT) thus aiding in axonal transport and supporting the structure of neurons (Cleveland et al., 1977; Kosik, 1993). Tau is predominantly located within the neurons (Drubin and Kirschner, 1986) where it may work synergistically with other microtubule associated proteins (De Vos et al., 2008). The protein contains an acidic N-terminal region known as the projection domain, which is thought to maintain spacing between microtubules and to promote interactions with other cytoskeletal proteins (Avila et al., 2004; Mandelkow et al., 2007). The middle region consists of a proline rich domain that binds proteins and the C-terminal portion is known as the assembly domain, which contains a tubulin binding domain to promote MT assembly (Mandelkow et al., 2007).

### 1.2.1 Tau isoforms

There are 6 tau protein isoforms that are expressed in the brain due to alternative splicing of the RNA transcript (Andreadis et al., 1992) (Figure 1.2). These range from 352-441 amino acids in length and contain either 3 (3R) or 4 (4R) microtubule binding repeat sequences that are in the C-terminus of the protein (Goedert et al., 1989a; Goedert et al., 1989b; Himmler et al., 1989). The microtubule repeats are encoded by exons 9-12 and contain either 3 or 4 repeats dependent on the presence or absence of exon 10. The affinity for MT binding increases with the number of repeats (Spires-Jones et al., 2009).

The isoforms also differ in N-terminal inserts due to the alternative splicing of exons 2 and 3. This results in isoforms containing both exons (2N), only exon 2 (1N) or neither exon 2 nor 3 (0N). The shortest of the isoforms (0N3R) is known as foetal tau as it is present at birth, while the other isoforms are developmentally regulated such that all 6 isoforms are expressed in the adult brain (Goedert et al., 1989a).

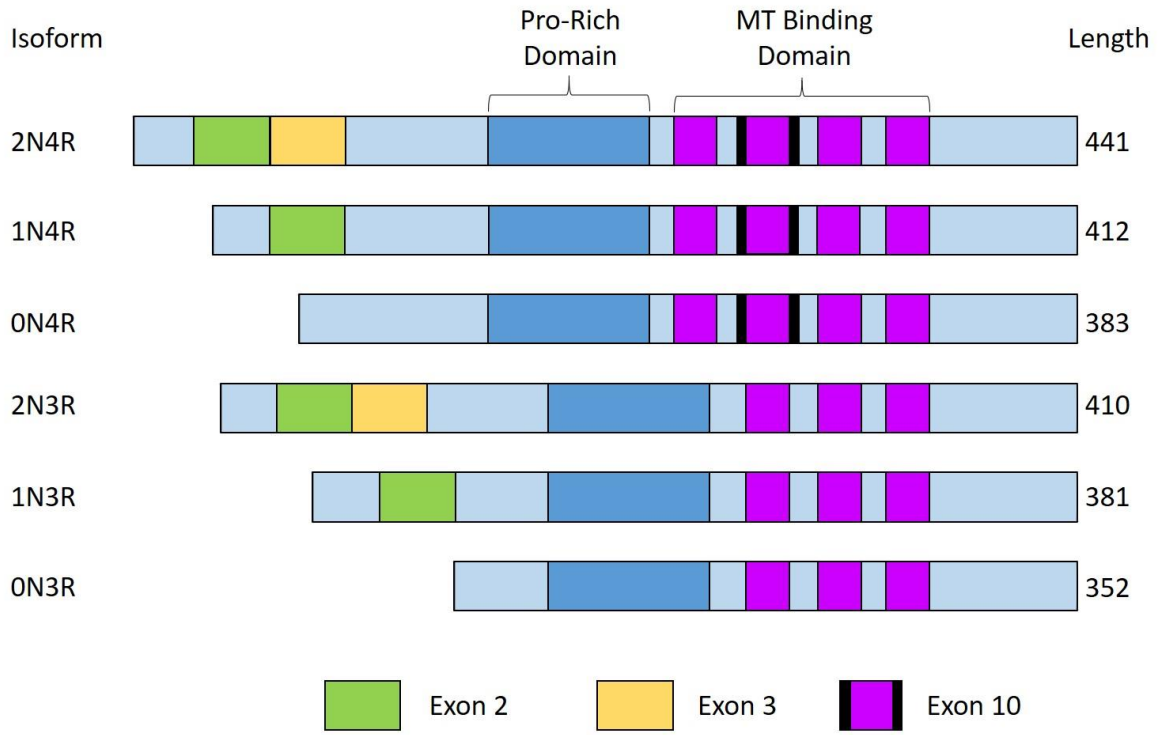


**Figure 2. Tau protein isoforms.** Alternative splicing of MAPT produces six isoforms differing in sequences from exons 2 and 3 and the presence or absence of exon 10. The shortest isoform with neither exon 2 or 3 in the N-terminal (0N) and absence of exon 10 and therefore only has three MTBR's (3R) is the foetal form and denoted as (0N3R). The other isoforms are developmentally regulated to express all six isoforms in the adult brain. (Adapted from (Guo et al., 2017; Lee et al., 2001; Spillantini and Goedert, 1998))

### 1.2.2 Tau phosphorylation and aggregation

Normally tau binds to and is released from microtubules dependent on the phosphorylation state of the protein. Phosphorylation of tau negatively affects its ability to bind to MT, while tau dephosphorylation increases the affinity to bind and stabilise MT (Cleveland et al., 1977; Lindwall and Cole, 1984). There are over 80 phosphorylation sites on the longest tau isoform, 71 of which have been implicated in either physiological or pathological conditions (Buée et al., 2000; Hanger et al., 2007), with over 20 kinases that phosphorylate at these sites. One of the major tau kinases found to employ significant roles in the regulation of tau phosphorylation during normal and pathological circumstances is GSK-3β (Lee et al., 2002). In pathological conditions further hyperphosphorylation of tau is the main contributing factor in the formation of tau aggregates (Figure 1.3). These aggregates

can adopt many conformations, but the most commonly found is neurofibrillary tangles (NFT) composed of paired helical filaments (PHF) made up of all six tau isoforms (Goedert et al., 1988; Grundke-Iqbal et al., 1986; Wischik et al., 1988). NFT are found in disorders such as Alzheimer's disease (AD), Down's syndrome (DS), Progressive supranuclear palsy (PSP), Parkinsonism-dementia complex of Guam and corticobasal degeneration (Buée et al., 2000). These diseases, characterised by the accumulation of abnormally phosphorylated and aggregated tau, are collectively known as tauopathies. Although tau is the main neurotoxic protein found in these diseases, other proteins have been found to colocalise and interact with tau (also within other disorders) suggesting possible synergistic relationships between neurodegenerative proteins (Table 1.2). The relationship between these neurological proteins and tau will be discussed.

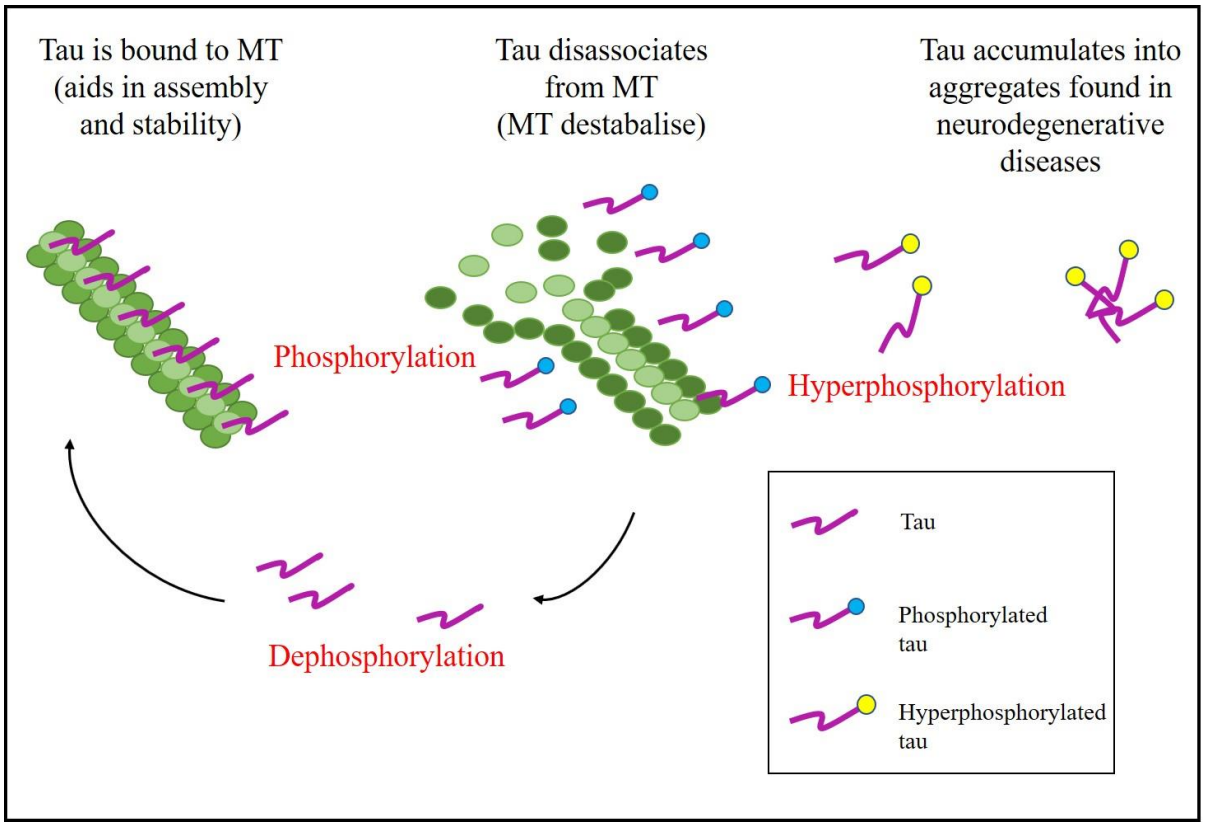


**Figure 1.3. Tau phosphorylation and accumulation into aggregates.** Tau binds on and off microtubules (MTs) depending on its phosphorylation state. Phosphorylation causes tau to dissociate from the microtubules leading to their destabilization. Dephosphorylated tau regains its affinity for and binds to MT. Further hyperphosphorylation leads to the accumulation of tau protein into the aggregates found in tauopathies and other neurodegenerative diseases. (Adapted from Paula et al. (2009)).

**Table 1.2. Tau-associated proteins in neurodegenerative disease.**

| Disease | Tau aggregate | Associated proteins |
|---|---|---|
| Alzheimer's disease | NFT | Amyloid-beta<br>α-synuclein<br>Filamin<br>Myosin |
| Parkinson's disease | Neurites | α-synuclein |
| Pick's disease | Pick bodies<br>Neurites | DJ-1 |
| Corticobasal degeneration | NFT | DJ-1 |
| Prion disease | NFT | PrP |
| FTDP-17 | NFT<br>Neuropil threads | Amyloid-beta<br>α-synuclein<br>Filamin<br>Myosin |

In tauopathies and other neurological diseases, tau is observed in addition to other proteins implicated in neurodegeneration. Tau aggregates and associated proteins can differ between diseases.

### 1.2.3 Tau and mitochondrial dysfunction

Mitochondria are important organelles which contribute to a wide range of functions, establishing cellular homeostasis. The main function of the mitochondria is creating ATP through oxidative phosphorylation (OXPHOS) as an energy source for cellular functions. They also participate in a range of other functions including intracellular signalling, apoptosis, metabolism of lipids, cholesterol, amino acids, as well as transport of organelles and calcium regulation (Brand and Nicholls, 2011; Chinnery and Schon, 2003). Tau oligomers have been seen to colocalise with mitochondria (Lasagna-Reeves et al., 2011) and the toxic aggregation of tau in diseases like AD, PD and other tauopathies appears to coincide with mitochondrial impairment associated with transport, dynamics and bioenergetics of the mitochondria (reviewed by (Cabezas-Opazo et al., 2015; Eckert et al., 2011; Gibson et al., 2010; Pérez et al., 2018a; Pèrez et al., 2018)).

Mitochondria are transported throughout the neuron along MT by microtubule associated proteins (MAPs) including tau (Wang et al., 2014). As tau has a direct involvement with mitochondrial trafficking, the disassociation of tau from MT can cause mislocalisation of the mitochondria, reducing localisation to axons, with 4R tau having a greater impact than 3R tau (Stoothoff et al., 2009). The transport and distribution of mitochondria are affected by the overexpression and

hyperphosphorylation of tau in many cellular and mouse models of tauopathies (Ebneth et al., 1998; Kopeikina et al., 2011; Rodríguez-Martín et al., 2013; Shahpasand et al., 2012). Other mitochondrial abnormalities include impaired oxidative phosphorylation in a mouse model of AD (Rhein et al., 2009) and impaired mitochondrial dynamics by truncated tau in immortalised cortical neurons and primary cortical neurons from tau knockout mice (Pérez et al., 2018b). The overexpression of tau in neuronal cultures decreased ATP production, the ratio of ATP/ADP and inhibited Complex I activity (Li et al., 2016). It has also been suggested that tau impairs mitochondrial function while simultaneously inhibiting the degradation of damaged mitochondria leading to a cycle of mitochondrial dysfunction (Cummins et al., 2019). In patients with FTDP-17, the 4R isoforms are predominant and mitochondrial functions are altered in neurons resulting in decreased ATP production and higher mitochondrial membrane potential, which leads to increased reactive oxygen species (ROS) causing oxidative stress and neuronal death (Esteras et al., 2017).

## 1.3 Interactions of tau with other proteins in neurodegenerative disease

### 1.3.1 Alzheimer's disease and amyloid beta

The most common tauopathy is Alzheimer's disease. The classical hallmarks of AD, namely neurofibrillary tangles and amyloid plaques, were first discovered in 1906 by Alois Alzheimer (Stelzmann et al., 1995). In 1984, Glenner and Wong (1984b) purified the short amyloid protein from AD brains which showed a beta sheet structure and named it the amyloid beta (Aβ) protein. Aβ is generated from the amyloid-β precursor protein (APP) which, when cleaved by β and γ secretases releases the major Aβ isoforms, Aβ40 and Aβ42 (Selkoe, 1999). In sporadic forms of AD, Aβ40 has been found at a 10-fold higher concentration than the other predominant isoform (Näslund et al., 1994), although Aβ42 is thought to be the more toxic form.

In familial AD, there is genetic evidence to link Aβ aggregation leading to events inducing tau hyperphosphorylation and aggregation (Haass and Selkoe, 2007) with Aβ correlating with synaptic dysfunction and cognitive decline. This corresponds with the amyloid cascade hypothesis (Figure 1.4) originally proposed in the early 90's (Hardy and Higgins, 1992). The consensus was that toxic Aβ deposits are an early event and the main cause of AD pathology, leading to the formation of tau NFT and the death of neurons. Thus commenced many investigations into the brain pathology of AD patients using numerous cell and animal models of AD to elucidate the roles of tau and Aβ and their possible interaction.

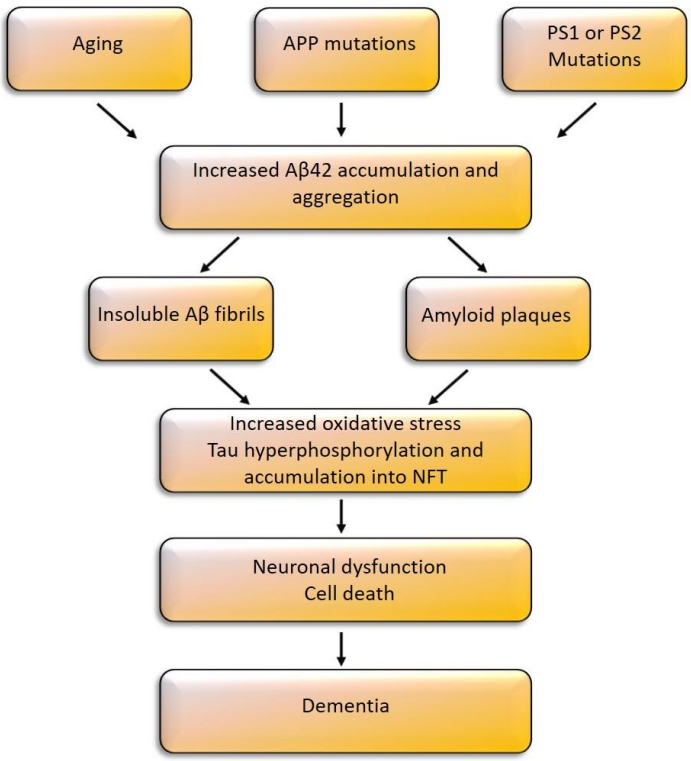


**Figure 1.4 The amyloid cascade hypothesis.** Originally suggested by Hardy and Higgins (1992), this proposes the sequence of pathological events leading to AD and dementia. In this hypothesis, Aβ neurotoxicity is an early event preceding tau filament formation and aggregation to neurofibrillary tangles (NFTs).

Oddo et al. (2003) created a triple transgenic mouse model with mutations in Presenilin-1 (a subunit of γ secretase), APP and tau. In this model, mice progressively developed plaque and tangle pathology, with Aβ deposits occurring at an earlier age (6 months) while extensive tau pathology did not occur until 12 months. This is consistent with the amyloid cascade hypothesis as Aβ deposits develop much earlier than tau NFTs. Another study using transgenic mice showed that NFT pathology was elevated in mice harbouring the tau point mutation P301L as well as a mutation in APP (Tau/APP), when compared to mice carrying only the mutant tau (Lewis et al., 2001). This provides some evidence that APP or Aβ may influence NFT formation. However, the double mutant, tau/APP mice developed amyloid deposits at the same time as mice with only the APP mutation. This suggests that the tau mutation did not exacerbate the development of Aβ pathology.

Nevertheless, there is also evidence that tau is a toxic protein that contributes to Aβ pathology. Rapoport et al. (2002) used cultured hippocampal neurons that were taken from tau knockout (KO) mice or mice expressing either the wildtype mouse or human tau gene. When these neurons were treated with fibrillar Aβ, neurons that contained either mouse or human tau displayed degeneration, while the tau KO neurons did not exhibit this degeneration. This suggests that tau is necessary for the development of the downstream cytopathology caused by Aβ fibrils. It has also been reported that

tau knockdown can lead to a reduction in Aβ40 and Aβ42 levels *in vitro* in primary human cortical neurons (Bright et al., 2015). Exogenous addition of extracellular tau to the cultured neurons increased Aβ levels, suggesting tau to be a driver of Aβ accumulation.

### 1.3.2 Prion diseases

Prion diseases are a group of neurodegenerative disorders that are transmissible and contain genetic familial forms caused by abnormal isoforms of the prion protein (Prusiner, 1991). In 1992, the familial Gertsmann-Stauvisler-Scheinker (GSS) disease, associated with mutations in prion proteins (PrP), was discovered for the first time to contain both PrP amyloid plaques and NFT (Hsiao et al., 1992). NFT with amyloid plaques reacting to prion protein antibodies were detected in the neocortex, together with the accumulation of protease resistant PrP. Two families with GSS have been studied and found to contain NFT composed of PHF of abnormally phosphorylated tau and the accumulation of PrP (Ghetti et al., 1994).

The interaction of tau and PrP has been investigated in cellular and mouse models. CHO cells transfected with constructs to express both tau and PrP showed colocalization of the two proteins using immunofluorescence microscopy (Han et al., 2006). Tau interacted with both the native PrP and protease resistant (toxic) PrP isoforms. This interaction occurred on the N-terminal residues of PrP. More recently phosphorylated tau and PrP were studied in mouse models that were inoculated with prion agents and developed PrP amyloid without any indication of prion disease (Piccardo et al., 2017). Replication and transmissibility of the PrP was confirmed by serially infecting subsequent passages of mice, and phosphorylated tau was consistently present. However, tau phosphorylation was hardly seen in mice harbouring the PrP amyloid plaques without the replication of PrP (Piccardo et al., 2017). Therefore, the authors suggested that toxicity or replication of the prion protein, not conformation of PrP may contribute to tau phosphorylation and fibril formation.

### 1.3.3 α-synuclein in tauopathies

Aβ is not the only protein seen to be present with tau in AD. Another protein profoundly involved in neurodegenerative disease is α-synuclein. This protein is the foremost component of Lewy bodies (LB) found in neurodegenerative diseases and has also been found to coexist with tau. In two studies of sporadic cases of AD, LB were found to exist in 60 % of affected brains (Hamilton, 2000), and α-synuclein positive structures were detected in 13/27 other AD cases (Arai et al., 2001). In both of these reports deposits were mainly confined to the amygdala. α-synuclein is encoded by the *SNCA* gene, is 140 amino acids in length, natively unfolded and heat stable (Tofaris and Spillantini, 2007). Like tau, it is richly expressed in neurons, predominantly in the presynaptic regions (Maroteaux et al., 1988). The normal functioning of the protein is still not well understood, but it is believed to have roles in

membrane dynamics, synaptic transmission, and recycling of synaptic vesicles (Burré, 2015; Burré et al., 2018; Murphy et al., 2000; Sharon et al., 2003). In pathological conditions, α-synuclein misfolds to form oligomers and ultimately into amyloid fibrils, the insoluble and dominate protein aggregate of LB (Burré et al., 2018; Conway et al., 1998; Lashuel et al., 2013; Paleček et al., 2008). Aggregates of α-synuclein containing LB is a hallmark of a group of neurodegenerative diseases classified as the synucleinopathies. Although α-synuclein is the most abundant aggregated protein in these disorders, other proteins like tau have been seen to colocalise within these aggregates as well suggesting an overlap of the tau- and synuclein-opathies.

### 1.3.4 Down's Syndrome

Down syndrome (DS) is a disease resulting from a trisomy of chromosome 21 in which the amyloid precursor protein (APP) is located. It is included as a tauopathy as AD pathology is found in nearly all patients with DS by the time they reach 40 years of age. Hyperphosphorylated Tau conforms into PHF as in AD. Both amyloid plaques and NFT are found within the CNS, wherein NFT are established later than plaque formation, however, directly correlate with the presence of dementia (Jones et al., 2008). Immunohistochemical examination with α-synuclein antibodies detected LB in 50 % of cases of Down's syndrome with AD (Lippa et al., 1999). These were more frequent in the amygdala and the LB sometimes colocalised with NFT.

### 1.3.5 Progressive supranuclear palsy

PSP is a neurodegenerative disease eventuating in neuronal death characterised by the pathological accumulation of insoluble Tau filaments (Williams and Lee, 2012). The symptoms of this tauopathy may also become apparent in other neurological syndromes. These include a loss of balance, and primarily affect motor and also ocular control, so the patient often bumps into objects. In later stages of the disease dementia becomes evident. In PSP, hyperphosphorylated Tau filaments are found within neurons and glia as components of astrocytic tuffs and glubose NFT, these are individual characteristics of PSP (Boeve, 2012). There is a difference in the distribution and composition of Tau in PSP when compared to AD. In PSP pathogenic Tau is localised mainly to the subcortical regions of the brain and as stated, found within neurons and also glial cells. Whereas in AD, neurofibrillary degeneration is more widespread throughout the CNS and filamentous Tau is located only in neurons (Baker et al., 1999). LB have also been detected in a small number of progressive supranuclear palsy (PSP) cases (Jellinger, 2004; Mori et al., 2002). Mori et al. (2002) found with LB pathology and colocalisation of tau and α-synuclein in some neurons in 5 out of 16 patients with PSP.

### 1.3.6 Corticobasal degeneration (CBD) and DJ-1

CBD affects movement and displays many different cortical features, with symptoms often overlapping with other tauopathies. Diagnosis of CBD is possible only by autopsy so the term 'Corticobasal syndrome' is often used to describe the clinical representation of the disease (Boeve et al., 2003). Signs of the disease arise between the ages of 60-80 and are characterized by neuronal loss and gliosis (Hassan et al., 2010). Glial pathology of the disease presents in the form of astrocytic plaques, which are not found in any other tauopathies (Lee et al., 2001; Ludolph et al., 2009). Tau in both straight and PHF are present within astrocytes and oligodendrocytes located in white matter, and another defining feature of the CBD is the vast accumulation of neuropil threads in both grey and white matter (Lee et al., 2001). Here, tau is not seen to colocalise with α-synuclein but another protein known as DJ-1. Antibodies against DJ-1 have been used to test its prevalence in a range of synucleinopathies and tauopathies. In tauopathies, neuronal tau deposits reacted positively to DJ-1 in CBD but also in Pick's disease (PiD), PSP and AD (Neumann et al., 2004). Patrizia et al. (2004) observed DJ-1 reactivity in Pick's bodies in PiD, with up to 50% of tau-positive inclusions staining positive for DJ-1 in the hippocampus.

### 1.3.7 FTDP-17

Most of these tauopathies are sporadically contracted and are due to the abnormal phosphorylation and accumulation of Tau. However, mutations in *MAPT* have been found to occur in Fronto-temporal dementia with Parkinsonism linked to chromosome 17 (FTDP-17) which may also be inherited. More than 35 MAPT mutations have been identified from over 150 families affecting all 6 isoforms (Shiarli et al., 2006). As these mutations cause a genetic form of a tauopathy, many studies using the most commonly found mutation (P301L) have been directed at assessing the different protein interactions with tau. The P301L transgenic mouse model has been extensively used. Injections of Aβ fibrils directly into the brain of P301L mice cause a 5-fold increase in NFT numbers around the site of injection (Gotz et al., 2001). The NFT formed contained tau phosphorylated at Serine 212/Threonine 214 and Serine 422. Oligomeric and fibrillar species of Aβ have also been shown to decrease mitochondrial membrane potential and impair mitochondrial function in tau mutant mice (Eckert et al., 2008). The P301L mutation also increases the propensity of tau to form NFT when cross-seeded with preformed α-synuclein fibrils. A wild type tau cellular model generated a small number of NFT when cross-seeded with α-synuclein, whereas cells with the P301L mutation converted over 50 % of total tau to NFT (Waxman and Giasson, 2011).

FTDP-17 brains have also been studied and found to contain tau colocalising with the cytoskeletal proteins Filamin-A and Myosin-VI (Feuillette et al., 2010a). Filamin A was a component in the NFT, neuropil threads and in coiled bodies with myosin VI-positive "ghost tangles". The accumulation of

these two proteins was also seen in AD brains, but not those of PiD and PSP. Since these proteins are involved in the cytoskeletal network, the authors proposed that tau toxicity may be compounded by the breakdown of the actin network.

### 1.4 Parkinson's disease and other synucleinopathies

As mentioned previously, neurodegenerative disorders that implicate α-synuclein as the dominant pathological protein are termed synucleinopathies. Diseases include Lewy Body Dementia, multiple system atrophy and Parkinsonism with dementia, but Parkinson's disease (PD) is the most common (Galpern and Lang, 2006; Savica et al., 2013).

Both idiopathic and familial forms of PD occur, with α-synuclein-containing LB the prominent pathological feature. Tau is often seen to coexist with α-synuclein and this is also evident in cases of PD. Mutations in SNCA, which encodes α-synuclein, cause a familial form of PD. However, the question arises as to whether a genetic predisposition for idiopathic PD may also exist. A complete genome screen of PD was conducted in 2001 with the aim to determine genetic risk factors of genes associated with idiopathic PD (Scott et al., 2001). An observed linkage to a region on chromosome 17 that contains the tau gene was identified. This led the investigators to conduct a study of 235 families with 426 affected with PD and 579 non- affected individuals. They implicated MAPT as a susceptibility gene for late-onset idiopathic PD as they found a MAPT haplotype that strongly correlated with an increased risk of inheriting PD (Martin et al., 2001). There have been many studies on PD brains and model systems used to determine whether there is an interaction between these two proteins, and there is much evidence to suggest this.

Post-mortem PD brains with dementia (PDD) and without (PD), showed an increase in tau hyperphosphorylated at Ser262 and Serine396/404 (known residues associated with pathological conditions) (Wills et al., 2010). This was localised to the striatum of the brain. Higher levels of active, phosphorylated (at Thr216) GSK-3β, one of the known tau kinases, were found in both PD and PDD when compared with the controls tested. It is thought that α-synuclein stimulates the phosphorylation of GSK-3β at Thr216 which leads in turn to GSK-3β phosphorylating tau, converting it into its toxic form.

The Contursi kindred is a large extended family from the Italian village of Contursi, in whom the first familial form of PD was discovered and subsequently found to be caused by an autosomal dominant α-synuclein mutation (A53T). Within brain tissues from the Contursi kindred, there has been a notable coexistence of α-synuclein and tau. One study found rare LB pathology and previously unrecognised α-synuclein pathology (Duda et al., 2002). Within these neurites, tau inclusions were also unexpectantly found, and in some inclusions colocalised with α-synuclein. Another study conducted

on an individual from the filamentous tau in specific areas of the brain (Kotzbauer et al., 2004). Large spheroids reacted positively to tau immunoreactivity and tau and α-synuclein were sometimes stained in the same inclusion. The authors speculated the α-synuclein A53T mutation may play a role in the fibrillisation of tau. Therefore, they performed *in vitro* fibrillisation assays using α-synuclein, α-synuclein with the A53T mutation and tau. The results indicated that the A53T mutation promotes faster fibrillisation of α-synuclein and tau filament formation as well as synergistically enhancing tau and α-synuclein cofibrillisation (Kotzbauer et al., 2004).

As directly studying the interaction of α-synuclein and tau in PD patients was limited to investigating postmortem brains, many models have been used to gain insights to the possible mechanisms and toxicity that coexpression of these proteins may cause. The A30P missense mutation in SNCA causes an autosomal dominant form of PD and mice expressing A30P α-synuclein were found to develop a four-fold increase in tau phosphorylated at Serine 396/404 (a pathological residue) when compared to controls (Frasier et al., 2005). Although a strong colocalisation of α-synuclein and tau was not seen in this study, it has been known to occur. When tau and α-synuclein were expressed in Chinese hampster ovary (CHO) cells, tau and α-synuclein were seen to largely colocalise except in the nucleus (Esposito et al., 2007). However, the authors acknowledged that this was not indicative of an interaction of these two proteins. Waxman and Giasson (2011) made similar findings when two plasmids containing tau and α-synuclein were expressed in cells derived from human embryonic kidney cells. Again, colocalisation seemed coincidental. However, when these cells were treated with recombinant prefibrillised α-synuclein protein, large intracellular aggregates were formed containing both α-synuclein and tau.

Two studies have used the MMP+/MPTP model of PD to study the interaction of tau and α-synuclein. MPTP (1-methyl-4-phenyl-1,2,3,6-tetrahydropyridine) is metabolised into MMP+ (1-methyl-4-phenylpyridinium) a neurotoxin that produces severe PD (Tieu, 2011). MMP+/MPTP-induced PD models have been created in cell lines and transgenic mice (Duka et al., 2009; Qureshi and Paudel, 2011). In some of these models, GSK-3β is heavily activated as seen in transgenic mice overexpressing α-synuclein and in the post-mortem striatum of PD patients (Duka et al., 2009). MPTP activated tau phosphorylation by GSK-3β in the transgenic mouse model and this was dependent on the presence of α-synuclein. A physical interaction between α-synuclein, GSK-3β and tau was confirmed by co-immunoprecipitation, indicating that these proteins form a complex.

MPTP has also been used in models with mutations in α-synuclein. In human neuroblastoma M17 cells treated with MPTP, α-synuclein was found to bind to Ser214 of tau and induce the phosphorylation of tau at Serine 262 (Qureshi and Paudel, 2011). MPTP-induced Tau phosphorylation at this site was

suppressed in knockout α-synuclein mice, suggesting that MPTP enhances the ability of intracellular α-synuclein to stimulate the increased phosphorylation of tau. In a similar vein, in MPTP-treated HEK-293 cells, α-synuclein mutants (A30P, E4KR & A53T) contributed to destabilisation of the cytoskeleton (Qureshi and Paudel, 2011). When these mutant forms of α-synuclein were coexpressed with tau, MT destabilisation was significantly more pronounced compared to coexpression with wild type α-synuclein. This indicates that point mutations in SNCA may contribute to tau pathology in neurodegeneration.

A similar suggestion that these proteins enhance neurodegenerative pathology when combined comes from a study of neurotoxicity using a *Drosophila* model of PD. Roy and Jackson (2014) mis-expressed α-synuclein and tau singly and in combination in *Drosophila* and used three 3 different tissues to gain insights into interactions between these two proteins. Misexpression of α-synuclein alone caused no phenotype in the retina while tau caused a rough eye phenotype and produced smaller eyes, a phenotype that was enhanced when both tau and α-synuclein were expressed together. Likewise, the ectopic expression of α-synuclein enhanced tau-induced motor dysfunction, and coexpression resulted in abnormal MT organisation and actin cytoskeletal disorganisation. These results suggest a synergistic interaction between tau and α-synuclein in producing cytoskeletal cytopathologies.

Although there is much evidence that tau and α-synuclein work together in PD to produce neurodegeneration, this is not the only neurological disorder in which α-synuclein is a pathological protein. Other examples of cooperative tau and α-synuclein pathology are found in other synucleinopathies. Badiola et al. (2011) used different cellular models of synucleinopathies to investigate the effects of tau on α-synuclein aggregation. Tau and α-synuclein colocalised in both human cell lines and primary neuronal cultures. They were seen to be colocalised in aggregates and in other parts of the cell, where tau phosphorylated and dephosphorylated forms were detected. The overexpression of tau in these cells led to an increased number and decreased size of α-synuclein aggregates. Overall, the study concluded that tau enhanced α-synuclein cytotoxicity.

Postmortem brains of patients with Dementia with Lewy Bodies disease (DLBD) were examined to determine the frequency of neurons that contained both LB and NFT (Iseki et al., 1999). Neurons positive for both inclusions were frequently seen in the limbic areas. Generally, α-synuclein-positive LB were surrounded with small, randomly oriented PHF. Coaggregation of tau and α-synuclein was also seen in LB taken from patients with LB disease. Double immunostaining in LB cases found tau-containing LB in 80 % of cases where LB were present in the medulla (Ishizawa et al., 2003).

## 1.5 *Dictyostelium discoideum* as a model organism

As seen in earlier sections, both cellular and animal models have been used to study tauopathies, protein-protein interactions and the pathological processes of neurodegenerative disorders. These highlight the usefulness of model systems to study complex disease mechanisms. *Dictyostelium discoideum* is a novel eukaryotic model organism recognised by the National Institute of Health (NIH) in the U.S.A for its importance in biomedical research (Martín-González et al., 2021). It has been used as a biomedical model for studying human diseases including neurodegeneration, lysosomal trafficking disorders and mitochondrial disease (Annesley and Fisher, 2009a; Francione et al., 2011; Maniak, 2011; Martín-González et al., 2021). The complete nuclear (Eichinger et al., 2005) and also mitochondrial (Ogawa et al., 2000) genomes have been sequenced, allowing for orthologues of human genes to be studied. Of interest is the distinctive life cycle of *D. discoideum* in which there are both unicellular and multicellular stages with numerous cell types (Figure 1.5). This allows diverse, reproducible phenotypic traits to serve as "readouts" of disease gene-related disturbances in cellular processes and the signalling pathways that control them (Annesley and Fisher, 2009a). Additionally, *D. discoideum* is greatly accessible for use in biomedical research, genetically manipulable and easily grown clonally.

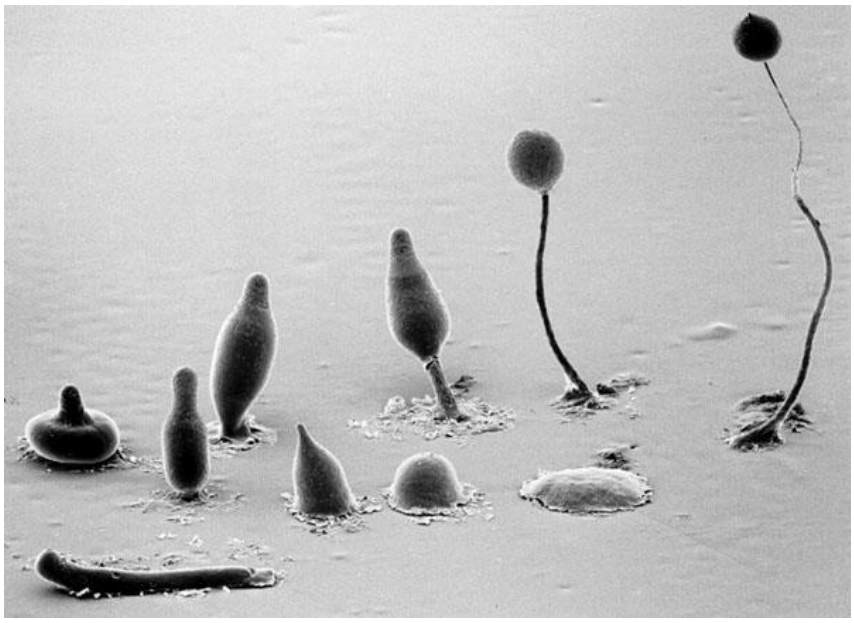

**Figure 1.5 The *Dictyostelium discoideum* life cycle.** When cells starve, chemical attraction towards cAMP results in aggregation and multicellular development. Aggregates of cells form the slug which migrates to more favourable conditions and culminates. This results in the formation of fruiting bodies consisting of a droplet of spores (sorus) atop a thin stalk and a basal disc. The differentiated stalk/disc and spore cells make up approximately 20% and 80% of the cells respectively (Jermyn et al., 1996; Kaiser, 1986; Loomis, 1982; Strmecki et al., 2005). Unicellular stages enable phenotypic investigation of growth by phagocytosis and macropinocytosis. While multicellular signalling pathways may be explored at numerous stages in the life cycle such as migrating slug and fruiting body formation.

Figure from http://dictybase.org/Multimedia/LarryBlanton/dev.html (accessed 31-01-2022) Copyright, M.J. Grimson & R.L. Blanton, Biological Sciences Electron Microscopy Laboratory, Texas Tech University).

### 1.5.1 *D. discoideum* models of neurodegeneration

*D. discoideum* has already been used as a model to study elements involved in AD. Orthologues of the presenilin proteins and other γ secretase subunits that cause the cleavage of amyloid precursor protein (APP) to Aβ have been identified in *D. discoideum,* and have similar functionality to the mammalian complex (Ludtmann et al., 2014; McMains et al., 2010). Mutations in the presenilin genes have been known to cause early-onset familial AD (De Strooper and Annaert, 2010). In *D. discoideum*, the knockout of the presenilin genes resulted in a developmental block in aggregation, which was restored with the expression of human presenilin 1 (Ludtmann et al., 2014). Also importantly, *D. discoideum* was seen to process ectopically expressed human APP to the amyloid-β peptides $A\beta_{40}$ and $A\beta_{42}$, while in strains that were deficient in γ secretase this APP processing was blocked (McMains et al., 2010). As is the case with APP, there are no homologues of tau in *D. discoideum,* but many of the proteins that interact with tau have been evolutionarily conserved such as the kinases AMPK and glycogen synthase kinase 3 (GSK3) as well as cytoskeletal proteins tubulin and filamin. This allows the study of the cytotoxic effects of tau directly without the complication of the endogenously expressed protein or homologue.

### 1.5.2 Mitochondrial disease in *Dictyostelium*

Mitochondrial dysfunction has been associated with neurodegenerative disease like AD and PD (Beharry et al., 2014). Specifically, tau has been implicated in mitochondrial dysfunction involving trafficking, dynamics and bioenergetics of the mitochondria. Studying mitochondrial diseases in complex organisms can often be hampered due to the complex relationship between genotype and phenotypic presentation of disease. In humans, mutations in genes encoding mitochondrial proteins results in various clinical presentations without a clear link to genotype (Garone et al., 2018). The same genetic defect can cause significantly different phenotypic outcomes, and similar clinical representations can be caused by a range of genetic mutations (Sofou et al., 2018). The phenotypic outcome of mitochondrial disease seems to be determined by how many mutant mitochondrial genomes are present in an individual (Pearce et al., 2019). This number can vary greatly between persons and in tissues of an individual, with this affected proportion of the mitochondrial population known as the 'mutant load' (Stewart and Chinnery, 2015). For this reason, using the simple model *D. discoideum* has proved advantageous when studying mitochondrial biology. Mitochondrial disease has been created and well characterised in *D. discoideum.* Through the knockdown of nuclear encoded mitochondrial proteins or disruption of mitochondrial genes, a clear set of phenotypes was exhibited

in each case (reviewed by Francione and Fisher (2011)). Among these phenotypes were: decreased growth on bacterial lawns and in axenic medium, aberrant fruiting body with shorter and thicker stalks, defective slug phototaxis and increased susceptibility to *Legionella* proliferation. These mitochondrially diseased *D. discoideum* phenotypes were attributed to the chronic activation of the energy sensing protein AMP-activated protein kinase (AMPK) by Bokko et al. (2007) and Francione et al. (2009) that showed when AMPK was knocked down by antisense inhibition, the defective phenotypes returned to wildtype levels and chronic activation of AMPK mimicked the disease phenotypes.

### 1.5.3 α-synuclein toxicity in *Dictyostelium*

Like tau α-synuclein has also been implicated in defects associated with mitochondrial dynamics and bioenergetics as well as inhibition of the electron transport chain and specifically Complex I (Ryan et al., 2015). Both tau and α-synuclein are found in axons and presynaptic compartments of neurons where tau stabilises MT and α-synuclein is involved in vesicular trafficking (Yan et al., 2020). Additionally, tau and α-synuclein share many similar properties such as hydrophobic regions, modification by phosphorylation and are both prone to aggregation (Lee et al., 2004). α-synuclein has also be found to associate with tubulin (Zhou et al., 2010).

α-synuclein cytotoxicity has previously been investigated in *D. discoideum*. Like tau, there is no endogenous gene in *Dictyostelium*, so phenotypic affects are a direct result of the human gene successfully being expressed. Wildtype α-synuclein was expressed as well as mutant forms to see whether there was a role in mitochondrial dysfunction (Fernando et al., 2020). α-synuclein localises to the membrane in *Dictyostelium* dependent on the presence of the C-terminus of α-synuclein. The expression of α-synuclein significantly protected *D. discoideum* cells from *Legionella* proliferation and had no effect on axenic growth or pinocytosis. Conversely, it had effects on plaque expansion rates, phagocytosis, and the PD associated point mutation (A53T) and truncated mutants impaired phototaxis. These impaired phenotypes were rescued or partially rescued with the coexpression of an AMPK antisense construct, suggesting that mitochondrial dysfunction may be attributing to at least some of the defective phenotypes. However, when mitochondrial function was directly measured, α-synuclein displayed an increased mitochondrial respiration rather than a dysfunction (Fernando et al., 2020). This was in line with other PD models in which mitochondrial respiration was seen to be increased including α-synuclein fibrils in neuroblastoma cells (Ugalde et al., 2020), lymphoblast cell lines made from idiopathic PD patients (iPD) (Annesley et al., 2016), *D. discoideum* Roco4 knockout cells (Rosenbusch et al., 2021), and fibroblasts from iPD patients (Haylett et al., 2016). As tau and α-synuclein share so many biochemical similarities it is interesting to test whether tau shares a similar phenotypic pattern as α-synuclein in *D. discoideum*. As they are found colocalised in many types of

pathological aggregates it is also worth determining the phenotypic outcomes when both proteins are expressed together.

## 1.6 Aims

Since Tau is not native in this organism, non-mutated forms of Tau can be expressed and studied without the complications of an endogenously expressed gene. The overarching aim of this project was to establish a *D. discoideum* model to study tauopathies and interactions between proteins involved in neurodegeneration. To achieve this, I aimed to determine if tau could be ectopically expressed and phosphorylated in *D. discoideum*, if tau was cytotoxic within *D. discoideum* and whether the expression of tau caused phenotypes which mimicked mitochondrially diseased strains. As there is mounting evidence of an interaction of tau and α-synuclein in neurodegeneration, this project also aimed to express tau and α-synuclein in combination and determine if they had a physical and/or a functional relationship.

# 2.0 MATERIALS AND METHODS

## 2.1 General information

### 2.1.1 Sterilization

All media, pipette tips and glassware were sterilized by autoclaving at 100 kPa for 20 min at 120˚C. Sterile distilled water was used as the solvent for all media and buffers unless otherwise stated.

### 2.1.2 Chemicals

A list of chemicals and their suppliers used during the course of this project are listed in Appendix I.

### 2.1.3 Buffers and media

A list of buffers and media used during the course of this project can be found in Appendix II

### 2.1.4 Enzymes and experimental kits

All enzymes and experimental kits used are listed in Appendix III.

### *2.1.5 D. discoideum* and bacterial strains

**Table 2.1 Origin and genotypes of *Dictyostelium* strains**

| Strain | Parent | Genotype and expressing construct | Construct copy number | Reference |
|---|---|---|---|---|
| AX2 | AX4 | *axe*A1, *axe*B1, *axe*C1 | | Darmon *et al.* (1975) |
| Tau1 | AX2 | pPROF665, expresses tau | 383 | This thesis |
| Tau2 | AX2 | pPROF665, expresses tau | 303 | This thesis |
| Tau4 | AX2 | pPROF665, expresses tau | 176 | This thesis |
| Tau13 | AX2 | pPROF665, expresses tau | 344 | This thesis |
| Tau58 | AX2 | pPROF665, expresses tau | 381 | This thesis |
| Tau60 | AX2 | pPROF665, expresses tau | 432 | This thesis |
| Tau70 | AX2 | pPROF665, expresses tau | 67 | This thesis |
| Tau70 | AX2 | pPROF665, expresses tau | 123 | This thesis |
| Tau105 | AX2 | pPROF665, expresses tau | 235 | This thesis |
| Tau174 | AX2 | pPROF665, expresses tau | 257 | This thesis |
| Tau182 | AX2 | pPROF665, expresses tau | 152 | This thesis |

| | | | | |
|---|---|---|---|---|
| Tau188 | AX2 | pPROF665, expresses tau | 301 | This thesis |
| Tau191 | AX2 | pPROF665, expresses tau | 336 | This thesis |
| Co6 | AX2 | pPROF665 and pPROF629, expresses both tau and α-synuclein | Tau-189 α-syn-92 | This thesis |
| Co8 | AX2 | pPROF665 and pPROF629, expresses both tau and α-synuclein | Tau-130 α-syn-32 | This thesis |
| Co10 | AX2 | pPROF665 and pPROF629, expresses both tau and α-synuclein | Tau-232 α-syn-32 | This thesis |
| Co18 | AX2 | pPROF665 and pPROF629, expresses both tau and α-synuclein | Tau-149 α-syn-12 | This thesis |
| Co21 | AX2 | pPROF665 and pPROF629, expresses both tau and α-synuclein | Tau-137 α-syn-45 | This thesis |
| Co22 | AX2 | pPROF665 and pPROF629, expresses both tau and α-synuclein | Tau-223 α-syn-43 | This thesis |
| Co25 | AX2 | pPROF665 and pPROF629, expresses both tau and α-synuclein | Tau-127 α-syn-16 | This thesis |
| Co29 | AX2 | pPROF665 and pPROF629, expresses both tau and α-synuclein | Tau-128 α-syn-8 | This thesis |
| Co38 | AX2 | pPROF665 and pPROF629, expresses both tau and α-synuclein | Tau-503 α-syn-13 | This thesis |
| Co39 | AX2 | pPROF665 and pPROF629, expresses both tau and α-synuclein | Tau-76 α-syn-34 | This thesis |
| Co41 | AX2 | pPROF665 and pPROF629, expresses both tau and α-synuclein | Tau-250 α-syn-11 | This thesis |
| Co42 | AX2 | pPROF665 and pPROF629, expresses both tau and α-synuclein | Tau- 116 α-syn-92 | This thesis |
| HPF881 | AX2 | pPROF629, expresses α-synuclein | 12 | Fernando, 2012 |
| HPF882 | AX2 | pPROF629, expresses α-synuclein | 12 | Fernando, 2012 |
| HPF883 | AX2 | pPROF629, expresses α-synuclein | 109 | Fernando, 2012 |
| HPF885 | AX2 | pPROF629, expresses α-synuclein | 127 | Fernando, 2012 |
| HPF886 | AX2 | pPROF629, expresses α-synuclein | 65 | Fernando, 2012 |
| HPF887 | AX2 | pPROF629, expresses α-synuclein | 4 | Fernando, 2012 |
| HPF888 | AX2 | pPROF629, expresses α-synuclein | 37 | Fernando, 2012 |
| HPF890 | AX2 | pPROF629, expresses α-synuclein | 122 | Fernando, 2012 |
| HPF891 | AX2 | pPROF629, expresses α-synuclein | 96 | Fernando, 2012 |
| HPF892 | AX2 | pPROF629, expresses α-synuclein | 188 | Fernando, 2012 |

| | | | | |
|---|---|---|---|---|
| HPF893 | AX2 | pPROF629, expresses α-synuclein | 5 | Fernando, 2012 |
| Tau/As13 | AX2 | pPROF665 and pPROF362, expresses tau and antisense AMPK | Tau-140 As-120 | This thesis |
| Tau/As22 | AX2 | pPROF665 and pPROF362, expresses tau and antisense AMPK | Tau-36 As-131 | This thesis |
| Tau/As23 | AX2 | pPROF665 and pPROF362, expresses tau and antisense AMPK | Tau-67 As-178 | This thesis |
| Tau/As31 | AX2 | pPROF665 and pPROF362, expresses tau and antisense AMPK | Tau-37 As-18 | This thesis |
| Tau/As40 | AX2 | pPROF665 and pPROF362, expresses tau and antisense AMPK | Tau-59 As-114 | This thesis |
| Tau/As50 | AX2 | pPROF665 and pPROF362, expresses tau and antisense AMPK | Tau-131 As-117 | This thesis |
| Tau/As53 | AX2 | pPROF665 and pPROF362, expresses tau and antisense AMPK | Tau-184 As-260 | This thesis |
| Tau/As65 | AX2 | pPROF665 and pPROF362, expresses tau and antisense AMPK | Tau-167 As-7 | This thesis |
| Tau/As66 | AX2 | pPROF665 and pPROF362, expresses tau and antisense AMPK | Tau-70 As-155 | This thesis |
| Tau/As67 | AX2 | pPROF665 and pPROF362, expresses tau and antisense AMPK | Tau-133 As-97 | This thesis |
| Tau/As69 | AX2 | pPROF665 and pPROF362, expresses tau and antisense AMPK | Tau-52 As-62 | This thesis |
| Tau/As70 | AX2 | pPROF665 and pPROF362, expresses tau and antisense AMPK | Tau-210 As-39 | This thesis |
| Tau/As72 | AX2 | pPROF665 and pPROF362, expresses tau and antisense AMPK | Tau-86 As-164 | This thesis |
| Tau/As73 | AX2 | pPROF665 and pPROF362, expresses tau and antisense AMPK | Tau-88 As-94 | This thesis |
| Tau/As74 | AX2 | pPROF665 and pPROF362, expresses tau and antisense AMPK | Tau-95 As-55 | This thesis |
| Tau/As75 | AX2 | pPROF665 and pPROF362, expresses tau and antisense AMPK | Tau-52 As-139 | This thesis |

**Abbreviations:**

| **Genotype** | **Phenotype** |
|---|---|
| *axe* | Allows growth in axenic medium |

**Constructs**

**Table 2.2 Plasmid constructs**

| Construct | Plasmid vector | Cloned gene | Reference |
|---|---|---|---|
| **pPROF362** | pDNeo2 | *snfA* Antisense | Bokko *et al.,* 2007 |
| **pPROF629** | pA15GFP | *SNCA* | Fernando et al., 2020 |
| **pPROF665** | pPROF267 | *MAPT* | This thesis |

**Table 2.3 Genotypes of bacterial strains**

| Strain | Genotype | Reference |
|---|---|---|
| ***E. coli* (DH5α)** | F' *end*A1 *hsd*R17 ($r_k^- m_k^+$) *sup*E44 *thi*-1 *rec*A1 *gyr*A ($Nal^r$) *rel*A1 Δ(*lac*ZYA-*agr*F)$_{U169}$ (m80*lac*ZΔM15) | Hanahan, 1983 |

**Abbreviations:**

| Genotype | Phenotype |
|---|---|
| *end*A1 | Mutation suppressing endonuclease A-dependent degradation of plasmid DNA |
| F' | Lacks F plasmid |
| *gln*V44 | Suppression of stop codons (UAG) by insertion of glutamine |
| *gyr*A(Nalr) | DNA gyrase mutation-nalidixic acid resistance |
| *hsd*R17 | Restriction negative modification positive |
| *lac*ZΔM15 | Partial deletion of lacZ gene, allows α complementation of β-galactosidase gene, required for blue/white screening |
| *rec*A1 | Does not allow for general recombination |
| *rel*A1 | RNA-synthesis is relaxed and permitted in the absence of protein synthesis |
| *sup*E44 | Carries a tRNA suppressor gene |
| *thi*-1 | Requires thiamine for growth |

### 2.1.6 Plasmids

The plasmid constructs used during this project are illustrated in Figures 2.1 - 2.4

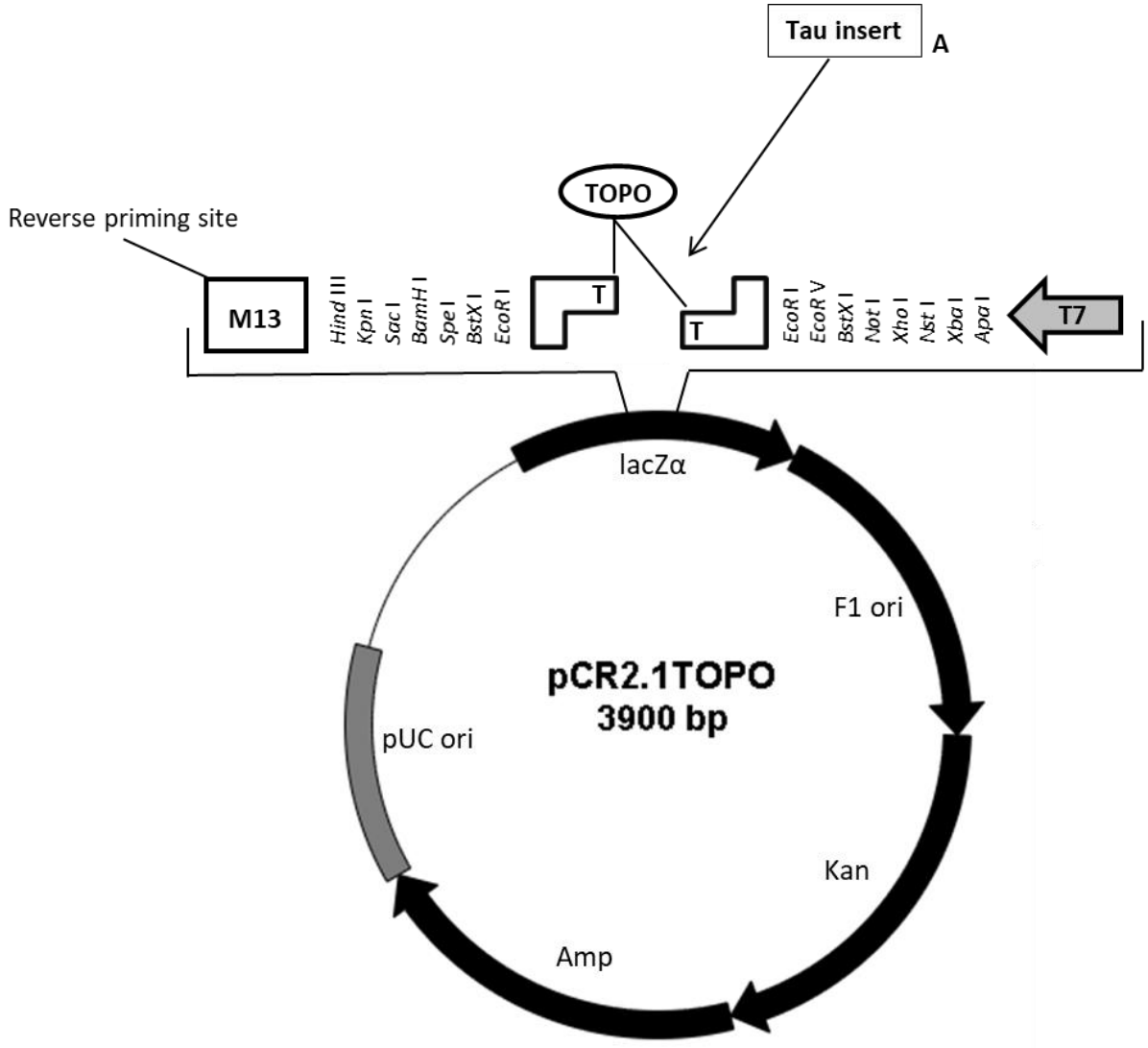


**Figure 2.1. Circular plasmid map of pCR®2.1-TOPO indicating the site of insertion of the tau gene**. PCR amplified tau was directly cloned into pCR®2.1-TOPO as an initial step in two phase cloning. Linearized pCR2.1TOPO vector possesses 3' deoxythimidine (T) overhangs. As a high fidelity *Taq* was used in the amplification, a deoxyadenosine (A) tailing reaction was performed and allowed for the direct ligation of the PCR product with the pCR2.1TOPO vector. The plasmid contains a T7 promoter to control gene expression and allows for selection as it contains ampicillin (Amp) and kanamycin (Kan) resistance cassettes.

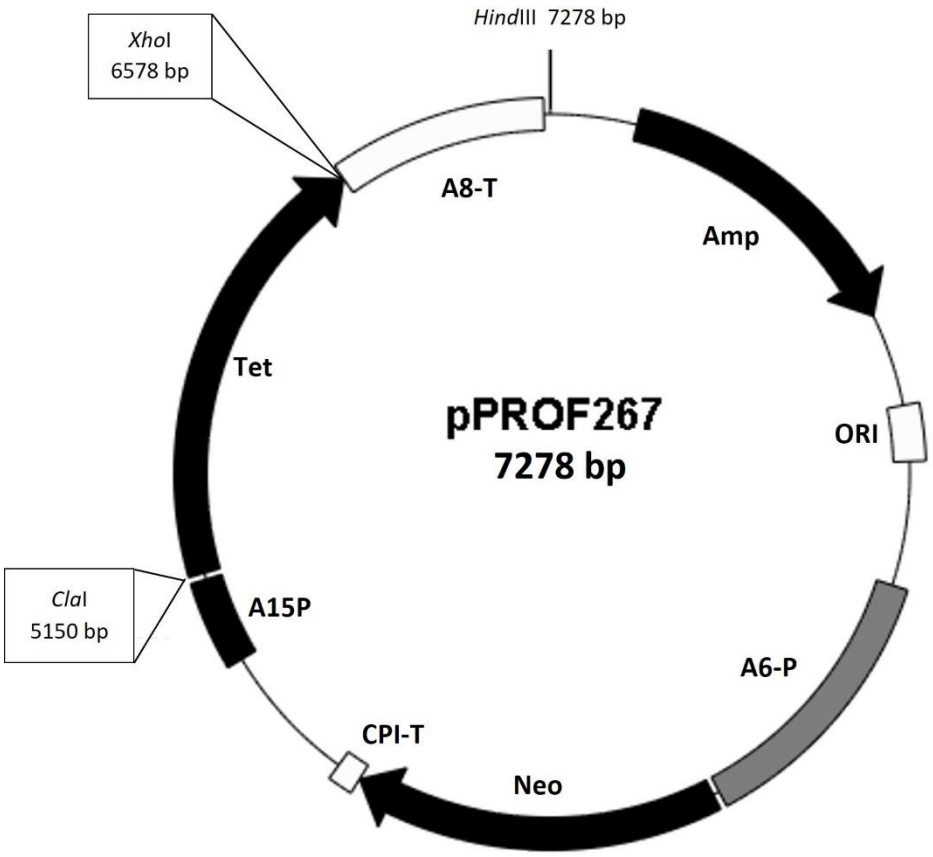


**Figure 2.2: Circular plasmid map of *D. discoideum* expression vector pPROF267.** pPROF267 was created by excising the GFP gene from pA15GFP using *Xho*I and *Cla*I and replacing it with a tetracycline cassette. The *tet* cassette was amplified by PCR from pPROF74 using primers that incorporated the additional enzyme sites (*Xho*I & *Cla*I)(Annesley, unpublished). The *Xho*I and *Cla*I restriction sites were used to excise the *tet* cassette and replace it with a copy of the full-length Tau coding sequence.

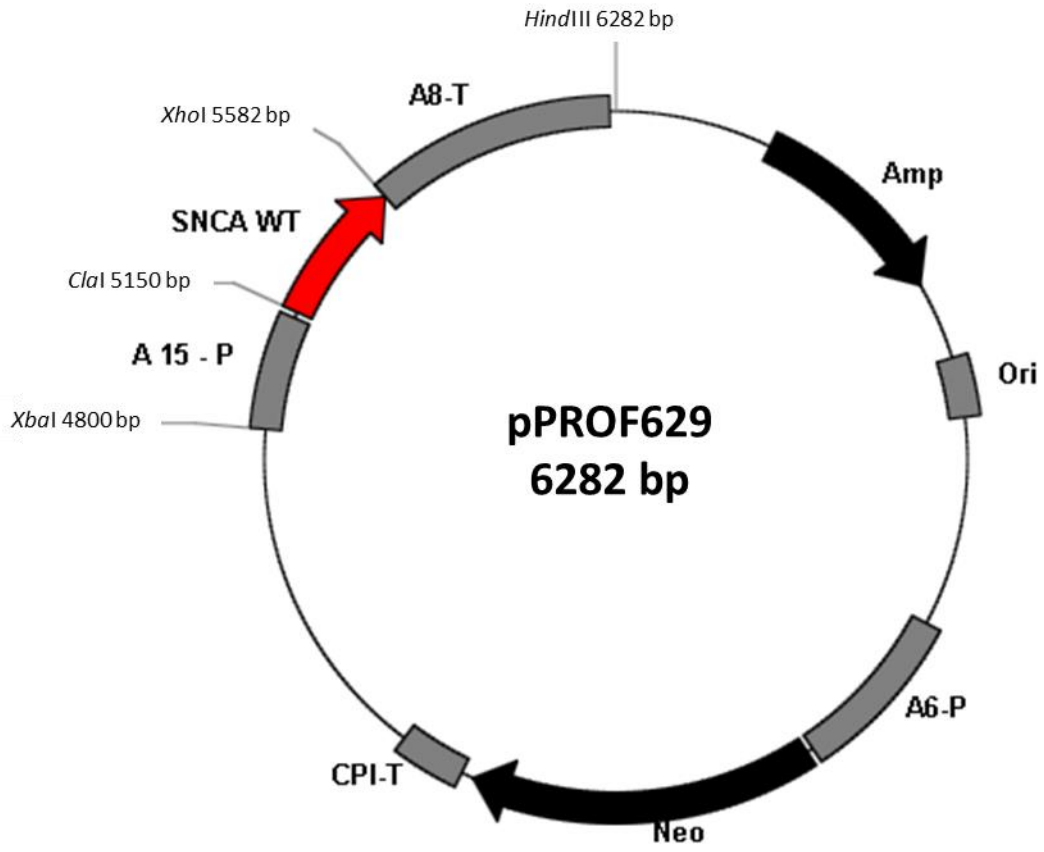


**Figure 2.3: Circular plasmid map of *D. discoideum* expression vector pPROF629.** pPROF629 was created by excising the GFP gene from pA15GFP using *Xho*I and *Cla*I and replacing it with the human α-synuclein gene (SNCA). pPROF629 contains a neomycin (Neo) resistance cassette under the control of the actin 6 promoter (A6-P) and an ampicillin resistance cassette (Amp) (Fernando et al., 2020).

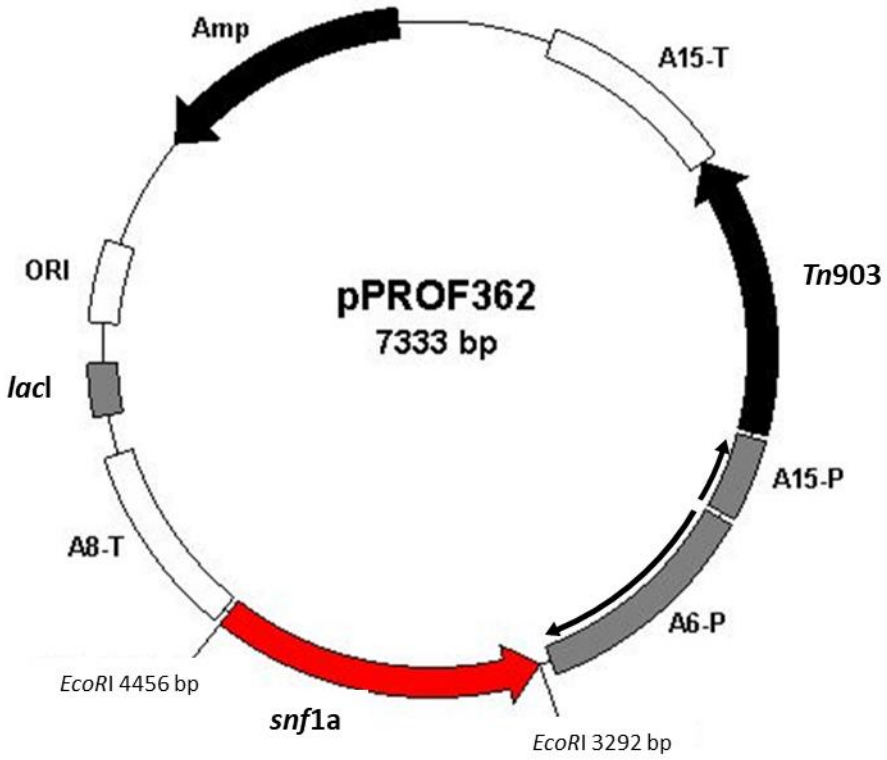


**Figure 2.4 Circular map of *Dictyostelium* construct pPROF362.**

The construct pPROF362 was created by cloning 1166 bp of *DdsnfA* (*snf*1a) into *D. discoideum* expression vector pDNeo2 at the *Eco*R1 site in the polylinker region in an antisense orientation. The expression is under the control of the *D. discoideum* actin-6 promoter (A6-P) and actin -8 terminator (A8-T). The construct contains an ampicillin resistance cassette (Amp) and a bacterial Tn903 neomycin resistance gene expressed under the control of the actin-15 promoter (A15-P) and transcription terminator (A15-T), providing G418 resistance (Bokko et al., 2007)

### 2.1.7 Growth and maintenance of bacterial and *D. discoideum* strains on solid and liquid medium

*Micrococcus luteus* and *Enterobacter aerogenes* were subcultured weekly onto SM agar plates containing geneticin (20 µg $ml^{-1}$) and *E. coli* B2 was subcultured on SM plates as needed. *E. coli* B2 and *E. aerogenes* were incubated overnight at 37˚C and *M. luteus* was grown at 21˚C for ~48 hr. All bacterial plates were stored at 4˚C for use within one week.

Transformed *D. discoideum* cells were grown axenically initially by inoculating 2-3 fruiting bodies (that were taken from transformants grown on SM plates) into 1 ml of HL-5 containing ampicillin (100 µg $ml^{-1}$), tetracycline (5 µg $ml^{-1}$), streptomycin (20 µg $ml^{-1}$) and geneticin (20 µg $ml^{-1}$) at 21˚C until they reached a cell density of 2-3 x $10^6$ cells $ml^{-1}$. Afterwards, *D. discoideum* was subcultured in HL-5 weekly both in a 24 well Nunc™ Costar Plate and on SM agar plates with 20 µg G418 $ml^{-1}$ and a lawn of *E. aerogenes* as a food source. The parental strain AX2 was also grown axenically in HL-5 and on lawns of *E. aerogenes* without the addition of geneticin.

### 2.1.8 Long term storage of *Dictyostelium* and bacterial strains

*Dictyostelium* strains were grown on SM plates with a lawn of *E. aerogenes* as a food source. Using a toothpick, amoeba were scraped from the edge of colonies and inoculated in 300 µl of *Dictyostelium* storage buffer in an Eppendorf tube. This was stored at -80 °C until required.

*E. coli* strains were grown in LB medium to an optical density of 0.5-0.6 at $OD_{600}$. Aliquots of 1 ml of culture were placed into Eppendorf tubes, pelleted and the supernatant removed. The pellet was resuspended in 100 µl of 10 % glycerol solution and stored at -80 °C.

## 2.2 Extraction of plasmid DNA

## 2.2.1 Large scale plasmid isolation

To extract large amounts of plasmid DNA, the Invitrogen PureLink™ HiPure plasmid kit was used according to the manufacturer's protocol. A single colony of *E. coli* containing plasmid was inoculated into 200 ml of LB containing ampicillin (100 µg $ml^{-1}$) and incubated at 37 ˚C overnight on a shaker. Cells were harvested by centrifugation at 4000 *x g* for 10 min using a Sorvall GSA rotor at 4˚C. Whilst harvesting, the HiPure Filter Maxi Column was equilibrated by applying 30 ml of Equilibration Buffer (EQ1) directly into the filtration cartridge inserted into the filter column.

The pellet was resuspended with 10 ml of Resuspension Buffer (R3) with RNase A until homogenous, then transferred into a 50 ml centrifuge tube. The cells were lysed with the addition of 10 ml of Lysis Buffer (L3) and mixed by inversion until homogenous, then incubated at RT for no longer than 5 min. Ten ml of Precipitation Buffer (N3) was added, mixed by inversion until homogenous and the precipitated lysate was then transferred into the equilibrated HiPure Filter Maxi Column. This filtered through by gravity flow for 10-15 min. To increase the final DNA yield, the residual bacterial lysate was washed with 10 ml of Wash Buffer (W8) and left to filter through by gravity flow. After the flow had stopped the inner Filtration Cartridge was removed and the Maxi Column washed with 50 ml of W8. This was left to drain by gravity flow and the flow through was discarded.

The PureLink™ HiPure Precipitator Module was used to elute the plasmid DNA. A sterile 50 ml elution tube was placed under the HiPure Filter Maxi Column, 15 ml of Elution Buffer (E4) was added to the column and allowed to drain by gravity flow. The column was discarded and 10.5 ml of isopropanol was added to the tube containing the eluted plasmid DNA and incubated at RT for 2 min. The PureLink™ HiPure Precipitator was attached to a 30 ml syringe in which the precipitated DNA was loaded and pushed through with the plunger using a slow and constant force. The flow through was discarded. Then 5 ml of 70 % (v/v) ethanol was added to the syringe and pushed slowly through the precipitator to wash the DNA. The flow through was discarded. The membrane was dried by passing air through the syringe twice. To elute the DNA, the precipitator was removed and attached to a 5 ml syringe in which 500 µl of TE buffer was added and pushed through into a sterile Eppendorf tube. A second elution was performed to ensure maximum recovery of the plasmid DNA. The eluted DNA was stored at -20˚C until needed.

### 2.2.2 Small scale plasmid isolation (alkaline lysis mini preps)

This method was used to extract small amounts of plasmid DNA and was adapted from Birnboim and Doly (1979) and Birnboim (1983). Three ml of LB containing ampicillin (100 µg $ml^{-1}$) was inoculated with a single *E. coli* colony containing plasmid and incubated overnight at 37 ˚C whilst shaking. A 1.5 ml aliquot of culture was pelleted by centrifugation and the pellet resuspended in 100 µl of resuspension buffer containing RNase A. 200 µl of NaOH/SDS solution was added to lyse the bacteria then neutralised with 150 µl of potassium acetate, mixed by inversion, causing the plasmid DNA to rapidly reanneal. This mixture was

centrifuged again to pellet cell debris and chromosomal DNA. The supernatant was transferred into a fresh Eppendorf tube containing 900 µl of absolute ethanol and incubated for 15 min at RT to precipitate plasmid DNA. The mixture was pelleted, then the pellet washed with 1 ml of 70 % (v/v) ethanol and dried in a Speed-vac on low speed for 10 min. This was resuspended in 20 µl of distilled $H_20$ and stored at -20 ˚C. The mini preps were screened using restriction enzyme digests with the appropriate enzymes to select for required clones (Section 2.3.1).

## 2.3 Gene Cloning Procedures

### 2.3.1 Restriction endonuclease digestion of DNA

Restriction endonuclease digestions were performed using the buffer recommended by the manufacturer or One-Phor-All buffer at 37 ˚C for 1-3 hr. The restriction enzymes were inactivated by the addition of 3 X SBE or 10 X blue juice (diluted to 1 x in the reaction). The digestion was then run on an agarose gel using electrophoresis (Section 2.3.2).

### 2.3.2 Agarose gel electrophoresis

Agarose gel electrophoresis was used for screening and for the purification of plasmid DNA. Gels of 1-2.5 % (w/v) agarose were prepared and immersed in 1 X TBE in an electrophoresis tank. A 1 kb Gene Ruler (Fermentas™ ) was used as a standard (500 µg $ml^{-1}$) and gels were electrophoresed at 100 mV for 2-4 hr. The DNA bands were observed using a UV transilluminator and then digitally documented with a AlphaDigiDoc™ RT camera.

### 2.3.3 Recovery of DNA from agarose gel

To recover DNA fragments of interest from an agarose gel, the PureLink™ Quick Gel Extraction Kit was used according to the manufacturer's instructions (Invitrogen™). The desired DNA was excised from the gel using a sterile blade, transferred into a 1.5 ml Eppendorf tube and weighed (≤ 400 mg of gel per tube was used). For ≤2 % agarose gel, 3 gel volumes of Gel Solubilization Buffer (L3) was added and dissolved using a heat block at 50 ˚C for at least 10 min. The tube was then incubated for an additional 5 min. For optimal DNA yields, 1 gel volume of isopropanol was added to the dissolved gel and mixed well. The DNA was purified by centrifugation through placing a Quick Gel Extraction Column inside of a wash tube and loading the gel mixture into the centre of the column. This was centrifuged at maximum speed for 1 min, then 500 µl of Wash Buffer (W1) containing ethanol was added and

recentrifuged for 1 min. The flow-through was discarded and the column spun again at maximum speed to remove any residual ethanol. The wash tube was then discarded and the column was placed into a recovery tube to which 30-50 µl of $dH_2O$ was added to the centre of the tube and incubated for 1 min at RT. This was recentrifuged at maximum speed for one minute to elute the purified DNA into the recovery tube. DNA was stored at 4˚C for immediate use or at -20 ˚C for long term storage.

### 2.3.4 Ligation of vector and insert DNA

For ligations, both vector and insert DNA were prepared by digesting with the appropriate enzymes in order to create complementary termini and were added to the ligation mix in a 1:3 ratio of vector to insert DNA. The ligations were generally performed in a 30 µl reaction volume containing 1.5 µl T4 DNA ligase and ligation buffer overnight at 16 ˚C.

For ligations involving the pCR2.1 TOPO vector a 1:4 (µl) ratio of vector to insert DNA was used and 1 µl of salt solution (200 mM NaCl; 10 mM $MgCl_2$) was added. As *Taq* polymerase adds a single adenosine (A) to the 3' end of PCR products to produce A overhangs, and the vector exhibits a single 3' thymidine (T) overhang, this allowed direct ligation of the vector with the insert DNA. The mixture was incubated at room temperature for 10 min. Ligations were microdialysed prior to transformations (Section 2.3.5).

### 2.3.5 Microdialysis

To maximise electroporation efficiency and avoid arcing due to high salt, the concentration of electrolytes from restriction and ligation buffers was reduced by microdialysis. The ligation mixtures were placed on Millipore type VS, filter paper (0.025 µM pore size) floating on $dH_2O$ for approximately 0.5-1 hr preceding electroporation.

### 2.3.6 DNA sequencing

DNA sequencing was performed by AGRF (Australian Genome Research Facility), Brisbane, QLD. Eppendorf tubes containing ~800 ng of plasmid DNA along with 100 pmol of the required forward or reverse primers were sent for sequencing.

## 2.4 PCR amplification of Tau gene fragment

### 2.4.1 Primer design

To amplify the entire tau gene, forward and reverse primers were designed and were synthesised by Gene Works Ltd. Each primer incorporated restriction sites to assist in cloning of the amplified gene product (Figure 2.3).

### 2.4.2 PCR reaction conditions

The polymerase chain reaction was used to amplify the tau gene *in vitro* using the specifically designed oligonucleotide primers. The reaction was carried out in a 0.5 ml Eppendorf tube in a total volume of 100 µl. The optimal conditions and reaction set up are listed in Table 2.4.

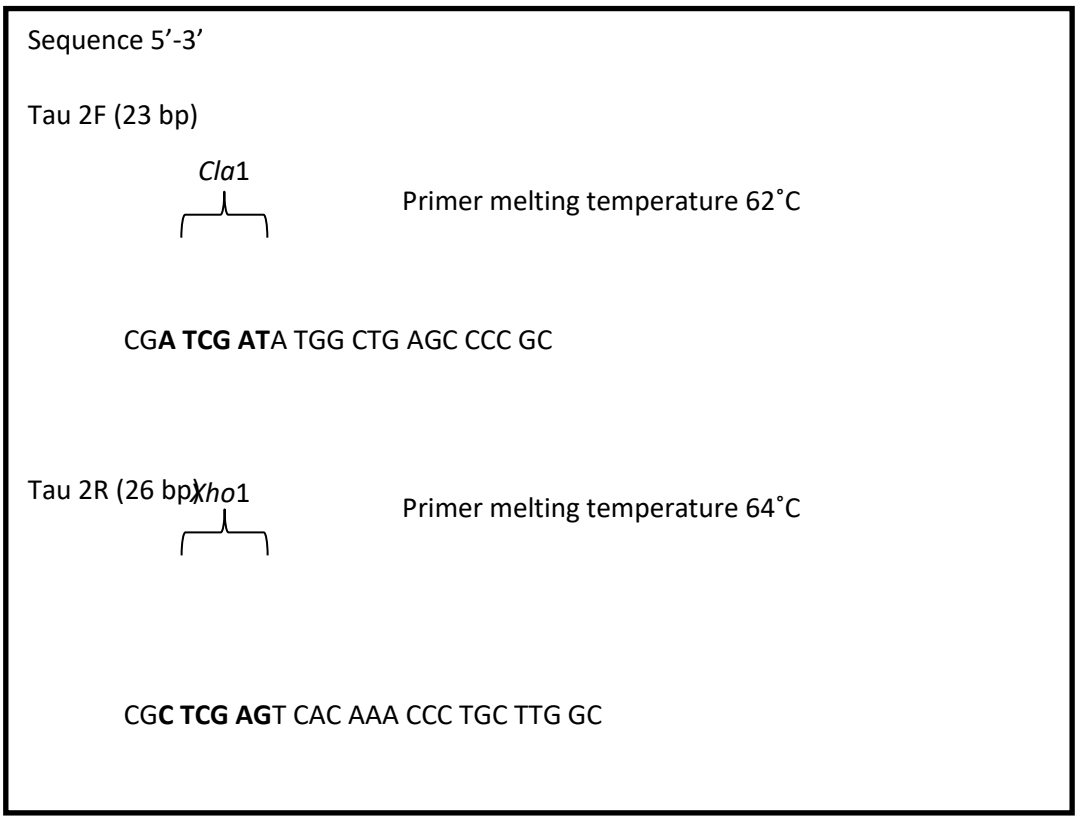


**Figure 2.5 Primer sequences for the amplification of tau insert.**

**Table 2.4 PCR components and reaction condition for amplification of tau.**

| **PCR components** | |
|---|---|
| 83 µl $dH_2O$<br>10 µl *Pfu*1 reaction buffer<br>2 µl dNTPs<br>1 µl Forward primer<br>1 µl Reverse primer<br>2 µl DNA (tau)<br>1 µl *Pfu*1 Taq polymerase<br><br>Total - 100 µl | |
| **PCR conditions** | |
| **Step** | **Temperature/duration** |
| Initial denaturation | 95˚C for 5 min |
| 35 cycles of | |
| Denaturation | 95˚C for 30 sec |
| Annealing | 55˚C for 30 sec |
| Elongation | 72˚C for 3 min |
| Final elongation | 72˚C for 7 min |

## 2.5 Transformation of *E. coli* cells with plasmid DNA

### 2.5.1 Preparation of electro competent cells

Electro competent *E. coli* strain DH5α cells was used for the electroporation of plasmid DNA. DH5α cells were treated using a method for maximum efficiency based on the described

process in Current Protocols of Molecular Biology (1989). One litre of LB was inoculated with 1/200 volume of a fresh overnight culture. The cells were then grown at 37 ˚C whilst shaking until this reached an optical density of 0.5-0.6 ($ABS_{600nm}$). The cells were harvested at 4,500 *x g* for 10 min in four GSA bottles in a GSA rotor at 4 ˚C. The cells were resuspended in 1 L of cold $dH_2O$ and centrifuged as previous, and then combined into two GSA bottles and resuspended in 0.5 litres of cold $dH_2O$ and centrifuged. Cells were then resuspended in ~20 ml of 10 % (v/v) glycerol and centrifuged again. The cells were resuspended to a final volume of 2-3 ml in 10 % (v/v) glycerol (to avoid cell damage by ice crystallisation) at a cell concentration of approximately 3 x $10^{10}$ cells $ml^{-1}$. Aliquots of 100 µl were dispensed into Eppendorf tubes and stored at -70 ˚C until required.

### 2.5.2 Electro transformation of *E. coli* competent cells

*E. coli* DH5α cells were transformed with plasmid DNA according to the following protocol adapted for Dower *et al.* (1988). An aliquot of 100 µl of DH5α cells in an Eppendorf tube were thawed at RT and placed on ice. About 10 µl of ligated plasmid DNA was microdialysed and added to DH5α cells. This was mixed well and placed on ice for approximately 1 min. The cells were transferred into a cold 0.2 cm Bio Rad *E. coli* Pulser cuvette and tapped to settle on the bottom. The cuvette was placed in the safety chamber and pulsed at 25 µF capacitance, 2.5 kV at a resistance of 200 Ω, the cuvette was immediately removed from the chamber and 1 ml of RT SOC medium was added to the cuvette and the cells were quickly resuspended with a pasteur pipette to maximize the recovery of transformants. The suspension was transferred into a polypropylene tube and incubated shaking at 37 ˚C for 1 hr, before 100-200 µl aliquots of serial dilutions from neat to $10^{-2}$ were plated onto LB agar plates containing ampicillin (100 µg $ml^{-1}$). These were incubated at 37 ˚C overnight.

### 2.5.3 Screening of *E. coli* transformants

Blue/white screening was used to detect positive clones in the pCR®2.1-TOPO vector. Serial dilutions from neat to $10^{-2}$ of transformed DH5α cells were spread onto LB plates (previously spread with X-gal (40 mg $ml^{-1}$)) containing ampicillin (100 µg $ml^{-1}$), at volumes of 50-100 µl. The plates were incubated at 37 ˚C overnight. Negative clones displayed as blue colonies, while white colonies indicated the insertion of DNA into the multiple cloning site resulting in the disruption of the lacZα gene.

## 2.6 Transformation of *D. discoideum* (AX2) cells

### 2.6.1 Transformation of AX2 with calcium chloride co-precipitate

The protocol for the transformation of AX2 with plasmid constructs by using calcium phosphate coprecipitation was adapted from Nellen et al. (1984) and was performed as follows. AX2 was grown in 50 ml of HL5 (Section 2.1.7) at 21 ˚C on an orbital shaker. Approximately 1-1.5 x $10^7$ cells were dispensed onto a 9 cm tissue culture dish (for each transformation) for the construct as well as for a negative and positive control and were allowed to adhere to the bottom of the dish for 30 min. The HL5 was then removed and replaced with 10 ml of MES-HL5 for 1.5-2.0 hr to equilibrate. During this time the DNA precipitate was made up in 1 x HBS. 600 µl of $dH_2O$ containing 12 µg of DNA (negative control contained only $dH_2O$) was added to 600 µl of 2 x HBS in a 1.5 ml Eppendorf tube. The DNA was precipitated with 76 µl of 2 M $CaCl_2$ which was slowly added drop wise to the solution while slowly vortexing for 10 sec. After 1 min the solution was again vortexed for 10 sec and incubated at RT for 25 min. The MES-HL5 was removed, 1.2 ml of DNA solution was added to each plate and incubated for 1 hr with occasional rocking to prevent cells from drying out then 10 ml of MES-HL5 medium was directly added to each dish and incubated for 4-6 hr. Following this, 2 ml of 15 % (v/v) glycerol solution in 1 x HBS was added and rocked gently to cover all cells. This was incubated for no more than 2 min, then the glycerol solution was carefully aspirated off the plate and 10 ml of standard HL5 medium was added and the cells were left to incubate at RT overnight.

### 2.6.2 Selection of *Dictyostelium* transformants on *M. luteus* lawns

Selection of G418 resistant *Dictyostelium* transformants was achieved on lawns of *Micrococcus luteus* as described by Wilczynska and Fisher (1994). Transformed cells prepared in Section 2.6.1 were resuspended in the HL5 medium with a pipette and 1 ml of suspension was inoculated onto 3 day old *M. luteus* lawns and suspended using a sterile glass spreader. These were left to incubate at 21 ˚C for 10-20 d during which the amoebae formed plaques. Amoebae from each plaque were subcultured onto *E. aerogenes* lawns using the flat edge of a sterile toothpick. The transformants were purified by streak dilution on *E. aerogenes* lawns on SM plates supplemented with 20 µg G418 $ml^{-1}$.

## 2.7 Isolation of genomic DNA and quantitative analysis of transformants

### 2.7.1 Isolation of genomic DNA using DNAzol®

The isolation of genomic DNA from *D. discoideum* cells was obtained using DNAzol®, a lysing solution that hydrolyses RNA and allows for the selective precipitation of DNA from cell lysates. Transformed and wildtype *D. discoideum* cells were grown axenically on an orbital shaker at 150 rpm and 21 ˚C and $10^7$ cells were harvested. One ml of DNAzol was added to the pellet, and the cells were lysed by repeated pipetting. Sedimentation of the homogenate was performed by centrifugation for 10 min at 10,000 *x g* at RT, then the resulting supernatant was transferred into fresh Eppendorf tubes. 500 µl of 100 % ethanol was added to each tube to precipitate the DNA from the lysate. The samples were mixed by inversion and incubated at RT for 10 min, then centrifuged at 10,000 *x g* for 5 min at RT to pellet the precipitated DNA. The pellet was then washed twice with 800 µl of 75 % (v/v) ethanol. The tubes were stored upright for 1 min to allow the DNA to settle to the bottom and the ethanol was removed and the DNA pellet air dried. DNA was resuspended in 30 µl MilliQ $dH_2O$.

### 2.7.2 Quantitative real time Polymerase Chain Reaction (qPCR)

To quantify the plasmid copy number of tau and α-synuclein constructs in transformants, qPCR was performed. Two calibration curves were prepared, one to estimate loading using genomic DNA of the wildtype AX2 (100 ng to 10 pg) and the filamin primers to estimate the total quantity of genomic DNA, and the second using purified plasmids and gene specific primers (Table 2.5) to determine the quantity of inserted plasmid constructs. For cotransformants a total of three calibration curves were prepared, including one for each of the plasmid constructs. The pPROF665 and/or pPROF629 constructs were used in serial dilutions ranging from 57 pg to $57^{-8}$ pg and 47 pg to $47^{-8}$ pg respectively in combination with primers to amplify tau and α-synuclein respectively. All measurements of nucleic acid concentrations were completed using Qubit® DNA dye in a Qubit® fluorometer (Invitrogen). Primers were designed using Primerquest software

(http://www.idtdna.com/Scitools/Applications/Primerquest/) and were synthesized by Geneworks.

**Table 2.5 Primer sequences for qPCR amplification.** This depicts the forward and reverse primers for the amplification of Filamin, tau and α-synuclein from AX2 and transformants.

| | |
|---|---|
| **Filamin Primers** | |
| Forward 5’ | CCACAGAGATATTGGAGTTGCGTACC |
| Reverse 5’ | CAACTCAACCAATGTGCCTGCCAA |
| **Tau Primers** | |
| Forward 5’ | AAGAGCACTCCAACAGCGGAAGAT |
| Reverse 5’ | GTGTCTCCAATGCCTGCTTCTTCA |
| **α-synuclein Primers** | |
| Forward 5’ | GCGCTCTAGAATCGATATGGATGTATTCATGAAAGGACTTTCAAAGGCC |
| Reverse 5’ | GCGCTCTAGACTCGAGTTAAGGATCCACAGGCATATCTTCCAGAATTCC |

PCR was carried out in a total volume of 20 µl containing 10 µl of 2 x SYBR Green Supermix (Bio-Rad). The amplification was performed using iCycler IQ Multicolor Real-Time PCR Detection System (BioRad). The optimal conditions and components used in the reaction are listed in Table 2.4 below.

**Table 2.6 qPCR amplification components and reaction conditions.**

| **qPCR components** |
|---|
| 7 µl MilliQ $H_20$ |
| 10 µl iQ™SYBR® Green Super-Mix (2x) (Bio-Rad®) |
| 1 µl Forward primer |
| 1 µl Reverse primer |
| 1 µl gDNA |
| Total - 20 µl |

| **qPCR conditions** | |
|---|---|
| **Step** | **Temperature/duration** |
| Initial denaturation | 95 ˚C for 3 min |
| 40 cycles of | |
| Denaturation | 95 ˚C for 30 sec |
| Annealing | 55 ˚C for 30 sec |
| Elongation | 72 ˚C for 30 sec |
| Final elongation | 72 ˚C for 3 min |

To calculate the number of copies of each gene the standard curves with known concentrations of DNA were used along with their threshold cycle ($C_t$) values. Estimates of the amount of DNA for each sample were calculated from the standard curves and represented as the starting quantity (SQ). Samples were duplicated and an average was calculated (SQ mean). The SQ mean for filamin gave an estimate of the total amount of gDNA and the following formula was used to calculate construct copy numbers.

Copy number = $\left(\frac{X}{Y}\right) \times \left(\frac{60\times10^6}{F}\right)$

X = quantity of DNA fragment of interest (ng)

Y = quantity of genomic DNA (ng)

F = amplified gene fragment size (bp)

60 x $10^6$ = *Dictyostelium* genome size (bp)

## 2.8 Protein Analysis

### 2.8.1 Preparation of protein samples

An aliquot of 1 x $10^7$ cells of *D. discoideum* wildtype and either tau or cotransformant strains were pelleted at maximum speed in a microcentrifuge for 2 min. The supernatant was removed and the pellet was resuspended in 75 µl of Laemmli 2x Sample Buffer (LSB). The samples were boiled for 10 min to denature the proteins and put into a -20 ˚C freezer for 1 min. Samples were then spun for 15 sec to remove any condensation.

Mini-PROTEAN®TAX™ pre-cast gels of 10-15 % (w/v) agarose were used to separate the proteins. The gel was positioned in a Mini-tetra protein tank in 1 x TGS running buffer. 15 µl of each protein sample was loaded onto a gel with 15 µl of prestained protein ladder (in order to assess the molecular weights of proteins). The gel was electrophoresed for 30-45 min at 200 V or until the protein ladder had sufficiently separated.

### 2.8.2 Western Blot

Upon completion of electrophoresis, gels were transferred to mini format 0.2 µm PVDF membranes using a Trans-Blot® Turbo™ transfer pack in a Bio-Rad Trans-Blot®Turbo at a high molecular weight setting of 1.3 A at 25 V for 10 min.

### 2.8.3 Detection of proteins

Once transfer was complete, the membrane was washed twice with 1 X TBS for 10 min at RT before the non-specific sites on the membrane were blocked by incubating the membrane at RT for 1-2 hr in blocking buffer (5 % skim milk in TBS buffer) on an orbital shaker at high speed. The membrane was washed 3 x in TBS-Tween buffer (10 mM TrisCl, 500 mM NaCl, 0.05 % (v/v) Tween-20 in $dH_20$). To detect tau, membranes were incubated with mouse monoclonal anti-tau antibody [Tau-5] (Abcam, Cambridge, UK ab80579) (1:2000), to detect α-synuclein membranes were incubated with mouse monoclonal anti-alpha-synuclein antibody [syn211] (Abcam, Cambridge, UK ab80627) (1:2000) and to detect phosphorylated tau membranes were incubated with rabbit monoclonal recombinant anti-tau (phosphor S404) antibody [EPR2605] (Abcam, Cambridge, UK ab92676) (1:500). Mouse β-actin antibody (1:2500) was used as a loading control. All antibodies were diluted in blocking buffer and incubated on a high speed orbital shaker at 4˚C overnight. The membrane was washed 3 x in TBST for 10 min to remove any unbound primary antibody. The membranes were then incubated with (goat)

anti-mouse or anti-rabbit cross-adsorbed secondary antibody Alexa-Fluor™ 647 (Thermo Fisher, Waltham, MA, USA, A32728) (1:1000) diluted in blocking buffer and covered with aluminium foil for 1 hr at RT (and remained covered during the remaining steps). The membrane was washed 2 x in TBST and once with 1 x TBS before viewing results. The Storm 860$^{TM}$ fluoroimager (Amersham Biosciences) was used to visually detect proteins. β-actin was used in order to quantitate the amount of protein present in each sample as levels of β-actin are known to be reasonably consistent between *D. discoideum* cells.

## 2.9 Immunofluorescence

### 2.9.1 Preparation of microscope slides with *D. discoideum* cells

*D. discoideum* transformed and wildtype cells were grown axenically to a density of 2-3 x $10^6$ cells $ml^{-1}$ (Section 2.1.7) and then transferred onto sterile coverslips in six-well Costar plates (Nunc$^{TM}$). The cells were allowed to settle for 30 min before the media was replaced with Lo-Flo HL-5 for 1 hr to equilibrate the cells. The media was aspirated off and the coverslips rinsed in PBS then cells were fixed with the addition of prechilled (-20 ˚C) methanol/acetone solution (1:1), left at -20 ˚C for 10 min and again rinsed in PBS.

### 2.9.2 Immunofluorescence assay and microscopy

The coverslips were then removed from the wells and inverted onto 30 µl of mouse monoclonal anti-tau antibody [Tau-5] (Abcam, Cambridge, UK ab80579) or a combination of Tau-5 and rabbit monoclonal anti-alpha + beta synuclein antibody [EP1646Y] (Abcam, Cambridge, UK ab51252) diluted (1:100) in blocking buffer (1 % (w/v) bovine serum albumin (BSA) and 1 % (v/v) cold-water fish skin gelatin) in PBS on parafilm for 1 hr. Coverslips were then placed back into wells (cell side up) and rinsed in PBS with 0.1 % (w/v) BSA twice for 5 min before again being removed and placed onto 30 µl of secondary antibody (goat anti-mouse Alexa-Fluor594 (Molecular Probes$^{TM}$ Invitrogen$^{TM}$) or a combination of Alexa-Fluor594 and (goat) anti-rabbit Alexa-Fluor-488 conjugated IgG antibody (Thermo Fisher, Waltham, MA, USA, A11034) for cotransformants, diluted (1:500) in PBS with 1 % (w/v) BSA on parafilm and left to incubate for 45 min in the dark. The coverslips were placed back into the wells, rinsed once and washed twice for 5 min in PBS, then DAPI diluted (1:1000) in PBS was added and incubated for 5 min. The cells were rinsed in PBS then in MilliQ $H_2O$ after which the coverslips were drained and mounted onto a microscope slide with Ultramount No 4 (Fronine Laboratory Supplies) and left to dry for 4 hr or overnight before visualisation. The cells were

detected on an Olympus (Shinjuku City, Tokyo, Japan) BX61T fluorescent microscope and images were digitally captured with the use of an Olympus DP80 camera.

### 2.9.3 Duolink®In Situ

To detect protein interactions using IF techniques, the Duolink® system was used as per manufacturer's instructions. *Dictyostelium* transformed and wildtype cells were axenically grown to a density of 2-3 x $10^6$ cells $ml^{-1}$. Coverslips were lined with a Mini PAP pen (Invitrogen™) to create a 1 $cm^2$ area. Coverslips were then put into a six well Costar plate (Nunc™) had 200 µl of cells dispensed onto them and left to settle for 30 min. Cells were rinsed in PBS and fixed using 300 µl of 1:1 methanol acetone and incubated at -20 ˚C for 10 min. Coverslips were rinsed with PBS before beginning the Duolink® protocol.

The protocol suggested using a humidity chamber for the entirety of the experiment, this was achieved in wells using wet paper towel moulded into the bottom of the plate. The reaction volume used for each reaction was 40 µl.

Two drops of blocking solution was added to each coverslip and incubated at 37 ˚C for 30 min. Primary antibody (AB) was diluted in AB diluent. Cells were stained in combinations using mouse monoclonal anti-tau antibody Tau-5, rabbit monoclonal anti-tau antibody (E178) (Abcam, Cambridge, UK ab32057), rabbit monoclonal anti-alpha + beta synuclein antibody [EP1646Y] and mouse monoclonal anti-alpha-tubulin antibody [12G10] (developed by Frankel & Nelsen, Developmental Studies Hybridoma Bank, created by the NICHD of the NIH and maintained at The University of Iowa, Department of Biology, Iowa City, IA 52242). The blocking solution was aspirated off and 40 µl of primary AB solution was added onto coverslips and incubated at RT for 1 hr. PLA probes (+ and -) were diluted 1:5 in AB diluent. In some experiments the secondary AB Alexa-fluor 488 was also added into the solution to visualise tubulin. This was achieved by making a 1:4 dilution in AB diluent and then 1 µl of this was added into PLA probe solution. The primary AB solution was aspirated off and the coverslips were washed 2 x 5 min in wash buffer A. The PLA solutions were added, incubated at 37 ˚C for 1 hr and covered to exclude light. The ligation stock solution was diluted 1:5 in MQ $H_2O$ (keeping in mind that ligase also needs to be added to the 40 µl reaction e.g. 8 µl ligation stock, 31 µl MQ $H_20$, then 1 µl ligase). Coverslips were washed in wash buffer A, 2 x 5 min, ligase was removed from the freezer and immediately added to ligation solution, vortexed and added to each sample. Samples were incubated at 37 ˚C for 30 min in the dark. The

amplification stock was diluted 1:5 in MQ $H_2O$ (taking into account later addition of polymerase 0.5 µl). Ligase was tapped off coverslips and washed 2 x 2 min in wash buffer A. Polymerase was added to the amplification solution and then onto each sample and incubated for 100 min at 37 ˚C. The amplification solution was tapped off and coverslips washed in 1 x wash buffer B for 2 x 10 min and once in 0.01 % wash buffer B for 1 min. Slides were air dried before being mounted using the minimal amount of mounting media containing DAPI (provided in kit). Coverslips were sealed with nail polish and viewed and digitally captured as in Section 2.8.2. Protein-protein interactions were observed (as red dots) indicating a proximity of the targets within 40 nm.

## 2.10 Phenotypic analysis of transformants

### 2.10.1 Qualitative Phototaxis

Qualitative phototaxis and quantitative photo- and thermo-taxis were performed as previously described (Annesley and Fisher, 2009b). Non nutrient charcoal agar plates were inoculated in two adjacent spots with amoebae of each strain. This was performed by scraping the edge of *D. discoideum* plaques growing on *E. aerogenes* lawns (using the flat edge of a sterile toothpick) and spotting onto the charcoal media. The plates were then transferred into dark polyvinylchloride (PVC) boxes with a 4 mm hole located on one side to provide a single lateral light source. The boxes were kept at 21 ˚C in the same orientation with a constant light source for 48 hr. During this time the amoebae consumed the remaining *E. aerogenes* and began to starve initiating a chemotactic response leading to the aggregation of cells and formation of a multicellular slug. The slugs migrated towards the light source through an extracellular matrix leaving behind a trail which was transferred to PVC discs, to be stained (Section 2.9.3) and digitised (Section 2.9.4).

### 2.10.2 Quantitative phototaxis and thermotaxis

Mass plates were produced for each strain by inoculating SM plates with 0.1 ml each of amoebal suspension (~2 x $10^6$ cells $ml^{-1}$) and *E. aerogenes* suspension. When clearing of the plates had begun, cells were harvested (2-3 plates per strain) and pooled into 50 ml of cold SS in a Falcon tube. Cells were spun at 2,000 *x g* in a benchtop centrifuge at 4 ˚C for 5 min. The supernatant was removed and the cells were washed 4 more times in this way to remove bacteria. After the final wash the supernatant was removed and the pellet was vortexed to ensure even distribution of amoebae, this was the 100 % concentration. To calculate the exact

cell density a 1:1000 dilution of the pellet was made in cold SS and a haemocytometer was used to count cells.

For phototaxis experiments dilutions of 80, 60, 40, 20, 10 and 5 % were made in SS. 20 µl of these cell suspensions were plated onto duplicate charcoal agar plates in a 1 $cm^2$ area in the middle of the plate. For the 10 % and 5 % dilutions, 4 and 6 plates were used to plate cells to ensure enough slugs formed for analysis. Plates were left to dry completely before transfer into PVC boxes with a single 4 mm hole light source and incubated at 21 ˚C for 42-48 hrs. The slug trails of AX2 wildtype and transformants were transferred to PVC discs and stained (Section 2.10.3).

For thermotaxis experiments, cells were diluted to a 30 % density and 10 µl of this suspension was plated onto a 1 $cm^2$ area in the centre of 16 water agar plates. Plates were allowed to dry before placing them into PVC boxes with no light source. These were then placed on a heat bar producing a 0.2 °C $cm^{-1}$ temperature gradient at the agar surface. Plates were placed in duplicate at arbitrary temperature points from 1-8 with T1 corresponding to 14 °C and increasing in 2 °C increments to reach 28 °C at T8. Slug trails of AX2 wildtype and transformants were transferred to PVC discs and stained (Section 2.10.3).

### 2.10.3 Staining slug trails on PVC discs using Coomassie brilliant blue

PVC discs (85 mm diameter and 0.02 mm thick) were pressed onto the charcoal agar plates following the phototaxis and thermotaxis assays making sure all air bubbles were removed so as not to disrupt the adhesion of slug trails. The discs were carefully removed using tweezers and visually observed to validate that the slug trails had transferred to the discs. These were then placed face down into a glass dish containing Coomassie blue in ethanol/acetic acid/water at a ratio of 5:1:4. The discs were left to stain for 5 min, and then removed and rinsed under a running tap to remove the excess stain. The discs were air dried and then slug trails were digitally analysed (Section 2.9.4).

### 2.10.4 Digital analysis of slug trails

Slug trails of AX2 and transformed strains were digitised using a Summagraphics MM1201 digitizing tablet linked to a SUN workstation. The qualitative digitizing was performed as described by Darcy *et al* (1994a) by tracing entire slug trails with a light source at 0 ˚. Trails were plotted from the site of inoculation to give an overall impression of the transformants

phototactic response and compared with wildtype AX2. For quantitative phototaxis and thermotaxis only the beginning and end points of the slug trails were digitized. The directions of slug trails were analysed using directional statistics, to determine the accuracy of orientation towards the light source.

### 2.10.5 Plaque expansion on bacterial lawns

*D. discoideum* wildtype and transformed cells were scraped from the edge of plaques growing on *E. aerogenes* lawns (using a toothpick) and transferred to the centre of normal agar plates containing lawns of *E. coli* B2 as a food source. Plates were incubated at 21 °C. The diameter of plaque expansion due to the clearing of bacteria by the amoebae was measured once 24 hr after inoculation, then twice daily over a period of approximately 100 hr. The plaque expansion rate (mm $hr^{-1}$) for each strain was calculated using the statistical computing and graphics software program "R" by linear regression.

### 2.10.6 Growth rates in liquid

*D. discoideum* cells were axenically grown in 10 ml of HL-5 until exponential phase was reached. From these cultures, 50 ml of HL-5 in a 250 ml conical flask was inoculated with 1 x $10^4$ cells $ml^{-1}$and the density was verified using a haemocytometer. Cells were grown with shaking at 150 rpm at 21 ˚C and cell cultures were counted twice each day over a period of 100 hr. The generation times (gens/hr) of each strain was calculated in R by log linear regression during exponential growth phase.

### 2.10.7 Fruiting body morphology

*D. discoideum* cells were grown on SM agar plates containing a lawn of *E. aerogenes* (Section 2.1.7) at 21 ˚C for 5-7 d. This period of time allowed for the differentiation of the cellular slime mould into a multicellular fruiting body which was observed under an Olympus S761 dissecting microscope. Photographs were taken from above the plates at different magnifications (2x and 4x) to get an overall view of the populations as well as side view pictures of singular fruiting bodies. This was obtained by slicing out a thin section of agar and placing it on its side so that the entire fruiting body could be seen. The images were captured using a digital Moticam 2300TM camera.

### 2.10.8 Phagocytosis

The *E.coli* DsRed strain was used to measure bacterial uptake in *D. discoideum* wildtype and transformants. This strain contains a construct encoding a pink fluorescent protein known as DsRed (Maselli et al., 2002).

*E. coli* DsRed was streak diluted onto 3-4 LB plates containing 100 $\mu g^{-1}$ ml ampicillin and grown at 37 ˚C for approximately 3 days or until cells were visibly pink. The cells were harvested from plates and resuspended in approximately 20 ml of cold 20 mM phosphate buffer.

*D. discoideum* strains were grown in parallel in HL5 media at 21 ˚C until exponential phase was reached. Cells were counted and harvested to a density of 6 x $10^6$ cells and resuspended in 1.2 ml of phosphate buffer. Then, 1 ml of this suspension was transferred to a scintillation vial and cells were starved for 30 min at 21 ˚C with shaking.

Meanwhile, duplicate 10 ml Falcon tubes were prepared for $T_0$ and $T_{30}$ time points with 3 ml of 20 mM phosphate buffer supplemented with 5 mM sodium azide and left on ice. After 30 min, 1 ml of the *E.coli* DsRed suspension was added to each *D. discoideum* sample, mixed and immediately 400 µl of cell suspension was transferred into each of the duplicate $T_0$ tubes and placed on ice. The scintillation vials were returned to the shaker at 21 ˚C for 30 min after which 400 µl of cell suspension was transferred into each of the duplicate tubes at $T_{30}$ and incubated on ice.

For each time point cells were pelleted for 2 min at 2,000 *x g*, supernatant was removed and cells were washed again with 3 ml of 20 mM phosphate buffer containing 5 mM sodium azide to remove the surface bound *E. coli* cells, then pelleted as previous. For the final wash the pellet was resuspended in 20 mM phosphate buffer only, cells were counted and cells were pelleted as previous. The supernatant was discarded and the pellet resuspended in 2 ml of 0.25 % Triton-X-100 in 100 mM $Na_2HPO_4$ and vortexed to lyse cells immediately before measuring fluorescence. The hourly rate of bacterial consumption was determined by measuring fluorescence at both time points using a Special Module (530 nm excitation and 580 nm emission) in a Modulus Fluorometer (Turner Biosystems, Sunnyvale, CA, USA). The increase in fluorescence over 30 min, the amoebal density and the fluorescence signal per million bacteria (separately determined) were used to calculate the rates of bacterial consumption.

### 2.10.9 Macropinocytosis

Macropinocytosis was determined by measuring the rate of uptake of Fluorescein Isothiocyanate (FITC)-dextran (Klein and Satre, 1986). *D. discoideum* strains were grown axenically for 2-3 days in HL5 at 21 ˚C. Cells were harvested to a density of 1 x $10^7$ cells and resuspended in 1 ml of HL5 and transferred to a scintillation vial. Cells were starved for 30 min at 21 ˚C and shaking. Concomitantly, duplicate 10 ml Falcon tubes for $T_0$ and $T_{70}$ were prepared and incubated on ice containing 3 ml of Sorensen phosphate buffer (17 mM). After 30 min FITC dextran (Sigma-Aldrich, St. Louis, MI, USA, average mol. mass 70 kDa) was added to the cell suspension at a concentration of 2 µg $ml^{-1}$ (100 µl of a 20 mg $ml^{-1}$ in HL5), samples were mixed and 200 µl was immediately removed and transferred to the duplicate $T_0$ tubes on ice. Scintillation vials were returned to the shaker at 21 ˚C for 70 min after which 200 µl of suspension was transferred to the $T_{70}$ tubes on ice.

All samples were centrifuged at 2,000 *x g* for 2 min to pellet cells, supernatant was discarded and the pellet resuspended in cold Sorensen buffer and recentrifuged as previous. The supernatant was discarded and the pellet was resuspended in 3 ml of Sorensen buffer. The cells were counted using a haemocytometer and remaining cells were pelleted as previous. After this final wash the supernatant was removed and 2 ml of 0.25 % Triton-X-100 in 100 mM $Na_2HPO_4$ was added to lyse cells. Immediately after the fluorescence was measured in the Modulus Fluorometer using the Green Module (525 nm excitation and 580–640 nm emission). The hourly rate of uptake of the medium was calculated using a calibration curve relating to fluorescence signal to volume of fluorescence medium, the cell density and the increase in fluorescence over 70 min.

### 2.10.10 *Legionella* infection assay

*Legionella pneumophila* infection and proliferation rates in *D. discoideum* was measured as previously described (Francione et al., 2009) and was adapted from Hagele et al. (2000) and Otto et al. (2004). Wildtype and transformant strains were grown to exponential phase axenically in HL5 at 25 °C with shaking. Cells were pelleted, washed twice in Sorensen 1x C buffer (17 mM $KH_2PO_4/Na_2PO_4$, 50 µM $CaCl_2$, pH 6.0) at 600 *x g* for 3 min and resuspended in modified broth (MB) medium at 5 x $10^5$ cells $ml^{-1}$. Each suspension was aliquoted into 5 wells of a 96 well tissue culture plate to a final density of 1 x $10^5$ cells to be used at a series of time

points (0, 24, 48, 72 & 96 hr) along with a negative control of only MB, and allowed to adhere for 30 min at 21°C.

The *L. pneumophila* strains used were derivatives of the pathogenic Corby strain (Mampel et al., 2006) and grown on buffered charcoal yeast extract (BCYE) agar containing 5 µg $ml^{-1}$ chloramphenicol at 37°C with 5 % $CO_2$ atmosphere for 3 days. After this time, the bacteria were harvested and resuspended in distilled water and used to infect the *D. discoideum* strains at a multiplicity of infection (MOI) of 1:1. This was achieved by reading the absorbance of the bacterial suspension at $OD_{600}$ and the approximated concentration of bacteria was determined using Table A6.1 (Appendix 6). Initial adherence of the *L. pneumophila* to *D. discoideum* cells was performed by centrifugation at 1,370 *x g* for 10 min. At each time point 50 µg $ml^{-1}$ gentamycin sulphate was added to each well for 30 min to kill the extracellular *L. pneumophila.* Then cells were resuspended and pelleted at 13,000 *x g* for 12 min in a microcentrifuge, washed twice and resuspended in Sorenson 1 x C buffer. The cells were lysed with 0.02 % (w/v) Saponin and vortexed vigorously to release the intracellular *L. pneumophila*. A 10-fold dilution series of the harvested bacteria was prepared up to 1000-fold for the first two time points and from $10^{-1}$ to $10^{-5}$ for time points 48 hrs and over. This was plated onto BCYE agar plates and incubated at 25-26 °C with 5 % $CO_2$ for 7 days in order to determine the colony-forming units (c.f.u.).

**2.10.11 Seahorse respirometry**

Mitochondrial respiration of *D. discoideum* wildtype and transformed strains were measured using the Seahorse Extracellular Flux Analyser (Seahorse Biosciences, North Billerica, MA, USA) as described previously (Lay et al., 2016). A combination of drugs were used in sequential order to measure the Oxygen Consumption Rate (OCR) of specific elements of mitochondrial respiration (10 µM DCCD (N,N0-dicyclohexylcarbodimide, an ATP synthase inhibitor (Sigma-Aldrich, St. Louis, MI, USA), 10 µM CCCP (carbonyl cyanide 3-chlorophenol hydrazone, a protonophore (Sigma-Aldrich, St. Louis, MI, USA)), 20 µM rotenone (Complex I inhibitor (Sigma-Aldrich, St. Louis, MI, USA)) and either 10 µM antimycin A (Complex III inhibitor (Sigma-Aldrich, St. Louis, MI, USA)) or 1.5 mM BHAM (benzohydroxamic acid, alternative oxidase (AOX) inhibitor (Sigma-Aldrich, St. Louis, MI, USA)). To do this, axenically grown *Dictyostelium* were harvested and washed, then resuspended in SIH medium (Formedium, Hunstanton, Norfolk, United Kingdom) supplemented with 20 mM sodium pyruvate and 5

mM sodium malate (pH 7.4). Each strain to be analysed was plated into 8 wells of an assay plate for the Seahorse XFe24 Flux Analyser (Seahorse Biosciences, North Billerica, MA, USA). The wells were precoated in Matrigel and the cells were left to settle for 30 min. Measurement cycles consisting of 3 min mix, 2 min wait and 3 min measurement time were completed before and after each sequentially added drug, at least three cycles per condition was performed. For each condition there were 8 replicates of a strain except the last condition in which either BHAM or Antimycin A were added to 4 replicate wells. The wildtype AX2 was included as a control in every experiment in 4 replicate wells, and 2 each for the final condition of BHAM and Antimycin A. From the measurements taken before and after the addition of the pharmacological agents averages of the Basal OCR, maximum CCCP-uncoupled OCR, respiration dedicated to ATP synthesis, respiration from sources other than the mitochondria, Complex I and Complex II dedicated respiration and proton leak were able to be calculated.

## 2.11 Proteomics

### 2.11.1 Whole Cell Proteomics

For proteomic analysis each sample (5 x $10^6$ cells in 100 µl of PBS) was prepared for analysis by the La Trobe University Comprehensive Proteomics Platform according to the following protocol: Cell pellets were dissolved in digestion buffer (8 M urea, 50 mM $NH_4HCO_3$, 10 mM dithiothreitol) and incubated at 25 °C for 5 h. Iodoacetamide (IAA) was added to a final concentration of 55 mM and incubated for 35 min at 20 °C in the dark to alkylate thiol groups. The preparation was then diluted to 1 M urea in 25 mM ammonium bicarbonate (pH 8.5) and sequencing-grade trypsin (Promega) was added to a ratio of 1:50 (wt/wt) to the sample and incubated for 16 h at 37 °C. The digests were acidified with 1 % (v/v) trifluoroacetic acid (TFA), dried in a SpeedVac centrifuge followed by a desalting step on SDB-XC StageTips (Empore, SDB-XC reversed-phase material, 3M, St. Paul, USA). Briefly: digested proteins were resuspended in 100 µL of 1 % (v/v) formic acid and centrifuged at 14,000 rpm for 2 min. The solid-phase extraction was performed according to Rappsilber et al. (2007) with the following modifications: the membrane was conditioned with 50 µL of 80 % (v/v) acetonitrile, 0.1 % (w/v) trifluoroacetic acid, and then washed with 50 µL of 0.1 % trifluoroacetic acid before the tryptic peptides were bound to the membrane. The bound peptides were eluted by 50 µL 80 % (v/v) acetonitrile, 0.1 % (w/v) trifluoroacetic acid, and dried in a SpeedVac centrifuge.

Peptides reconstituted in 0.1 % TFA and 2 % acetonitrile (ACN) were loaded using a Thermo Scientific™ UltiMate™ 3000 RSLCnano system onto a trap column (C18 PepMap 300 µm ID × 2 cm trapping column, Thermo-Fisher Scientific) at 15 µl $min^{-1}$ for 6 min. The valve was then switched to allow the precolumn to be in line with the analytical column (Vydac MS C18, 3 µm, 300 Å and 75 µm ID × 25 cm, Grace Pty. Ltd.). The separation of peptides was performed at 300 nl $min^{-1}$ at 45 °C using a linear ACN gradient of buffer A (water with 0.1 % formic acid, 2 % ACN) and buffer B (water with 0.1 % formic acid, 80 % ACN), starting at 5 % buffer B to 45 % over 105 min, then 95 % buffer B for 5 min followed by an equilibration step of 15 min (water with 0.1 % formic acid, 2 % ACN). Data were collected on an Orbitrap Elite (Thermo-Fisher Scientific) in Data Dependent Acquisition mode using m/z 300–1500 as MS scan range, CID MS/MS spectra were collected for the 10 most intense ions performed at a normalized collision energy of 35 % and an isolation width of 2.0 m/z. Dynamic exclusion parameters were set as follows: repeat count 1, duration 90 sec, the exclusion list size was set at 500 with early expiration disabled. Other instrument parameters for the Orbitrap were the following: MS scan at 120,000 resolution, maximum injection time 150 ms, AGC target $1 \times 10^6$ for a maximum injection time of 75 ms with AGT target of 5000.

The spectra obtained from the instrument were used to search against *Dictyostelium* database (February 2018), together with common contaminants using the Mascot search engine (Matrix Science Ltd., London, UK. Briefly, carbamidomethylation of cysteines was set as a fixed modification, acetylation of protein N-termini, methionine oxidation was included as variable modifications. Precursor mass tolerance was 10 ppm, product ions were searched at 0.5 Da tolerances, minimum peptide length defined at 6, maximum peptide length 144, and peptide spectral matches (PSM) were validated using Percolator based on q-values at a 1 % false discovery rate (FDR).

**2.11.2 Quantification and Statistical Analysis**

Proteomics data was analysed using Scaffold (Proteome Software) before exporting data to Excel for further analysis. Proteins detected in fewer than 5 samples were excluded from analysis. Intensity-Based Absolute Quantitation abundance values were normalised for each set of transformants to the mean total abundance of the parental strain AX2. Data was exported to Excel in which genes/proteins were assigned to one of either two groups on whether they were significantly up or significantly down compared to the WT using the p-

values of a two sample t-test. Gene enrichment in biological functions and cellular components associated with these resultant gene lists were determined in FunRich software using hypergeometric analysis and Bonferroni method to gain p-values. Lists were also entered into the STRING database for a visual representation and false discovery rates of biological processes.

# 3.0 RESULTS

## 3.1 Introduction

Tau is a MT associated protein that predominantly occurs in neurons where it aids in assembly and stability of MT, subsequently supporting axonal transport (Cleveland et al., 1977; Kosik, 1993). It does this through the mechanism of phosphorylation; when dephosphorylated it binds to MT, and phosphorylation promotes the disassociation of tau with MT (Cleveland et al., 1977; Lindwall and Cole, 1984). Further hyperphosphorylation results in the accumulation of the tau protein into aggregates, an indication of neurodegeneration (Grundke-Iqbal et al., 1986). Although the predominate feature of the accumulated protein in tauopathies is pathological tau, other neurological proteins associated with neurodegeneration have been found colocalised in these aggregates. One of these proteins is α-synuclein, a protein also highly expressed in neurons, mainly at presynaptic terminals (Iwai et al., 1995; Jakes et al., 1994). Often the aggregation of tau and α-synuclein coincides with mitochondrial dysfunction. In the case of tau, hyperphosphorylation and overexpression can lead to impaired axonal transport of the mitochondria as well as effecting mitochondrial dynamics and bioenergetics impacting the health of neurons (Eckert et al., 2014). Mitochondrial disease has been well characterised in *D. discoideum* with a clear set of phenotypes (Annesley and Fisher, 2009a; Francione et al., 2011). These were attributed to the chronic activation of energy sensing protein AMP-activated protein kinase (AMPK) (Bokko et al., 2007) which when knocked down, returned affected phenotypes to wildtype levels (Francione et al., 2009).

To establish whether tau is cytotoxic to *D. discoideum* and whether this organism can be used as a model to study tauopathies *D. discoideum* cells were transformed with an expression vector to allow ectopic expression of tau. This chapter will describe the localisation of the protein, its ability to be phosphorylated by *Dictyostelium* kinases and the phenotypic consequences of tau expression in this model system. *D. discoideum* cells were also transformed with tau and α-synuclein combined to assess any differences in phenotypes with the co-expression of these proteins. Phenotypic analysis indicated a possible mitochondrial dysfunction with the expression of tau, so aerobic respiration was measured directly. Finally, to gain an understanding of the underlying cellular processes contributing to phenotypic abnormalities, whole cell proteomics was performed.

The outcomes of these tests help to establish that tau is correctly expressed in *Dictyostelium* and is phosphorylated by *D. discoideum* kinases. Tau interacts with both tubulin and α-synuclein, and tau expression results in defective phenotypes similar to that of mitochondrially diseased cells.

## 3.2 Expression of tau alone and the coexpression with α-synuclein

### 3.2.1 PCR amplification of the tau gene and cloning into *E. coli* and *Dictyostelium* expression vectors.

There are 6 tau isoforms expressed in the human brain, the longest of these is 2N4R which contains both exons 2 and 3, and four repeats of the MT binding domain (Figure 1.1). There is no tau homolog endogenously expressed in *D. discoideum* and as such individual isoforms can be expressed without endogenous expression of other tau isoforms. For this project, a cloned copy of isoform 2N4R was commercially purchased from Add gene (plasmid #16316) and used as a gene template in constructing a *Dictyostelium* tau expression construct. The tau gene was amplified using synthesized primers that incorporated new *Xho*I and *Cla*I restriction cut sites to the 5' and 3' ends respectively of the PCR product for use in downstream cloning. The PCR product was initially cloned into the *E. coli* vector pCR2.1TOPO to produce pPROF664 and verified by restriction digest using *Xho*I and *Cla*I (Figure 3.1). Subsequently, the tau insert was subcloned into a *D. discoideum* expression vector by replacing the existing tetracycline cassette in pPROF267. The *Dictyostelium* vector has highly AT-rich regions that are prone to recombination by insertions and deletions in *E. coli*. Therefore, the 2-step cloning process increases cloning efficiency and reduces difficulties in cloning poorly cut PCR product into the *Dictyostelium* vector. The tau construct was verified by DNA sequencing performed at AGRF. The resultant clone was called pPROF665. Restriction digestion using *Cla*I/*Xho*I and internal cut sites *Hin*dIII and *Sac*I were performed to confirm successful subcloning of the tau gene (Figure 3.2).Page Break

Page Break

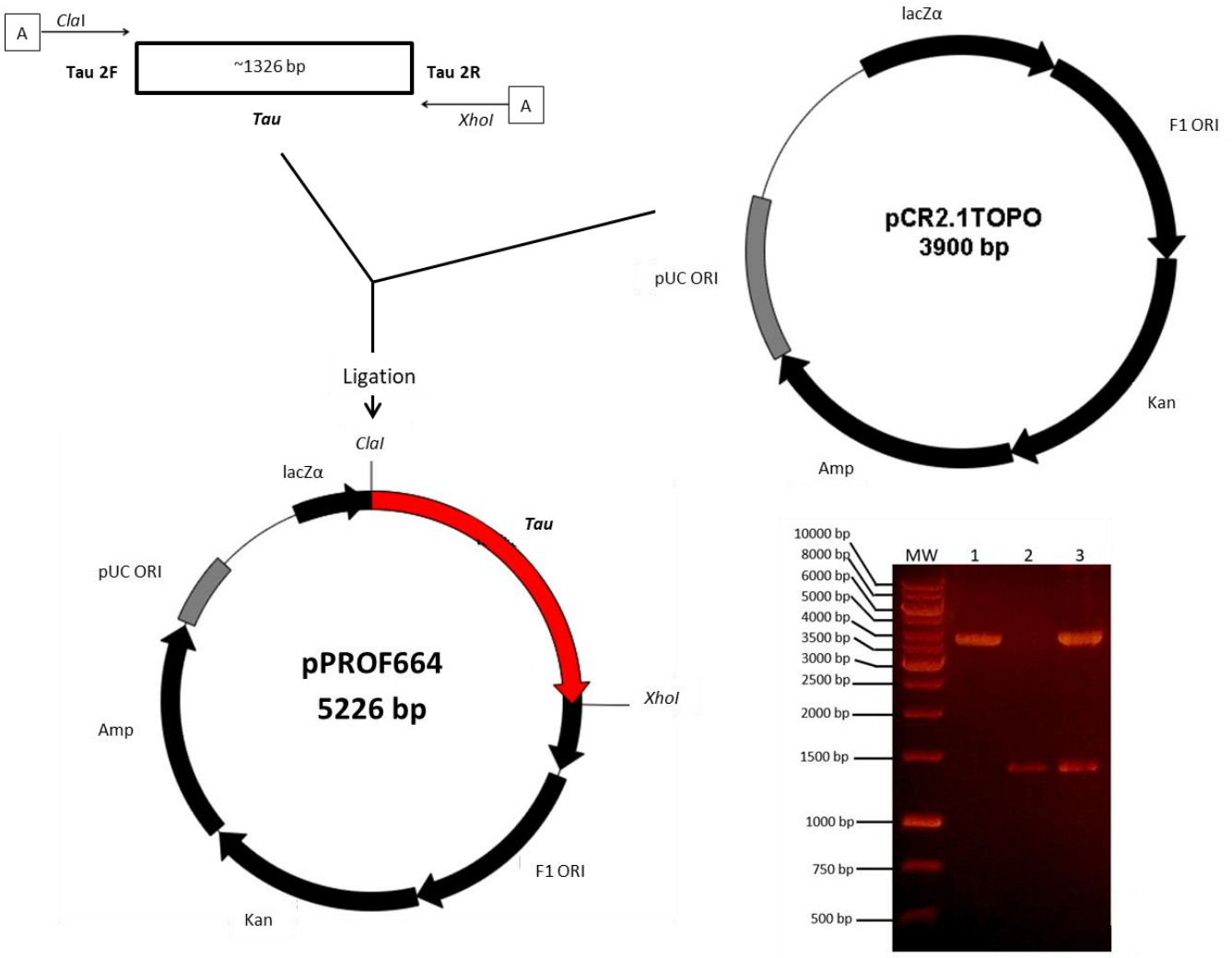


**Figure 3.1 Cloning of tau insert into pCR®2.1-TOPO vector to create pPROF664**. The human tau gene was PCR amplified with Taq polymerase which produces A overhangs. This was cloned into the pCR2.1TOPO vector which allows direct insertion of the PCR product as it comprises 3' T overhangs. The resulting plasmid was named pPROF664. Restriction digest reactions were run on a 1 % agarose gel at 100 V for 2.5 hr. The gel shows the linearized vector in Lane 1, the tau insert in Lane 2, and verification of pPROF664 using restriction enzymes *Xho*I and *Cla*I to release the cloned tau insert. Predicted band size of the cloning vector is 3900 bp and the tau insert 1326 bp.

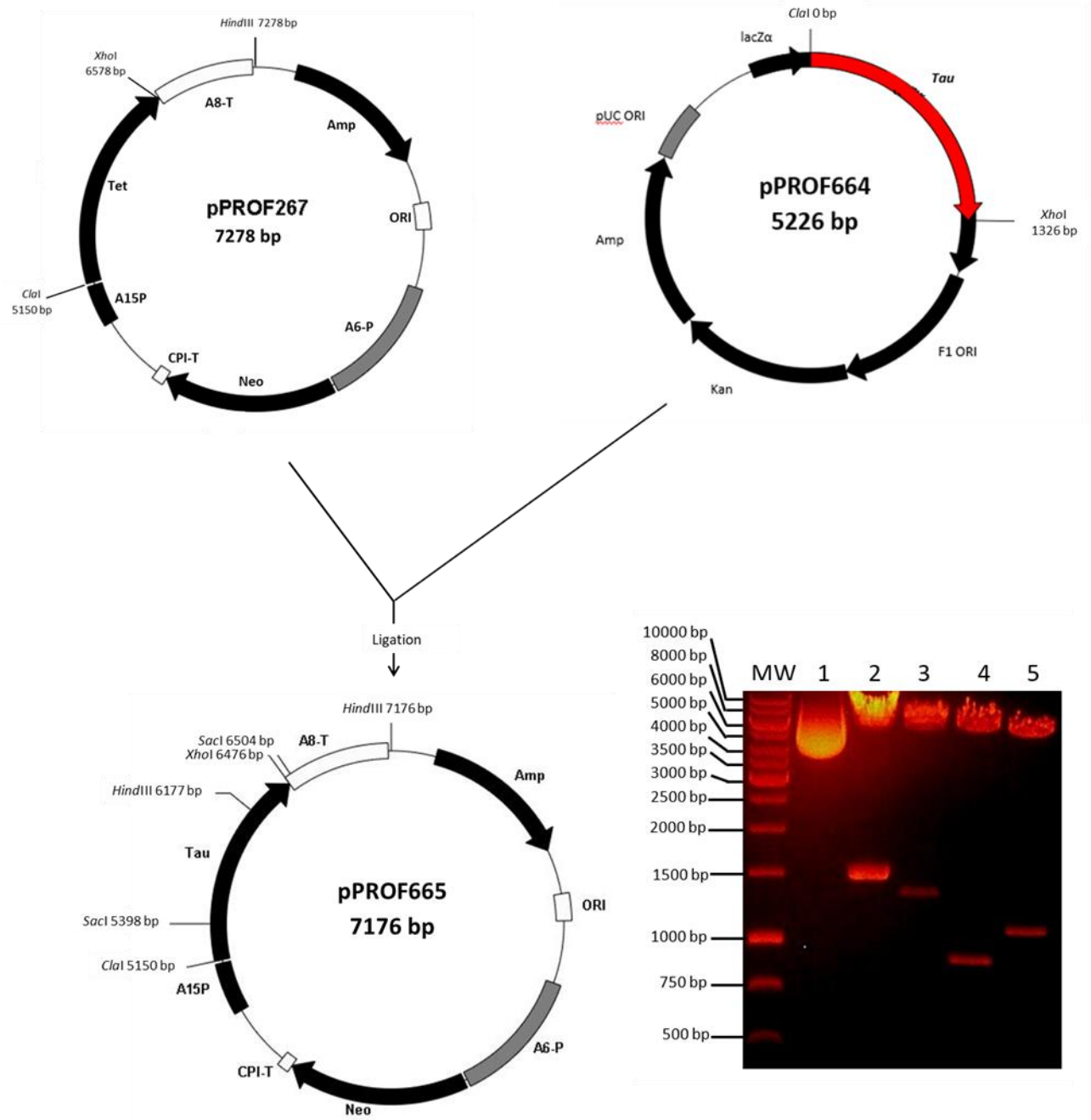


**Figure 3.2 Subcloning of tau insert into *Dictyostellium* vector pPROF267 to create pPROF665**. The tau insert was excised from pPROF664 and subcloned into a *D. discoideum* expression vector pPROF267 by replacing the tet cassette, resulting in pPROF665. Restriction digest reactions were run on a 1 % agarose gel at 100 V for 2.5 hr. The gel shows Lane1: circular plasmid DNA of pPROF267, Lane 2: restriction digest of pPROF267 with *Xho*I and *Cla*I to reveal pPROF267 backbone (5850 bp) and release of tet cassette (1428 bp), lane 3: confirmation of pPROF665 construct via digestion with *Xho*I and *Cla*I to produce pPROF267 backbone (5850 bp) and tau insert (1326 bp), Lanes 4 & 5: verification of pPROF665 using internal restriction sites of *Hin*dIII (predicted band sizes 6177 bp & 999 bp) and *Sac*I (predicted band sizes (5348 bp and 1106 bp).

### 3.2.2 Transformation of *D. discoideum* with plasmid constructs

To generate transformants expressing tau singularly and in combination with α-synuclein, the plasmids pPROF665 (tau) and pPROF629 (α-synuclein) were transformed into *D. discoideum* cells by the calcium chloride coprecipitation method (Section 2.6.1). Transformants were isolated under selection of G418 on lawns of *Micrococcus luteus*. The plasmid expression constructs enter the *D. discoideum* genome through rolling circle replication, this results in transformants each with a varying number of copies of the construct and therefore different expression levels.

In order to verify the number of copies of inserted constructs in each strain, qPCR was performed (Section 2.7.2), and to detect the expression of tau and α-synuclein in the transformants, western blots were performed. To detect tau, a tau mouse monoclonal (tau-5) antibody (Abcam®) was used and to detect α-synuclein a mouse monoclonal α-synuclein (syn211) antibody (Abcam®) was used. Expression of tau was detected in all tau single transformants and in the tau/α-synuclein cotransformants, with a visible band at 69 kDa. α-synuclein expression was detected with a band visible at 18 kDa in all cotransformants. Western blots with a sample of tau transformants and cotransformants can be seen in Figure 3.3A and 3.3B respectively.

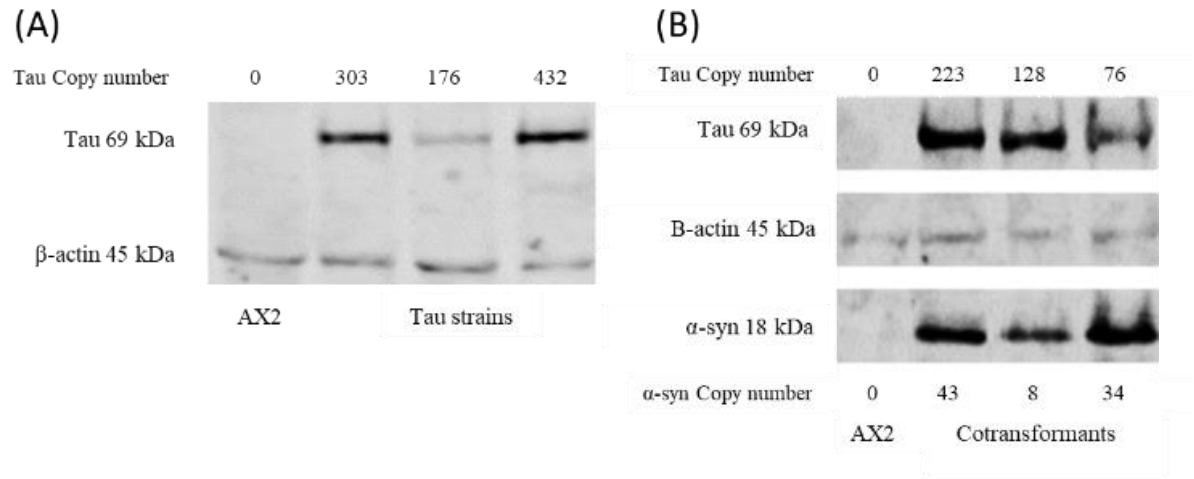


**Figure 3.3 Expression of tau and α-synuclein in *D. discoideum*. (A)** Human tau can be expressed in *D. discoideum*. A western blot showing the expression of the tau protein in *D. discoideum*. The parental strain AX2 was used as a negative control and β-actin as the loading control. Tau construct copy numbers as estimated by qPCR are indicated at the top of the figure. **(B)**. Tau can be expressed in combination with α-synuclein in *D. discoideum*. A western blot showing the expression of both tau and α-synuclein in cotransformant strains. The parental strain AX2 was used as a negative control and β-actin as the loading control. Construct copy numbers are displayed for both tau and α-synuclein. tau runs at 69 kDa while α-synuclein runs at 18 kDa.

### 3.2.3 Human tau can be is phosphorylated in *D. discoideum*

Tau is phosphorylated by a number of kinases and phosphorylation is important for its normal role in MT stability and also in disease pathways. In normal circumstances tau binds on and off MT depending on the phosphorylation state of the protein. Phosphorylation causes tau to disassociate from MT while regained affinity to bind to MT occurs with dephosphorylation (Cleveland et al., 1977; Lindwall and Cole, 1984). Further hyperphosphorylation of the protein leads to aggregation and the pathological conformations of tau seen in the tauopathies (Grundke-Iqbal et al., 1986). As phosphorylation is a major factor in the accumulation of the tau protein, it was important to determine whether it could be phosphorylated in *Dictyostelium*. *D. discoideum* has homologues of many of the kinases that phosphorylate tau in the human brain such as AMPK and glycogen synthase kinase 3 (GSK3). To detect tau phosphorylation a rabbit monoclonal recombinant anti-tau (phosphor S404 [EPR2605]) antibody (Abcam®) was used. As evident in Figure 3.4, human tau is phosphorylated at least at residue S404 in *D. discoideum.*

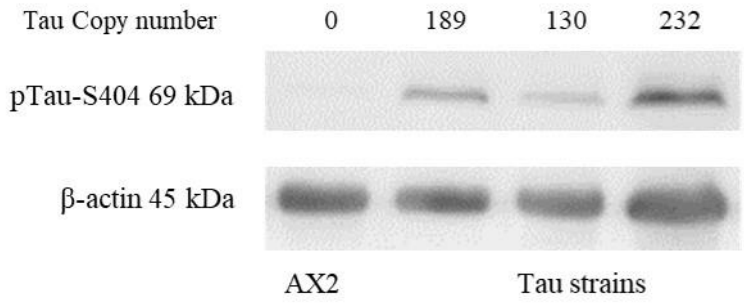


**Figure 3.4 Tau is phosphorylated in *D. discoideum***. One of the phosphorylation sites implicated in pathological accumulation and aggregation of the tau protein is S404 (Augustinack et al., 2002). An antibody against phosphorylation at this site was used and indicated that tau can be phosphorylated in *D. discoideum*. Construct copy numbers are displayed at the top of each lane. β-actin was used as the loading control and the parental strain AX2 as the negative control.

## 3.3 Localisation of tau and α-synuclein in *D. discoideum cells.*

### 3.3.1 Tau is localised throughout the cytoplasm in *D. discoideum* whereas α-synuclein is localised to the cortex.

In humans, tau is prodominantly found in axons of neurons where it binds to and stabilises MT (Binder et al., 1985; Drubin and Kirschner, 1986; Kosik and Finch, 1987; Mandell and Banker, 1996; Migheli et al., 1988). To visualise the localization of tau in *D. discoideum* immunofluorescence microscopy was performed (Section 2.9.2). Tau was detected using an anti-tau antibody coupled with Alexa-Fluor 594-conjugated secondary antibody which immunolabels tau with red fluorescence. Tau was observed throughout the cytoplasm of the cell (Figure 3.5A). α-synuclein had previously been seen to localise to the cortex of the cell in *D. discoideum* and was also the case here (Fernando et al., 2020). To detect α-synuclein and tau in the cotranformants anti-tau and anti-α-synuclein antibodies were coupled with Alexa-Fluor 594 and 488-conjugated secondary antibodies respectively. In the cotransformants tau was again located throughout the cytoplasm and α-synuclein (immunolabelled with green fluorescence) was seen primarily at the cortex (Figure 3.5B). From these results, it was unclear whether there was colocalisation at the cortex and hence further investigation was required.

### 3.3.2 Do tau and α-synuclein colocalise in *D. discoideum?*

Tau and α-synuclein have been found to colocalise in many neurodegenerative diseases where they may enhance the pathological process of the other protein. Evidence suggesting a possible interaction between these two proteins is found with the colocalisation of tau and α-synuclein in pathological aggregates in diseased brains (Arima et al., 2000; Hamilton, 2000; Iseki et al., 1999; Ishizawa et al., 2003; Lippa et al., 1999). To investigate whether tau and α-synuclein colocalise within *D. discoideum*, proximity ligation assays (PLA) were performed using the Duolink™ *in situ* protein-protein interaction detection assay (Section 2.9.3). This assay allows for the detection of protein-protein interactions within 40 nm. The mouse anti-tau antibody and rabbit anti-α-synuclein primary antibodies were bound by secondary antibodies coupled with oligonucleotides (PLA probes). If the proteins were within 40 nm of each other the PLA probes would be ligated with connector oligos, resulting in a closed, circular DNA template. This is amplified by DNA polymerase and complementary oligos coupled to fluorochromes then hybridised to repeat sequences in the amplicons. Fluorescence microscopy was then used to visualise protein-protein interaction, and positive interactions were observed as discrete red dots. Tau and α-synuclein were found to colocalise at the cortex of the cell where α-synuclein was primarily concentrated (Figure 3.5C).

### 3.3.3 Does human tau and α-synuclein interact with *D. discoideum* tubulin?

In humans, tau binds to microtubules aiding in their assembly and stability and supporting axonal transport. To determine whether tau interacts with tubulin in *D. discoideum* the Duolink™ detection assay was again used. This time using a mouse-anti-tubulin primary antibody and rabbit-anti-tau or anti-α-synuclein antibodies. As microtubules are dynamic and diverse within the cell, an additional Alexa-Fluor 488 conjugated secondary antibody was added in with the proximity probes in order to visualise tubulin and aid in the observation of the interactions. Tau was seen to localise with tubulin throughout the cytoplasm of the cell (Figure 3.5.D). Tubulin and α-synuclein were also seen to colocalise, however this interaction was seen at the cortex of the cell where α-synuclein is primarily located (Figure 3.5.E).

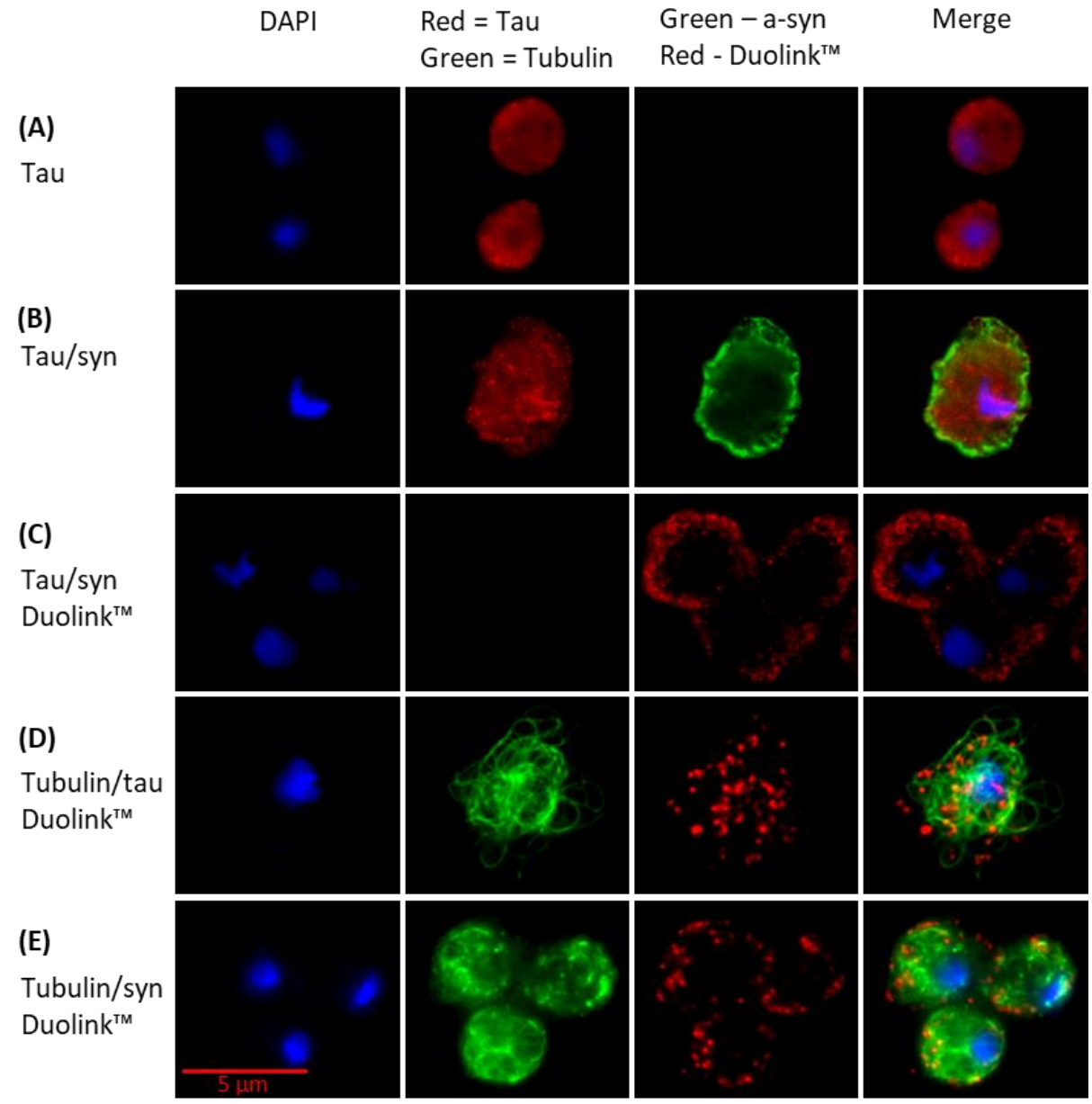

**Figure 3.5. Human tau and α-synuclein can interact with *D. discoideum* tubulin and each other**. In *D. discoideum* tau localises throughout the cytoplasm of the cell while α-synuclein concentrates at the cortex. The colocalization of the two proteins takes place at the cortex of the cell where α-synuclein is most concentrated. **(A)** Tau was detected in the tau transformant using an anti-tau primary antibody and observed using Alexa-Fluor 594 conjugated secondary antibody. **(B)** α-synuclein was detected using an anti-α-synuclein antibody and visualised using Alexa Fluor 488 conjugated secondary antibody along with tau detection in the cotransformant. **(C)** To view colocalization of tau and α-synuclein the cotransformants were stained with mouse anti-tau antibody and rabbit anti-α-synuclein antibody, the protein-protein interaction was observed (as red dots) using secondary proximity probes, anti-rabbit MINUS and anti-mouse PLUS in the Duolink™ in situ detection kit (Sigma-Aldrich). To visualise colocalization of tau or α-synuclein with tubulin Duolink™ was again used, this time using a mouse-anti-tubulin primary antibody and rabbit-anti-tau or anti-α-synuclein antibodies. An additional Alexa-Fluor 488 conjugated secondary antibody was added in with the proximity probes in order to visualise tubulin. **(D)** tau colocalised with tubulin throughout the cytoplasm of the cell. **(E)** The colocalization of tubulin and α-synuclein occurred at the cortex of the cell where α-synuclein is most abundant.

## 3.4 Phenotypic analysis – is there evidence of a mitochondrial defect?

Both tau and α-synuclein have been implicated in mitochondrial dysfunction in neurodegeneration. As mitochondrial disease has been well characterised in *D. discoideum,* a phenotypic analysis was performed on transformants to determine if there was any evidence of a mitochondrial defect in these strains. In *D. discoideum*, mitochondrially diseased strains exhibit a clear set of phenotypes, these being decreased growth both on bacterial lawns and in axenic medium, defective slug phototaxis, increased susceptibility to *Legionella* proliferation and aberrant fruiting body morphology with shorter and thicker stalks when compared to the parental strain AX2. This allowed for the comparison with tau and cotransformant strains to determine if a possible defect in the mitochondria was present.

### 3.4.1 Fruiting body morphology

Loss of a food source induces chemotaxis among unicellular *D. discoideum* leading to aggregation and multicellular development culminating in the development of a fruiting body consisting of a sorus of spores atop a slender stalk. Fruiting body morphology previously seen in α-synuclein expressing strains resembles that of the parental strain AX2 (Fernando et al., 2020). The expression of tau however produces an abnormal stalk (shorter and thicker) with enlarged basal disc when compared to the parental strain. Cells in the stalk and the basal disc have undergone a programmed cell death and the result suggests that expression of tau increases the number of cells entering this pathway. This phenotype was also observed in *D. discoideum* strains characterised as mitochondrially diseased. The strains expressing both tau and α-synuclein have a larger sorus and thicker stalk, suggesting that they form larger aggregates.

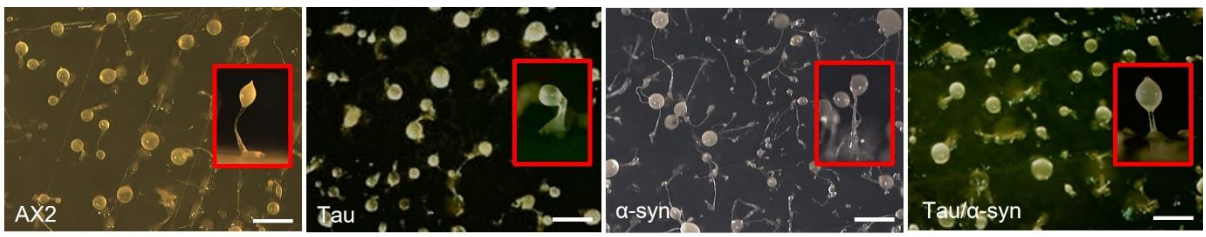


**Figure 3.6. Tau negatively affects fruiting body morphology.** Fruiting body morphology by AX2, strains expressing tau and α-synuclein singularly and coexpression of the two proteins (tau/α -syn). Tau strains produce an abnormal stalk which is shorter but thicker and an enlarged basal disc when compared to the parental strain. The α-synuclein strains resemble that of the parental strain AX2 (Fernando et al., 2020). The strains expressing both tau and α-synuclein have a thicker stalk and larger sorus suggesting that these strains produce larger aggregates than AX2. Aerial view of plates with insets showing the side view of a single representative fruiting body of each strain. Scale bar indicates 1 mm.

### 3.4.2 Phototaxis and Thermotaxis

#### 3.4.2.1 Qualitative Phototaxis

Prior to culmination into a fruiting body the aggregated amoebae can form a motile slug which is phototactic and thermotactic enabling it to migrate and find more favourable conditions in which to form the fruiting body. As the slugs migrate, they leave behind a trail of collapsed slime sheath providing visual evidence of their migration paths. Defects in the photosensory pathway have been observed repeatedly in mitochondrially diseased *D. discoideum* and it has been suggested to be sensitive to alterations in energy production (Francione et al., 2011). To determine if tau alone and in combination with α-synuclein have any effects on the accuracy of phototaxis reminiscent of mitochondrially diseased cells, qualitative phototaxis (section 2.10.1) was performed (Figure 3.7).

In agreement with previous studies WT α-synuclein expressing strains exhibited no phototaxis defect when compared with the wildtype (Fernando et al., 2020). The tau strains displayed a mild defect in accuracy of phototaxis which was more severe in the strains expressing both tau and α-synuclein. This was independent of copy number. The increased severity of the phototaxis defect when both tau and α-synuclein were expressed together hints at a functional interaction between the two proteins. This is consistent with yeast models of a synergistic relationship between the two proteins, with enhanced defects when both proteins are expressed (Ciaccioli et al., 2013).

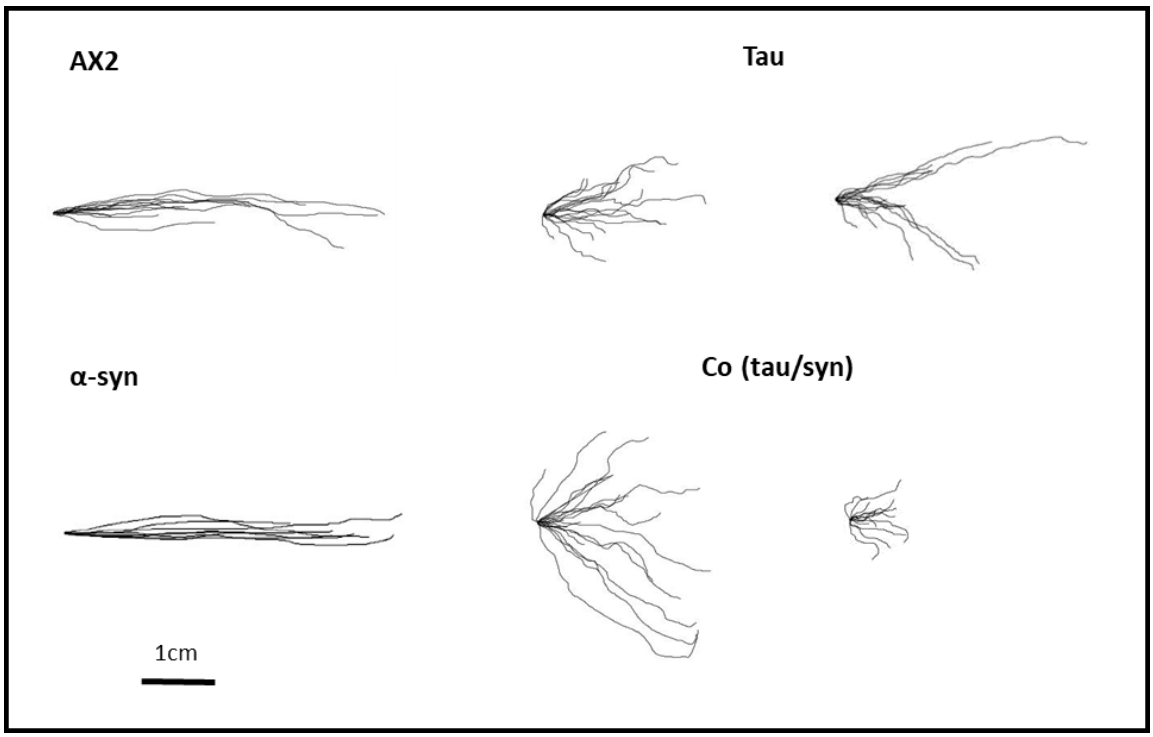


**Figure 3.7. Tau causes an impairment in phototaxis which is enhanced by the coexpression with α-synuclein.** *D. discoideum* slugs migrate towards the light source at the right of the figure. Slug trails of WT AX2, tau, α-synuclein and cotransformants (tau/syn) were stained, traced and digitised. Strains expressing α-synuclein showed no defect in phototaxis when compared to WT. Tau strains exhibited a reduced accuracy of phototaxis which was enhanced by the coexpression with α-synuclein. There was no copy number effect on any of these strains. Scale bar represents 1 cm compared to the trails.

### 3.4.2.2 Quantitative Phototaxis

As the qualitative phototaxis results suggested a defect in the tau strains which was enhanced by the co-expression of α-synuclein, quantitative phototaxis was performed to determine the degree of this impairment (Section 2.10.2). Accuracy of phototaxis was measured and plotted against cell density. The α-synuclein expressing strains again resemble the parental strain AX2 with similar accuracies of phototaxis at all densities (Fernando et al., 2020) (Figure 3.8.B). The tau strains showed a defect in the accuracy of phototaxis at all cell densities when compared to AX2 which was enhanced by the coexpression with α-synuclein (Figure 3.8.A). This was confirmed by a multiple regression analysis (Figure 3.9).

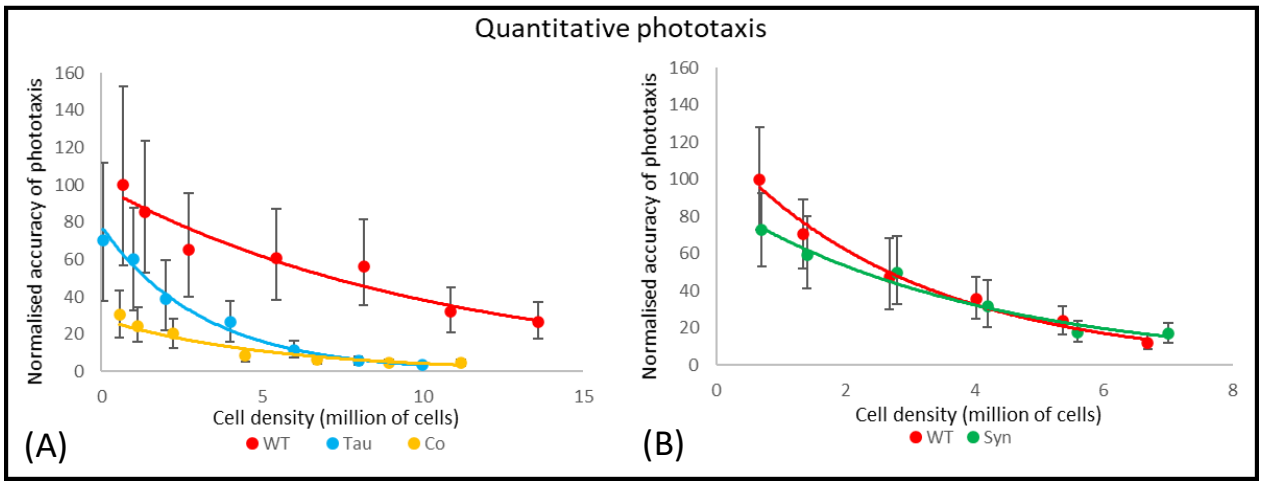


**Figure 3.8 Accuracy of phototaxis is impaired by tau and is decreased further with the coexpression with α-synuclein**. Parental strain AX2 (WT), tau, α-synuclein (Syn) and cotransformant strains (Co) were statistically analysed to measure the accuracy of phototaxis (κ) normalised to the parental AX2 strain, and plotted againt cell density. **(A)** Tau expressing strains displayed an impaired accuracy of phototaxis when compared with the WT AX2. This defect was more severe in the strains expressing tau and α-synuclein in combination. **(B)** α-synuclein expressing strains resemble the parental strain. Error bars represent 90% confidence intervals.

(A)

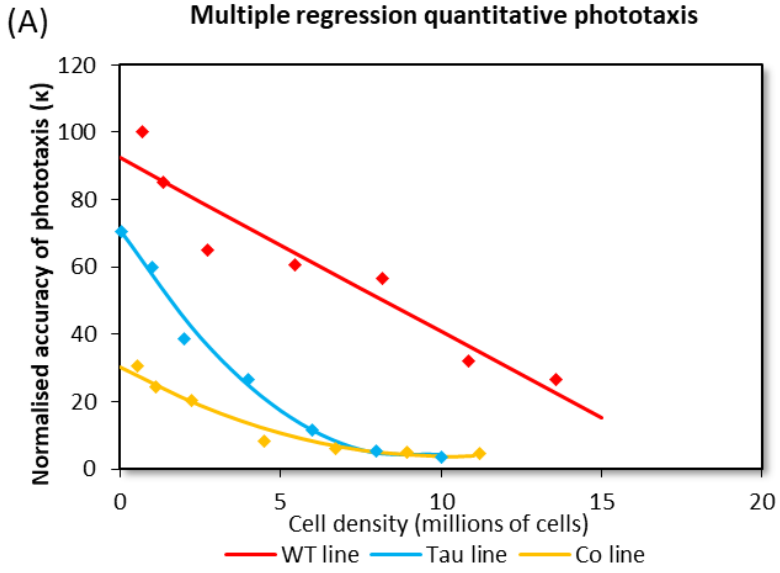


(B)

| *Backwards regression analysis* | *Coefficient* | *Coefficient value* | *Conf. (±)* | *Std.Error* | *t Stat* | *P-value* |
|---|---|---|---|---|---|---|
| Intercept AX2 | a | 92.31601 | 7.67864 | 3.58014 | 25.78557 | 3.35E-13 |
| Density slope AX2 | b | -5.14061 | 0.99715 | 0.46492 | -11.05706 | 2.65E-08 |
| Intercept Tau | d | -21.48998 | 12.41068 | 5.78644 | -3.71385 | 0.00231 |
| Density Slope Tau | e | -9.61612 | 5.24062 | 2.44342 | -3.93551 | 0.00149 |
| Density$^2$ Slope Tau | f | 0.81016 | 0.50371 | 0.23485 | 3.44963 | 0.00391 |
| Intercept Co | g | -62.22501 | 8.94027 | 4.16837 | -14.92789 | 5.42E-10 |
| Density$^2$ Slope Co | i | 0.25210 | 0.13409 | 0.06252 | 4.03219 | 0.001236 |

**Figure 3.9. Multiple regression analysis of quantitative phototaxis.** Tau and cotransformant strains exhibited significantly impaired phototaxis compared with the WT. Regression model: κ = Accuracy of phototaxis, *D*=cell density (millions of cells/cm$^2$)

Full regression model: $\kappa = a+bD+cD^2+d+eD+fD^2+g+hD+iD^2$

**(A)** Tau and cotransformant strains displayed an impaired accuracy of phototaxis when compared with the WT AX2. Fitted lines are a result of the multiple regression analysis. **(B)** Coefficients retained as significant ($p<0.05$) after multiple regression with 'backwards' stepwise removal of insignificant terms. Significances (P-values) for each coefficient retained in the final regression model are highlighted in green. Lines plotted in **(A)** are those for the final fitted regression model with the coefficients in **(B).**

### 3.4.2.3 Thermotaxis

In *D. discoideum*, phototaxis and thermotaxis pathways share many downstream genes (Darcy, Wilczynska, & Fisher, 1994), so that when a phototaxis defect is detected, a thermotaxis defect is usually also present. As there was a phototaxis defect seen in tau strains which was enhanced with the expression of α-synuclein, thermotaxis experiments (Section 2.10.2) were also performed on these strains. Strains expressing tau displayed reduced accuracies of thermotaxis with a maximum accuracy between the temperatures T3 and T4 (Figure 3.10.A). Strains expressing α-synuclein displayed no defect in thermotaxis and accuracies similar to AX2, with a maximum accuracy of positive thermotaxis between the temperatures T4 and T5 (Figure 3.10.B). The tau and α-synuclein strains align with the phototaxis results. However, cotransformants expressing both tau and α-synuclein showed reduced accuracies of thermotaxis at a similar magnitude to the tau expressing strains suggesting that α-synuclein imparts no additional defect in contrast to phototaxis (Figure 3.10.A).

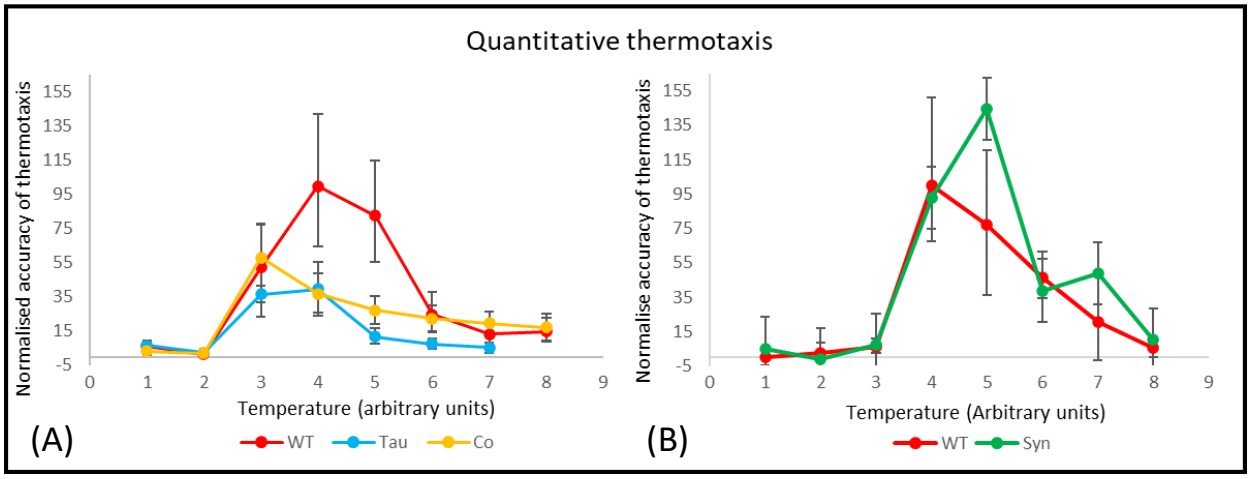


**Figure 3.10 Tau impairs thermotaxis while α-synuclein has no affect.** AX2 (WT), tau strain, α-synuclein (Syn) (HPF885 – data taken from (Fernando et al., 2020)) and cotransformants were measured for accuracy of thermotaxis (κ), normalised and plotted against temperature. Temperature is expressed in arbitrary units (1-8) corresponding to agar surface temperatures of 14 °C to 28 °C with increasing 2 °C increments. **(A)** The tau and cotransformant strains displayed a similar reduction in accuracy of thermotaxis. **(B)** α-synuclein caused no thermotaxis defect in comparison to the WT. Error bars represent 90% confidence intervals, indicating a significance between strains at time points where there is no overlap.

### 3.4.3 Growth rates

As tau expression led to aberrant fruiting body morphology and deranged phototaxis phenocopying mitochondrially diseased strains, growth rates were examined to determine if these phenotypes were also affected. *D. discoideum* strains expressing tau and α-synuclein alone and in combination were grown on lawns of *E.coli* B2 to measure plaque expansion rates (Section 2.10.5). Previous experiments showed a decrease in plaque expansion rates and no affect on axenic growth by α-synuclein expressing strains (Fernando et al., 2020). Tau strains produced plaque expansion rates similar to AX2, while the cotransformant had slightly faster plaque expansion rates. This could indicate an interaction between tau and α-synuclein that rescues the α-synuclein defect (Figure 3.11.A). To measure axenic growth rates, *Dictyostellium* cells were grown in liquid medium during exponential growth (Section 2.10.6). Axenic growth was slightly impaired in both tau and cotransformant strains with slightly longer generation times (Figure 3.11.B). These results differ from those seen with mitochondrially diseased strains which displayed decreased growth on both solid and in liquid media.

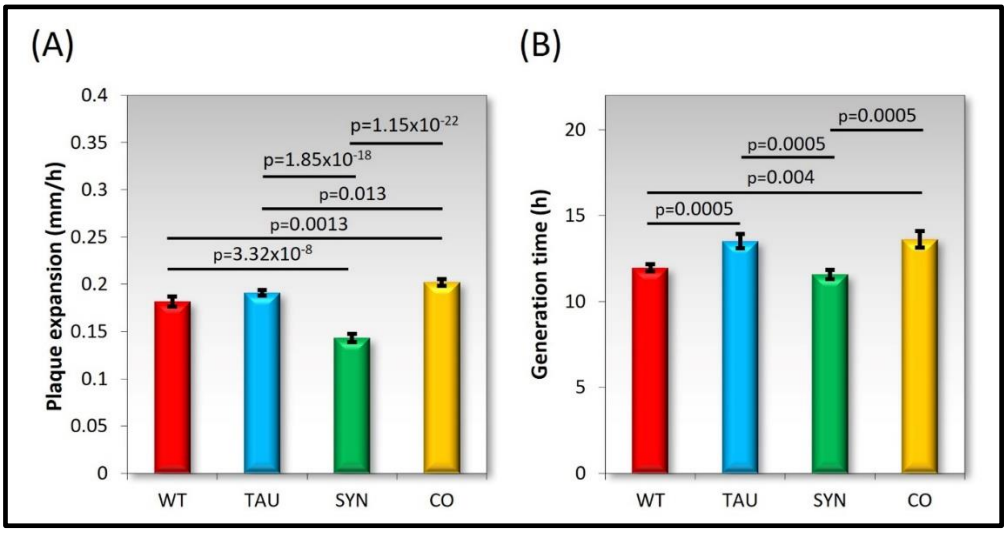


**Figure 3.11. Coexpression of tau and α-synuclein positively affects growth on plates but negatively affects axenic growth.** Wild type AX2 (WT) and strains expressing tau (TAU), α-synuclein (SYN) or both tau and α-synuclein (CO) were tested. **(A)** Plaque expansion rates were measured during growth on bacterial lawns of *E. coli* B2. Plaques were measured twice daily over one hundred hours. Experiments were performed in triplicate in four different experiments. As previously seen (Fernando et al., 2020) α-synuclein-expressing strains display slower growth on bacterial lawns when compared to the WT AX2. Tau does not affect growth on bacterial lawns, but strains expressing both tau and α-synuclein grew slightly but significantly faster than WT AX2 and strains expressing tau alone. **(B)** Axenic growth rates were measured by determining the generation time of strains (doubling in exponential growth phase). Strains were grown in HL5 liquid medium on a shaker at 21 °C for one hundred hours. Experiments were performed on tau and cotransformant strains over four separate experiments. As previously shown, α-synuclein did not affect axenic growth (Fernando et al., 2020). Strains expressing tau or both tau and α-synuclein showed significantly longer generation times than AX2. Error bars are standard errors of the mean, p-values represent statistically significant values using a two sample *t*-test.

### 3.4.4 Phagocytosis and Macropinocytosis

*D. discoideum* consume nutrients through endocytosis. When feeding on bacterial lawns, bacteria are ingested through phagocytosis, and in liquid media nutrients are taken up through macropinocytosis (pinocytosis). The normalised rates of endocytosis can be seen in Figure 3.12. Tau did not affect phagocytosis or pinocytosis rates, which resembles the phenotypes of mitochondrially diseased cells (Bokko et al., 2007). Phagocytosis but not pinocytosis was affected in α-synuclein strains, indicating the impaired growth on bacterial lawns was due at least partly to a phagocytosis defect and most likely not due to mitochondrial dysfunction. The cotransformants had an increased phagocytosis rate suggesting that the increased growth rate on bacterial lawns was also due to elevated rates of phagocytosis. Pinocytosis was not affected in these strains and therefore not the cause of the impaired axenic growth of the tau and cotransformant strains.

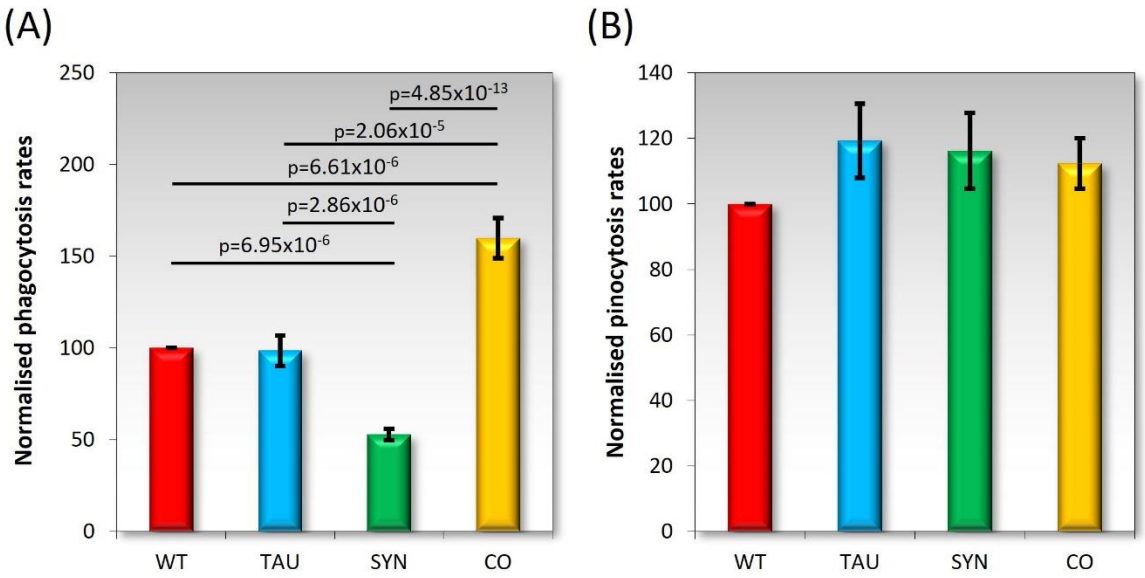


**Figure 3.12. Combined expression of tau and α-synuclein cause increased phagocytosis rates while pinocytosis is not affected**. **(A)** Phagocytosis rates were determined by measuring the uptake of fluorescent *E. coli* DS-Red by *D. discoideum* amoeba. The uptake rates of bacteria were normalised to the rate of uptake of AX2 (WT). Tau did not affect phagocytosis rates and shows a similar uptake rate to AX2. Previously, α-synuclein expression caused a significant decrease in phagocytosis rates (two-sample *t*-test pictured). The coexpression of tau and α-synuclein significantly increased the rate of phagocytosis (two-sample *t*-test). Cell lines were assayed in at least three separate experiments **(B)** *D. discoideum* pinocytosis rates were determined by measuring the uptake of FITC-dextran in HL5 media. Cell lines were assayed in at least 3 separate experiments. Pinocytosis rates were not significantly affected by the expression of tau, α-synuclein (Fernando et al., 2020) or the combined expression of these two proteins.

### 3.4.5 *Legionella* proliferation

*D. discoideum* is naturally found in soil environments where it consumes bacteria as a food source. *Legionella* also reside in moist soil environments where they can infect and proliferate within amoebae by exploiting phagocytosis. In healthy *D. discoideum* cells, *Legionella* is taken up and proliferates, but in mitochondrially diseased cells, *Legionella* proliferation is enhanced by up to 2-fold when compared to wildtype (Francione et al., 2009). To measure *Legionella* infection and intracellular proliferation rates, *D. discoideum* amoebae were plated in a monolayer in a tissue culture plate and infected with *L. pneumophila* Corby. Viable counts of *L. pneumophila* were determined over 5 days at time points 0-96 hrs (Figure3.13.A). As the *Legionella* proliferation rates can vary and occur on different days of the measurement period, the maximum proliferation of these groups of strains was also statistically analysed for direct comparison (Figure 3.13.B). Tau strains and cotransformants exhibited significantly increased *L. pneumophila* proliferation compared to the parental strain AX2, which corresponds to previous results seen in mitochondrially diseased cells. *D. discoideum* strains expressing α-synuclein showed a decrease in *L. pneumophila* proliferation.

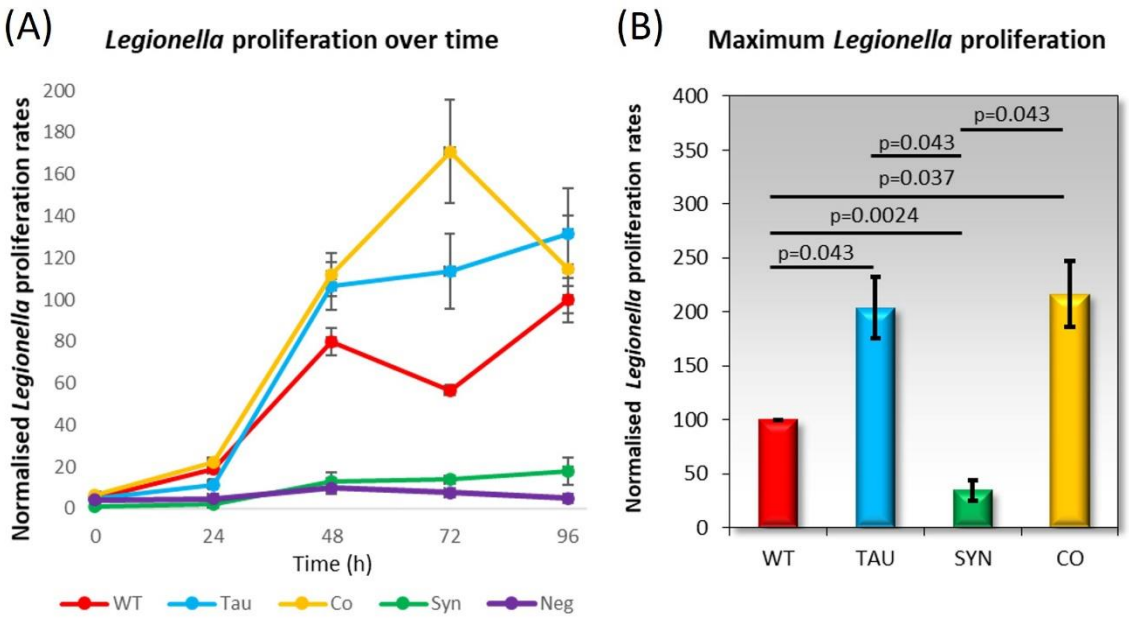


**Figure 3.13. *Legionella* proliferation is increased in tau and cotransformant strains.**
*Legionella* infection rates were measured by creating a monolayer of *D. discoideum* amoebae in a cell culture plate and infection with *L. pneumophila* Corby. The parental strain AX2 (WT), tau expressing strains (TAU), α-synuclein expressing strains (SYN) and cotransformants expressing tau and α-synuclein (CO) were infected with *L. pneumophila* and assayed for viable counts across five days at time periods 0 hr, 24 hr, 48 hr, 72 hr and 96 hr. Extracellular *L. pneumophila* was killed by the addition of Gentamycin sulphate (G418) 30 mins before cells were harvested for viable counts. **(A)** The normalised viable counts resulting from the intracellular *L. pneumophila* released by the *D. discoideum* cells were plotted against the corresponding time periods. A negative control was included for

comparison and did not contain *D. discoideum* cells. *L. pneumophila* proliferation was increased in tau and cotransformant strains when compared to AX2. The plot values are an average of 3-6 strains per time period and were assayed in at least three individual experiments. The error bars are standard errors of the mean. **(B)** The maximum *L. pneumophila* proliferation rates were normalised to the proliferation in AX2 (WT). *L. pneumophila* proliferation was significantly decreased in α-synuclein expressing strains compared to the WT. There was a significant increase in *L. pneumophila* proliferation in the tau and cotransformant strains in comparison to the parental strain. p-values represent statistical significance using an ANOVA with pairwise comparisons using the Least Squares Difference test. Error bars are the standard errors of the mean.

## 3.5 Phototaxis defect is mediated by AMPK

Some of the phenotypes with tau-expressing stains resemble phenotypes which mimic mitochondrial dysfunction in *D. discoideum.* These phenotypes have previously been attributed to the chronic activation of AMPK, an energy-sensing enzyme important in cellular homeostasis. One of the main phenotypes associated with mitochondrial dysfunction and chronic activation of AMPK is a defective slug phototaxis. This was observed in strains in which Cpn60 had been antisense inhibited (Bokko et al., 2007), the mitochondrial protein MidA was knocked out (Carilla-Latorre et al., 2010) and mitochondrial genes were disrupted in a subset of mitochondrial genomes (Francione et al., 2011; Francione and Fisher, 2011). The phototaxis defect in mitochondrially diseased strains is rescued by antisense inhibition of AMPK. Therefore, the phototaxis phenotype was again investigated to determine whether the defect caused by the expression of tau and the more severe defect present in the cotransformants was mediated by increased AMPK activity. To do this, cotransformants were created expressing tau and an AMPK antisense construct. As the expression of tau and α-synuclein combined yielded a more severe phototaxis defect, strains expressing tau, α-synuclein and AMPK knockdown were also produced. Copy numbers of the tau, AMPK antisense and α-synuclein expression constructs were determined by qPCR. AMPK antisense inhibition rescued the phototaxis defect caused by both the expression of tau and the more severe impairment observed in the α-synuclein/tau cotransformants (Figure 3.14). The slug trails resemble the parental strain in accuracies towards the light source, suggesting that the phototaxis defect in these strains is mediated by chronic AMPK hyperactivity as is known to be the case for mitochondrially diseased strains. It would be of interest in future work to determine if the phenotypes produced by tau that mimic those of mitochondrial disease are also mediated by AMPK. These include the defective fruiting body morphology, axenic growth, thermotaxis and enhanced *L. pneumophila* proliferation.

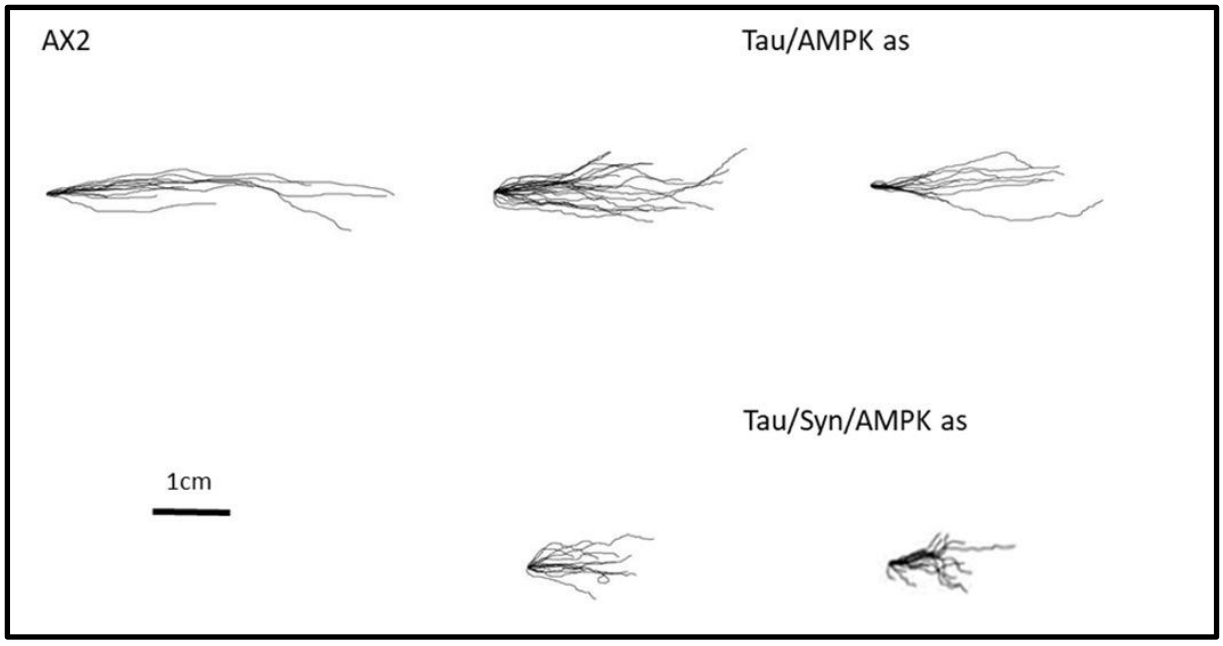


**Figure 3.14. Aberrant phenotypes associated with mitochondrial disease are rescued with antisense inhibition of AMPK.** The slug trails of WT AX2 and cotransformants expressing tau or tau and α-synuclein combined with antisense inhibition of AMPK (Tau/AMPK as, Tau/Syn/AMPK as respectively) were stained, traced and digitised. *D. discoideum* slugs migrate towards the light source at the right of the figure. Both sets of strains display phototaxis accuracies resembling AX2. Scale bar represents 1 cm.

## 3.6 Analysing aerobic respiration

The previously described phenotypes caused by ectopic tau expression suggest a mitochondrial defect producing at least some AMPK-dependent cytopathological outcomes. To measure mitochondrial function more directly the Seahorse Extracellular Flux Analyser in combination with a series of inhibiting drugs added in sequential order was employed (Section 2.10.11). This allows the analysis of various components of mitochondrial respiration using the Oxygen Consumption Rate (OCR) as a readout of mitochondrial activity (Figure 3.15.B-M).

Figure 3.15(a) shows a typical example of a Seahorse experiment and indicates how each of the components are measured. In agreement with previously conducted experiments, the α-synuclein-expressing strains showed significant increases in mitochondrial respiration and also an increase in the OCR by non-mitochondrial processes. There was no significant difference in the contribution of each component to basal respiration or maximum respiration rates suggesting that all complexes and components are functionally normal but hyperactive, as previously reported (Fernando et al., 2020). The expression of tau did not affect total mitochondrial respiration but there was a significant decrease in OCR dedicated to ATP synthesis both in absolute terms (pmol/min) and relative to the basal mitochondrial respiration rate. Tau did not affect the maximum uncoupled $O_2$ consumption rate, or the contributions to this by Complex I and Complex II. These results suggest a specific defect in Complex V, the mitochondrial ATP synthase. It was accompanied by a significant increase in the $O_2$ consumption rate attributable to 'proton leak', a measure of electron transport-driven oxygen consumption by mitochondrial activities other than ATP synthesis, both the absolute rate and the proportion it contributed to basal respiration. This could reflect compensatory upregulation of mitochondrial transport processes responsible for provisioning the mitochondria with oxidizable substrates and other molecules. The coexpression of tau and α-synuclein rescued all of these defects and these strains displayed normal mitochondrial function resembling the wild type AX2 strain. This again signifies a functional interaction between the two proteins.

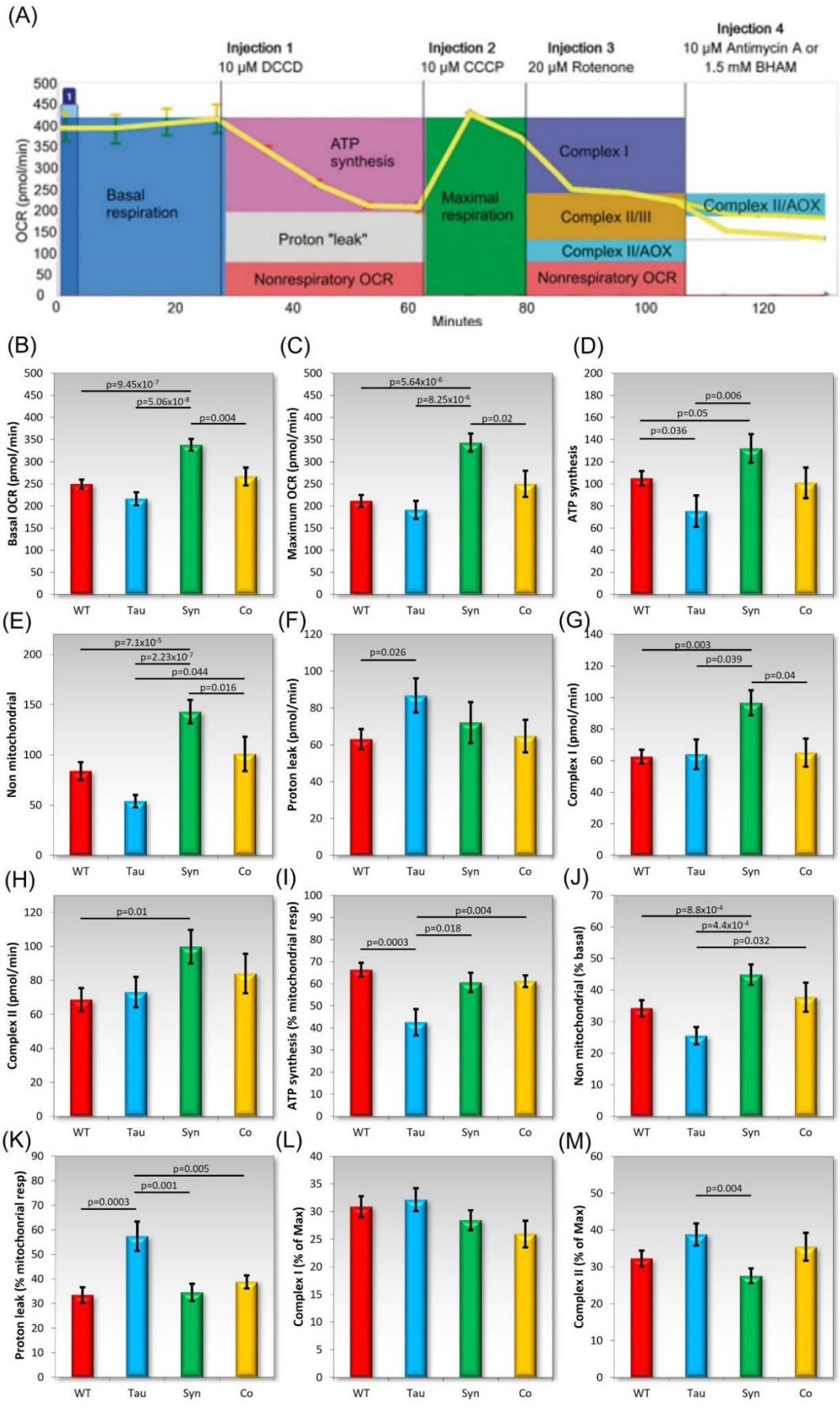
(A)
Injection 1
10 µM DCCD
Injection 2
10 µM CCCP
Injection 3
20 µM Rotenone
Injection 4
10 µM Antimycin A or
1.5 mM BHAM
OCR (pmol/min)
Minutes
Basal respiration
ATP synthesis
Proton "leak"
Nonrespiratory OCR
Maximal respiration
Complex I
Complex II/III
Complex II/AOX
Nonrespiratory OCR
Complex II/AOX
(B)
Basal OCR (pmol/min)
p=9.45x10-7
p=5.06x10-8
p=0.004
(C)
Maximum OCR (pmol/min)
p=5.64x10-6
p=8.25x10-6
p=0.02
(D)
ATP synthesis
p=0.006
p=0.05
p=0.036
(E)
Non mitochondrial
p=7.1x10-5
p=2.23x10-7
p=0.044
p=0.016
(F)
Proton leak (pmol/min)
p=0.026
(G)
Complex I (pmol/min)
p=0.003
p=0.039
p=0.04
(H)
Complex II (pmol/min)
p=0.01
(I)
ATP synthesis (% mitochondrial resp)
p=0.004
p=0.018
p=0.0003
(J)
Non mitochondrial (% basal)
p=8.8x10-4
p=4.4x10-4
p=0.032
(K)
Proton leak (% mitochonrial resp)
p=0.005
p=0.001
p=0.0003
(L)
Complex I (% of Max)
(M)
Complex II (% of Max)
p=0.004
WT
Tau
Syn
Co

**Figure 3.15. Tau impairs mitochondrial ATP synthesis and coexpression with α-synuclein rescues the defect.**

In each experiment, cells of the *D. discoideum* parental strain (AX2), and strains expressing tau or α-synuclein alone or in combination were plated in four wells per sample of a Seahorse XFe24 plate. Mitochondrial respiration was measured as the oxygen consumption rate (OCR) using the Seahorse XFe24 Analyzer following the addition of pharmacological agents. The following agents were added sequentially (as seen in (A) and into all wells: DCCD (dicyclohexylcarbodimide), CCCP (carbonyl cyanide m-chlorophenyl hydrazone) and rotenone. Then either Antimycin A or BHAM (benzohydroxamic acid) was added to the wells. The coloured boxes in panel **(A)** indicate how each component of the respiratory chain was measured (Lay et al., 2016). Total activity for Complex II was calculated by adding the effects of Antimycin A and BHAM. Panels b-h represent each component of mitochondrial respiration measured by the OCR. Each strain was assayed as four replicates per experiment across an average of 3-6 experiments. Horizontal bars with *p* values represent statistically significant pairwise comparisons using the *t*-test. All other pairwise differences were not statistically significant. Error bars are a standard error of the mean. The following components were measured: **(B)** Basal OCR, **(C)**, maximum OCR, **(D)** ATP synthesis, **(E)** non-mitochondrial respiration, **(F)** proton leak, **(G)** Complex I activity and **(H)** Complex II activity. As seen previously, *D. discoideum* expressing α-synuclein showed an increase in mitochondrial respiration and also an increase in oxygen consumption rates as a result of non-mitochondrial processes. In contrast tau expressing strains displayed a reduced OCR dedicated to ATP synthesis **(D)** and an increased proton leak **(F)** and the two appeared to balance each other out as basal respiration was unchanged **(A)** The proportion of ATP synthesis and proton leak to basal respiration was also significantly affected suggesting functional defects in Complex V and proton leak. There were significant differences between tau and α-synuclein expressing strains in the basal and maximum OCRs, ATP synthesis, non-mitochondrial respiration and Complex I activity. In all cases α-synuclein displayed higher OCR measurements than tau strains. The effects on either of these strains seemed to be 'balanced' out with the combination of the two proteins being expressed together. The cotransformants showed similar results to the parental strain and did not differ significantly in any component when compared to AX2. **(I-M)** The following were plotted as a proportion of either the Basal, maximum, or mitochondrial respiration dedicated OCR in order to determine the contribution of each component to the relative respiration rates. Shown in these panels are the OCR attributed to ATP synthesis as a % of mitochondrial OCR **(I)**, non-mitochondrial OCR as a % of Basal OCR **(J),** the 'proton leak' or the mitochondrial OCR rate not contributed to by ATP synthesis; as a % of mitochondrial respiration **(K),** relative contribution of Complex I activity as a % of Maximum OCR **(L)** and the relative contribution of Complex II activity as a % of Maximum OCR **(M).** Strains expressing α-synuclein increase in non-mitochondrial OCR as a % of basal. Tau expressing strains displayed a decrease in OCR attributed to ATP synthesis relative to mitochondrial OCR but an increase in mitochondrial OCR attributed to by the 'proton leak'. Once again, the cotransformants expressing both tau and α-synuclein did not differ from the parental strain indicating all complexes were functioning normally, making similar relative contributions to respiration as in the parental strain AX2.

## 3.7 Proteomics

To investigate whether any of the phenotypes caused by the expression of tau, α-synuclein or the cotransformant strains were associated with differentially regulated proteins, whole cell proteomics was performed (Section 2.11.1) and analysed (Section 2.11.2) to compare protein abundances between strains. The number of up- and down-regulated proteins of each strain when compared to AX2 was determined using data exported to Excel from Scaffold and using the p-values of two sample t-tests. The number of proteins differentially expressed in the tau, α-synuclein and cotransformant strains can be seen in Figure 3.16. There were more proteins down-regulated (tau n=99, α-synuclein n=53, cotransformants n=144) in all groups compared to proteins that were up-regulated (tau n=42, α-synuclein n=27, cotransformants n=59), and the cotransformants had more proteins differentially expressed than either the tau or α-synuclein alone. Lists of up- and down-regulated proteins can be found in Appendix 7.

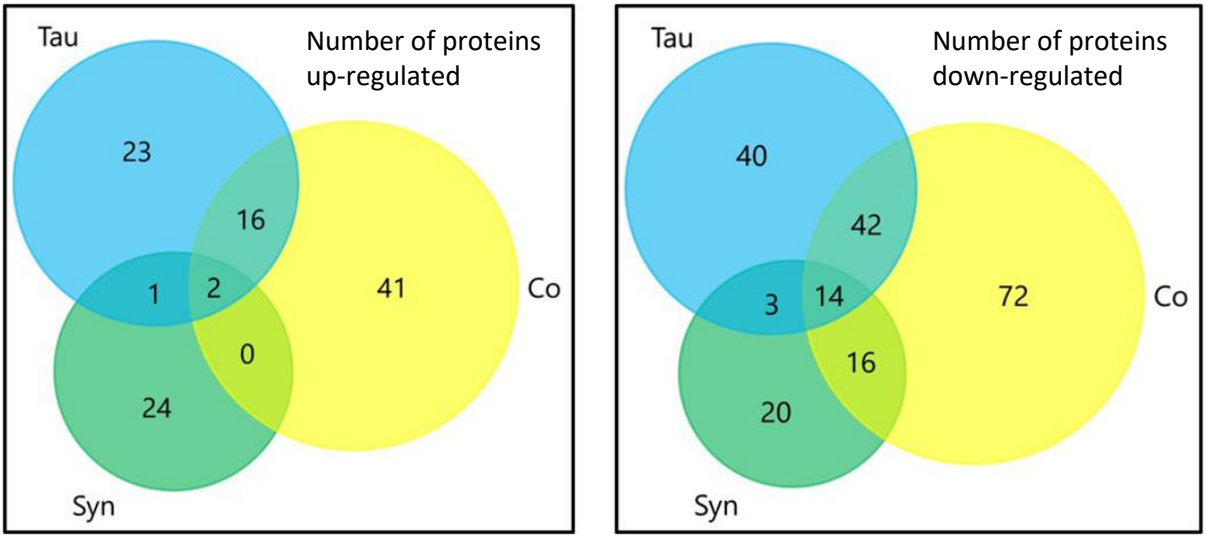


**Figure 3.16. Proteins are differentially expressed in each strain**. Venn diagrams representing the number of proteins that were differentially expressed in each strain when compared to AX2. (Tau expressing strains, α-synuclein (Syn) and the cotransformant expressing both tau and α-synuclein (Co)). There were more proteins down-regulated in each of the sets of strains compared to the number that were up-regulated. The coexpression of tau and α-synuclein lead to the expression of more proteins being up- or down-regulated than either did alone.

Enrichment analysis using FunRich software (Figure 3.17.A & B) revealed that of the proteins up-regulated in the tau strains there were significantly more genes affecting protein catabolism (p=<0.0001), the proteasome (p=<0.0001) and translation (p=0.0001) indicating that protein degradation and synthesis *ie* turnover are up-regulated. α-synuclein did not have any effect on these processes while the cotransformants up-regulated fewer proteins involved in protein catabolism but

more in the process of protein synthesis (translation, p=0.0001). Thus, the biological processes up-regulated by α-synuclein were unlike those up-regulated by tau. Tau induces protein catabolism, possibly as part of a spectrum of homeostatic compensatory processes that favour energy production by alternative catabolic processes in the face of defective mitochondrial ATP synthesis. By contrast, α-synuclein expression enhances mitochondrial respiration and perhaps in support of this elevated activity, these strains exhibited higher levels of expression of enzymes involved in carbohydrate metabolism. This may provide the energy to support elevated rates of protein biosynthesis.

In α-synuclein-expressing strains, proteins involved in responding to bacteria were up-regulated as well as proteins associated with the pathogen-containing vacuole (p=0.0001). This accords with the *L. pneumophila* infection and proliferation experiments in which α-synuclein was significantly less susceptible to proliferation when compared with the parental strain AX2. These observations suggest that in α-synuclein-expressing strains, *Legionella*-containing vacuoles may be up-regulated increasing the capacity of the cell to directly handle the pathogens through the endolysosomal *Legionella*-destroying pathway.

In accord with their different subcellular localizations, tau up-regulated proteins in the cytosol and cytoplasm where it was localised (as well as the nucleus), while α-synuclein up-regulated proteins in the plasma membrane, extracellular matrix and phagocytic vesicle which are all associated with the cell cortex. STRING was used as a visual representation of the interacting protein groups up-regulated in the tau and cotransformant strains and the False Discovery Rates of each biological process affected (Figure 3.17.C). There were too few up-regulated proteins in the α-synuclein expressing strains for valid comparisons.

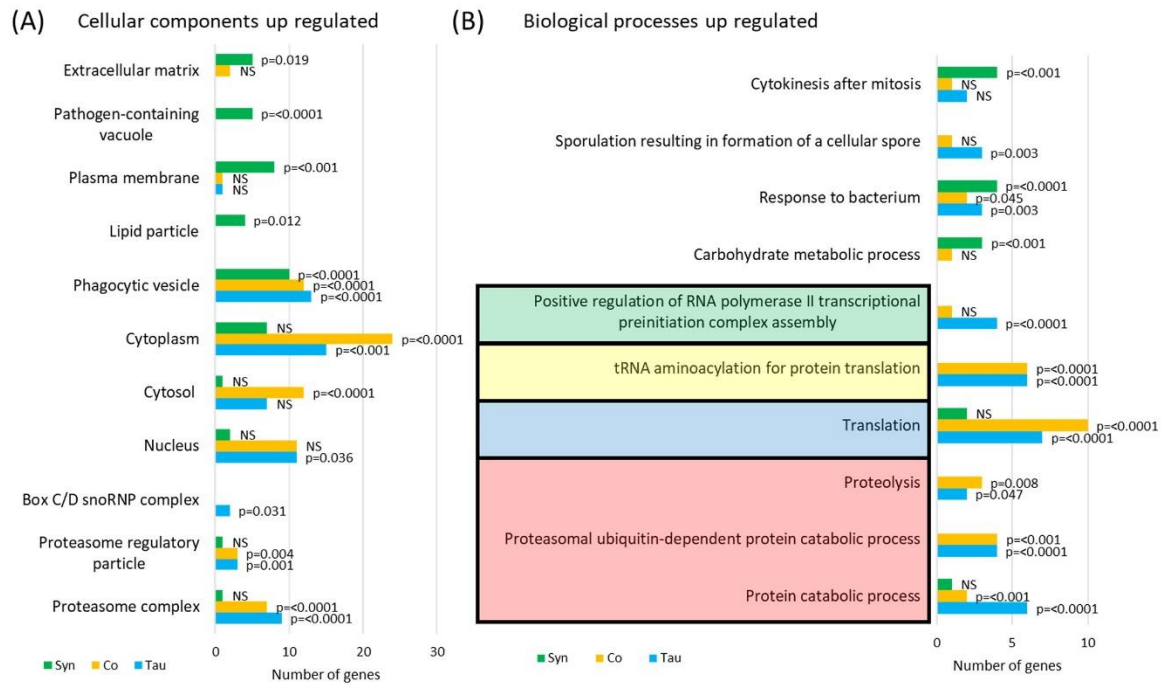


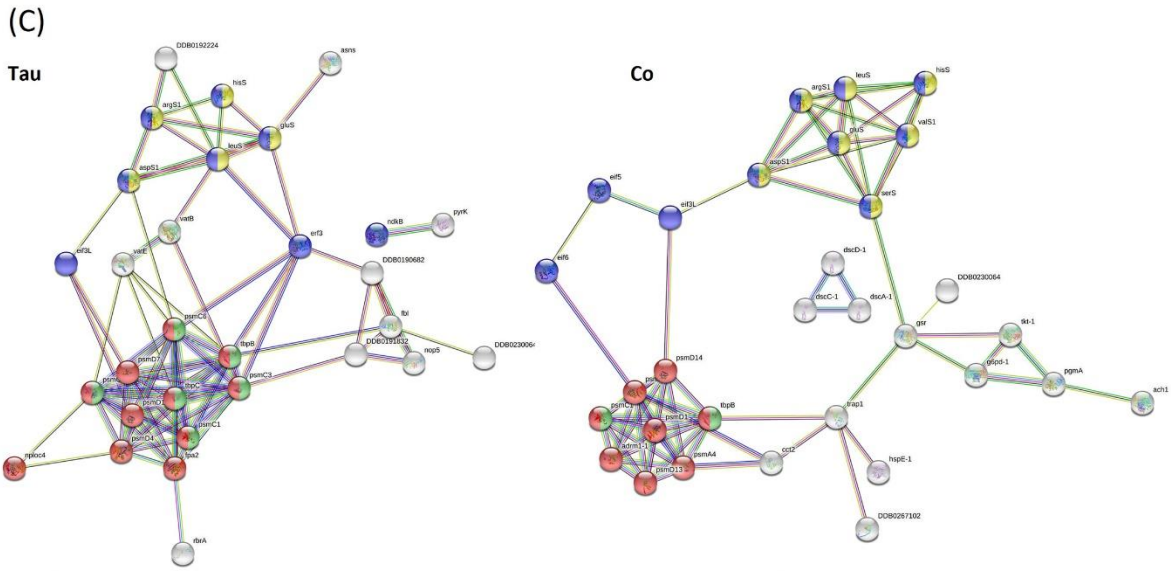


| Biological process | Colour | Tau (FDR) | Co (FDR) |
|---|---|---|---|
| Proteolysis | Red | $p=5.89\times10^{-11}$ | $p=1.18\times10^{-6}$ |
| Positive regulation of RNA polymerase II transcriptional preinitiation complex | Green | $p=1.15\times10^{-11}$ | NS |
| Translation | Blue | $p=4.09\times10^{-7}$ | $p=1.15\times10^{-8}$ |
| tRNA aminoacylation for protein translation | Yellow | $p=5.97\times10^{-7}$ | $p=1.18\times10^{-8}$ |

**Figure 3.17. Cellular components and biological processes up-regulated in strains expressing tau and/or α-synuclein.** Funrich enrichment analysis of cellular components **(A)** and biological processes **(B)** indicate that tau affects the proteasome and proteolytic processes as well as translation. The expression of α-synuclein resulted in different biological processes and therefore different cellular components being affected. The cotransformants displayed patterns of up-regulated expression similar to those in strains expressing tau alone. The reported p-values are based on hypergeometric tests **(A)** and corrected using the Bonferroni method **(B)** calculated in FunRich software. This is based on the number of genes up-regulated within each strain divided by the total number of genes generated for each process/component using the Gene Ontology database for *D. discoideum.* (In

green ‘Syn’ represents α-synuclein expressing strains, in yellow ‘Co’ represents the cotransformants expressing both tau and α-synuclein and ‘Tau’ is in blue). To give a visual representation of protein groups, STRING was used to view the groups of interacting proteins involved in the major up-regulated processes in the tau-expressing strains and cotransformants and calculate False Discovery Rates (FDR) **(C)** which indicate statistical significance of the overrepresentation of these biological processes in the list of interacting up-regulated proteins. There was insufficient data to provide a network of interacting up-regulated proteins in the α-synuclein expressing strains using STRING. (Not pictured). Proteins and STRING protein annotations can be found in supplementary material Tables 1, 3 & 5.

More biological process and cellular components were down- than up-regulated in all three strain groups (Figure 3.18). Proteins involved with the cytoskeleton were down-regulated in all strains ($p=<0.0001$), with the highest number of proteins down-regulated in strains expressing both tau and α-synuclein. This is another indication of functional interactions between these cytotoxic proteins and is not surprising as the cytoskeleton is involved in many processes that were affected in these strains, including phagocytosis, phototaxis and thermotaxis, differentiation, and development (Noegel and Schleicher, 2000). Of note, the biological processes of cell motility ($p=0.012$), polarity ($p=0.018$), morphogenesis ($p=0.01$) and filopodium assembly ($p=0.005$) were only significantly down-regulated in the cotransformants. This corresponds with the more severe phototaxis defect in the cotransformants which also displayed a possible motility defect, as the slugs did not travel as far as other strains. It would be of interest to measure single cell motility and chemotaxis in these strains.

Several proteins involved in the response to bacteria were down-regulated in all strain groups, however this was more significant and there were more proteins affected in the tau-expressing and cotransformant strains ($p=0.0001$) when compared to those expressing α-synuclein alone ($p=0.005$). Proteins upregulated in this pathway in the α-synuclein strains were downregulated in the cotransformants. This again relates to the *L. pneumophila* results, wherein the tau and cotransformants both displayed an increased susceptibility to *L. pneumophila* proliferation when compared to the parental strain. Oxidation-reduction processes are significantly down regulated in the tau and cotransformant strains. Most of the proteins involved in these processes are involved in response to oxidative stress and the biosynthetic pathways of amino acid, fatty acid and lipid synthesis.

Lipid metabolism has been found to be dysregulated in association with tau pathology in AD and α-synuclein in synucleinopathies including PD. For reviews see (Bok et al., 2021) and (Alecu and Bennett, 2019). Lewy bodies, the α-synuclein-containing aggregates that are the pathological hallmark of PD, contain high lipid content and lipid membranes (Shahmoradian et al., 2019), while membrane lipids such as those associated with cholesterol have been associated with PHF in AD brains (Gellermann et al., 2006). Here tau and α-synuclein when expressed alone significantly reduced lipid and sterol

metabolic pathways, but when coexpressed, the down-regulation was rescued. This resembles the results of mitochondrial respiration where the coexpression of both proteins resulted in respiration rescued to normal levels. Again, this signifies a functional interaction between tau and α-synuclein. STRING was used as a visual representation of the protein groups down-regulated in three sets of strains and the False Discovery Rates of each biological process affected (Figure 3.19).

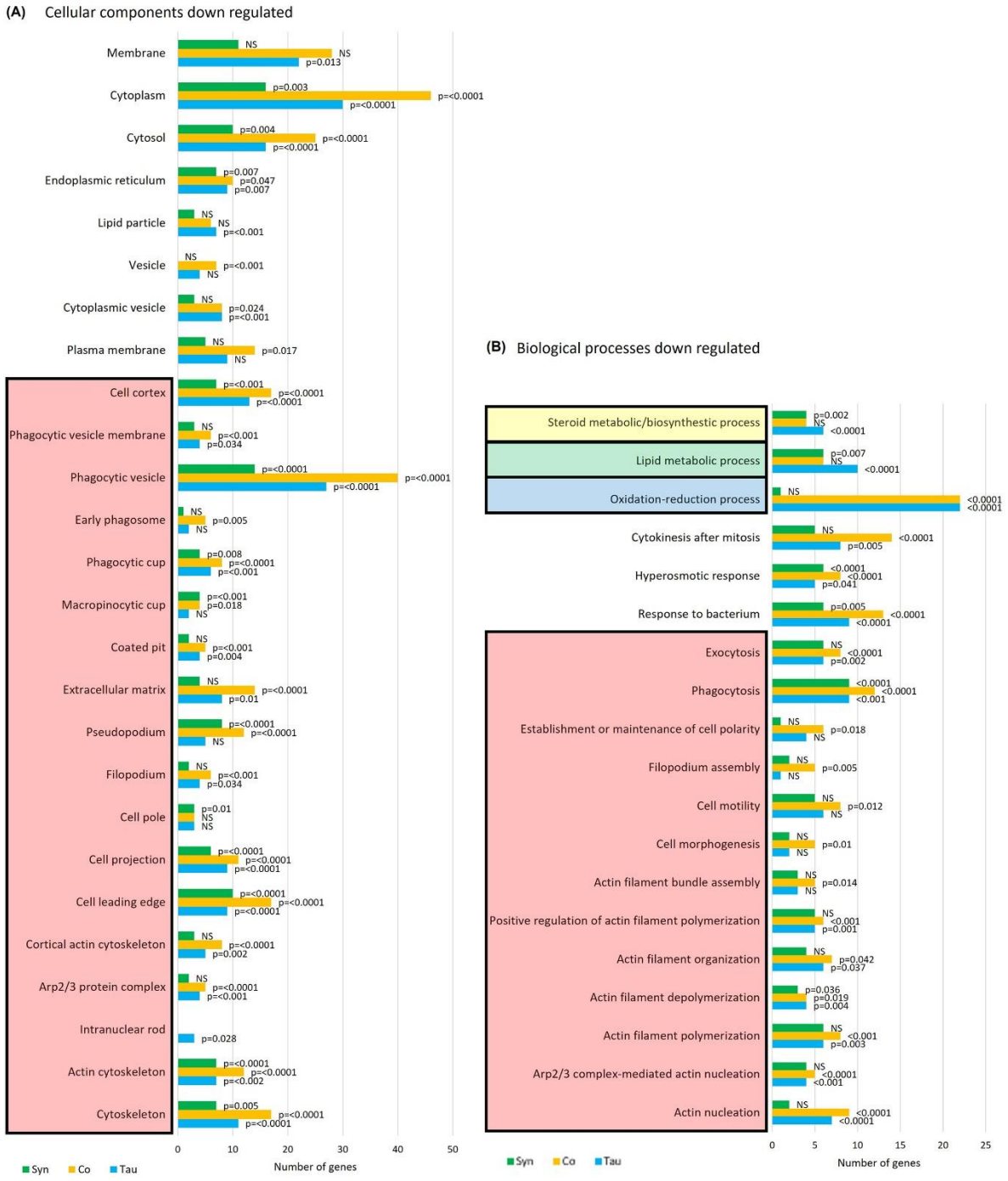


**Figure 3.18. Cellular components and biological processes down-regulated in strains expressing tau and/or α-synuclein.** Funrich enrichment analysis of cellular components **(A)** and biological processes **(B)** indicate that the cytoskeleton is significantly down-regulated in all strains. The coexpression of tau and α-synuclein compounded the effect. The reported p-values are based on hypergeometric tests using the Bonferroni method of correction calculated in FunRich software. This is based on the number of proteins down-regulated within each strain divided by the total number of proteins generated for each process/component using the Gene Ontology database for *D. discoideum*. (In green 'Syn' represents α-synuclein expressing strains, in yellow 'Co' represents the cotransformants expressing both tau and α-synuclein and 'Tau' is in blue).

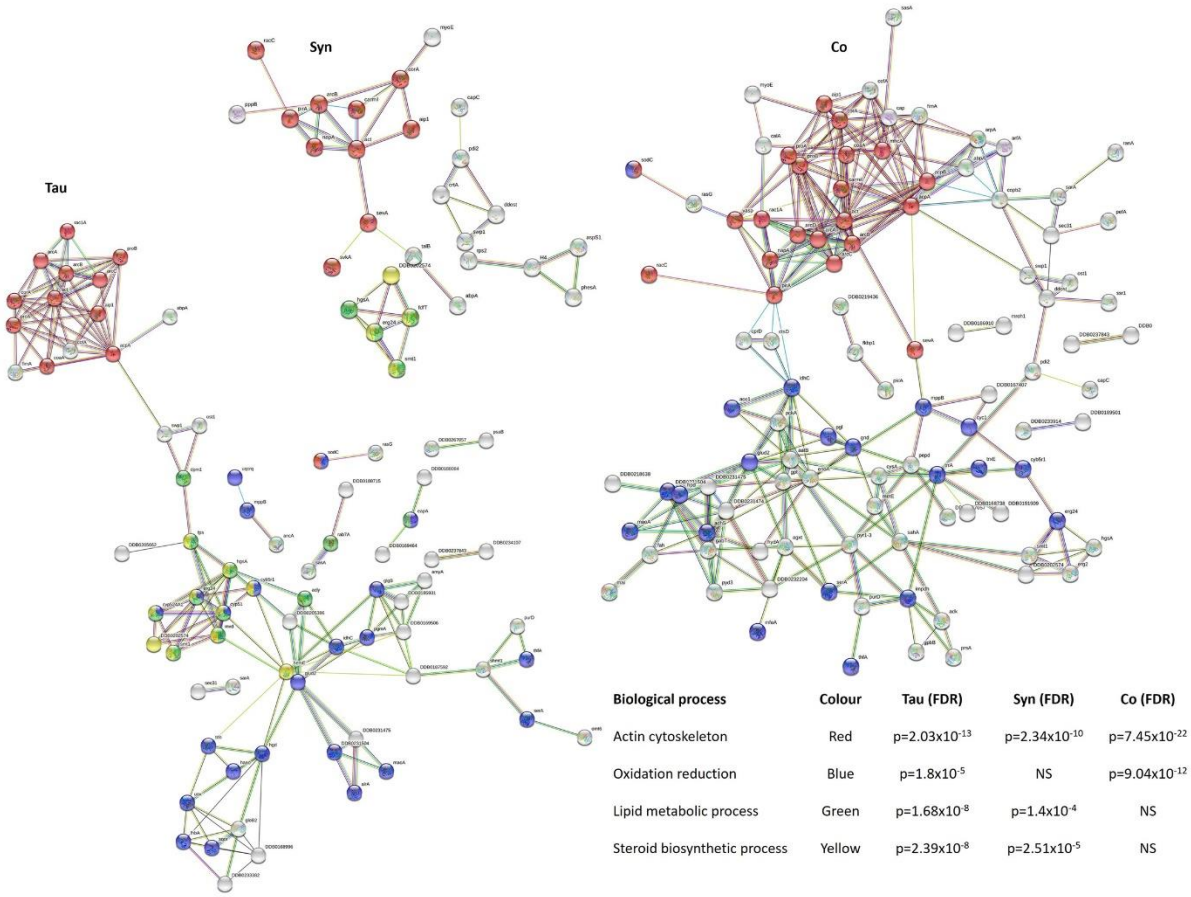


| Biological process | Colour | Tau (FDR) | Syn (FDR) | Co (FDR) |
|---|---|---|---|---|
| Actin cytoskeleton | Red | $p=2.03\times10^{-13}$ | $p=2.34\times10^{-10}$ | $p=7.45\times10^{-22}$ |
| Oxidation reduction | Blue | $p=1.8\times10^{-5}$ | NS | $p=9.04\times10^{-12}$ |
| Lipid metabolic process | Green | $p=1.68\times10^{-8}$ | $p=1.4\times10^{-4}$ | NS |
| Steroid biosynthetic process | Yellow | $p=2.39\times10^{-8}$ | $p=2.51\times10^{-5}$ | NS |

**Figure 3.19. Down-regulated biological processes in strains expressing tau and/or α-synuclein.** To give a visual representation of protein groups, STRING was used to view the interacting protein clusters in the main processes down-regulated in the tau (Tau), α-synuclein (Syn) and cotransformants (Co) and calculated False Discovery Rates (FDR) which indicate statistical significance of the overrepresentation of these processes in the list of interacting proteins. Proteins and STRING protein annotations can be found in supplementary material Tables 2, 4 & 6.

# 4.0 DISCUSSION

Tauopathies are a diverse set of neurodegenerative diseases characterised by the accumulation of the tau protein into aggregates. Tau is important in the stabilisation of MT and axonal transport and binds to microtubules based on the phosphorylation state of the protein. Phosphorylation of tau leads to disassociation of tau and MT, and further hyperphosphorylation causes the accumulation of tau into aggregates, while dephosphorylation restores tau/MT binding. In this project the full-length human tau isoform (2N4R) was expressed in *D. discoideum,* and it was shown to be phosphorylated at residue S404.

Tau is regulated by many different kinases and phosphatases (Avila, 2008) and there are over 80 different phosphorylation sites on the 2N4R isoform (Buée et al., 2000; Hanger et al., 1998). Over 20 kinases have been identified which are able to phosphorylate tau and these can be divided into two main groups - the proline directed protein kinases (PDPKs) and non-PDPKs. The PDPKs phosphorylate tau at Serine/Threonine residues including S404 and have been linked to the process of neurodegeneration (De Vos et al., 2011; Sergeant et al., 2008). Some common PDPKs are GSK-3β, mitogen activated protein kinase and cyclin dependent kinases which all have homologues in *D. discoideum* (Augustinack et al., 2002; Goldberg et al., 2006). Phosphatases of tau have also been defined and include protein phosphatase 1 (PP1), 2A (PP2A), 2B (PP2B) and 5 (PP5), all of which have homologues in *D. discoideum.* The S404 residue is an important residue in the process of aggregation of the tau protein. Mondragón-Rodríguez et al. (2014) found that the double phosphorylation of Ser396 and Ser404 was an early event in AD and Down's syndrome. They saw early pathological tau structures (not yet defined NFT) correlating with phosphorylation at Ser396/404, while other phosphorylation sites corresponded with mature NFT. Pseudophosphorylation of tau (achieved by mutating the serine to glutamic acid to mimic phosphorylation) at this epitope has also been found to be an early event in the hyperphosphorylation and aggregation of tau *in vitro* (Abraha et al., 2000; Haase et al., 2004). Phosphorylation specifically at S404 has been shown by kinases including GSK-3β and the mitogen activating protein kinase ERK2 (Reynolds et al., 2000). Phosphopeptide mapping and sequencing of endogenous tau in neuroblastoma cells and from brain tissue and recombinant tau expressed in *E. coli* shows that GSK-3β displays pronounced phosphorylation at S404 (Augustinack et al., 2002; Godemann et al., 1999; Illenberger et al., 1998; Mandelkow et al., 1992; Zheng-Fischhöfer et al., 1998). Phosphorylation of tau was also seen in other simple models including the yeast model of tauopathy, in which human tau was phosphorylated and dephosphorylated by yeast kinases and phosphatases (De Vos et al., 2011), and site specific phosphorylation resulted in tau aggregates and damage to MT (Vanhelmont et al., 2010). As tau is phosphorylated at S404 in *D. discoideum*, and many tau kinases are conserved in *D. discoideum* it is likely that it is also phosphorylated at other residues.

Despite there being no tau orthologue in *D. discoideum*, the presence of homologous kinases that phosphorylate tau and the demonstration that at least one of them does act on tau suggest that the cellular machinery that regulates tau is ancient and could act on it in a similar way in *D. discoideum* as it is in mammals. This is not unlike the case of Amyloid Precursor Protein (APP) which has no orthologue in *D. discoideum,* but which has been shown to be processed by γ-secretase in *D. discoideum* as in mammalian cells (McMains et al., 2010). As phosphorylation is the first step in the eventual pathological accumulation of tau, the next steps could be to investigate tau aggregation as well as other posttranslational modifications and structural conformations of the protein in *D. discoideum.* It would also be useful to investigate total vs phosphorylated tau to allow further analysis of this signalling pathway in *Dictyostelium*.

In normal healthy cells, tau binds on and off MT depending on the phosphorylation state of the protein. The longest tau isoform has a high affinity for MT as it has 4 MTBR. Here, tau was localised in the cytoplasm of the cell where it interacted with tubulin, although not necessarily on the MT. As tau was phosphorylated, this could have caused MT disassembly as it does in human neurons. However, as tau is not endogenously expressed in *D. discoideum* it is not necessary for MT stability. Immunofluorescence microscopy using an anti-tubulin antibody did not show any evidence of MT disassembly when tau was ectopically expressed in *D. discoideum,* although this was not directly measured. Therefore, it is unclear if tau impacts on MT stability in *Dictyostelium*, however it did cause cytotoxic effects suggesting that tau can exert cytopathological effects that are not related to dysregulated MT assembly/disassembly. This is in agreement with the ectopic expression of tau in *Drosophila* which revealed that, unlike the endogenous *Drosophila* orthologue, it interacted poorly with *Drosophila* microtubules but was nonetheless cytotoxic (Feuillette et al., 2010b).

There has been much evidence to suggest that mitochondrial dysfunction is involved in neurodegenerative diseases (Lin and Beal, 2006) and both tau and α-synuclein have been implicated. As *D. discoideum* has been well characterised as a model for mitochondrial disease which results in a clear set of phenotypes, the phenotypes of strains expressing tau, α-synuclein or both were analysed to determine their similarity to mitochondrially diseased strains. The α-synuclein-mediated phenotypes and those caused by mitochondrial dysfunction have been compared previously and shown to be distinct (Fernando *et al.,* 2020). Impaired mitochondrial function caused greater intracellular *L. pneumophila* proliferation as well as defects in phototaxis, thermotaxis, growth and development, but did not impair phagocytosis or pinocytosis. Despite similarities in some of these phenotypes, the expression of wild type α-synuclein differed in that it impaired phagocytosis and *L. pneumophila* proliferation, while having no significant effect on growth in liquid, phototaxis, thermotaxis or fruiting body morphology. In fact, direct assay of mitochondrial function showed that

α-synuclein expression did not impair but enhanced mitochondrial respiration. The overall pattern of phenotypes suggested that α-synuclein cytotoxicity lies not in mitochondrial defects but in its impairment of specific endocytic pathways (Fernando et al., 2020).

In this work, tau expression increases *L. pneumophila* susceptibility, has no significant effect on phagocytosis or pinocytosis, impairs growth in liquid but not on bacterial lawns, and causes moderate phototaxis and thermotaxis defects as well as aberrant fruiting bodies with shorter, thicker stalks. This pattern of phenotypic outcomes is very distinct to those caused by α-synuclein expression and indicates that tau and α-synuclein cause different cytotoxic effects in *D. discoideum*. In fact, the phenotypic consequences of tau expression are reminiscent of mitochondrial disease phenotypes, with the exception of the normal plaque expansion rates in tau-expressing strains. When mitochondrial respiratory function was measured using Seahorse respirometry, an isolated defect in ATP synthesis by complex V was found, accompanied by an elevation of the mitochondrial "proton leak" (the use of the mitochondrial proton gradient to drive diverse mitochondrial transport processes other than ATP synthesis). Were it not for the normal growth on bacterial lawns, the cytopathological effects of tau expression in *D. discoideum* could thus be attributed entirely to this mitochondrial defect. This raises the question of what other mechanisms might be involved.

The proteomics results suggested that ectopic tau expression had a major impact on protein turnover with both protein degradation (proteasomal) and protein biosynthesis (transcription and translation) being up-regulated. The phosphorylation state of tau could impact the proteins involved in the proteasome as seen by Ren et al. (2007). Here, tau was expressed in embryonic kidney cells and phosphorylation of tau increased proteasome activity while further hyperphosphorylation decreased activity by the proteasome. The phenotypic abnormalities caused by tau all involved the cytoskeleton and this also corresponds with the downregulation of actin cytoskeletal proteins found in the proteomic analysis. Tau impaired axenic growth with a slower generation time in liquid compared to the WT, but this was not mediated by a pinocytosis defect and there was no significant downregulation of proteins associated with the macropinocytic cup. This suggests that other pathways mediating cell proliferation could be causing the defect. This could be a defect in cytokinesis as proteins involved in this process were down-regulated. *Dictyostelium* cytokinesis during growth in suspension in liquid medium depends entirely on the actomyosin cytoskeleton (Bosgraaf and van Haastert, 2006; Zang et al., 1997), whereas on surfaces it can take place by a different mechanism (De Lozanne and Spudich, 1987; Knecht and Loomis, 1987). In the tau transformant the Rho-related protein racE was downregulated. Larochelle et al. (1996) showed that racE was necessary for cytokinesis as *D. discoideum* mutants that did not express racE did not grow in suspension due to a cytokinesis defect. The same group found that racE cells containing an expression vector for racE were able to produce

racE to wildtype levels and had no defect in cytokinesis and growth rates in suspension (Larochelle et al., 1997). A study detailing the effect of an *abiA* null mutant (part of the SCAR/WAVE complex that drives actin polymerisation) in *D. discoideum* showed that the axenic growth defect was due to a defect in cytokinesis (Pollitt and Insall, 2008). Cytokinesis defects can be readily measured in Dictyostelium and could be performed in future analysis (Pakes et al., 2012). Tau-expressing strains also exhibited an increased susceptibility to intracellular *L. pneumophila* proliferation, which again corresponded with proteomics data that indicated proteins responsible for the cellular response to bacteria were down-regulated.

As many neurodegenerative diseases including the tauopathies suggest a synergistic relationship between pathological proteins, tau was also expressed in combination with α-synuclein to investigate the interaction between these two proteins. Like tau, α-synuclein has been reported to interact with tubulin heterodimers in the cytosol (Payton et al., 2001) but also with MT, where it altered the cell surface recruitment of the dopamine transporter (Wersinger and Sidhu, 2005). A study by Alim et al. (2002) found that tubulin was a binding partner of α-synuclein and colocalised in LB in a case of PD. However, colocalization of proteins in the aggregates of Lewy Bodies does not necessarily reflect their normal interactions in the absence of such aggregates. In this study, although tau primarily localised in the cytosol, both tubulin and tau colocalise with α-synuclein in *D. discoideum* in the cortex of the cell where α-synuclein is concentrated. It is also here in the cortical regions of the cell that the cytopathological effects of ectopically expressed α-synuclein are exercised – in the inhibition of phagocytosis and *L. pneumophila* proliferation. Furthermore, the proteomics revealed significant dysregulation of proteins involved in these processes with α-synuclein-expressing cells having lower levels of proteins involved in phagocytosis, but elevated levels of proteins involved in the response to and uptake of bacteria into pathogen-containing vesicles. The phagocytic vesicle associated proteins that were upregulated were mainly related to membrane fusion and protein transport. While the down regulated proteins were associated mainly with actin binding and the cytoskeleton. In relation to response to bacterium, proteins involved in vesicle transport were upregulated (rab1A, rab5A, rasG, sasA and vatC). The interaction of tau with α-synuclein in these same cortical regions can explain the ability of tau to reverse the inhibition of phagocytosis by α-synuclein, when tau on its own has no effect on this phenotype, despite also downregulating expression of proteins involved in this pathway.

The colocalization of tau and α-synuclein at the cortex has been observed in cellular models where tau and α-synuclein have both been found to interact with the plasma membrane (Brandt et al., 1995; Nakamura et al., 2001) and α-synuclein stimulated phosphorylation of tau has been seen to occur here too (Jensen et al., 1999). Esposito et al. (2007) proposed a membrane-bound functional complex with tau and α-synuclein that may involve the actin cytoskeleton. In a Chinese hamster ovary cell line, α-

synuclein was found interacting with actin at the plasma membrane and the colocalization of tau and α-synuclein was highest at the cell periphery. The colocalization of tau and α-synuclein has been seen in autopsied brain sections of patients with AD (Arai et al., 2001; Hamilton, 2000), cellular models (Badiola et al., 2011) and in LB from patients with LBD (Ishizawa et al., 2003). *D. discoideum* is an accepted model for investigating microtubule dynamics and interactions with microtubule associated proteins (MAPs) and is the best understood model for actin dynamics and function in eukaryotic cells (Eichinger et al., 1999; Gerisch, 2009; Noegel and Schleicher, 2000). An interaction between actin and MTs at the cell cortex has been established (Hestermann et al., 2002) and *D. discoideum* has many homologues of the mammalian MAPs (Graf et al., 2000; Koch et al., 2006; Rehberg and Gräf, 2002; Rehberg et al., 2005). The results presented here indicate an interaction of tau, tubulin and α-synuclein which could be further investigated exploiting the well-established cytoskeletal genetics and molecular biology of the *D. discoideum* model.

In view of the distinctive and sometimes opposite phenotypic outcomes of expressing tau and α-synuclein in *D. discoideum*, the question arises as to what happens in cotransformants expressing both proteins. Here, the cotransformants displayed a third distinct pattern of phenotypes, with the presence of the second protein either exacerbating (phototaxis, fruiting body morphology), reversing (phagocytosis, growth on plates, mitochondrial respiratory function, *L. pneumophila* proliferation) or having no significant impact (growth in liquid) on defects caused by the other. This indicates clear functional interactions of the two proteins in several phenotypic pathways and in some cases a synergistic effect. There is similar evidence to suggest an interaction and synergistic cytotoxicity of these two proteins in other model systems coexpressing tau and α-synuclein. In cellular models Badiola et al. (2011) found that tau and α-synuclein colocalised in primary neuronal cultures and the overexpression of tau lead to enhanced α-synuclein cytotoxicity. In a *Drosophila* model of PD, Roy and Jackson (2014) misexpressed tau and α-synuclein singly and in combination. They found that the expression of α-synuclein produced no phenotype associated with the eye, while the expression of tau caused the rough eye phenotype with smaller eyes and the combined expression of the two proteins resulted in a more severe phenotype. This accords with α-synuclein exacerbating tau-mediated defects in phototaxis and fruiting body morphology. Similarly in yeast, tau exacerbated the growth defects caused by α-synuclein (tau alone produced no defect) (Ciaccioli et al., 2013).

Even though the results support a cytotoxic interaction between the two proteins in some phenotypes, it was also found that in relation to other phenotypes the two proteins exerted opposing actions. Thus, the significantly impaired growth on bacterial lawns and the phagocytosis defect observed in the α-synuclein strains were reversed in the cotransformants. In the case of intracellular *L. pneumophila* proliferation, tau not only reversed the reduction caused by α-synuclein but increased

the proliferation of the pathogen to the same elevated levels as observed when tau was expressed singly. There is evidence that tau affects neuronal phagocytosis (Xie et al., 2019) and α-synuclein affects synaptic endocytosis (Lautenschläger et al., 2017), but the effect of combined expression on endocytic pathways has not been previously reported.

Another of the phenotypes in which coexpression of tau and α-synuclein had opposing effects was in mitochondrial respiratory function. Previously, α-synuclein did not cause an impairment in mitochondrial function but instead it increased respiratory activity coordinately in all components measured (Fernando et al., 2020). This result was consistent with increases in mitochondrial respiration seen in lymphoblast cell lines made from iPD patients (Annesley et al., 2016), fibroblasts from iPD patients (Haylett et al., 2016) and when neuroblastoma cells were seeded with α-synuclein fibrils (Ugalde et al., 2020). In this project, tau expression caused a significant decrease in the OCR dedicated to ATP synthesis thereby revealing a specific defect in Complex V. A decrease in ATP production has been seen in neuronal cultures overexpressing tau by Li et al. (2016) and this was accompanied by decreases in Complex I activity and in the ratio of ATP/ADP. Here, no Complex I defect was evident in the tau expressing *D. discoideum* strains. The combined expression of tau and α-synuclein returned mitochondrial respiration to normal, reversing the elevated mitochondrial respiration caused by α-synuclein as well as the Complex V defect and elevated proton leak caused by tau. Altered mitochondrial function is associated with many neurodegenerative diseases and this result highlights that it may occur through different mechanisms and the importance of looking at neuronal protein-protein interactions to advance our understanding of the part played by mitochondria in neurodegeneration. This emphasises the usefulness of using a simple model to study complex interactions and processes.

Many of the defective phenotypes observed in the tau-expressing strains were in line with mitochondrial dysfunction and previously this has been shown to be due to the chronic activation of AMPK (Bokko *et al*., 2007; Francione *et al.,*2009). To determine if there was a functional relationship between tau and AMPK in *D. discoideum,* cotransformants were created which expressed tau or tau and α-synuclein and antisense inhibited AMPK. As phototaxis is a signature defect of impaired mitochondrial function this phenotype was investigated to see whether it was mediated by increased AMPK activity. The antisense inhibition of AMPK in tau strains and strains expressing both tau and α-synuclein resulted in a rescue of the phototaxis defect, suggesting that AMPK mediates the phototaxis defect caused by tau and exacerbated by α-synuclein coexpression. This suggests that AMPK may have been upregulated in the transformants however this could not be measured directly as AMPK could not be detected in any of the transformants or wild type strains. In neurons containing tau pathology in AD and many other tauopathies, AMPK levels and degree of activation (phosphorylation) are

elevated (Vingtdeux et al., 2011). In cell culture a physical interaction between AMPK and tau was established and overexpression of AMPK increased tau toxicity and phosphorylation (Galasso et al., 2017). Interestingly, the inhibition of AMPK might serve as neuronal protection in neurodegenerative diseases (McCullough et al., 2005). Models of motor neuron disease and amylotrophic lateral sclerosis found benefits of downregulating AMPK (Lim et al., 2012). In *Drosophila* expressing tau, downregulation of the AMPKα subunit partially rescued the tau rough eye phenotype. In future studies, determining if AMPK knockdown can rescue the other tau-mediated phenotypes would be beneficial, as would investigating whether AMPK phosphorylates tau in *D. discoideum.*

Proteomics analysis revealed that there were a number of proteins up- and down-regulated in these strains. In all strains more proteins were down-regulated than up-regulated, and the combined effect of tau and α-synuclein coexpression dysregulated the expression of more proteins than did expression of either protein on its own. The pattern of dysregulation caused by tau and α-synuclein expression were quite distinct from each other. Tau significantly up-regulated protein degradation and turnover, possibly in response to the defect in ATP synthesis, while α-synuclein up-regulated proteins involved in the response to bacterium corresponding with decreased *Legionella* susceptibility possibly as a result of a more efficient endolysosomal pathway. All strains exhibited a down-regulation of cytoskeletal proteins, which was exacerbated in the cotransformants. Interestingly here, the cotransformants displayed unique downregulation in some aspects of the cytoskeleton relating to cell motility, polarity, morphogenesis and filopodium assembly corresponding with the more severe phototaxis defect. Both tau and α-synuclein down-regulated proteins involved in lipid and steroid metabolism, which are dysregulated in diseases like AD and PD. However, these pathways were not compounded in the cotransformants but instead were rescued suggesting a complex functional interaction between these two proteins that is sometimes beneficial rather than cytotoxic.

The work described in this thesis shows that *D. discoideum* can be a useful model to study the biological functions of tau and the interactions with other neurodegeneration-associated proteins. Tau was expressed alone and in combination with α-synuclein to investigate the cytotoxic effects and interactions between the proteins in this simple model system. The results showed that tau and α-synuclein have different subcellular distributions but they colocalize in the cortical regions of the cell. They affect different pathways and phenotypes when expressed singly and, depending on the pathway and phenotype, these effects can be enhanced or reversed by the expression of both proteins at once. Thus, the *D. discoideum* model has revealed that the α-synuclein/tau interaction is clear but more complex than a simple synergistic cytotoxicity. These complexities are worthy of further investigation in models like *D. discoideum* in which they can be studied without concerns about the possible effects of endogenous orthologues.

# 5.0 REFERENCES


Abraha, A., N. Ghoshal, T.C. Gamblin, V. Cryns, R.W. Berry, J. Kuret, and L.I. Binder. 2000. C-terminal inhibition of tau assembly in vitro and in Alzheimer's disease. *J Cell Sci*. 113:3737-3745.

Alecu, I., and S.A.L. Bennett. 2019. Dysregulated Lipid Metabolism and Its Role in α-Synucleinopathy in Parkinson's Disease. *Frontiers in Neuroscience*. 13.

Alim, M.A., M.S. Hossain, K. Arima, K. Takeda, Y. Izumiyama, M. Nakamura, H. Kaji, T. Shinoda, S. Hisanaga, and K. Uéda. 2002. Tubulin Seeds α-Synuclein Fibril Formation. *Journal of Biological Chemistry*. 277:2112-2117.

Andreadis, A., W.M. Brown, and K.S. Kosik. 1992. Structure and novel exons of the Human-tau Gene. *Biochemistry*. 31:10626-10633.

Annesley, S.J., and P.R. Fisher. 2009a. Dictyostelium discoideum--a model for many reasons. *Molecular and cellular biochemistry*. 329:73-91.

Annesley, S.J., and P.R. Fisher. 2009b. Dictyostelium Slug Phototaxis. *In* Chemotaxis: Methods and Protocols. T. Jin and D. Hereld, editors. Humana Press, Totowa, NJ. 67-76.

Annesley, S.J., S.T. Lay, S.W. De Piazza, O. Sanislav, E. Hammersley, C.Y. Allan, L.M. Francione, M.Q. Bui, Z.-P. Chen, K.R.W. Ngoei, F. Tassone, B.E. Kemp, E. Storey, A. Evans, D.Z. Loesch, and P.R. Fisher. 2016. Immortalized Parkinson's disease lymphocytes have enhanced mitochondrial respiratory activity. *Disease models & mechanisms : DMM.* 9:1295-1305.

Arai, Y., M. Yamazaki, O. Mori, H. Muramatsu, G. Asano, and Y. Katayama. 2001. α-Synuclein-positive structures in cases with sporadic Alzheimer's disease: morphology and its relationship to tau aggregation. *Brain Research*. 888:287-296.

Arima, K., T. Mizutani, M.A. Alim, H. Tonozuka-Uehara, Y. Izumiyama, S. Hirai, and K. Uéda. 2000. NACP/α-synuclein and tau constitute two distinctive subsets of filaments in the same neuronal inclusions in brains from a family of parkinsonism and dementia with Lewy bodies: double-immunolabeling fluorescence and electron microscopic studies. *Acta Neuropathologica*. 100:115-121.

Augustinack, J., A. Schneider, E.-M. Mandelkow, and B. Hyman. 2002. Specific tau phosphorylation sites correlate with severity of neuronal cytopathology in Alzheimer's disease. *Acta Neuropathologica*. 103:26-35.

Avila, J. 2008. Tau kinases and phosphatases. *J Cell Mol Med*. 12:258-259.

Avila, J., J.J. Lucas, M. Perez, and F. Hernandaz. 2004. Role of Tau Protein in Both Physiological and Pathological Conditions. *Physiol Rev*. 84:361-384.

Badiola, N., R.M. de Oliveira, F. Herrera, C. Guardia-Laguarta, S.A. Goncalves, M. Pera, M. Suarez-Calvet, J. Clarimon, T.F. Outeiro, and A. Lleo. 2011. Tau Enhances alpha-Synuclein Aggregation and Toxicity in Cellular Models of Synucleinopathy. *PLoS One*. 6.

Baker, M., I. Litvan, H. Houlden, J. Adamson, D. Dickson, J. Perez-Tur, J. Hardy, T. Lynch, E. Bigio, and M. Hutton. 1999. Association of an Extended Haplotype in the Tau Gene with Progressive Supranuclear Palsy. *Human Molecular Genetics*. 8:711-715.

Beharry, C., L. Cohen, J. Di, K. Ibrahim, S. Briffa-Mirabella, and A. Alonso. 2014. Tau-induced neurodegeneration: mechanisms and targets. *Neurosci. Bull.* 30:346-358.

Binder, L., A. Frankfurter, and L. Rebhun. 1985. The distribution of tau in the mammalian central nervous system. *J Cell Biol*. 101:1371 - 1378.

Boeve, B.F. 2012. Progressive supranuclear palsy. *Parkinsonism & Related Disorders*. 18, Supplement 1:S192-S194.

Boeve, B.F., A.E. Lang, and I. Litvan. 2003. Corticobasal degeneration and its relationship to progressive supranuclear palsy and frontotemporal dementia. *Ann Neurol*. 54:S15-S19.

Bok, E., E. Leem, B.-R. Lee, J.M. Lee, C.J. Yoo, E.M. Lee, and J. Kim. 2021. Role of the Lipid Membrane and Membrane Proteins in Tau Pathology. *Frontiers in Cell and Developmental Biology*. 9.

Bokko, P.B., L. Francione, E. Bandala-Sanchez, A.U. Ahmed, S.J. Annesley, X. Huang, T. Khurana, A.R. Kimmel, and P.R. Fisher. 2007. Diverse Cytopathologies in Mitochondrial Disease Are Caused by AMP-activated Protein Kinase Signaling. *Molecular Biology of the Cell*. 18:1874-1886.

Bosgraaf, L., and P.J.M. van Haastert. 2006. The regulation of myosin II in Dictyostelium. *European journal of cell biology.* 85:969-979.

Brand, M.D., and D.G. Nicholls. 2011. Assessing mitochondrial dysfunction in cells. *The biochemical journal.* 435:297-312.

Brandt, R., J. Léger, and G. Lee. 1995. Interaction of tau with the neural plasma membrane mediated by tau's amino-terminal projection domain. *The journal of cell biology.* 131:1327-1340.

Bright, J., S. Hussain, V. Dang, S. Wright, B. Cooper, T. Byun, C. Ramos, A. Singh, G. Parry, N. Stagliano, and I. Griswold-Prenner. 2015. Human secreted tau increases amyloid-beta production. *Neurobiology of Aging*. 36:693-709.

Buée, L., T. Bussière, V. Buée-Scherrer, A. Delacourte, and P.R. Hof. 2000. Tau protein isoforms, phosphorylation and role in neurodegenerative disorders. *Brain Research Reviews*. 33:95-130.

Burré, J. 2015. The Synaptic Function of α-Synuclein. *Journal of Parkinson's Disease*. 5:699-713.

Burré, J., M. Sharma, and T.C. Südhof. 2018. Cell Biology and Pathophysiology of α-Synuclein. *Cold Spring Harbor Perspectives in Medicine*. 8.

Cabezas-Opazo, F.A., K. Vergara-Pulgar, M.J. Pérez, C. Jara, C. Osorio-Fuentealba, and R.A. Quintanilla. 2015. Mitochondrial Dysfunction Contributes to the Pathogenesis of Alzheimer's Disease. *Oxid Med Cell Longev*. 2015:509654.

Carilla-Latorre, S., M.E. Gallardo, S.J. Annesley, J. Calvo-Garrido, O. Graña, S.L. Accari, P.K. Smith, A. Valencia, R. Garesse, P.R. Fisher, and R. Escalante. 2010. MidA is a putative methyltransferase that is required for mitochondrial complex I function. *Journal of cell science.* 123:1674-1683.

Chinnery, P.F., and E.A. Schon. 2003. Mitochondria. *Journal of neurology, neurosurgery and psychiatry.* 74:1188-1199.

Ciaccioli, G., A. Martins, C. Rodrigues, H. Vieira, and P. Calado. 2013. A Powerful Yeast Model to Investigate the Synergistic Interaction of α-Synuclein and Tau in Neurodegeneration. *PLoS One*. 8.

Cleveland, D.W., S.-Y. Hwo, and M.W. Kirschner. 1977. Physical and chemical properties of purified tau factor and the role of tau in microtubule assembly. *Journal of Molecular Biology*. 116:227-247.

Conway, K.A., J.D. Harper, and P.T. Lansbury. 1998. Accelerated in vitro fibril formation by a mutant α-synuclein linked to early-onset Parkinson disease. *Nature medicine.* 4:1318-1320.

Cummins, N., A. Tweedie, S. Zuryn, J. Bertran-Gonzalez, and J. Götz. 2019. Disease-associated tau impairs mitophagy by inhibiting Parkin translocation to mitochondria. *The EMBO Journal*. 38:e99360.

De Lozanne, A., and J.A. Spudich. 1987. Disruption of the Dictyostelium myosin heavy chain gene by homologous recombination. *Science*. 236:1086-1091.

De Strooper, B., and W. Annaert. 2010. Novel Research Horizons for Presenilins and γ-Secretases in Cell Biology and Disease. *Annual review of cell and developmental biology.* 26:235-260.

De Vos, A., J. Anandhakumar, J. Van den Brande, M. Verduyckt, V. Franssens, J. Winderickx, and E. Swinnen. 2011. Yeast as a model system to study tau biology. *Int J Alzheimer's Dis*. 2011:1-16.

De Vos, K.J., A.J. Grierson, S. Ackerley, and C.C.J. Miller. 2008. Role of Axonal Transport in Neurodegenerative Diseases. *Annual Review of Neuroscience*. 31:151-173.

Drubin, D.G., and M.W. Kirschner. 1986. Tau protein function in living cells. *The Journal of Cell Biology*. 103:2739-2746.

Duda, J.E., B.I. Giasson, M.E. Mabon, D.C. Miller, L.I. Golbe, V.M.-Y. Lee, and J.Q. Trojanowski. 2002. Concurrence of alpha-synuclein and tau brain pathology in the contursi kindred. *Acta Neuropathol*. 104:7-11.

Duka, T., V. Duka, J.N. Joyce, and A. Sidhu. 2009. α-Synuclein contributes to GSK-3β-catalyzed Tau phosphorylation in Parkinson's disease models. *The FASEB Journal*. 23:2820-2830.

Ebneth, A., R. Godemann, K. Stamer, S. Illenberger, B. Trinczek, and E. Mandelkow. 1998. Overexpression of tau protein inhibits kinesin-dependent trafficking of vesicles, mitochondria, and endoplasmic reticulum: implications for Alzheimer's disease. *J Cell Biol*. 143:777-794.

Eckert, A., S. Hauptmann, I. Scherping, J. Meinhardt, V. Rhein, S. Drose, U. Brandt, M. Fandrich, W.E. Muller, and J. Gotz. 2008. Oligomeric and fibrillar species of betaamyloid (A beta 42) both impair mitochondrial function in P301L tau transgenic mice. *J Mol Med*. 86.

Eckert, A., R. Nisbet, A. Grimm, and J. Götz. 2014. March separate, strike together — Role of phosphorylated TAU in mitochondrial dysfunction in Alzheimer's disease. *Biochimica et Biophysica Acta (BBA) - Molecular Basis of Disease*. 1842:1258-1266.

Eckert, A., K. Schmitt, and J. Götz. 2011. Mitochondrial dysfunction - the beginning of the end in Alzheimer's disease? Separate and synergistic modes of tau and amyloid-β toxicity. *Alzheimer's Research & Therapy*. 3:1-11.

Eichinger, L., S.S. Lee, and M. Schleicher. 1999. Dictyostelium as model system for studies of the actin cytoskeleton by molecular genetics. *Microsc Res Tech*. 47:124-134.

Eichinger, L., J.A. Pachebat, R.S. G. Glo¨ ckner M.-A. Rajandream, M. Berriman, J. Song, R. Olsen, K. Szafransk, Q. Xu,, S.K. B. Tunggal, M. Madera, B. A. Konfortov, F. Rivero, A. T. Bankier, R. Lehmann, N. Hamlin, R. Davies, P. Gaudet,, K.P. P. Fey, G. Chen, D. Saunders, E. Sodergren, P. Davis, A. Kerhornou, X. Nie, N. Hall, C. Anjard, L. Hemphill, N. Bason,, B.D. P. Farbrother, E. Just, T. Morio, R. Rost, C. Churcher, J. Cooper, S. Haydock, N. van Driessche, A. Cronin, I. Goodhead,, T.M. D. Muzny, A. Pain, M. Lu, D. Harper, R. Lindsay, H. Hauser, K. James,M. Quiles, M. Madan Babu, T. Saito, C. Buchrieser,, M.F. A. Wardroper, M. Thangavelu, D. Johnson, A. Knights, H. Loulseged, K. Mungall, K. Oliver, C. Price, M. A. Quail,, J.H. H. Urushihara, E. Rabbinowitsch, D. Steffen, M. Sanders, J. Ma, Y. Kohara, S. Sharp, M. Simmonds, S. Spiegler,, S.S. A. Tivey, B. White, D. Walker, J. Woodward, T. Winckler, Y. Tanaka, G. Shaulsky, M. Schleicher, G. Weinstock,, E.C.C. A. Rosenthal, R. L. Chisholm, R. Gibbs, W. F. Loomis, M. Platzer, R. R. Kay, J. Williams, P. H. Dear, A. A. Noegel,, and B.B.A. Kuspa. 2005. The genome of the social amoeba *Dictyostelium discoideum*. *Nature*. 435:43-57.

Esposito, A., C.P. Dohm, P. Kermer, M. Bähr, and F.S. Wouters. 2007. α-Synuclein and its disease-related mutants interact differentially with the microtubule protein tau and associate with the actin cytoskeleton. *Neurobiology of Disease*. 26:521-531.

Esteras, N., J.D. Rohrer, J. Hardy, S. Wray, and A.Y. Abramov. 2017. Mitochondrial hyperpolarization in iPSC-derived neurons from patients of FTDP-17 with 10+16 MAPT mutation leads to oxidative stress and neurodegeneration. *Redox Biol*. 12:410-422.

Fernando, S., C.Y. Allan, K. Mroczek, X. Pearce, O. Sanislav, P.R. Fisher, and S.J. Annesley. 2020. Cytotoxicity and Mitochondrial Dysregulation Caused by α-Synuclein in Dictyostelium discoideum. *Cells*. 9:2289.

Fernando, S.G. 2012. Alpha-synuclein cytotoxicity in Dictyostelium: a model of Parkinson's disease. i. La Trobe University degree granting, editor. Thesis () -- La Trobe University.

Ferrer, I.M.D.P., I.B. López-González, M.T. Carmona, L.B. Arregui, E.P. Dalfó, B.P. Torrejón-Escribano, R.M.D. Diehl, and G.G.M.D.P. Kovacs. 2014. Glial and Neuronal Tau Pathology in Tauopathies: Characterization of Disease-Specific Phenotypes and Tau Pathology Progression. *Journal of Neuropathology and Experimental Neurology*. 73:81-97.

Feuillette, S., V. Deramecourt, A. Laquerriere, C. Duyckaerts, M.-B. Delisle, C.-A. Maurage, D. Blum, L. Buée, T. Frébourg, D. Campion, and M. Lecourtois. 2010a. Filamin-A and Myosin VI colocalize with fibrillary Tau protein in Alzheimer's disease and FTDP-17 brains. *Brain Research*. 1345:182-189.

Feuillette, S., L. Miguel, T. Frébourg, D. Campion, and M. Lecourtois. 2010b. Drosophila models of human tauopathies indicate that Tau protein toxicity in vivo is mediated by soluble cytosolic phosphorylated forms of the protein. *Journal of neurochemistry.* 113:895-903.

Francione, L., P.K. Smith, S.L. Accari, P.E. Taylor, P.B. Bokko, S. Bozzaro, P.L. Beech, and P.R. Fisher. 2009. Legionella pneumophila multiplication is enhanced by chronic AMPK signalling in mitochondrially diseased Dictyostelium cells. *Disease Models & Mechanisms*. 2:479-489.

Francione, L.M., S.J. Annesley, S. Carilla-Latorre, R. Escalante, and P.R. Fisher. 2011. The Dictyostelium model for mitochondrial disease. *Seminars in cell & developmental biology*. 22:120-130.

Francione, L.M., and P.R. Fisher. 2011. Heteroplasmic mitochondrial disease in Dictyostelium discoideum. *Biochemical pharmacology.* 82:1510-1520.

Frasier, M., M. Walzer, L. McCarthy, D. Magnuson, J.M. Lee, C. Haas, P. Kahle, and B. Wolozin. 2005. Tau phosphorylation increases in symptomatic mice overexpressing A30P α-synuclein. *Experimental Neurology*. 192:274-287.

Galasso, A., C.S. Cameron, B.G. Frenguelli, and K.G. Moffat. 2017. An AMPK-dependent regulatory pathway in tau-mediated toxicity. *Biol Open*. 6:1434-1444.

Galpern, W.R., and A.E. Lang. 2006. Interface between tauopathies and synucleinopathies: a tale of two proteins. *Ann Neurol*. 59:449-458.

Gammon, K. 2014. Neurodegenerative disease: Brain windfall. *Nature*. 515:299-300.

Garone, C., M. Minczuk, S.L. Stenton, and H. Prokisch. 2018. Advancing genomic approaches to the molecular diagnosis of mitochondrial disease. *Essays in biochemistry.* 62:399-408.

Gellermann, G.P., T.R. Appel, P. Davies, and S. Diekmann. 2006. Paired helical filaments contain small amounts of cholesterol, phosphatidylcholine and sphingolipids. 387:1267-1274.

Gerisch, G. 2009. Imaging actin cytoskeleton dynamics in Dictyostelium chemotaxis. *Methods Mol Biol*. 571:385-400.

Ghetti, B., F. Tagliavini, G. Giaccone, O. Bugiani, B. Frangione, M.R. Farlow, and S.R. Dlouhy. 1994. Familial Gerstmann-Sträussler-Scheinker disease with neurofibrillary tangles. *Molecular Neurobiology*. 8:41-48.

Gibson, G.E., Q. Shi, X. Zhu, M.F. Beal, X. Wang, G. Perry, and M.A. Smith. 2010. A Mitocentric View of Alzheimer's Disease Suggests Multi-Faceted Treatments. *Journal of Alzheimer's disease*. 20:S591-S607.

Glenner, G.G., and C.W. Wong. 1984a. Alzheimer's disease and Down's syndrome: Sharing of a unique cerebrovascular amyloid fibril protein. *Biochemical and Biophysical Research Communications*. 122:1131-1135.

Glenner, G.G., and C.W. Wong. 1984b. Alzheimer's disease: Initial report of the purification and characterization of a novel cerebrovascular amyloid protein. *Biochemical and Biophysical Research Communications*. 120:885-890.

Godemann, R., J. Biernat, E. Mandelkow, and E.M. Mandelkow. 1999. Phosphorylation of tau protein by recombinant GSK-3β: pronounced phosphorylation at select Ser/Thr-Pro motifs but no phosphorylation at Ser262 in the repeat domain. *FEBS letters.* 454:157-164.

Goedert, M., W. C.M, R.A. Crowther, J.E. Walker, and A. Klug. 1988. Cloning and sequencing of the cDNA encoding a core protein of the paired helical filament of Alzheimer disease: identification as the microtubule-associated protein tau. *Proc Natl Acad Sci U S A*. 85:4051-4055.

Goedert, M., and M.G. Spillantini. 2011. Pathogenesis of the tauopathies. *J Mol Neurosci*. 45:425-431.

Goedert, M., M.G. Spillantini, R. Jakes, D. Rutherford, and R.A. Crowther. 1989a. Multiple isoforms of human microtubule-associated protein tau: sequences and localization in neurofibrillary tangles of Alzheimer's disease. *Neuron*. 3:519-526.

Goedert, M., M.G. Spillantini, M.C. Potier, J. Ulrich, and R.A. Crowther. 1989b. Cloning and sequencing of the cDNA encoding an isoform of microtubule-associated protein tau containing four tandem repeats: differential expression of tau protein mRNAs in human brain. *The EMBO Journal*. 8:393-399.

Goldberg, J.M., G. Manning, A. Liu, P. Fey, K.E. Pilcher, Y. Xu, and J.L. Smith. 2006. The *Dictyostelium* Kinome—Analysis of the Protein Kinases from a Simple Model Organism. *PLoS Genet*. 2:e38.

Gotz, J., F. Chen, J. van Dorpe, ., and R.M. Nitsch. 2001. Formation of neurofibrillary tangles in P301l tau transgenic mice induced by Abeta 42 fibrils. *Science*. 293:1491-1495.

Graf, R., C. Daunderer, and M. Schliwa. 2000. Dictyostelium DdCP224 is a microtubule-associated protein and a permanent centrosomal resident involved in centrosome duplication. *Journal of Cell Science*. 113:1747-1758.

Grundke-Iqbal, I., K. Iqbal, M. Quinlan, Y.C. Tung, M.S. Zaidi, and H.M. Wisniewski. 1986. Microtubule-associated protein tau. A component of Alzheimer paired helical filaments. *Journal of Biological Chemistry*. 261:6084-6089.

Guo, T., W. Noble, and D.P. Hanger. 2017. Roles of tau protein in health and disease. *Acta Neuropathologica*. 133:665-704.

Haase, C., J.T. Stieler, T. Arendt, and M. Holzer. 2004. Pseudophosphorylation of tau protein alters its ability for self-aggregation. *J Neurochem*. 88:1509-1520.

Haass, C., and D.J. Selkoe. 2007. Soluble protein oligomers in neurodegeneration: lessons from the Alzheimer's amyloid β-peptide. *Nature Reviews Molecular Cell Biology*. 8:101.

Hagele, S., R. Kohler, H. Merkert, M. Schleicher, J. Hacker, and M. Steinert. 2000. Dictyostelium discoideum: a new host model system for intracellular pathogens of the genus Legionella. *Cellular microbiology.* 2:165-171.

Hamilton, R.L. 2000. Lewy Bodies in Alzheimer's Disease: A Neuropathological Review of 145 Cases Using α-Synuclein Immunohistochemistry. *Brain Pathology*. 10:378-384.

Han, J., J. Zhang, Y. Hailan, X. Wang, F. Li, L. Chen, C. Goa, J. Gao, K. Nie, W. Zhou, and X. Dong. 2006. Study on interaction between microtubule associated protein tau and prion protein. *Science in China: Series C Life Sciences*. 49:1-7.

Hanger, D.P., J.C. Betts, T.L.F. Loviny, W.P. Blackstock, and B.H. Anderton. 1998. New Phosphorylation Sites Identified in Hyperphosphorylated Tau (Paired Helical Filament-Tau) from Alzheimer's Disease Brain Using Nanoelectrospray Mass Spectrometry. *Journal of Neurochemistry*. 71:2465-2476.

Hanger, D.P., H.L. Byers, S. Wray, K.-Y. Leung, M.J. Saxton, A. Seereeram, C.H. Reynolds, M.A. Ward, and B.H. Anderton. 2007. Novel Phosphorylation Sites in Tau from Alzheimer Brain Support a Role for Casein Kinase 1 in Disease Pathogenesis. *Journal of Biological Chemistry*. 282:23645-23654.

Hardy, J.A., and G.A. Higgins. 1992. Alzheimer's disease: the amyloid cascade hypothesis. *Science*. 256:184+.

Hassan, A., J.L. Whitwell, B.F. Boeve, C.R. Jack Jr, J.E. Parisi, D.W. Dickson, and K.A. Josephs. 2010. Symmetric corticobasal degeneration (S-CBD). *Parkinsonism Relat D*. 16:208-214.

Haylett, W., C. Swart, F. van der Westhuizen, H. van Dyk, L. van der Merwe, C. van der Merwe, B. Loos, J. Carr, C. Kinnear, and S. Bardien. 2016. Altered Mitochondrial Respiration and Other Features of Mitochondrial Function in Parkin-Mutant Fibroblasts from Parkinson's Disease Patients. *Parkinson's disease.* 2016:1819209.

Hestermann, A., M. Rehberg, and R. Gräf. 2002. Centrosomal microtubule plus end tracking proteins and their role in Dictyostelium cell dynamics. *Journal of Muscle Research & Cell Motility*. 23:621-630.

Himmler, A., D. Drechsel, M.W. Kirschner, and D.W. Martin. 1989. Tau consists of a set of proteins with repeated C-terminal microtubule-binding domains and variable N-terminal domains. *Molecular and Cellular Biology*. 9:1381-1388.

Hsiao, K., S.R. Dlouhy, M.R. Farlow, C. Cass, M. Da Costa, M. Conneally, P, M.E. Hodes, B. Ghetti, and S.B. Prusiner. 1992. Mutant prion proteins in Gerstmann-Straussler-Scheinker disease with neurofibrillary tangles. *Nature genetics*. 1:68-71.

Illenberger, S., Q. Zheng-Fischhöfer, U. Preuss, K. Stamer, K. Baumann, B. Trinczek, J. Biernat, R. Godemann, E.-M. Mandelkow, and E. Mandelkow. 1998. The Endogenous and Cell Cycle-dependent Phosphorylation of tau Protein in Living Cells: Implications for Alzheimer's Disease. *Molecular Biology of the Cell*. 9:1495-1512.

Iqbal, K., A. del C. Alonso, S. Chen, M.O. Chohan, E. El-Akkad, C.-X. Gong, S. Khatoon, B. Li, F. Liu, A. Rahman, H. Tanimukai, and I. Grundke-Iqbal. 2005. Tau pathology in Alzheimer disease and other tauopathies. *Biochimica et Biophysica Acta (BBA) - Molecular Basis of Disease*. 1739:198-210.

Iseki, E., W. Marui, K. Kosaka, and K. Uéda. 1999. Frequent coexistence of Lewy bodies and neurofibrillary tangles in the same neurons of patients with diffuse Lewy body disease. *Neuroscience Letters*. 265:9-12.

Ishizawa, T., P. Mattila, P. Davies, D. Wang, and D.W. Dickson. 2003. Colocalization of Tau and Alpha-Synuclein Epitopes in Lewy Bodies. *Journal of Neuropathology and Experimental Neurology*. 62:389-397.

Iwai, A., E. Masliah, M. Yoshimoto, N. Ge, L. Flanagan, H.A. Rohan de Silva, A. Kittel, and T. Saitoh. 1995. The precursor protein of non-Aβ component of Alzheimer's disease amyloid is a presynaptic protein of the central nervous system. *Neuron*. 14:467-475.

Jakes, R., M.G. Spillantini, and M. Goedert. 1994. Identification of two distinct synucleins from human brain. *FEBS Letters*. 345:27-32.

Jellinger, K.A. 2004. Lewy body-related α-synucleinopathy in the aged human brain. *Journal of Neural Transmission*. 111:1219-1235.

Jensen, P.H., H. Hager, M.S. Nielsen, P. Højrup, J. Gliemann, and R. Jakes. 1999. α-Synuclein Binds to Tau and Stimulates the Protein Kinase A-catalyzed Tau Phosphorylation of Serine Residues 262 and 356. *Journal of Biological Chemistry*. 274:25481-25489.

Jermyn, K., D. Traynor, and J. Williams. 1996. The initiation of basal disc formation in Dictyostelium discoideum is an early event in culmination. *Development*. 122:753-760.

Jones, E., M. Margallo-Iana, V. Prasher, and C. Ballard. 2008. The extended tau haplotype and the age of onset dementia in Down Syndrome. *Dement Geriatr Cogn Disord*. 26:199-202.

Kaiser, D. 1986. Control of multicellular development: *Dictyostelium* and *Myxococcus*. *Ann Rev Genet*. 20:539-566.

Knecht, D.A., and W.F. Loomis. 1987. Antisense RNA inactivation of myosin heavy chain gene expression in Dictyostelium discoideum. *Science*. 236:1081-1086.

Koch, K.V., Y. Reinders, T.-H. Ho, A. Sickmann, and R. Gräf. 2006. Identification and isolation of Dictyostelium microtubule-associated protein interactors by tandem affinity purification. *European Journal of Cell Biology*. 85:1079-1090.

Kopeikina, K.J., G.A. Carlson, R. Pitstick, A.E. Ludvigson, A. Peters, J.I. Luebke, R.M. Koffie, M.P. Frosch, B.T. Hyman, and T.L. Spires-Jones. 2011. Tau accumulation causes mitochondrial distribution deficits in neurons in a mouse model of tauopathy and in human Alzheimer's disease brain. *Am J Pathol*. 179:2071-2082.

Kosik, K., and E. Finch. 1987. MAP2 and tau segregate into dendritic and axonal domains after the elaboration of morphologically distinct neurites: an immunocytochemical study of cultured rat cerebrum. *The Journal of Neuroscience*. 7:3142-3153.

Kosik, K.S. 1993. The Molecular and Cellular Biology of Tau. *Brain Pathology*. 3:39-43.

Kotzbauer, P.T., B.I. Giasson, A.V. Kravitz, L.I. Golbe, M.H. Mark, J.Q. Trojanowski, and V.M.Y. Lee. 2004. Fibrillization of α-synuclein and tau in familial Parkinson's disease caused by the A53T α-synuclein mutation. *Experimental Neurology*. 187:279-288.

Larochelle, D.A., K.K. Vithalani, and A. De Lozanne. 1996. A novel member of the rho family of small GTP-binding proteins is specifically required for cytokinesis. *The journal of cell biology.* 133:1321-1329.

Larochelle, D.A., K.K. Vithalani, and A. De Lozanne. 1997. Role of Dictyostelium racE in cytokinesis: mutational analysis and localization studies by use of green fluorescent protein. *Molecular biology of the cell.* 8:935-944.

Lasagna-Reeves, C., D. Castillo-Carranza, U. Sengupta, A. Clos, G. Jackson, and R. Kayed. 2011. Tau oligomers impair memory and induce synaptic and mitochondrial dysfunction in wild-type mice. *Mol Neurodegen*. 6:39.

Lashuel, H.A., C.R. Overk, A. Oueslati, and E. Masliah. 2013. The many faces of α-synuclein: from structure and toxicity to therapeutic target. *Nature Reviews Neuroscience*. 14:38-48.

Lautenschläger, J., C.F. Kaminski, and G.S. Kaminski Schierle. 2017. α-Synuclein – Regulator of Exocytosis, Endocytosis, or Both? *Trends in Cell Biology*. 27:468-479.

Lee, C.W.C., K.F. Lau, C.C.J. Miller, and P.C. Shaw. 2002. Glycogen synthase kinase-3b-mediated tau phosphorylation in cultured cell lines. *Mol Neurosci*. 14:257-260.

Lee, V., M. Goedert, and J. Trojanowski. 2001. Neurodegenerative tauopathies. *Annu Rev Neurosci*. 24:1121 - 1159.

Lee, V.M.Y., B.I. Giasson, and J.Q. Trojanowski. 2004. More than just two peas in a pod: common amyloidogenic properties of tau and α-synuclein in neurodegenerative diseases. *Trends in Neurosciences*. 27:129-134.

Lewis, J., D.W. Dickson, W.-L. Lin, L. Chisholm, A. Corral, G. Jones, S.-H. Yen, N. Sahara, L. Skipper, D. Yager, C. Eckman, J. Hardy, M. Hutton, and E. McGowan. 2001. Enhanced Neurofibrillary Degeneration in Transgenic Mice Expressing Mutant Tau and APP. *Science*. 293:1487.

Li, X.-C., Y. Hu, Z.-h. Wang, Y. Luo, Y. Zhang, X.-P. Liu, Q. Feng, Q. Wang, K. Ye, G.-P. Liu, and J.-Z. Wang. 2016. Human wild-type full-length tau accumulation disrupts mitochondrial dynamics and the functions via increasing mitofusins. *Scientific reports*. 6:24756-24756.

Lim, M.A., M.A. Selak, Z. Xiang, D. Krainc, R.L. Neve, B.C. Kraemer, J.L. Watts, and R.G. Kalb. 2012. Reduced activity of AMP-activated protein kinase protects against genetic models of motor neuron disease. *The journal of neuroscience : the official journal of the Society for Neuroscience.* 32:1123-1141.

Lin, M.T., and M.F. Beal. 2006. Mitochondrial dysfunction and oxidative stress in neurodegenerative diseases. *Nature*. 443:787-795.

Lindwall, G., and R.D. Cole. 1984. Phosphorylation affects the ability of tau protein to promote microtubule assembly. *Journal of Biological Chemistry*. 259:5301-5305.

Lippa, C.F., M.L. Schmidt, V.M.Y. Lee, and J.Q. Trojanowski. 1999. Antibodies to α-synuclein detect Lewy bodies in many Down's syndrome brains with Alzheimer's disease. *Annals of Neurology*. 45:353-357.

Loomis, W.F. 1982. The development of Dictyostelium discoideum. Academic Press, New York.

Ludolph, A.C., J. Kassubek, B.G. Landwehrmeyer, E. Mandelkow, E.M. Mandelkow, D.J. Burn, D. Caparros-Lefebvre, K.A. Frey, J.G. de Yebenes, T. Gasser, P. Heutink, G. Hoglinger, Z. Jamrozik, K.A. Jellinger, A. Kazantsev, H. Kretzschmar, A.E. Lang, I. Litvan, J.J. Lucas, P.L. McGeer, S. Melquist, W. Oertel, M. Otto, D. Paviour, T. Reum, A. Saint-Raymond, J.C. Steele, M. Tolnay, H. Tumani, J.C. van Swieten, M.T. Vanier, J.P. Vonsattel, S. Wagner, and Z.K. Wszolek. 2009. Tauopathies with parkinsonism: clinical spectrum, neuropathologic basis, biological markers, and treatment options. *Eur J Neurol*. 16:297-309.

Ludtmann, M.H.R., G.P. Otto, C. Schilde, Z.-H. Chen, C.Y. Allan, S. Brace, P.W. Beesley, A.R. Kimmel, P. Fisher, R. Killick, and R.S.B. Williams. 2014. An ancestral non-proteolytic role for presenilin proteins in multicellular development of the social amoeba Dictyostelium discoideum. *Journal of Cell Science*. 127:1576-1584.

Mandelkow, E., M. von Bergen, J. Biernat, and E.M. Mandelkow. 2007. Structural principles of tau and the paired helical filaments of Alzheimer's disease. *Brain Pathol*. 17:83-90.

Mandelkow, E.M., G. Drewes, J. Biernat, N. Gustke, J. Van Lint, J.R. Vandenheede, and E. Mandelkow. 1992. Glycogen synthase kinase-3 and the Alzheimer-like state of microtubule-associated protein tau. *FEBS letters.* 314:315-321.

Mandell, J.W., and G.A. Banker. 1996. A Spatial Gradient of Tau Protein Phosphorylation in Nascent Axons. *The Journal of Neuroscience*. 16:5727-5740.

Maniak, M. 2011. Dictyostelium as a model for human lysosomal and trafficking diseases. *Seminars in cell & developmental biology*. 22:114-119.

Maroteaux, L., J. Campanelli, and R. Scheller. 1988. Synuclein: a neuron-specific protein localized to the nucleus and presynaptic nerve terminal. *The Journal of Neuroscience*. 8:2804-2815.

Martín-González, J., J.-F. Montero-Bullón, and J. Lacal. 2021. Dictyostelium discoideum as a non-mammalian biomedical model. *Microbial Biotechnology*. 14:111-125.

Martin, E.R., W.K. Scott, M.A. Nance, and et al. 2001. Association of single-nucleotide polymorphisms of the tau gene with late-onset parkinson disease. *JAMA*. 286:2245-2250.

Maselli, A., G. Laevsky, and D.A. Knecht. 2002. Kinetics of binding, uptake and degradation of live fluorescent (DsRed) bacteria by Dictyostelium discoideum. *Microbiology*. 148:413-420.

McCullough, L.D., Z. Zeng, H. Li, L.E. Landree, J. McFadden, and G.V. Ronnett. 2005. Pharmacological Inhibition of AMP-activated Protein Kinase Provides Neuroprotection in Stroke. *Journal of Biological Chemistry*. 280:20493-20502.

McMains, V.C., M. Myre, L. Kreppel, and A.R. Kimmel. 2010. Dictyostelium possesses highly diverged presenilin/gamma-secretase that regulates growth and cell-fate specification and can accurately process human APP: a system for functional studies of the presenilin/gamma-secretase complex. *Dis Model Mech*. 3.

Migheli, A., M. Butler, K. Brown, and M. Shelanski. 1988. Light and electron microscope localization of the microtubule- associated tau protein in rat brain. *The Journal of Neuroscience*. 8:1846-1851.

Mondragón-Rodríguez, S., G. Perry, J. Luna-Muñoz, M.C. Acevedo-Aquino, and S. Williams. 2014. Phosphorylation of tau protein at sites Ser 396-404 is one of the earliest events in Alzheimer's disease and Down syndrome. *Neuropathology and applied neurobiology.* 40:121-135.

Mori, H., M. Oda, T. Komori, N. Arai, M. Takanashi, T. Mizutani, S. Hirai, and Y. Mizuno. 2002. Lewy bodies in progressive supranuclear palsy. *Acta Neuropathologica*. 104:273-278.

Murphy, D.D., S.M. Rueter, J.Q. Trojanowski, and V.M. Lee. 2000. Synucleins are developmentally expressed, and alpha-synuclein regulates the size of the presynaptic vesicular pool in primary hippocampal neurons. *The journal of neuroscience : the official journal of the Society for Neuroscience.* 20:3214-3220.

Nakamura, T., H. Yamashita, T. Takahashi, and S. Nakamura. 2001. Activated Fyn Phosphorylates α-Synuclein at Tyrosine Residue 125. *Biochemical and Biophysical Research Communications*. 280:1085-1092.

Näslund, J., A. Schierhorn, U. Hellman, L. Lannfelt, A.D. Roses, L.O. Tjernberg, J. Silberring, S.E. Gandy, B. Winblad, and P. Greengard. 1994. Relative abundance of Alzheimer A beta amyloid peptide variants in Alzheimer disease and normal aging. *Proceedings of the National Academy of Sciences*. 91:8378-8382.

Nellen, W., C. Silan, and R.A. Firtel. 1984. DNA-mediated transformation in Dictyostelium discoideum: regulated expression of an actin gene fusion. *Mol Cell Biol*. 4:2890-2898.

Neumann, M., V. Müller, K. Görner, H.A. Kretzschmar, C. Haass, and P.J. Kahle. 2004. Pathological properties of the Parkinson's disease-associated protein DJ-1 in α-synucleinopathies and tauopathies: relevance for multiple system atrophy and Pick's disease. *Acta Neuropathologica*. 107:489-496.

Noegel, A.A., and M. Schleicher. 2000. The actin cytoskeleton of Dictyostelium: a story told by mutants. *Journal of Cell Science*. 113:759-766.

Oddo, S., A. Caccamo, J.D. Shepherd, M.P. Murphy, T.E. Golde, R. Kayed, R. Metherate, M.P. Mattson, Y. Akbari, and F.M. LaFerla. 2003. Triple-Transgenic Model of Alzheimer's Disease with Plaques and Tangles. *Neuron*. 39:409-421.

Ogawa, S., R. Yoshino, K. Angata, M. Iwamoto, M. Pi, K. Kuroe, K. Matsuo, T. Morio, H. Urushihara, K. Yanagisawa, and Y. Tanaka. 2000. The mitochondrial DNA of Dictyostelium discoideum: complete sequence, gene content and genome organization. *Molecular and general genetics : MGG.* 263:514-519.

Otto, G.P., M.Y. Wu, M. Clarke, H. Lu, O.R. Anderson, H. Hilbi, H.A. Shuman, and R.H. Kessin. 2004. Macroautophagy is dispensable for intracellular replication of Legionella pneumophila in Dictyostelium discoideum. *Molecular microbiology.* 51:63-72.

Pakes, N.K., D.M. Veltman, F. Rivero, J. Nasir, R. Insall, and R.S.B. Williams. 2012. The Rac GEF ZizB regulates development, cell motility and cytokinesis in Dictyostelium. *Journal of Cell Science*. 125:2457-2465.

Paleček, E., V. Ostatná, M. Masařík, C.W. Bertoncini, and T.M. Jovin. 2008. Changes in interfacial properties of α-synuclein preceding its aggregation. *Analyst*. 133:76-84.

Patrizia, R., H.D. A., Z. Victoria, B. Vincenzo, S. Lies-Anne, M. Daniel, R. Rivka, K. Wouter, E.J. H., L.V. M.-Y., T.J. Q., and H. Peter. 2004. DJ-1 colocalizes with tau inclusions: A link between parkinsonism and dementia. *Annals of Neurology*. 55:113-118.

Paula, V.d.J.R.d., F.M. Guimarães, B.S. Diniz, and O.V. Forlenza. 2009. Neurobiological pathways to Alzheimer's disease: Amyloid-beta, TAU protein or both? *Dementia & neuropsychologia.* 3:188-194.

Payton, J.E., R.J. Perrin, D.F. Clayton, and J.M. George. 2001. Protein–protein interactions of alpha-synuclein in brain homogenates and transfected cells. *Molecular Brain Research*. 95:138-145.

Pearce, X.G., S.J. Annesley, and P.R. Fisher. 2019. The Dictyostelium model for mitochondrial biology and disease. *Int J Dev Biol*. 63:497-508.

Pérez, M.J., C. Jara, and R.A. Quintanilla. 2018a. Contribution of Tau Pathology to Mitochondrial Impairment in Neurodegeneration. *Frontiers in Neuroscience*. 12.

Pérez, M.J., K. Vergara-Pulgar, C. Jara, F. Cabezas-Opazo, and R.A. Quintanilla. 2018b. Caspase-Cleaved Tau Impairs Mitochondrial Dynamics in Alzheimer's Disease. *Molecular neurobiology.* 55:1004-1018.

Piccardo, P., D. King, D. Brown, and R.M. Barron. 2017. Variable tau accumulation in murine models with abnormal prion protein deposits. *Journal of the Neurological Sciences*. 383:142-150.

Pollitt, A.Y., and R.H. Insall. 2008. Abi Mutants in Dictyostelium Reveal Specific Roles for the SCAR/WAVE Complex in Cytokinesis. *Current Biology*. 18:203-210.

Prusiner, S.B. 1991. Molecular biology of prion diseases. *Science*. 252:1515+.

Pèrez, M.a.J., C. Jara, and R.A. Quintanilla. 2018. Contribution of Tau Pathology to Mitochondrial Impairment in Neurodegeneration. *Frontiers in neuroscience.* 12:441.

Qureshi, H.Y., and H.K. Paudel. 2011. Parkinsonian neurotoxin 1-Methyl-4-phenyl-1,2,3,6-tetrahydropyridine (MPTP) and α-synuclein mutations promote tau protein phosphorylation at Ser262 and destabilize microtubule cytoskeleton in vitro. *J. Biol Chem*. 286:5055-5068.

Rapoport, M., H.N. Dawson, L.I. Binder, M.P. Vitek, and A. Ferreira. 2002. Tau is essential to β-amyloid-induced neurotoxicity. *Proceedings of the National Academy of Sciences*. 99:6364-6369.

Rappsilber, J., M. Mann, and Y. Ishihama. 2007. Protocol for micro-purification, enrichment, pre-fractionation and storage of peptides for proteomics using StageTips. *Nature Protocols*. 2.

Rehberg, M., and R. Gräf. 2002. Dictyostelium EB1 Is a Genuine Centrosomal Component Required for Proper Spindle Formation. *Molecular Biology of the Cell*. 13:2301-2310.

Rehberg, M., J. Kleylein-Sohn, J. Faix, T.-H. Ho, I. Schulz, and R. Gräf. 2005. Dictyostelium LIS1 Is a Centrosomal Protein Required for Microtubule/Cell Cortex Interactions, Nucleus/Centrosome Linkage, and Actin Dynamics. *Molecular Biology of the Cell*. 16:2759-2771.

Ren, Q.-G., X.-M. Liao, X.-Q. Chen, G.-P. Liu, and J.-Z. Wang. 2007. Effects of tau phosphorylation on proteasome activity. *FEBS Letters*. 581:1521-1528.

Reynolds, C.H., J.C. Betts, W.P. Blackstock, A.R. Nebreda, and B.H. Anderton. 2000. Phosphorylation Sites on Tau Identified by Nanoelectrospray Mass Spectrometry. *Journal of Neurochemistry*. 74:1587-1595.

Rhein, V., X. Song, A. Wiesner, L.M. Ittner, G. Baysang, F. Meier, L. Ozmen, H. Bluethmann, S. Dröse, U. Brandt, E. Savaskan, C. Czech, J. Götz, and A. Eckert. 2009. Amyloid-beta and tau synergistically impair the oxidative phosphorylation system in triple transgenic Alzheimer's disease mice. *Proc Natl Acad Sci USA*. 106.

Rodríguez-Martín, T., I. Cuchillo-Ibáñez, W. Noble, F. Nyenya, B.H. Anderton, and D.P. Hanger. 2013. Tau phosphorylation affects its axonal transport and degradation. *Neurobiol Aging*. 34:2146-2157.

Rosenbusch, K.E., A. Oun, O. Sanislav, S.T. Lay, I. Keizer-Gunnink, S.J. Annesley, P.R. Fisher, A.M. Dolga, and A. Kortholt. 2021. A Conserved Role for LRRK2 and Roco Proteins in the Regulation of Mitochondrial Activity. *Frontiers in Cell and Developmental Biology*. 9.

Roy, B., and G.R. Jackson. 2014. Interactions between Tau and α-synuclein augment neurotoxicity in a Drosophila model of Parkinson's disease. *Human Molecular Genetics*. 23:3008-3023.

Ryan, B.J., S. Hoek, E.A. Fon, and R. Wade-Martins. 2015. Mitochondrial dysfunction and mitophagy in Parkinson's: from familial to sporadic disease. *Trends in biochemical sciences.* 40:200-210.

Savica, R., B.R. Grossardt, J.H. Bower, J. Ahlskog, and W.A. Rocca. 2013. INcidence and pathology of synucleinopathies and tauopathies related to parkinsonism. *JAMA Neurology*. 70:859-866.

Scott, W.K., M.A. Nance, R.L. Watts, and et al. 2001. Complete genomic screen in parkinson disease: Evidence for multiple genes. *JAMA*. 286:2239-2244.

Selkoe, D.J. 1999. Translating cell biology into therapeutic advances in Alzheimer's disease. *Nature*. 399:A23-A31.

Sergeant, N., A. Bretteville, M. Hamdane, M.-L. Caillet-Boudin, P. Grognet, S. Bombois, D. Blum, A. Delacourte, F. Pasquier, E. Vanmechelen, S. Schraen-Maschke, and L. Buee. 2008. Biochemistry of tau in Alzheimer's disease and related neurological disorders. *Expert Rev Proteomic*. 5:207-224.

Shahmoradian, S.H., A.J. Lewis, C. Genoud, J. Hench, T.E. Moors, P.P. Navarro, D. Castaño-Díez, G. Schweighauser, A. Graff-Meyer, K.N. Goldie, R. Sütterlin, E. Huisman, A. Ingrassia, Y.d. Gier, A.J.M. Rozemuller, J. Wang, A.D. Paepe, J. Erny, A. Staempfli, J. Hoernschemeyer, F. Großerüschkamp, D. Niedieker, S.F. El-Mashtoly, M. Quadri, W.F.J. Van Ijcken, V. Bonifati, K. Gerwert, B. Bohrmann, S. Frank, M. Britschgi, H. Stahlberg, W.D.J. Van de Berg, and M.E. Lauer. 2019. Lewy pathology in Parkinson's disease consists of crowded organelles and lipid membranes. *Nature Neuroscience*. 22:1099-1109.

Shahpasand, K., I. Uemura, T. Saito, T. Asano, K. Hata, K. Shibata, Y. Toyoshima, M. Hasegawa, and S. Hisanaga. 2012. Regulation of mitochondrial transport and inter-microtubule spacing by tau phosphorylation at the sites hyperphosphorylated in Alzheimer's disease. *J Neurosci*. 32:2430-2441.

Sharon, R., I. Bar-Joseph, M.P. Frosch, D.M. Walsh, J.A. Hamilton, and D.J. Selkoe. 2003. The Formation of Highly Soluble Oligomers of α-Synuclein Is Regulated by Fatty Acids and Enhanced in Parkinson's Disease. *Neuron*. 37:583-595.

Shiarli, A.M., R. Jennings, J. Shi, K. Bailey, Y. Davidson, J. Tian, E.H. Bigio, B. Ghetti, J.R. Murrell, M.B. Delisle, S. Mirra, B. Crain, P. Zolo, K. Arima, E. Iseki, S. Murayama, H. Kretzschmar, M. Neumann, C. Lippa, G. Halliday, J. MacKenzie, N. Khan, R. Ravid, D. Dickson, Z. Wszolek, T. Iwatsubo, S.M. Pickering-Brown, and D.M.A. Mann. 2006. Comparison of extent of tau pathology in patients with frontotemporal dementia with Parkinsonism linked to chromosome 17 (FTDP-17), frontotemporal lobar degeneration with Pick bodies and early onset Alzheimer's disease. *Neuropath Appl Neuro*. 32:374-387.

Sofou, K., I.F.M. de Coo, E. Ostergaard, P. Isohanni, K. Naess, L. De Meirleir, C. Tzoulis, J. Uusimaa, T. Lönnqvist, L.A. Bindoff, M. Tulinius, and N. Darin. 2018. Phenotype-genotype correlations in Leigh syndrome: new insights from a multicentre study of 96 patients. *Journal of medical genetics : eJMG.* 55:21-27.

Spillantini, M.G., and M. Goedert. 1998. Tau protein pathology in neurodegenerative diseases. *Trends in Neurosciences*. 21:428-433.

Spires-Jones, T.L., W.H. Stoothoff, A. de Calignon, P.B. Jones, and B.T. Hyman. 2009. Tau pathophysiology in neurodegeneration: a tangled issue. *Trends Neurosci*. 32:150-159.

Stelzmann, R.A., N.H. Schnitzlein, and R.F. Murtagh. 1995. An english translation of alzheimer's 1907 paper, "über eine eigenartige erkankung der hirnrinde". *Clinical Anatomy*. 8:429-431.

Stewart, J.B., and P.F. Chinnery. 2015. The dynamics of mitochondrial DNA heteroplasmy: implications for human health and disease. *Nature reviews.* 16:530-542.

Stoothoff, W.H., P.B. Jones, T.L. Spires-Jones, J. D., E. Chhabra, K. Bercury, Z. Fan, H. Xie, B. Bacskai, J. Edd, D. Irimia, and B.T. Hyman. 2009. Differential effect of three-repeat and four-repeat tau on mitochonrial axonal transport. *Journal of Neurochemistry*. 111:417-427.

Strmecki, L., D.M. Greene, and C.J. Pears. 2005. Developmental decisions in Dictyostelium discoideum. *Developmental Biology*. 284:25-36.

Tieu, K. 2011. A Guide to Neurotoxic Animal Models of Parkinson's Disease. *Cold Spring Harbor Perspectives in Medicine*. 1.

Tofaris, G.K., and M.G. Spillantini. 2007. Physiological and pathological properties of α-synuclein. *Cell. Mol. Life Sci.* 64:2194-2201.

Ugalde, C.L., S.J. Annesley, S.E. Gordon, K. Mroczek, M.A. Perugini, V.A. Lawson, P.R. Fisher, D.I. Finkelstein, and A.F. Hill. 2020. Misfolded α-synuclein causes hyperactive respiration without functional deficit in live neuroblastoma cells. *Disease models & mechanisms : DMM.* 13.

Vanhelmont, T., T. Vandebroek, A.D. Vos, D. Terwel, K. Lamaire, J. Anandhakumar, V. Franssens, E. Swinnen, F.V. Leuven, and J. Winderickx. 2010. Serine-409 phosphorylation and oxidative damage define aggregation of human protein tau in yeast. *FEMS Yeast Res*. 10:992-1005.

Vingtdeux, V., P. Davies, D.W. Dickson, and P. Marambaud. 2011. AMPK is abnormally activated in tangle- and pre-tangle-bearing neurons in Alzheimer's disease and other tauopathies. *Acta Neuropathol*. 121:337-349.

Wang, X., W. Wang, L. Li, G. Perry, H.G. Lee, and X. Zhu. 2014. Oxidative stress and mitochondrial dysfunction in Alzheimer's disease. *Biochimica et biophysica acta*. 1842:1240-1247.

Waxman, E.A., and B.I. Giasson. 2011. Induction of intracellular tau aggregation is promoted by alpha-synuclein seeds and provides novel insights into the hyperphosphorylation of tau. *J Neurosci*. 31:7604-7618.

Wersinger, C., and A. Sidhu. 2005. Disruption of the Interaction of α-Synuclein with Microtubules Enhances Cell Surface Recruitment of the Dopamine Transporter. *Biochemistry.* 44:13612-13624.

Wilczynska, Z., and P.R. Fisher. 1994. Analysis of a Complex Plasmid Insertion in a Phototaxis-Deficient Transformant of Dictyostelium discoideum Selected on a Micrococcus luteus Lawn. *Plasmid*. 32:182-194.

Williams, D., and W. Lee. 2012. Clinical features and criteria for the diagnosis of progressive supranuclear palsy. *Neurodegen Dis Man*. 2:125.

Wills, J., J. Jones, T. Haggerty, V. Duka, J.N. Joyce, and A. Sidhu. 2010. Elevated tauopathy and alpha-synuclein pathology in postmortem Parkinson's disease brains with and without dementia. *Experimental Neurology*. 225:210-218.

Wischik, C.M., M. Novak, H.C. Thogersen, P.C. Edwards, M.J. Runswick, R. Jakes, J.E. Walker, C. Milstein, M. Roth, and A. Klug. 1988. Isolation of a fragment of tau derived from the core of the paired helical filament of Alzheimer disease. *Proc Natl Acad Sci U S A*. 85:4506-4510.

Xie, A.J., T.Y. Hou, W. Xiong, H.Z. Huang, J. Zheng, K. Li, H.Y. Man, Y.Z. Hu, Z.T. Han, H.H. Zhang, N. Wei, J.Z. Wang, D. Liu, Y. Lu, and L.Q. Zhu. 2019. Tau overexpression impairs neuronal endocytosis by decreasing the GTPase dynamin 1 through the miR-132/MeCP2 pathway. *Aging Cell*. 18:e12929.

Yan, X., R.-L. Uronen, and H.J. Huttunen. 2020. The interaction of α-synuclein and Tau: A molecular conspiracy in neurodegeneration? *Seminars in cell & developmental biology.* 99:55-64.

Zang, J.-H., G. Cavet, J.H. Sabry, P. Wagner, S.L. Moores, and J.A. Spudich. 1997. On the Role of Myosin-II in Cytokinesis: Division of Dictyostelium Cells under Adhesive and Nonadhesive Conditions. *Molecular biology of the cell.* 8:2617-2629.

Zheng-Fischhöfer, Q., J. Biernat, E.M. Mandelkow, S. Illenberger, R. Godemann, and E. Mandelkow. 1998. Sequential phosphorylation of Tau by glycogen synthase kinase-3beta and protein kinase A at Thr212 and Ser214 generates the Alzheimer-specific epitope of antibody AT100 and requires a paired-helical-filament-like conformation. *Eur J Biochem*. 252:542-552.

Zhou, R.M., Y.X. Huang, X.L. Li, C. Chen, Q. Shi, G.R. Wang, C. Tian, Z.Y. Wang, Y.Y. Jing, C. Gao, and X.P. Dong. 2010. Molecular interaction of α-synuclein with tubulin influences on the polymerization of microtubule in vitro and structure of microtubule in cells. *Molecular biology reports.* 37:3183-3192.

# APPENDIX 1 CHEMICALS AND SUPPLIERS

| | |
|---|---|
| ACES | Sigma-Aldrich |
| Acetic acid | Ajax chemicals |
| Agar (Technical NO. 3) | Oxoid |
| Agarose | Promega |
| Ampicillin | Roche |
| Ammonium persulfate (APS) | Sigma-Aldrich |
| Antimycin A | Sigma-Aldrich |
| Bacteriological peptone | Oxoid |
| Bacto® proteose peptone | Difco Laboratories |
| Bacto® tryptone | Difco Laboratories |
| Bacto® yeast extract | Difco Laboratories |
| BHAM (benzohydroxamic acid) | Sigma-Aldrich |
| Boric acid | Sigma-Aldrich |
| Bovine serum albumin | Sigma-Aldrich |
| Bromophenol blue | Sigma-Aldrich |
| Calcium chloride | Ajax chemicals |
| CCCP (carbonyl cyanide 3-chlorophenol hydrazone) | Sigma-Aldrich |
| Charcoal activated | Sigma-Aldrich |
| Chloroform | Ajax |
| Chloramphenicol | Sigma-Aldrich |
| Coomassie Brilliant Blue | Sigma-Aldrich |
| D-glucose anhydrous | BHD |
| DCCD (N,N0-dicyclohexylcarbodimide) | Sigma-Aldrich |
| Dimethyl sulphoxide (DMSO) | Ajax chemicals |
| DNazol | Invitrogen |
| Ethanol (absolute) | May & Baker Australia |
| Ethidium bromide | Sigma-Aldrich |
| Ethylenediamine-tetracetic acid (EDTA) | Sigma-Aldrich |
| Fluorescein isothiocyanate (FITC)-dextran | Sigma-Aldrich |
| Gene Ruler™ 1kb DNA ladder | Thermo Fisher Scientific |
| Geneticin | Gibco |
| Glacial acetic acid | Roche |

| | |
|---|---|
| Glycerol | Ajax Chemical Co. |
| Glycine | APS |
| HEPES(N-Hydroxyethylpiperazine-N-2-ehtanesuphonic acid) | Sigma-Aldrich |
| HL-5 medium without glucose | Formedium |
| Horse Blood Serum | Sigma-Aldrich |
| Hydrochloric acid | Ajax Chemicals |
| Isopropanol | Ajax Chemicals |
| L-cystine | Sigma-Aldrich |
| Magnesium acetate | Ajax Chemicals |
| Magnesium chloride | Ajax Chemicals |
| Magnesium sulphate | Ajax Chemicals |
| Corning®Matrigel® | Sigma-Aldrich |
| MES (2-(N-Morpholino) ethane-sulphonic acid) | Sigma-Aldrich |
| Methanol | Ajax Chemicals |
| Mineral oil | Sigma-Aldrich |
| Nonidet P40 substitute (NP40) | Sigma-Aldrich |
| PAP pen | Abcam |
| Phenol | Sigma-Aldrich |
| Potassium acetate | Ajax |
| Potassium chloride | Ajax |
| Potassium di-hydrogen orthophosphate | Ajax Chemicals |
| Potassium hydroxide | APS |
| Proteose peptone | Difco |
| Potassium phosphate | APS |
| Rotenone | Sigma-Aldrich |
| SIH medium | Formedium |
| Skim milk powder | Bonland Dairies |
| SM agar | Formedium |
| Sodium acetate | BHD |
| Sodium azide | Sigma-Aldrich |
| Sodium chloride | Ajax Chemicals |
| Sodium di-hydrogen orthophosphate | Ajax Chemicals |
| Sodium dodecyl sulphate (SDS) | BHD |

| | |
|---|---|
| Sodium hydroxide | Ajax Chemicals |
| Sodium malate | Sigma-Aldrich |
| Sodium pyruvate | Sigma-Aldrich |
| Streptomycin | Roche |
| Sucrose | Ajax |
| TEMED | Sigma |
| Tetracycline | ICN |
| Tris | Sigma-Aldrich |
| Triton® X-100 | Sigma-Aldrich |
| Tryptone | Difco |
| Tween 20® (polyoxyethylene-sorbitan) | ICN |
| Ultramount | Thermo fisher Scientific |
| Yeast Extract | Sigma-Aldrich/Oxoid |

## Full names of suppliers

Ajax Chemicals Pty. Ltd., Auburn, NSW, AUS

APS Pty. Ltd., Seven Hills, NSW, AUS

BDH Chemicals Pty. Ltd., Kilysth, VIC, AUS

Bio-Rad Australia Pty. Ltd., Regents Park, NSW, AUS

Difco Laboratories Pty. Ltd., Detroit, MII, USA

ICN Biochemicals Inc., Aurora, OH, USA

Invitrogen Australia Pty. Ltd., Mount Waverley, VIC, AUS Jencons Australia, Noble Park, VIC, AUS

May & Baker Australia Pty. Ltd., West Footscray, VIC, AUS

Molecular Research Centre Inc., Cincinnati, OH, USA

Oxoid Ltd., Basingstoke, Hampshire, England, GB

Promega Corp., Madison, WI, USA

Roche Pty. Ltd., Castle Hill, NSW, AUS

Sigma-Aldrich Chemical Company Pty. Ltd., Castle Hill, NSW, AUS

Thermo Fisher Scientific, Scoresby, VIC, AUS TPS Pty. Ltd., Springwood, QLD, AUS

# APPENDIX 2 CHEMICAL COMPOSITION OF MEDIA AND BUFFERS

**A2.1 Media**

| Media | Composition | Chemical |
|---|---|---|
| **Bacterial culture** | | |
| Luria Broth | 1.0 % (w/v) | Difco Bacto tryptone |
| | 0.5 % (w/v) | Difco Bacto yeast extract |
| | 86 mM NaCl | NaCl |
| | 10 mM NaOH | NaOH |
| Luria Agar | Luria Broth | |
| | 1 % (w/v) | Oxoid agar |
| SOC | 0.25 % (w/v) | Difco yeast extract |
| | 2.0 % (w/v) | Difco bacto tryptone |
| | 10 mM | NaCl |
| | 2.5 mM | KCl |
| | 10 mM | $MgCl_2$ |
| | 10 mM | $MgSO_4$ |
| | 20 mM | Glucose |

***D. discoideum* medium**

| | | |
|---|---|---|
| Axenic medium (HL-5) | 1.0 % (w/v) | Difco Proteose Peptone |
| | 1.0 % (w/v) | Glucose |
| | 0.5 % (w/v) | Difco Yeast extract |
| | 2.8 mM | $Na_2HPO_4.2H_2O$ |
| | 2.6 mM | $KH_2PO_4$ |
| MES-HL-5 | 6 mM | MES |
| | 1.0 % (w/v) | Glucose |
| | 1.0 % (w/v) | Bacteriological peptone |
| | 0.6 % (w/v) | Yeast extract |
| Standard medium (SM) | 1.0 % (w/v) | Oxoid bacteriological peptone |
| | 1.0 % (w/v) | Oxoid agar |
| | 1.0 % (w/v) | Glucose |
| | 0.1 % (w/v) | Oxoid yeast extract |
| | 16.2 mM | $KH_2PO_4$ |
| | 5.8 mM | $K_2HPO_4$ |
| | 4.1 mM | $MgSO_4.7H_2O$ |
| Sterile saline (SS) | 10 mM | NaCl |
| | 10 mM | KCl |
| | 2.7 mM | $CaCl_2$ |

| | | |
|---|---|---|
| Charcoal Agar | 0.5 % (w/v) | Activated charcoal |
| | 1-1.5 % (w/v) | Oxoid agar |
| Water Agar | 1.5 % (w/v) | Oxoid agar |
| Normal agar | 2 % (w/v) | Difco bacto agar |
| | 0.1 % (w/v) | Difco bacto peptone |
| | 0.11 % (w/v) | Glucose |
| | 14.7 mM | $KH_2PO_4$ |
| | 3 mM | $Na_2HPO_4$ |

**A2.2 Composition of buffers**

**General**

| | | |
|---|---|---|
| Coomassie Blue | 50 % (v/v) | Ethanol |
| | 40 % (v/v) | $dH_2O$ |
| | 10 % (v/v) | Acetic acid |
| | 0.6 % (w/v) | Brilliant blue |
| *Dictyostelium* storage buffer | 45 % (v/v) | Horse Blood Serum |
| | 45 % (v/v) | SS |
| | 10 % (v/v) | DMSO |

| | | |
|---|---|---|
| EDTA | 0.5 M | EDTA |
| Ethidium bromide stock | 1 mg $ml^{-1}$ | Ethidium bromide |
| Phosphate Buffer | 110 mM | $Na_2HPO_4$ |
| | 146 mM | $KH_2PO_4$ |
| TE (pH 8.0) | 10 mM | Tris-HCl |
| | 1 mM | EDTA |

**Alkaline Lysis Minipreps**

| | | |
|---|---|---|
| Resuspension buffer | 10 mM | EDTA |
| | 50 mM | Tris-HCL (pH 8.0) |
| | 100 g $ml^{-1}$ | RNAse A |
| Lysis Solution | 0.2 M | Sodium hydroxide |
| | 1.0 % (w/v) | SDS |
| Neutralisation solution (pH 4.8) | 5 M | Potassium acetate |

**Restriction digests**

| | | |
|---|---|---|
| One-Phor-All buffer (10X) | 100 mM | Tris-acetate (pH 7.5) |
| | 100 mM | Magnesium acetate |
| | 500 mM | Potassium acetate |
| | 500 mM | Sodium chloride |

**Ligation of DNA**

| | | |
|---|---|---|
| 10x Ligation Buffer (pH 7.5) | 300 mM | Tris-HCL |
| | 100 mM | Magnesium chloride |
| | 100 mM | NaCl |
| | 100 mM | ATP |

**Polymerase Chain Reaction**

| | | |
|---|---|---|
| Taq polymerase enzyme | 5 U $ml^{-1}$ | |
| PCR Buffer (10x) (pH 4.8) | 500 mM | Potassium chloride |
| | 200 mM | Tris-HCL |
| Magnesium Chloride | 50 mM | $MgCl_2$ |
| DNA polymerization Mix (20 mM dNTPs) | 5 mM | dATP |
| | 5 mM | dCTP |
| | 5 mM | dGTP |
| | 5 mM | dTTP |

**qPCR**

| | | |
|---|---|---|
| iQTM SYBR® Green Supermix | 100 mM | KCL |
| | 40 mM | Tris-HCL |
| | 0.4 mM | dATP |
| | 0.4 mM | dCTP |
| | 0.4 mM | dGTP |
| | 0.4 mM | dTTP |
| | 50 U $ml^{-1}$ | *iTaq* DNA polymerase |
| | 6 mM | $MgCl_2$ |
| | 20 nM | fluorescein |
| | | SYBR Green 1 |

**Agarose Gel Electrophoresis**

| | | |
|---|---|---|
| Agarose Gel | 1-2% (w/v) | Agarose |
| | 10 % (v/v) | TBE (10x) |
| | 90 % (v/v) | Distilled water |
| | 0.5 µg $ml^{-1}$ | Ethidium Bromide |
| Loading Dye (SBE) | 50 % (w/v) | Sucrose |
| | 0.15 % (w/v) | Bromophenol blue |
| | 0.2 M | EDTA |
| 10x Running Buffer (10x TBE) | 0.89 M | Tris-HCL |
| | 0.89 M | Boric acid |
| | 0.02 M | EDTA |

| | | |
|---|---|---|
| Molecular weight marker | 500 mg $ml^{-1}$ | 1kb Gene Ruler DNA ladder |

**<u>*D. discoideum* Transformation</u>**

| | | |
|---|---|---|
| 2x HBS (Filter sterilised) | 42 mM | HEPES, pH 7.05 |
| | 274 mM | NaCl |
| | 9.4 mM | KCl |
| | 1.3 mM | $NaH_2PO_4.2H_2O$ |
| | 0.2 % (w/v) | Glucose |
| Calcium Chloride Solution | 2 M | $CaCl_2.2H_2O$ |
| Glycerol solution | 60 % (v/v) | Glycerol |

**<u>Staining of *D. discoideum* slug trails</u>**

| | | |
|---|---|---|
| Coomassie blue | 0.3 % (w/v) | Coomassie blue |
| | 50 % (v/v) | Ethanol |
| | 10 % (v/v) | Acetic acid |
| | 40 % (v/v) | $dH_2O$ |

**<u>Phagocytosis</u>**

| | | |
|---|---|---|
| Phosphate buffer 20 mM | 2.35 mM | $Na_2HPO_4$ |
| | 17.65 mM | $KH_2PO_4$ |
| Sodium Azide | 40 mM | Sodium Azide in Phosphate buffer |

**Pinocytosis**

| | | |
|---|---|---|
| FITC-dextran | 20 mg $ml^{-1}$ | FITC-dextran in HL-5 |
| Sorensen's phosphate buffer (pH 6.0) | 2 mM | $Na_2HPO_4.2H_2O$ |
| | 14.67 mM | $KH_2PO_4$ |
| Sodium Phosphate- Triton-X100 | 0.25 % (v/v) | Triton-X 100 |
| | 100 mM | $Na_2HPO_4$ |

***L. pneumophila* infection assay**

| | | |
|---|---|---|
| BYCE agar | 1 % (w/v) | ACES [N-(2-acetamido)-2-aminoethanesulfonic acid] |
| | 1 % (w/v) | Yeast extract (pH 6.9) |
| | 0.2 % (w/v) | Activated charcoal |
| | 1.5 % (w/v) | Agar |
| | 0.04 % (w/v) | L-cystein* |
| | 0.25 % (w/v) | $Fe(NO_3)_3.9H_2O$* |

*Filter sterilised and added to the autoclaved medium when cooled to 60 °C

| | | |
|---|---|---|
| Sorensen 1xC buffer | 17 mM | $KH_2PO_4/Na_2PO_4$ |
| | 50 µM | $CaCl_2$, pH 6.0 |

| | | |
|---|---|---|
| MB medium | 0.7 % (w/v) | Yeast extract |
| | 1.4 % (w/v) | Proteose peptone |
| | 0.062 % (w/v) | $Na_2HPO_4.2H_2O$ |
| | 0.049 % (w/v) | $KH_2PO_4$, pH 6.9 |

**Immunofluorescence microscopy**

| | | |
|---|---|---|
| LoFlo HL-5 medium (Filter sterilised) | 0.385 % (w/v) | D-Glucose |
| | 0.178 % (w/v) | Proteose peptone |
| | 0.045 % (w/v) | Yeast extract |
| | 0.0485 % (w/v) | $KH_2PO_4$ |
| | 0.12 % (w/v) | $Na_2HPO_4.12H_2O$ |
| Phosphate buffer (pH 6.5) | 12 mM | $Na_2HPO_4$ |
| | 12 mM | $Na_2H2PO_4$ |
| 10x PBS (pH 7.4) | 1.38 M | NaCl |
| | 27 mM | KCl |
| | 43 mM | $Na_2HPO_4.17H_2O$ |
| | 14.7 mM | $KH_2PO_4$ |
| Blocking buffer (In 1x PBS) | 0.05 % (v/v) | Tween 20 |
| | 1 % (w/v) | Bovine Serum Albumin |
| | 1 % (v/v) | Cold water fish skin gelatine |
| | 0.02 % (w/v) | Sodium azide |

**Polyacrylamide gel electrophoresis**

| | | |
|---|---|---|
| Running buffer | 25 mM | Tris base |
| | 129 mM | Glycine |
| | 0.01 % (w/v) | SDS |

**Western blotting and detection**

| | | |
|---|---|---|
| Laemmli 2x sample buffer | 4 % (w/v) | SDS |
| | 20 % (v/v) | Glycerol |
| | 0.004 % (w/v) | Bromophenol blue |
| | 0.125 M | Tris-Cl (pH 6.8) |
| Transfer buffer | 192 mM | Glycine |
| | 25 mM | Tris |
| | 20 % (v/v) | Methanol |
| TBS (pH 7.5) | 20 mM | Tris-Cl |
| | 137 mM | NaCl |
| TBST (TBS Tween) (pH 7.5) | 20 mM | Tris-Cl |
| | 137 mM | NaCl |
| | 0.05 % (v/v) | Tween 20 |
| Blocking buffer | 10 % (w/v) | Skim milk powder in TBS |

# APPENDIX 3 ENZYMES AND EXPERIMENTAL KITS

### A3.1 Enzymes

| Component | Supplier |
|---|---|
| DNase I | Roche |
| Restriction endonucleases | Promega |
| RNAse A | Roche |
| Taq DNA polymerase | Invitrogen |
| T4 DNA ligase | Promega |

### A3.2 Kits

| Component | Supplier |
|---|---|
| Duolink™ *in situ* detection kit | Sigma-Aldrich |
| PureLink™ HiPure Plasmid Filter Purification Kit | Invitrogen |
| PureLink™ HiPure Plasmid Filter Maxiprep Kit | Invitrogen |
| PureLink™ Quick Gel Extraction Kit | Invitrogen |
| PureLink™ HiPure precipitator module | Invitrogen |

# APPENDIX 4 TAU GENE SEQUENCE

Complete gene sequence of Tau, showing restriction sites (*Cla*I and *Xho*I) as well as internal cut sites (*Hind*III and *Sac*I) as cloned into pPROF267 in order to create pPROF665

**ATCGAT**ATGGCTGAGCCCCGCCAGGAGTTCGAAGTGATGGAAGATCACGCTGGGACGTACGGGTGGGGGAC
AGGAAAGATCAGGGGGGCTACACCATGCACCAAGACCAAGAGGGTGACACGGACGCTCCTGAAAGAATCTC
CCCTGCAGACCCCCACTGAGGACGGATCTGAGGAACCGGGCTCTGAAACCTCTGATGCTAAGAGCACTCCAA
CAGCGGAAGATGTGACAGCACCCTTAGTGGATGAGG**GAGCTC**CCGGCAAGCAGGCTGCCGCGCAGCCCCAC
ACGGAGATCCCAGAAGGAACCACAGCTGAAGAAGCAGGCATTGGAGACACCCCCAGCCTGGAAGACGAAGC
TGCTGGTCACGTGACCCAAGCTCGCATGGTCAGTAAAAGCAAAGACGGGACTGGAAGCGATGACAAAAAAG
CCAAGGGGGCTGATGGTAAAACGAAGATCGCCACACCGCGGGGAGCAGCCCCTCCAGGCCAGAAGGGCCAG
GCCAACGCCACCAGGATTCCAGCAAAAACCCCGCCCGCTCCAAAGACACCACCCAGCTCTGGTGAACCTCCAA
AATCAGGGGATCGCAGCGGCTACAGCAGCCCCGGCTCCCCAGGCACTCCCGGCAGCCGCTCCCGCACCCCGT
CCCTTCCAACCCCACCCACCCGGGAGCCCAAGAAGGTGGCAGTGGTCCGTACTCCACCCAAGTCGCCGTCTTC
CGCCAAGAGCCGCCTGCAGACAGCCCCCGTGCCCATGCCAGACCTGAAGAATGTCAAGTCCAAGATCGGCTC
CACTGAGAACCTGAAGCACCAGCCGGGAGGCGGGAAGGTGCAGATAATTAATAAGAAGCTGGATCTTAGCA
ACGTCCAGTCCAAGTGTGGCTCAAAGGATAATATCAAACACGTCCCGGGAGGCGGCAGTGTGCAAATAGTCT
ACAAACCAGTTGACCTGAGCAAGGTGACCTCCAAGTGTGGCTCATTAGGCAACATCCATCATAAACCAGGAG
GTGGCCAGGTGGAAGTAAAATCTGAG**AAGCTT**GACTTCAAGGACAGAGTCCAGTCGAAGATTGGGTCCCTGG
ACAATATCACCCACGTCCCTGGCGGAGGAAATAAAAAGATTGAAACCCACAAGCTGACCTTCCGCGAGAACG
CCAAAGCCAAGACAGACCACGGGGCGGAGATCGTGTACAAGTCGCCAGTGGTGTCTGGGGACACGTCTCCAC
GGCATCTCAGCAATGTCTCCTCCACCGGCAGCATCGACATGGTAGACTCGCCCCAGCTCGCCACGCTAGCTGA
CGAGGTGTCTGCCTCCCTGGCCAAGCAGGGTTTGTGA**CTCGAG**

Restriction enzyme cut sites in bold
**ATCGAT –** *Cla*I (5')

**CTCGAG –** *Xho*I (3')

**GAGCTC –** *Sac*I (248 bp)

**AAGCTT –** *Hind*III (1027 bp)

# APPENDIX 5: EXPERIMENTAL CONDITIONS AND COMPONENTS

**Restriction Enzyme Reactions**

| | |
|---|---|
| Reaction Components | DNA<br>Enzyme (2-10 µl)<br>Buffer for enzyme (1x)<br>$dH_20$<br>(Total volumes varied between 10-100 µl and amounts of each component depended on volume) |
| Reaction conditions | Incubation for 1-2.5 hr at 37˚C<br>Reaction stopped with the addition of 3x SBE |

**DNA Ligation**

| | |
|---|---|
| Ligation components | Vector<br>Insert<br>1 U T4 DNA ligase<br>$dH_2O$<br>(Total volume 30 µl) |
| Ligation conditions | Incubate at 16 ˚C for 16 hr |

# APPENDIX 6 *LEGIONELLA* VIABLE COUNTS CORRESPONDING TO VALUES OF $OD_{600}$

**A6.1**

| **$OD_{600}$** | **Bacteria/ml x $10^9$** |
|---|---|
| 0.47 | 0.36 |
| 0.52 | 0.39 |
| 0.57 | 0.43 |
| 0.63 | 0.47 |
| 0.69 | 0.51 |
| 0.76 | 0.56 |
| 0.84 | 0.62 |
| 0.92 | 0.68 |
| 1.01 | 0.74 |
| 1.10 | 0.82 |
| 1.20 | 0.90 |
| 1.31 | 0.99 |
| 1.42 | 1.08 |
| 1.54 | 1.18 |
| 1.66 | 1.29 |
| 1.79 | 1.41 |
| 1.93 | 1.54 |
| 2.07 | 1.69 |
| 2.22 | 1.84 |
| 2.37 | 2.00 |
| 2.53 | 2.17 |
| 2.69 | 2.36 |
| 2.87 | 2.56 |
| 3.04 | 2.77 |
| 3.23 | 3.00 |
| 3.42 | 3.24 |
| 3.61 | 3.50 |
| 3.81 | 3.78 |
| 4.02 | 4.07 |

# APPENDIX 7 PROTEIN ANNOTATIONS TAKEN FROM STRING

**Table A7.1: Tau up-regulated proteins**

*Proteins with multiple colours involved in more than one process.

**Up-regulated processes**

Proteolysis

Positive regulation of RNA polymerase II transcription preinitiation complex

Translation

tRNA aminoacylation for protein translation

Other

Disconnected node

| #node | Identifier | Annotation | Fold Change |
|---|---|---|---|
| DDB0168140 | DDB0168140 | annotation not available | 2.68 |
| DDB0190682 | DDB0233387 | annotation not available | 1.92 |
| DDB0191832 | DDB0233013 | annotation not available | 2.14 |
| DDB0192224 | DDB0192224 | annotation not available | 2.0 |
| DDB0204927 | DDB0204927 | annotation not available | 2.32 |
| DDB0217073 | DDB0234178 | annotation not available | 1.77 |
| DDB0218284 | DDB0218284 | annotation not available | 2.55 |
| DDB0230005 | DDB0230005 | CBS domain-containing protein DDB_G0289609 | 2.04 |
| DDB0230064 | DDB0230064 | annotation not available | 2.92 |
| DDB0233715 | DDB0233715 | annotation not available | 1.74 |
| argS1 | DDB0231324 | Probable arginine--tRNA ligase, cytoplasmic; Forms part of a macromolecular complex that catalyzes the attachment of specific amino acids to cognate tRNAs during protein synthesis | 3.29 |
| asns | DDB0230140 | Probable asparagine synthetase [glutamine-hydrolyzing] | 2.36 |

| | | | |
|---|---|---|---|
| aspS1 | DDB0231308 | Aspartyl-tRNA synthetase, cytoplasmic 1; Belongs to the class-II aminoacyl-tRNA synthetase family. Type 2 subfamily | 1.56 |
| cinB | DDB0220110 | Vegetative-specific protein H5; Belongs to the 'GDXG' lipolytic enzyme family | 4.12 |
| eif3L | DDB0233946 | Eukaryotic translation initiation factor 3 subunit L; Component of the eukaryotic translation initiation factor 3 (eIF-3) complex, which is involved in protein synthesis of a specialized repertoire of mRNAs and, together with other initiation factors, stimulates binding of mRNA and methionyl-tRNAi to the 40S ribosome. The eIF-3 complex specifically targets and initiates translation of a subset of mRNAs involved in cell proliferation | 1.75 |
| erf3 | DDB0214990 | Eukaryotic peptide chain release factor GTP-binding subunit; Involved in translation termination. Stimulates the activity of erf1. Binds guanine nucleotides (By similarity) | 1.78 |
| fbl | DDB0267046 | rRNA 2'-O-methyltransferase fibrillarin; S-adenosyl-L-methionine-dependent methyltransferase that has the ability to methylate both RNAs and proteins. Involved in pre-rRNA processing. Utilizes the methyl donor S-adenosyl-L- methionine to catalyze the site-specific 2'-hydroxyl methylation of ribose moieties in pre-ribosomal RNA. Site specificity is provided by a guide RNA that base pairs with the substrate. Methylation occurs at a characteristic distance from the sequence involved in base pairing with the guide RNA. Also acts as a protein methyltransferase by mediating methylation of 'G [...] | 2.83 |
| fpa2 | DDB0266780 | SCF ubiquitin ligase complex protein SKP1bSCF ubiquitin ligase complex protein SKP1b(4-162)SCF ubiquitin ligase complex protein SKP1b(6-162) | 2.05 |

| | | | |
|---|---|---|---|
| g6pd-1 | DDB0238739 | Glucose-6-phosphate 1-dehydrogenase; Catalyzes the rate-limiting step of the oxidative pentose-phosphate pathway, which represents a route for the dissimilation of carbohydrates besides glycolysis. The main function of this enzyme is to provide reducing power (NADPH) and pentose phosphates for fatty acid and nucleic acid synthesis (By similarity) | 1.57 |
| gluS | DDB0231321 | Probable glutamate--tRNA ligase, cytoplasmic; Catalyzes the attachment of glutamate to tRNA(Glu) in a two-step reaction: glutamate is first activated by ATP to form Glu-AMP and then transferred to the acceptor end of tRNA(Glu); Belongs to the class-I aminoacyl-tRNA synthetase family. Glutamate--tRNA ligase type 2 subfamily | 1.35 |
| gpaD | DDB0216411 | Guanine nucleotide-binding protein alpha-4 subunit; Guanine nucleotide-binding proteins (G proteins) are involved as modulators or transducers in various transmembrane signaling systems. G alpha-4 plays a role in morphogenesis of the multicellular structure | 1.53 |
| hisS | DDB0231332 | Histidine--tRNA ligase, cytoplasmic; Histidyl-tRNA synthetase, cytoplasmic; Belongs to the class-II aminoacyl-tRNA synthetase family | 1.78 |
| hspC | DDB0185048 | 32 kDa heat shock protein | 5.98 |
| leuS | DDB0231253 | Leucine--tRNA ligase, cytoplasmic; Leucyl-tRNA synthetase, cytoplasmic; Belongs to the class-I aminoacyl-tRNA synthetase family | 1.36 |
| ndkB | DDB0238334 | Nucleoside diphosphate kinase, cytosolic; Major role in the synthesis of nucleoside triphosphates other than ATP | 1.52 |
| nop5 | DDB0305289 | Nucleolar protein 58; Required for 60S ribosomal subunit biogenesis | 2.01 |
| nploc4 | DDB0233722 | Nuclear protein localization protein 4 homolog; May be part of a complex that binds ubiquitinated proteins | 1.99 |

| | | | |
|---|---|---|---|
| | | and that is necessary for the export of misfolded proteins from the ER to the cytoplasm, where they are degraded by the proteasome | |
| ppkA | DDB0216190 | Polyphosphate kinase; Catalyzes the reversible transfer of the terminal phosphate of ATP to form a long-chain polyphosphate (polyP). Produces polyP in a broad range of chain lengths (50-300 Pi residues). Involved in development (growth and fruiting body formation), sporulation, phagocytosis, cell division and the late stages of cytokinesis | 1.87 |
| psmC1 | DDB0232964 | 26S proteasome regulatory subunit 4 homolog; The 26S proteasome is involved in the ATP-dependent degradation of ubiquitinated proteins. The regulatory (or ATPase) complex confers ATP dependency and substrate specificity to the 26S complex (By similarity). Plays an important role in regulating both growth and multicellular development | 6.12 |
| psmC2 | DDB0232966 | 26S proteasome regulatory subunit 7; The 26S proteasome is involved in the ATP-dependent degradation of ubiquitinated proteins. The regulatory (or ATPase) complex confers ATP dependency and substrate specificity to the 26S complex (By similarity) | 2.99 |
| psmC3 | DDB0232967 | 26S proteasome regulatory subunit 6A homolog; The 26S proteasome is involved in the ATP-dependent degradation of ubiquitinated proteins. The regulatory (or ATPase) complex confers ATP dependency and substrate specificity to the 26S complex (By similarity) | 1.89 |
| psmC6 | DDB0232968 | 26S proteasome regulatory subunit 10B; The 26S proteasome is involved in the ATP-dependent degradation of ubiquitinated proteins. The regulatory (or ATPase) complex confers ATP dependency and | 1.54 |

| | | | |
|---|---|---|---|
| | | substrate specificity to the 26S complex (By similarity) | |
| psmD14 | DDB0191298 | 26S proteasome non-ATPase regulatory subunit 14; Metalloprotease component of the 26S proteasome that specifically cleaves 'Lys-63'-linked polyubiquitin chains. The 26S proteasome is involved in the ATP-dependent degradation of ubiquitinated proteins. The function of the 'Lys-63'-specific deubiquitination of the proteasome is unclear (By similarity) | 1.46 |
| psmD4 | DDB0232981 | 26S proteasome non-ATPase regulatory subunit 4; Binds and presumably selects ubiquitin-conjugates for destruction | 1.77 |
| psmD7 | DDB0232987 | 26S proteasome non-ATPase regulatory subunit 7; Acts as a regulatory subunit of the 26S proteasome which is involved in the ATP-dependent degradation of ubiquitinated proteins | 1.68 |
| pyrK | DDB0191367 | UMP-CMP kinase; Catalyzes the phosphorylation of pyrimidine nucleoside monophosphates at the expense of ATP. Plays an important role in de novo pyrimidine nucleotide biosynthesis. Has preference for UMP and CMP as phosphate acceptors; Belongs to the adenylate kinase family. UMP-CMP kinase subfamily | 1.61 |
| rbrA | DDB0191418 | Probable E3 ubiquitin-protein ligase rbrA; Might act as an E3 ubiquitin-protein ligase. Appears to be required for normal cell-type proportioning and cell sorting during multicellular development. In addition to being necessary for a normal percentage of prestalk cells and the organization of the slug, rbrA is also necessary for spore cell viability | 1.51 |
| tbpB | DDB0191435 | 26S proteasome regulatory subunit 6B homolog; The 26S proteasome is involved in the ATP-dependent degradation of ubiquitinated proteins. The regulatory (or ATPase) complex confers ATP dependency and | 1.96 |

| | | | |
|---|---|---|---|
| | | substrate specificity to the 26S complex (By similarity) | |
| tbpC | DDB0216230 | 26S proteasome regulatory subunit 8; The 26S proteasome is involved in the ATP-dependent degradation of ubiquitinated proteins. The regulatory (or ATPase) complex confers ATP dependency and substrate specificity to the 26S complex (By similarity) | 1.54 |
| udpB | DDB0230170 | annotation not available | 1.65 |
| vatB | DDB0185207 | V-type proton ATPase subunit B; Vacuolar ATPase is responsible for acidifying a variety of intracellular compartments in eukaryotic cells. The B subunit is non-catalytic but combines with other subunits to form the catalytic complex. V-ATPase is responsible for energizing electrophoretic K(+)/2H(+) antiport by generating a transmembrane voltage of more than 200 mV (By similarity) | 1.23 |
| vatE | DDB0185070 | V-type proton ATPase subunit E; Subunit of the peripheral V1 complex of vacuolar ATPase essential for assembly or catalytic function. V-ATPase is responsible for acidifying a variety of intracellular compartments in eukaryotic cells (By similarity) | 1.54 |

**Table A7.2: Tau down-regulated proteins**

*Proteins with multiple colours involved in more than one process.

**Down-regulated processes**

- Actin cytoskeleton
- Steroid biosynthetic process
- Oxidation/reduction
- Lipid metabolic process
- Other
- Disconnected node

| #node | Identifier | Annotation | Fold change |
|---|---|---|---|
| DDB0167402 | DDB0238277 | Uncharacterized protein; Belongs to the short-chain dehydrogenases/reductases (SDR) family | 0.62 |
| DDB0168996 | DDB0168996 | annotation not available | 0.41 |
| DDB0169413 | DDB0169413 | annotation not available | |
| DDB0169464 | DDB0234149 | annotation not available | 0.34 |
| DDB0169506 | DDB0231973 | annotation not available | 0.57 |
| DDB0185931 | DDB0185931 | annotation not available | 0.74 |
| DDB0186109 | DDB0186109 | annotation not available | 0.62 |
| DDB0187592 | DDB0187592 | annotation not available | 0.64 |
| DDB0188084 | DDB0234168 | annotation not available | 0.53 |
| DDB0188715 | DDB0234195 | annotation not available | 0.62 |
| DDB0188843 | DDB0188843 | annotation not available | 0.59 |
| DDB0191909 | DDB0191909 | Uncharacterized protein | 0.53 |
| DDB0202574 | DDB0202574 | annotation not available | 0.53 |
| DDB0205386 | DDB0235361 | annotation not available | 0.62 |
| DDB0205662 | DDB0205662 | annotation not available | 0.32 |
| DDB0219884 | DDB0233782 | annotation not available | 0.59 |

| | | | |
|---|---|---|---|
| DDB0231475 | DDB0231475 | Aldehyde dehydrogenase; Belongs to the aldehyde dehydrogenase family | 0.67 |
| DDB0231504 | DDB0231504 | Putative aldehyde dehydrogenase family 7 member A1 homolog; Belongs to the aldehyde dehydrogenase family | 0.78 |
| DDB0232204 | DDB0232204 | Aminotransferase class-III; Belongs to the class-III pyridoxal-phosphate-dependent aminotransferase family | 0.48 |
| DDB0233285 | DDB0233285 | PH domain-containing protein DDB_G0274775 | 0.55 |
| DDB0233382 | DDB0233382 | Short-chain dehydrogenase/reductase family protein; Belongs to the short-chain dehydrogenases/reductases (SDR) family | |
| DDB0234107 | DDB0234107 | annotation not available | 0.63 |
| DDB0234207 | DDB0234207 | annotation not available | 0.70 |
| DDB0237843 | DDB0237843 | annotation not available | 0.74 |
| DDB0267057 | DDB0267057 | Thimet-like oligopeptidase | 0.65 |
| abcG9 | DDB0214893 | ABC transporter G family member 9 | 0.40 |
| abpA | DDB0191133 | Alpha-actinin A; F-actin cross-linking protein which is thought to anchor actin to a variety of intracellular structures. This is a bundling protein. Increases the actin-stimulated ATPase activity of myosin. Involved in vegetative cell growth, phagocytosis, motility and development, probably through stabilization of the actin network in the cortical cytoskeleton | 0.69 |
| acly | DDB0235360 | Probable ATP-citrate synthase; ATP-citrate synthase is the primary enzyme responsible for the synthesis of cytosolic acetyl-CoA in many tissues; In the N-terminal section; belongs to the succinate/malate CoA ligase beta subunit family | 0.64 |
| acpA | DDB0191202 | F-actin-capping protein subunit beta; F-actin-capping proteins bind in a Ca(2+)-independent manner to the | 0.78 |

| | | | |
|---|---|---|---|
| | | fast growing ends of actin filaments (barbed end) thereby blocking the exchange of subunits at these ends. Unlike other capping proteins (such as gelsolin and severin), these proteins do not sever actin filaments | |
| act | DDB0219936 | Actin-related protein 3; Functions as ATP-binding component of the Arp2/3 complex which is involved in regulation of actin polymerization and together with an activating nucleation-promoting factor (NPF) mediates the formation of branched actin networks. Seems to contact the pointed end of the daughter actin filament. The Arp2/3 complex is involved in organizing the actin system in cell motility and chemotaxis, in phagocytosis and macropinocytosis, at late steps of endosome processing, and in mitosis. In concert with a group of other proteins, the Arp2/3 complex plays a general role in [...] | 0.75 |
| adprt1A | DDB0214818 | Poly [ADP-ribose] polymerase | 0.52 |
| aip1 | DDB0214916 | Actin-interacting protein 1; Implicated in both actin filament depolymerization and polymerization. May enhance chemotaxis by promoting cofilin- dependent actin assembly at cell leading edges | 0.66 |
| alrA | DDB0215363 | Aldose reductase A; Catalyzes the NADPH-dependent reduction of a wide variety of carbonyl-containing compounds to their corresponding alcohols with a broad range of catalytic efficiencies (By similarity). Probably affects several metabolic pathways in addition to converting glucose to sorbitol. Affects group size | 0.65 |
| amyA | DDB0214924 | Putative alpha-amylase; AmyA | 0.65 |
| ancA | DDB0201558 | Mitochondrial substrate carrier family protein ancA; Mitochondrial solute carriers shuttle metabolites, nucleotides, and cofactors through the mitochondrial | 0.74 |

| | | | |
|---|---|---|---|
| | | inner membrane. Catalyzes the exchange of ADP and ATP across the mitochondrial inner membrane | |
| arcA | DDB0214932 | Actin-related protein 2/3 complex subunit 1; Functions as component of the Arp2/3 complex which is involved in regulation of actin polymerization and together with an activating nucleation-promoting factor (NPF) mediates the formation of branched actin networks. Seems to contact the pointed end of the daughter actin filament. The Arp2/3 complex is involved in organizing the actin system in cell motility and chemotaxis, in phagocytosis and macropinocytosis, at late steps of endosome processing, and in mitosis. In concert with a group of other proteins, the Arp2/3 complex plays a general [...] | 0.69 |
| arcB | DDB0214935 | Actin-related protein 2/3 complex subunit 2; Functions as component of the Arp2/3 complex which is involved in regulation of actin polymerization and together with an activating nucleation-promoting factor (NPF) mediates the formation of branched actin networks. Seems to contact the pointed end of the daughter actin filament. The Arp2/3 complex is involved in organizing the actin system in cell motility and chemotaxis, in phagocytosis and macropinocytosis, at late steps of endosome processing, and in mitosis. In concert with a group of other proteins, the Arp2/3 complex plays a general [...] | 0.70 |
| arc | DDB0201632 | Actin-related protein 2/3 complex subunit 3; Functions as component of the Arp2/3 complex which is involved in regulation of actin polymerization and together with an activating nucleation-promoting factor (NPF) mediates the formation of branched actin networks. Seems to contact the pointed end of the daughter actin filament. The Arp2/3 complex is involved in organizing the actin system in cell motility and chemotaxis, in phagocytosis and | 0.73 |

| | | | |
|---|---|---|---|
| | | macropinocytosis, at late steps of endosome processing, and in mitosis. In concert with a group of other proteins, the Arp2/3 complex plays a general [...] | |
| cnrI | DDB0229864 | Putative countin receptor Cnr9; SET domain-containing protein | 0.71 |
| coaA | DDB0215369 | Coactosin; Binds to F-actin in a calcium independent manner. Binds to the filaments along their length | |
| cofA | DDB0214987 | Cofilin-1A; Controls reversibly actin polymerization and depolymerization in a pH-sensitive manner. It has the ability to bind G- and F-actin in a 1:1 ratio of cofilin to actin. It is the major component of intranuclear and cytoplasmic actin rods (By similarity) | 0.75 |
| corA | DDB0191115 | Coronin-A; Required for normal motility. Participates in cytokinesis | 0.77 |
| cyb5r1 | DDB0266821 | NADH-cytochrome b5 reductase 1; Electron donor reductase for cytochrome b5. The cytochrome b5/NADH cytochrome b5 reductase electron transfer system supports the catalytic activity of several sterol biosynthetic enzymes (By similarity) | 0.38 |
| cyp51 | DDB0232962 | Probable lanosterol 14-alpha demethylase; Catalyzes C14-demethylation of lanosterol which is critical for ergosterol biosynthesis. It transforms lanosterol into 4,4'-dimethyl cholesta-8,14,24-triene-3-beta-ol (By similarity) | 0.3 |
| cyp524A1 | DDB0233032 | Probable cytochrome P450 524A1 | 0.25 |
| dpm1 | DDB0231708 | Dolichol-phosphate mannosyltransferase subunit 1; Transfers mannose from GDP-mannose to dolichol monophosphate to form dolichol phosphate mannose (Dol-P-Man) which is the mannosyl donor in pathways leading to N-glycosylation, glycosyl phosphatidylinositol membrane anchoring, and O-mannosylation of proteins; catalytic subunit of the | 0.59 |

| | | | |
|---|---|---|---|
| | | dolichol- phosphate mannose (DPM) synthase complex | |
| eapA | DDB0191146 | Alkyldihydroxyacetonephosphate synthase; Catalyzes the exchange of an acyl for a long-chain alkyl group and the formation of the ether bond in the biosynthesis of ether phospholipids | 0.54 |
| empC | DDB0215345 | Emp24/gp25L/p24 family proteinPutative uncharacterized protein empC | 0.71 |
| erg24 | DDB0232079 | Delta(14)-sterol reductase; Reduces the C14=C15 double bond of 4,4-dimethyl- cholesta-8,14,24-trienol to produce 4,4-dimethyl-cholesta-8,24- dienol; Belongs to the ERG4/ERG24 family | 0.43 |
| fcsA | DDB0191105 | Fatty acyl-CoA synthetase A; Long chain fatty acid acyl-CoA synthetases catalyze the formation of a thiester bond between a free fatty acid and coenzyme A during fatty acid metabolic process. May mediate fatty acid retrieval from the lumen of endosomes into the cytoplasm; Belongs to the ATP-dependent AMP-binding enzyme family | 0.62 |
| fhbA | DDB0191099 | Flavohemoprotein A; Is involved in NO detoxification in an aerobic process, termed nitric oxide dioxygenase (NOD) reaction that utilizes O(2) and NAD(P)H to convert NO to nitrate, which protects the cell from various noxious nitrogen compounds. Therefore, plays a central role in the inducible response to nitrosative stress; In the C-terminal section; belongs to the flavoprotein pyridine nucleotide cytochrome reductase family | 0.38 |
| fimA | DDB0214994 | Fimbrin; Binds to actin | 0.67 |
| Fps | DDB0215017 | Farnesyl diphosphate synthase; Key enzyme in isoprenoid biosynthesis which catalyzes the formation of farnesyl diphosphate (FPP), a sterol precursor. | 0.71 |

| | | | |
|---|---|---|---|
| | | Involved in the inhibition of cell growth; Belongs to the FPP/GGPP synthase family | |
| glgB | DDB0214943 | 1,4-alpha-glucan-branching enzyme | 0.63 |
| gloB2 | DDB0230991 | Glyoxylase B2 | 0.38 |
| glud2 | DDB0233691 | Glutamate dehydrogenase 2; Belongs to the Glu/Leu/Phe/Val dehydrogenases family | 0.65 |
| haao | DDB0231359 | 3-hydroxyanthranilate 3,4-dioxygenase; Catalyzes the oxidative ring opening of 3- hydroxyanthranilate to 2-amino-3-carboxymuconate semialdehyde, which spontaneously cyclizes to quinolinate | 0.65 |
| hemE | DDB0231418 | Uroporphyrinogen decarboxylase; Catalyzes the decarboxylation of four acetate groups of uroporphyrinogen-III to yield coproporphyrinogen-III | 0.64 |
| hexa1 | DDB0191256 | Beta-hexosaminidase subunit A1; Responsible for the degradation of GM2 gangliosides, and a variety of other molecules containing terminal N-acetyl hexosamines. This enzyme plays a role during the slug stage of development in the maintenance of pseudoplasmodia of normal size; Belongs to the glycosyl hydrolase 20 family | 0.61 |
| Hgd | DDB0191461 | Homogentisate 1,2-dioxygenase | 0.46 |
| hgsA | DDB0219924 | Hydroxymethylglutaryl-CoA synthase A; Condenses acetyl-CoA with acetoacetyl-CoA to form HMG-CoA, which is the substrate for HMG-CoA reductase | 0.13 |
| idhC | DDB0231401 | Isocitrate dehydrogenase [NADP] cytoplasmic; Belongs to the isocitrate and isopropylmalate dehydrogenases family | 0.89 |
| maoA | DDB0231707 | Probable flavin-containing monoamine oxidase A; Belongs to the flavin monoamine oxidase family | 0.31 |
| mppB | DDB0231799 | Mitochondrial-processing peptidase subunit beta; The mitochondrial processing protease (MPP-I) cleaves | 0.76 |

| | | | |
|---|---|---|---|
| | | presequences from mitochondrial protein precursors. Most MPP-I cleavage sites follow an arginine at position -2. mppB is the catalytic subunit of the heterodimeric metallo-endopeptidase. Mitochondrial processing peptidase plays an essential role in mitochondrial biogenesis | |
| mvd | DDB0252847 | Diphosphomevalonate decarboxylase; Performs the first committed step in the biosynthesis of isoprenes; Belongs to the diphosphomevalonate decarboxylase family | 0.82 |
| nedd8 | DDB0238041 | NEDD8; Ubiquitin-like protein which plays an important role in cell cycle control, embryogenesis and neurogenesis. Covalent attachment to its substrates requires prior activation by the E1 complex ube1c/uba3-ula1 and linkage to the E2 enzyme ube2m/ubc12. Attachment of nedd8 to cullins activates their associated E3 ubiquitin ligase activity, and thus promotes polyubiquitination and proteasomal degradation of cyclins and other regulatory proteins (By similarity) | 0.86 |
| nxnA | DDB0232009 | Annexin A7; Calcium/phospholipid-binding protein which promotes membrane fusion and is involved in exocytosis | 0.64 |
| omt6 | DDB0229909 | Probable caffeoyl-CoA O-methyltransferase 2 | 0.66 |
| ost1 | DDB0233146 | Dolichyl-diphosphooligosaccharide--protein glycosyltransferase subunit 1; Essential subunit of the N-oligosaccharyl transferase (OST) complex which catalyzes the transfer of a high mannose oligosaccharide from a lipid-linked oligosaccharide donor to an asparagine residue within an Asn-X-Ser/Thr consensus motif in nascent polypeptide chains; Belongs to the OST1 family | 0.71 |

| | | | |
|---|---|---|---|
| pgmA | DDB0191348 | Phosphoglucomutase-1; This enzyme participates in both the breakdown and synthesis of glucose; Belongs to the phosphohexose mutase family | 0.76 |
| pkiA | DDB0216234 | Protein pkiA | 0.68 |
| pksB | DDB0214951 | PksBShort-chain dehydrogenase/reductase family protein; Belongs to the short-chain dehydrogenases/reductases (SDR) family | 0.65 |
| ponA | DDB0215380 | Ponticulin; Binds F-actin and nucleates actin assembly. Major high affinity link between the plasma membrane and the cortical actin network | 0.45 |
| prlA | DDB0232955 | Proliferation-associated protein A; Belongs to the peptidase M24 family | 0.76 |
| proA | DDB0191178 | Profilin-1; Binds to actin and affects the structure of the cytoskeleton. At high concentrations, profilin prevents the polymerization of actin, whereas it enhances it at low concentrations. By binding to PIP2, it inhibits the formation of IP3 and DG | 0.81 |
| proB | DDB0191249 | Profilin-2; Binds to actin and affects the structure of the cytoskeleton. At high concentrations, profilin prevents the polymerization of actin, whereas it enhances it at low concentrations. By binding to PIP2, it inhibits the formation of IP3 and DG | 0.78 |
| psaB | DDB0231240 | annotation not available | 0.8 |
| purD | DDB0230084 | Bifunctional purine biosynthetic protein purDPhosphoribosylamine--glycine ligasePhosphoribosylformylglycinamidine cyclo-ligase; In the N-terminal section; belongs to the GARS family | 0.67 |
| rab7A | DDB0191507 | Ras-related protein Rab-7A; Key regulator in endo-lysosomal trafficking. Governs early-to-late endosomal maturation, microtubule minus-end as well as plus-end directed endosomal migration and | 0.8 |

| | | | |
|---|---|---|---|
| | | positioning, and endosome-lysosome transport through different protein-protein interaction cascades (By similarity). Involved in lipophagy, a cytosolic lipase-independent autophagic pathway (By similarity) | |
| rac1A | DDB0214822 | Rho-related protein rac1A; Overexpression promotes the formation of filopodia and membrane ruffles; Belongs to the small GTPase superfamily. Rho family | 0.78 |
| racC | DDB0201659 | Rho-related protein racC; Belongs to the small GTPase superfamily. Rho family | 0.61 |
| racE | DDB0214825 | Rho-related protein racE; Specifically required for cytokinesis; Belongs to the small GTPase superfamily. Rho family | 0.66 |
| rasG | DDB0201663 | Ras-like protein rasG; Ras proteins bind GDP/GTP and possess intrinsic GTPase activity; Belongs to the small GTPase superfamily. Ras family | 0.7 |
| sarA | DDB0229965 | GTP-binding protein Sar1A; Component of the coat protein complex II (COPII) which promotes the formation of transport vesicles from the endoplasmic reticulum (ER). The coat has two main functions, the physical deformation of the endoplasmic reticulum membrane into vesicles and the selection of cargo molecules (By similarity) | 0.56 |
| sasA | DDB0214885 | Ras-related protein Rab-8A; Protein transport. Probably involved in vesicular traffic (By similarity) | 0.84 |
| sec31 | DDB0235185 | Protein transport protein SEC31; Component of the coat protein complex II (COPII) which promotes the formation of transport vesicles from the endoplasmic reticulum (ER). The coat has two main functions, the physical deformation of the endoplasmic reticulum membrane into vesicles and the selection of cargo molecules (By similarity) | 0.71 |

| | | | |
|---|---|---|---|
| serA | DDB0230052 | D-3-phosphoglycerate dehydrogenase; Catalyzes the reversible oxidation of 3-phospho-D- glycerate to 3-phosphonooxypyruvate, the first step of the phosphorylated L-serine biosynthesis pathway. Also catalyzes the reversible oxidation of 2-hydroxyglutarate to 2-oxoglutarate; Belongs to the D-isomer specific 2-hydroxyacid dehydrogenase family | 0.63 |
| shmt1 | DDB0230072 | Serine hydroxymethyltransferase 1; Interconversion of serine and glycine | 0.71 |
| smt1 | DDB0237965 | Probable cycloartenol-C-24-methyltransferase 1; Catalyzes the methyl transfer from S-adenosyl-methionine to the C-24 of cycloartenol to form 24-methylene cycloartenol | 0.31 |
| sodC | DDB0232186 | Extracellular superoxide dismutase [Cu-Zn] 3; Protect the extracellular space from toxic effect of reactive oxygen intermediates by converting superoxyde radicals into hydrogen peroxyde and oxygen | 0.55 |
| Sqor | DDB0252562 | Sulfide:quinone oxidoreductase, mitochondrial; Catalyzes the oxidation of hydrogen sulfide, with the help of a quinone | 0.47 |
| swp1 | DDB0233147 | Dolichyl-diphosphooligosaccharide--protein glycosyltransferase subunit swp1; Essential subunit of the N-oligosaccharyl transferase (OST) complex which catalyzes the transfer of a high mannose oligosaccharide from a lipid-linked oligosaccharide donor to an asparagine residue within an Asn-X-Ser/Thr consensus motif in nascent polypeptide chains | 0.62 |
| Tdo | DDB0231363 | Tryptophan 2,3-dioxygenase; Heme-dependent dioxygenase that catalyzes the oxidative cleavage of the L-tryptophan (L-Trp) pyrrole ring and converts L-tryptophan to N-formyl-L-kynurenine. Catalyzes the oxidative cleavage of the indole moiety | 0.51 |

| | | | |
|---|---|---|---|
| thfA | DDB0230118 | Methylenetetrahydrofolate dehydrogenase [NAD(+)]; Catalyzes oxidation of cytoplasmic one-carbon units for purine biosynthesis | 0.53 |
| trxE | DDB0237674 | Putative thioredoxin-5; Participates in various redox reactions through the reversible oxidation of its active center dithiol to a disulfide and catalyzes dithiol-disulfide exchange reactions | 0.74 |
| Uox | DDB0231470 | Uricase; Catalyzes the oxidation of uric acid to 5-hydroxyisourate, which is further processed to form (S)-allantoin; Belongs to the uricase family | 0.44 |
| uqcrq | DDB0267111 | Probable cytochrome b-c1 complex subunit 8; This is a component of the ubiquinol-cytochrome c reductase complex (complex III or cytochrome b-c1 complex), which is part of the mitochondrial respiratory chain. This subunit, together with cytochrome b, binds to ubiquinone (By similarity) | 0.71 |

**Table A7.3: α-synuclein up-regulated proteins**

| #node | Identifier | Annotation | Fold Change |
|---|---|---|---|
| DDB0191909 | DDB0191909 | Uncharacterized protein | 1.59 |
| DDB0219276 | DDB0219276 | annotation not available | 1.26 |
| DDB0233382 | DDB0233382 | Short-chain dehydrogenase/reductase family protein; Belongs to the short-chain dehydrogenases/reductases (SDR) family | 1.54 |
| DDB0233715 | DDB0233715 | annotation not available | 19.67 |
| arcE | DDB0191138 | Actin-related protein 2/3 complex subunit 5; Functions as component of the Arp2/3 complex which is involved in regulation of actin polymerization and together with an activating nucleation-promoting factor (NPF) mediates the formation of branched actin networks. Seems to contact the pointed end of the daughter actin filament. The Arp2/3 complex is involved in organizing the actin system in cell motility and chemotaxis, in phagocytosis and macropinocytosis, at late steps of endosome processing, and in mitosis. | 1.04 |
| cinB | DDB0220110 | Vegetative-specific protein H5; Belongs to the 'GDXG' lipolytic enzyme family | 2.28 |
| coaA | DDB0215369 | Coactosin; Binds to F-actin in a calcium independent manner. Binds to the filaments along their length | 1.24 |
| cytC | DDB0216257 | Cytochrome c; Electron carrier protein. The oxidized form of the cytochrome c heme group can accept an electron from the heme group of the cytochrome c1 subunit of cytochrome reductase. Cytochrome c then transfers this electron to the cytochrome oxidase complex, the final protein carrier in the mitochondrial electron-transport chain (By similarity) | 40.84 |

| | | | |
|---|---|---|---|
| erg2 | DDB0267016 | Protein erg2 homolog; May function in lipid transport from the endoplasmic reticulum and be involved in a wide array of cellular functions probably through regulation of the biogenesis of lipid microdomains at the plasma membrane. May regulate calcium efflux at the endoplasmic reticulum (By similarity) | 1.84 |
| gpaG | DDB0185045 | Guanine nucleotide-binding protein alpha-7 subunit; Guanine nucleotide-binding proteins (G proteins) are involved as modulators or transducers in various transmembrane signaling systems | 1.08 |
| hexa1 | DDB0191256 | Beta-hexosaminidase subunit A1; Responsible for the degradation of GM2 gangliosides, and a variety of other molecules containing terminal N-acetyl hexosamines. This enzyme plays a role during the slug stage of development in the maintenance of pseudoplasmodia of normal size; Belongs to the glycosyl hydrolase 20 family | 1.20 |
| mdhB | DDB0230188 | Probable malate dehydrogenase 2, mitochondrial; Catalyzes the reversible oxidation of malate to oxaloacetate; Belongs to the LDH/MDH superfamily. MDH type 2 family | 1.29 |
| gnpda1 | DDB0234126 | Glucosamine-6-phosphate isomerase | 1.53 |
| ndkM | DDB0214817 | Nucleoside diphosphate kinase, mitochondrial; Major role in the synthesis of nucleoside triphosphates other than ATP. The ATP gamma phosphate is transferred to the NDP beta phosphate via a ping-pong mechanism, using a phosphorylated active-site intermediate; Belongs to the NDK family | 2.63 |
| nxnA | DDB0232009 | Annexin A7; Calcium/phospholipid-binding protein which promotes membrane fusion and is involved in exocytosis | 3.53 |
| pefA | DDB0191092 | Penta-EF hand domain-containing protein 1; Belongs to the Peflin/Sorcin family | 1.15 |

| | | | |
|---|---|---|---|
| proB | DDB0191249 | Profilin-2; Binds to actin and affects the structure of the cytoskeleton. At high concentrations, profilin prevents the polymerization of actin, whereas it enhances it at low concentrations. By binding to PIP2, it inhibits the formation of IP3 and DG | 8.01 |
| psmC1 | DDB0232964 | 26S proteasome regulatory subunit 4 homolog; The 26S proteasome is involved in the ATP-dependent degradation of ubiquitinated proteins. The regulatory (or ATPase) complex confers ATP dependency and substrate specificity to the 26S complex (By similarity). Plays an important role in regulating both growth and multicellular development | 3.60 |
| rab1A | DDB0191476 | Ras-related protein Rab-1A | 1.26 |
| rab5A | DDB0229401 | Ras-related protein Rab-5A; Required for the fusion of plasma membranes and early endosomes | 1.12 |
| rasG | DDB0201663 | Ras-like protein rasG; Ras proteins bind GDP/GTP and possess intrinsic GTPase activity; Belongs to the small GTPase superfamily. Ras family | 1.62 |
| rpl34 | DDB0231151 | 60S ribosomal protein L34; Belongs to the eukaryotic ribosomal protein eL34 family | 8.52 |
| rpl6 | DDB0231338 | 60S ribosomal protein L6; Belongs to the eukaryotic ribosomal protein eL6 family | 1.47 |
| sasA | DDB0214885 | Ras-related protein Rab-8A; Protein transport. Probably involved in vesicular traffic (By similarity) | 2.30 |
| sodC | DDB0232186 | Extracellular superoxide dismutase [Cu-Zn] 3; Protect the extracellular space from toxic effect of reactive oxygen intermediates by converting superoxyde radicals into hydrogen peroxyde and oxygen | 1.04 |
| ssr1 | DDB0266492 | Translocon-associated protein subunit alpha; TRAP proteins are part of a complex whose function is to bind calcium to the ER membrane and thereby | 4.70 |

| | | | |
|---|---|---|---|
| | | regulate the retention of ER resident proteins; Belongs to the TRAP-alpha family | |
| vatC | DDB0191419 | V-type proton ATPase subunit C; Subunit of the peripheral V1 complex of vacuolar ATPase. Subunit C is necessary for the assembly of the catalytic sector of the enzyme and is likely to have a specific function in its catalytic activity. V-ATPase is responsible for acidifying a variety of intracellular compartments in eukaryotic cells (By similarity) | 1.39 |

**Table A7.4: α-synuclein down-regulated proteins**

*Proteins with multiple colours involved in more than one process.

**Down-regulated processes**

Actin cytoskeleton

Steroid biosynthetic process

Oxidation/reduction

Lipid metabolic process

Other

Disconnected node

| #node | Identifier | Annotation | Fold change |
|---|---|---|---|
| DDB0169270 | DDB0234153 | annotation not available | 0.32 |
| DDB0184078 | DDB0184078 | annotation not available | 0.42 |
| DDB0184409 | DDB0235225 | annotation not available | 0.14 |
| DDB0189501 | DDB0233903 | annotation not available | 0.56 |
| DDB0202574 | DDB0202574 | annotation not available | 0.64 |
| DDB0216913 | DDB0305102 | Uncharacterized protein | 0.68 |
| DDB0218146 | DDB0218146 | Uncharacterized protein; Gag | 0.69 |
| DDB0218284 | DDB0218284 | annotation not available | 0.45 |
| DDB0218308 | DDB0218308 | annotation not available | 0.92 |
| DDB0219884 | DDB0233782 | annotation not available | 0.10 |
| DDB0231477 | DDB0231477 | annotation not available | 0.75 |
| DDB0233285 | DDB0233285 | PH domain-containing protein DDB_G0274775 | 0.28 |
| DDB0233381 | DDB0233381 | annotation not available | 0.42 |
| DDB0304688 | DDB0304688 | Poly [ADP-ribose] polymerase; Ankyrin repeat-containing protein | 0.13 |

| | | | |
|---|---|---|---|
| H4 | DDB0201644 | Probable glutamine--tRNA ligase; Probable glutaminyl-tRNA synthetase; Belongs to the class-I aminoacyl-tRNA synthetase family | 0.69 |
| abcB2 | DDB0201670 | ABC transporter B family member 2 | 0.19 |
| abcG9 | DDB0214893 | ABC transporter G family member 9 | 0.07 |
| abpA | DDB0191133 | Alpha-actinin A; F-actin cross-linking protein which is thought to anchor actin to a variety of intracellular structures. This is a bundling protein. Increases the actin-stimulated ATPase activity of myosin. Involved in vegetative cell growth, phagocytosis, motility and development, probably through stabilization of the actin network in the cortical cytoskeleton | 0.23 |
| abpF | DDB0230207 | Actin-binding protein F | 0.03 |
| act | DDB0219936 | Actin-related protein 3; Functions as ATP-binding component of the Arp2/3 complex which is involved in regulation of actin polymerization and together with an activating nucleation-promoting factor (NPF) mediates the formation of branched actin networks. Seems to contact the pointed end of the daughter actin filament. The Arp2/3 complex is involved in organizing the actin system in cell motility and chemotaxis, in phagocytosis and macropinocytosis, at late steps of endosome processing, and in mitosis. | 0.26 |
| adprt1A | DDB0214818 | Poly [ADP-ribose] polymerase | 0.22 |
| aip1 | DDB0214916 | Actin-interacting protein 1; Implicated in both actin filament depolymerization and polymerization. May enhance chemotaxis by promoting cofilin- dependent actin assembly at cell leading edges | 0.25 |
| arcB | DDB0214935 | Actin-related protein 2/3 complex subunit 2; Functions as component of the Arp2/3 complex which is involved in regulation of actin polymerization and together with an activating nucleation-promoting factor (NPF) mediates the formation of branched actin | 0.74 |

| | | | |
|---|---|---|---|
| | | networks. Seems to contact the pointed end of the daughter actin filament. The Arp2/3 complex is involved in organizing the actin system in cell motility and chemotaxis, in phagocytosis and macropinocytosis, at late steps of endosome processing, and in mitosis. | |
| aspS1 | DDB0231308 | Aspartyl-tRNA synthetase, cytoplasmic 1; Belongs to the class-II aminoacyl-tRNA synthetase family. Type 2 subfamily | 0.54 |
| capC | DDB0219923 | Comitin; May have a role in cell motility. It has high affinity for both G-actin and F-actin. Binds to vesicle membranes via mannose residues and, by way of its interaction with actin, links these membranes to the cytoskeleton | 0.53 |
| carmil | DDB0185176 | Protein CARMIL; Serves as the scaffold for the assembly of a complex that links key players in the nucleation and termination of actin filament assembly with a ubiquitous barbed end-directed motor. This complex is composed of at least capping proteins (acpA and acpB), the Arp2/3 complex, type I myosins (myoB and myoC) and carmil. It has at least a modest ability to activate Arp2/3- dependent actin nucleation. CARMIL localizes along with the Arp2/3 complex, myoB, and myoC in the leading edge of cells | 0.10 |
| cnrI | DDB0229864 | Putative countin receptor Cnr9; SET domain-containing protein | 0.22 |
| corA | DDB0191115 | Coronin-A; Required for normal motility. Participates in cytokinesis | 0.50 |
| cpnA | DDB0215368 | Copine-A; Required for cytokinesis, contractile vacuole function and development; Belongs to the copine family | 0.60 |
| crtA | DDB0191384 | Calreticulin; Molecular calcium-binding chaperone promoting folding, oligomeric assembly and quality | 0.36 |

| | | | |
|---|---|---|---|
| | | control in the ER via the calreticulin/calnexin cycle. This lectin may interact transiently with almost all of the monoglucosylated glycoproteins that are synthesized in the ER (By similarity) | |
| ddost | DDB0233148 | Dolichyl-diphosphooligosaccharide--protein glycosyltransferase 48 kDa subunit; Essential subunit of the N-oligosaccharyl transferase (OST) complex which catalyzes the transfer of a high mannose oligosaccharide from a lipid-linked oligosaccharide donor to an asparagine residue within an Asn-X-Ser/Thr consensus motif in nascent polypeptide chains | 0.23 |
| erg24 | DDB0232079 | Delta(14)-sterol reductase; Reduces the C14=C15 double bond of 4,4-dimethyl- cholesta-8,14,24-trienol to produce 4,4-dimethyl-cholesta-8,24- dienol; Belongs to the ERG4/ERG24 family | 0.96 |
| fcsA | DDB0191105 | Fatty acyl-CoA synthetase A; Long chain fatty acid acyl-CoA synthetases catalyze the formation of a thiester bond between a free fatty acid and coenzyme A during fatty acid metabolic process. May mediate fatty acid retrieval from the lumen of endosomes into the cytoplasm; Belongs to the ATP-dependent AMP-binding enzyme family | 0.11 |
| fdfT | DDB0231376 | Squalene synthase; Belongs to the phytoene/squalene synthase family | 0.41 |
| gluA | DDB0215373 | Lysosomal beta glucosidase | 0.52 |
| hgsA | DDB0219924 | Hydroxymethylglutaryl-CoA synthase A; Condenses acetyl-CoA with acetoacetyl-CoA to form HMG-CoA, which is the substrate for HMG-CoA reductase | 0.78 |
| myoE | DDB0216200 | Myosin IE heavy chain; Myosin is a protein that binds to actin and has ATPase activity that is activated by actin. May play a role in moving membranes relative to actin | 0.20 |

| | | | |
|---|---|---|---|
| napA | DDB0231423 | Nck-associated protein 1 homolog; Involved in regulation of actin and microtubule organization. Involved in cell adhesion | 0.09 |
| omt9 | DDB0266734 | O-methyltransferase 9 | 0.99 |
| pdi2 | DDB0231409 | Protein disulfide-isomerase 2; Participates in the folding of proteins containing disulfide bonds, may be involved in glycosylation, prolyl hydroxylation and triglyceride transfer | 0.52 |
| phesA | DDB0231328 | Phenylalanine--tRNA ligase alpha subunit; Phenylalanyl-tRNA synthetase alpha chain | 0.39 |
| pirA | DDB0216270 | Protein pirA; Involved in regulation of actin and microtubule organization | 0.07 |
| plbA | DDB0185225 | Phospholipase B-like protein A; Phospholipase that removes both fatty-acid chains from phosphatidylcholine and produces the water-soluble glycerophosphorylcholine. In addition to phosphatidylcholine deacylation, it also hydrolyzes phosphatidylinositol and phosphatidylethanolamine | 0.90 |
| pppB | DDB0185058 | Serine/threonine-protein phosphatase PP1; Protein phosphatase activity in vitro; Belongs to the PPP phosphatase family | 0.40 |
| pyd3 | DDB0185221 | Beta-ureidopropionase; Converts N-carbamoyl-beta-aminoisobutyrate and N- carbamoyl-beta-alanine (3-ureidopropanoate) to, respectively, beta-aminoisobutyrate and beta-alanine, ammonia and carbon dioxide | 0.33 |
| racC | DDB0201659 | Rho-related protein racC; Belongs to the small GTPase superfamily. Rho family | 0.90 |
| rps2 | DDB0215391 | 40S ribosomal protein S2; Belongs to the universal ribosomal protein uS5 family | 0.43 |

| | | | |
|---|---|---|---|
| sevA | DDB0232954 | Severin; Severin blocks the ends of F-actin and causes the fragmentation and depolymerization of actin filaments in a Ca(2+) dependent manner | 0.45 |
| smt1 | DDB0237965 | Probable cycloartenol-C-24-methyltransferase 1; Catalyzes the methyl transfer from S-adenosyl-methionine to the C-24 of cycloartenol to form 24-methylene cycloartenol | 0.81 |
| snpA | DDB0231538 | Alpha-soluble NSF attachment protein; May be required for vesicular transport between the endoplasmic reticulum and the Golgi apparatus (By similarity). Involved in vesicle fusion with nsfA and probably SNARE proteins; Belongs to the SNAP family | 0.40 |
| svkA | DDB0191176 | Serine/threonine-protein kinase svkA; Involved in regulation of actin cytoskeleton organization during cell motility; F-actin fragmenting and capping protein allowing dynamic rearrangements of the actin cytoskeleton. Also part of a regulatory pathway from the centrosome to the midzone, thus regulating the completion of cell division | 0.25 |
| swp1 | DDB0233147 | Dolichyl-diphosphooligosaccharide--protein glycosyltransferase subunit swp1; Essential subunit of the N-oligosaccharyl transferase (OST) complex which catalyzes the transfer of a high mannose oligosaccharide from a lipid-linked oligosaccharide donor to an asparagine residue within an Asn-X-Ser/Thr consensus motif in nascent polypeptide chains | 0.20 |
| talB | DDB0191526 | Talin-B; Actin-binding protein required for multicellular morphogenesis. Substrate of pkgB and/or pkbA | 0.04 |

**Table A7.5: Cotransformant up-regulated proteins**

*Proteins with multiple colours involved in more than one process.

**Up-regulated processes**

Proteolysis

Positive regulation of RNA polymerase II transcription preinitiation complex

Translation

tRNA aminoacylation for protein translation

Other

Disconnected node

| #node | Identifier | Annotation | Fold change |
|---|---|---|---|
| DD7-1 | DDB0238141 | Galactose-binding domain-containing proteinPutative uncharacterized protein DD7-1 | 3.19 |
| DDB0167345 | DDB0238156 | Uncharacterized protein; Short-chain dehydrogenase/reductase family protein; Belongs to the short-chain dehydrogenases/reductases (SDR) family | 4.86 |
| DDB0167437 | DDB0167437 | annotation not available | 1.43 |
| DDB0167945 | DDB0238195 | annotation not available | 3.01 |
| DDB0168140 | DDB0168140 | annotation not available | 4.10 |
| DDB0169073 | DDB0237753 | annotation not available | 1.64 |
| DDB0190011 | DDB0305306 | Obg-like ATPase 1; Hydrolyzes ATP, and can also hydrolyze GTP with lower efficiency. Has lower affinity for GTP | 1.30 |
| DDB0217073 | DDB0234178 | annotation not available | 2.51 |
| DDB0217720 | DDB0217720 | Putative acetyltransferase DDB_G0275913; Belongs to the transferase hexapeptide repeat family | 3.43 |
| DDB0218284 | DDB0218284 | annotation not available | 2.45 |
| DDB0230005 | DDB0230005 | CBS domain-containing protein DDB_G0289609 | 2.04 |

| | | | |
|---|---|---|---|
| DDB0230064 | DDB0230064 | annotation not available | 2.68 |
| DDB0252581 | DDB0252581 | Probable GH family 25 lysozyme 5; Belongs to the glycosyl hydrolase 25 family | 1.72 |
| DDB0267102 | DDB0267102 | Probable nucleosome assembly protein; May modulate chromatin structure by regulation of histone octamer formation | 0.09 |
| V4 | DDB0215343 | Vegetative-specific protein V4; Unknown. Its expression during growth is not required for growth but for the proper initiation of development, therefore playing a role in the transition from growth to development | 1.64 |
| abpE-1 | DDB0302489 | Drebrin-like protein; Actin-binding adapter protein. Binds to F-actin but is not involved in actin polymerization, capping or bundling. Does not bind G-actin. Controls pseudopodium number and motility in early stages of chemotactic aggregation | 1.80 |
| ach1 | DDB0233380 | Acetyl-CoA hydrolase; Presumably involved in regulating the intracellular acetyl-CoA pool for fatty acid and cholesterol synthesis and fatty acid oxidation | 1.50 |
| adrm1-1 | DDB0238204 | Proteasomal ubiquitin receptor ADRM1 homolog; Functions as a proteasomal ubiquitin receptor. Recruits the deubiquitinating enzyme uchl5 at the 26S proteasome and promotes its activity (By similarity). Plays a role in the transition from growth to differentiation | 1.42 |
| ap2a1-2 | DDB0302453 | annotation not available | 2.13 |
| argS1 | DDB0231324 | Probable arginine--tRNA ligase, cytoplasmic; Forms part of a macromolecular complex that catalyzes the attachment of specific amino acids to cognate tRNAs during protein synthesis | 4.61 |

| | | | |
|---|---|---|---|
| aspS1 | DDB0231308 | Aspartyl-tRNA synthetase, cytoplasmic 1; Belongs to the class-II aminoacyl-tRNA synthetase family. Type 2 subfamily | 1.99 |
| cbp2 | DDB0191196 | Calcium-binding protein 2; Not known; probably binds four calcium ions | 5.59 |
| ccbl | DDB0231138 | Kynurenine--oxoglutarate transaminase; Catalyzes the irreversible transamination of the L- tryptophan metabolite L-kynurenine to form kynurenic acid (KA). Metabolizes the cysteine conjugates of certain halogenated alkenes and alkanes to form reactive metabolites. Catalyzes the beta- elimination of S-conjugates and Se-conjugates of L- (seleno)cysteine, resulting in the cleavage of the C-S or C-Se bond (By similarity); Belongs to the class-I pyridoxal-phosphate-dependent aminotransferase family | 2.10 |
| cct2 | DDB0233992 | T-complex protein 1 subunit beta; Molecular chaperone; assists the folding of proteins upon ATP hydrolysis. Known to play a role, in vitro, in the folding of actin and tubulin (By similarity) | 1.75 |
| cinB | DDB0220110 | Vegetative-specific protein H5; Belongs to the 'GDXG' lipolytic enzyme family | 5.67 |
| dpp3-1 | DDB0266802 | Dipeptidyl peptidase 3 | 2.21 |
| dscA-1 | DDB0266623 | Discoidin-1 subunit A; Galactose- and N-acetylgalactosamine-binding lectin. May play a role in cell-substratum adhesion rather than in cell-cell adhesion. May be necessary for the maintenance of normal elongate morphology during aggregation | 6.24 |
| dscC-1 | DDB0266624 | Discoidin-1 subunit B/C; Galactose- and N-acetylgalactosamine-binding lectin. May play a role in cell-substratum adhesion rather than in cell-cell adhesion. May be necessary for the maintenance of normal elongate morphology during aggregation | 6.40 |

| | | | |
|---|---|---|---|
| dscD-1 | DDB0266625 | Discoidin-1 subunit D; Galactose- and N-acetylgalactosamine-binding lectin. May play a role in cell-substratum adhesion rather than in cell-cell adhesion. May be necessary for the maintenance of normal elongate morphology during aggregation | 5.89 |
| dscE | DDB0215382 | Discoidin-2; Galactose-binding lectin. May be necessary for the primary process of spore formation and may be involved in spore coat formation | 1.45 |
| eif3L | DDB0233946 | Eukaryotic translation initiation factor 3 subunit L; Component of the eukaryotic translation initiation factor 3 (eIF-3) complex, which is involved in protein synthesis of a specialized repertoire of mRNAs and, together with other initiation factors, stimulates binding of mRNA and methionyl-tRNAi to the 40S ribosome. The eIF-3 complex specifically targets and initiates translation of a subset of mRNAs involved in cell proliferation | 1.52 |
| eif5 | DDB0234258 | Eukaryotic translation initiation factor 5; Catalyzes the hydrolysis of GTP bound to the 40S ribosomal initiation complex (40S.mRNA.Met-tRNA[F].eIF-2.GTP) with the subsequent joining of a 60S ribosomal subunit resulting in the release of eIF-2 and the guanine nucleotide. The subsequent joining of a 60S ribosomal subunit results in the formation of a functional 80S initiation complex (80S.mRNA.Met-tRNA[F]) (By similarity) | 1.63 |
| eif6 | DDB0234038 | Eukaryotic translation initiation factor 6; Binds to the 60S ribosomal subunit and prevents its association with the 40S ribosomal subunit to form the 80S initiation complex in the cytoplasm. May also be involved in ribosome biogenesis | 2.53 |
| etfa | DDB0267017 | Electron transfer flavoprotein subunit alpha, mitochondrial; The electron transfer flavoprotein serves as a specific electron acceptor for several | 1.47 |

| | | | |
|---|---|---|---|
| | | dehydrogenases, including five acyl- CoA dehydrogenases, glutaryl-CoA and sarcosine dehydrogenase. It transfers the electrons to the main mitochondrial respiratory chain via ETF-ubiquinone oxidoreductase (ETF dehydrogenase) (By similarity) | |
| g6pd-1 | DDB0238739 | Glucose-6-phosphate 1-dehydrogenase; Catalyzes the rate-limiting step of the oxidative pentose-phosphate pathway, which represents a route for the dissimilation of carbohydrates besides glycolysis. The main function of this enzyme is to provide reducing power (NADPH) and pentose phosphates for fatty acid and nucleic acid synthesis (By similarity) | 1.71 |
| gluS | DDB0231321 | Probable glutamate--tRNA ligase, cytoplasmic; Catalyzes the attachment of glutamate to tRNA(Glu) in a two-step reaction: glutamate is first activated by ATP to form Glu-AMP and then transferred to the acceptor end of tRNA(Glu); Belongs to the class-I aminoacyl-tRNA synthetase family. Glutamate--tRNA ligase type 2 subfamily | 1.42 |
| gp130 | DDB0214937 | Glycoprotein 130Lipid-anchored plasma membrane glycoprotein 130 | 1.89 |
| gsr | DDB0231410 | Glutathione reductase; Maintains high levels of reduced glutathione in the cytosol | 1.75 |
| hisS | DDB0231332 | Histidine--tRNA ligase, cytoplasmic; Histidyl-tRNA synthetase, cytoplasmic; Belongs to the class-II aminoacyl-tRNA synthetase family | 2.40 |
| hspC | DDB0185048 | 32 kDa heat shock protein | 12.49 |
| hspE-1 | DDB0238264 | Heat shock cognate 70 kDa protein 2; May function in protein folding and assembly, and disassembly of protein complexes | 1.84 |

| | | | |
|---|---|---|---|
| leuS | DDB0231253 | Leucine--tRNA ligase, cytoplasmic; Leucyl-tRNA synthetase, cytoplasmic; Belongs to the class-I aminoacyl-tRNA synthetase family | 1.68 |
| ndkB | DDB0238334 | Nucleoside diphosphate kinase, cytosolic; Major role in the synthesis of nucleoside triphosphates other than ATP | 1.82 |
| pgmA | DDB0191348 | Phosphoglucomutase-1; This enzyme participates in both the breakdown and synthesis of glucose; Belongs to the phosphohexose mutase family | 1.32 |
| psmA1 | DDB0214956 | Proteasome subunit alpha type-1; The proteasome is a multicatalytic proteinase complex which is characterized by its ability to cleave peptides with Arg, Phe, Tyr, Leu, and Glu adjacent to the leaving group at neutral or slightly basic pH. The proteasome has an ATP-dependent proteolytic activity; Belongs to the peptidase T1A family | 1.26 |
| psmA4 | DDB0214953 | Proteasome subunit alpha type-4; The proteasome is a multicatalytic proteinase complex which is characterized by its ability to cleave peptides with Arg, Phe, Tyr, Leu, and Glu adjacent to the leaving group at neutral or slightly basic pH. The proteasome has an ATP-dependent proteolytic activity; Belongs to the peptidase T1A family | 1.60 |
| psmC1 | DDB0232964 | 26S proteasome regulatory subunit 4 homolog; The 26S proteasome is involved in the ATP-dependent degradation of ubiquitinated proteins. The regulatory (or ATPase) complex confers ATP dependency and substrate specificity to the 26S complex (By similarity). Plays an important role in regulating both growth and multicellular development | 4.76 |
| psmD1 | DDB0232977 | 26S proteasome non-ATPase regulatory subunit 1; Acts as a regulatory subunit of the 26 proteasome | 1.94 |

| | | | |
|---|---|---|---|
| | | which is involved in the ATP-dependent degradation of ubiquitinated proteins | |
| psmD13 | DDB0233004 | 26S proteasome non-ATPase regulatory subunit 13; Acts as a regulatory subunit of the 26S proteasome which is involved in the ATP-dependent degradation of ubiquitinated proteins | 1.53 |
| psmD14 | DDB0191298 | 26S proteasome non-ATPase regulatory subunit 14; Metalloprotease component of the 26S proteasome that specifically cleaves 'Lys-63'-linked polyubiquitin chains. The 26S proteasome is involved in the ATP-dependent degradation of ubiquitinated proteins. The function of the 'Lys-63'-specific deubiquitination of the proteasome is unclear (By similarity) | 1.52 |
| qdpr | DDB0237752 | Dihydropteridine reductase; The product of this enzyme, tetrahydrobiopterin (BH-4), is an essential cofactor for phenylalanine, tyrosine, and tryptophan hydroxylases | 2.02 |
| serS | DDB0231305 | Serine--tRNA ligase, cytoplasmic; Catalyzes the attachment of serine to tRNA(Ser). Is also able to aminoacylate tRNA(Sec) with serine, to form the misacylated tRNA L-seryl-tRNA(Sec), which will be further converted into selenocysteinyl-tRNA(Sec) (By similarity) | 2.76 |
| tbpB | DDB0191435 | 26S proteasome regulatory subunit 6B homolog; The 26S proteasome is involved in the ATP-dependent degradation of ubiquitinated proteins. The regulatory (or ATPase) complex confers ATP dependency and substrate specificity to the 26S complex (By similarity) | |
| tkt-1 | DDB0266926 | Transketolase; Catalyzes the transfer of a two-carbon ketol group from a ketose donor to an aldose acceptor, via a covalent intermediate with the cofactor thiamine pyrophosphate | 2.10 |

| | | | |
|---|---|---|---|
| trap1 | DDB0185036 | TNF receptor-associated protein 1 homolog, mitochondrial; Chaperone that expresses an ATPase activity | 3.07 |
| valS1 | DDB0231269 | Probable valyl-tRNA synthetase, cytoplasmic; Belongs to the class-I aminoacyl-tRNA synthetase family | 2.17 |
| xpo1 | DDB0234066 | Exportin-1; Mediates the nuclear export of cellular proteins (cargos) bearing a leucine-rich nuclear export signal (NES) | 1.60 |
| zpr1 | DDB0304584 | Zinc finger protein ZPR1 homolog | 2.43 |

**Table A7.6: Cotransformant down-regulated proteins**

*Proteins with multiple colours involved in more than one process.

**Down-regulated processes**

Actin cytoskeleton

Steroid biosynthetic process

Oxidation/reduction

Lipid metabolic process

Other

Disconnected node

| #node | Identifier | Annotation | Fold change |
|---|---|---|---|
| DDB0167402 | DDB0238277 | Uncharacterized protein; Belongs to the short-chain dehydrogenases/reductases (SDR) family | 0.53 |
| DDB0167407 | DDB0167407 | annotation not available | 0.45 |
| DDB0168319 | DDB0233965 | annotation not available | 0.54 |
| DDB0168738 | DDB0232205 | annotation not available | 0.70 |
| DDB0184409 | DDB0235225 | annotation not available | 0.59 |
| DDB0184511 | DDB0233800 | annotation not available | 0.67 |
| DDB0186910 | DDB0238597 | annotation not available | 0.34 |
| DDB0188715 | DDB0234195 | annotation not available | 0.65 |
| DDB0188980 | DDB0235312 | annotation not available | 0.51 |
| DDB0189501 | DDB0233903 | annotation not available | 0.43 |
| DDB0191047 | DDB0302557 | annotation not available | 0.53 |
| DDB0191714 | DDB0191714 | annotation not available | 0.54 |
| DDB0191909 | DDB0191909 | Uncharacterized protein | 0.47 |
| DDB0202574 | DDB0202574 | annotation not available | 0.63 |
| DDB0204712 | DDB0204712 | annotation not available | 0.46 |
| DDB0205849 | DDB0235377 | annotation not available | 0.60 |

| | | | |
|---|---|---|---|
| DDB0218053 | DDB0304452 | annotation not available | 0.73 |
| DDB0218638 | DDB0237522 | annotation not available | 0.72 |
| DDB0219436 | DDB0233867 | Uncharacterized protein | 0.60 |
| DDB0231474 | DDB0231474 | Aldehyde dehydrogenase; Belongs to the aldehyde dehydrogenase family | 0.63 |
| DDB0231475 | DDB0231475 | Aldehyde dehydrogenase; Belongs to the aldehyde dehydrogenase family | 0.54 |
| DDB0231504 | DDB0231504 | Putative aldehyde dehydrogenase family 7 member A1 homolog; Belongs to the aldehyde dehydrogenase family | 0.73 |
| DDB0231658 | DDB0231658 | annotation not available | 0.53 |
| DDB0232204 | DDB0232204 | Aminotransferase class-III; Belongs to the class-III pyridoxal-phosphate-dependent aminotransferase family | 0.64 |
| DDB0233285 | DDB0233285 | PH domain-containing protein DDB_G0274775 | 0.53 |
| DDB0233382 | DDB0233382 | Short-chain dehydrogenase/reductase family protein; Belongs to the short-chain dehydrogenases/reductases (SDR) family | 0.56 |
| DDB0233914 | DDB0233914 | Putative methyltransferase DDB_G0268948 | 0.40 |
| DDB0234107 | DDB0234107 | annotation not available | 0.68 |
| DDB0234207 | DDB0234207 | annotation not available | 0.64 |
| DDB0237843 | DDB0237843 | annotation not available | 0.74 |
| DDB0266618 | DDB0266618 | SH3 domain-containing protein | 0.59 |
| DDB0267057 | DDB0267057 | Thimet-like oligopeptidase | 0.67 |
| aatB | DDB0230093 | Aspartate aminotransferase, cytoplasmic; Plays a key role in amino acid metabolism; Belongs to the class-I pyridoxal-phosphate-dependent aminotransferase family | 0.85 |

| | | | |
|---|---|---|---|
| abcB2 | DDB0201670 | ABC transporter B family member 2 | 0.36 |
| abpA | DDB0191133 | Alpha-actinin A; F-actin cross-linking protein which is thought to anchor actin to a variety of intracellular structures. This is a bundling protein. Increases the actin-stimulated ATPase activity of myosin. Involved in vegetative cell growth, phagocytosis, motility and development, probably through stabilization of the actin network in the cortical cytoskeleton | 0.59 |
| abpF | DDB0230207 | Actin-binding protein F | 0.34 |
| aco1 | DDB0229908 | Probable cytoplasmic aconitate hydratase; Catalyzes the isomerization of citrate to isocitrate via cis-aconitate; Belongs to the aconitase/IPM isomerase family | 0.85 |
| acpA | DDB0191202 | F-actin-capping protein subunit beta; F-actin-capping proteins bind in a Ca(2+)-independent manner to the fast growing ends of actin filaments (barbed end) thereby blocking the exchange of subunits at these ends. Unlike other capping proteins (such as gelsolin and severin), these proteins do not sever actin filaments | 0.67 |
| acpB | DDB0191243 | F-actin-capping protein subunit alpha; F-actin-capping proteins bind in a Ca(2+)-independent manner to the fast growing ends of actin filaments (barbed end) thereby blocking the exchange of subunits at these ends. Unlike other capping proteins (such as gelsolin and severin), these proteins do not sever actin filaments | 0.73 |
| act | DDB0219936 | Actin-related protein 3; Functions as ATP-binding component of the Arp2/3 complex which is involved in regulation of actin polymerization and together with an activating nucleation-promoting factor (NPF) mediates the formation of branched actin networks. Seems to contact the pointed end of the daughter actin filament. The Arp2/3 complex is involved in | 0.60 |

| | | | |
|---|---|---|---|
| | | organizing the actin system in cell motility and chemotaxis, in phagocytosis and macropinocytosis, at late steps of endosome processing, and in mitosis | |
| adh5 | DDB0238276 | Alcohol dehydrogenase class-3; Class-III ADH is remarkably ineffective in oxidizing ethanol, but it readily catalyzes the oxidation of long-chain primary alcohols and the oxidation of S-(hydroxymethyl) glutathione | 0.55 |
| adk | DDB0230174 | Adenosine kinase; ATP dependent phosphorylation of adenosine and other related nucleoside analogs to monophosphate derivatives | 0.61 |
| adprt1A | DDB0214818 | Poly [ADP-ribose] polymerase | 0.29 |
| agxt | DDB0237978 | Serine--pyruvate aminotransferase; Dual metabolic roles of gluconeogenesis and glyoxylate detoxification; Belongs to the class-V pyridoxal-phosphate-dependent aminotransferase family | 0.68 |
| aip1 | DDB0214916 | Actin-interacting protein 1; Implicated in both actin filament depolymerization and polymerization. May enhance chemotaxis by promoting cofilin- dependent actin assembly at cell leading edges | 0.63 |
| amyA | DDB0214924 | Putative alpha-amylase; AmyA | 0.71 |
| arcA | DDB0214932 | Actin-related protein 2/3 complex subunit 1; Functions as component of the Arp2/3 complex which is involved in regulation of actin polymerization and together with an activating nucleation-promoting factor (NPF) mediates the formation of branched actin networks. Seems to contact the pointed end of the daughter actin filament. The Arp2/3 complex is involved in organizing the actin system in cell motility and chemotaxis, in phagocytosis and macropinocytosis, at late steps of endosome processing, and in mitosis. | 0.67 |

| | | | |
|---|---|---|---|
| arcB | DDB0214935 | Actin-related protein 2/3 complex subunit 2; Functions as component of the Arp2/3 complex which is involved in regulation of actin polymerization and together with an activating nucleation-promoting factor (NPF) mediates the formation of branched actin networks. Seems to contact the pointed end of the daughter actin filament. The Arp2/3 complex is involved in organizing the actin system in cell motility and chemotaxis, in phagocytosis and macropinocytosis, at late steps of endosome processing, and in mitosis. | 0.61 |
| arcC | DDB0201632 | Actin-related protein 2/3 complex subunit 3; Functions as component of the Arp2/3 complex which is involved in regulation of actin polymerization and together with an activating nucleation-promoting factor (NPF) mediates the formation of branched actin networks. Seems to contact the pointed end of the daughter actin filament. The Arp2/3 complex is involved in organizing the actin system in cell motility and chemotaxis, in phagocytosis and macropinocytosis, at late steps of endosome processing, and in mitosis. | 0.69 |
| arcD | DDB0191121 | Actin-related protein 2/3 complex subunit 4; Functions as component of the Arp2/3 complex which is involved in regulation of actin polymerization and together with an activating nucleation-promoting factor (NPF) mediates the formation of branched actin networks. Seems to contact the pointed end of the daughter actin filament. The Arp2/3 complex is involved in organizing the actin system in cell motility and chemotaxis, in phagocytosis and macropinocytosis, at late steps of endosome processing, and in mitosis. | 0.69 |

| | | | |
|---|---|---|---|
| arfA | DDB0191101 | ADP-ribosylation factor 1; GTP-binding protein involved in protein trafficking; may modulate vesicle budding and uncoating within the Golgi apparatus | 0.80 |
| arpA | DDB0220489 | Centractin; Component of a multi-subunit complex, PPK2 (poly P kinase complex 2) involved in microtubule based vesicle motility. It is associated with the centrosome. PPK2 complex can synthesize a poly chain of hundreds of phosphate residues linked by ATP-like bonds | 0.71 |
| calA | DDB0214955 | Calmodulin; Calmodulin mediates the control of a large number of enzymes, ion channels and other proteins by Ca(2+). Among the enzymes to be stimulated by the calmodulin-Ca(2+) complex are a number of protein kinases and phosphatases | 0.68 |
| cap | DDB0191139 | Adenylyl cyclase-associated protein; May have a regulatory bifunctional role. Binds G-actin and PIP2. Involved in microfilament reorganization near the plasma membrane in a PIP2-regulated manner | 0.70 |
| capB | DDB0185023 | cAMP-binding protein 2; Belongs to the CAPAB/TerDEXZ family | 0.64 |
| capC | DDB0219923 | Comitin; May have a role in cell motility. It has high affinity for both G-actin and F-actin. Binds to vesicle membranes via mannose residues and, by way of its interaction with actin, links these membranes to the cytoskeleton | 0.71 |
| carmil | DDB0185176 | Protein CARMIL; Serves as the scaffold for the assembly of a complex that links key players in the nucleation and termination of actin filament assembly with a ubiquitous barbed end-directed motor. This complex is composed of at least capping proteins (acpA and acpB), the Arp2/3 complex, type I myosins (myoB and myoC) and carmil. It has at least a modest ability to activate Arp2/3- dependent actin nucleation. | 0.70 |

| | | | |
|---|---|---|---|
| | | CARMIL localizes along with the Arp2/3 complex, myoB, and myoC in the leading edge of cells | |
| cmfB | DDB0191095 | Conditioned medium factor receptor 1; Receptor for cmfA, that appears to mediate the G- independent cmfA signal transduction | 0.79 |
| cnrI | DDB0229864 | Putative countin receptor Cnr9; SET domain-containing protein | 0.57 |
| coaA | DDB0215369 | Coactosin; Binds to F-actin in a calcium independent manner. Binds to the filaments along their length | 0.72 |
| cofA | DDB0214987 | Cofilin-1A; Controls reversibly actin polymerization and depolymerization in a pH-sensitive manner. It has the ability to bind G- and F-actin in a 1:1 ratio of cofilin to actin. It is the major component of intranuclear and cytoplasmic actin rods (By similarity) | 0.72 |
| copb2 | DDB0233798 | Coatomer subunit beta; The coatomer is a cytosolic protein complex that binds to dilysine motifs and reversibly associates with Golgi non- clathrin-coated vesicles, which further mediate biosynthetic protein transport from the ER, via the Golgi up to the trans Golgi network. Coatomer complex is required for budding from Golgi membranes, and is essential for the retrograde Golgi-to-ER transport of dilysine-tagged proteins (By similarity) | 0.61 |
| corA | DDB0191115 | Coronin-A; Required for normal motility. Participates in cytokinesis | 0.71 |
| cprD | DDB0214999 | Cysteine proteinase 4 | 0.61 |
| ctsD | DDB0215012 | Cathepsin D; Protease that may act during cell growth and/or development; Belongs to the peptidase A1 family | 0.74 |
| cyb5r1 | DDB0266821 | NADH-cytochrome b5 reductase 1; Electron donor reductase for cytochrome b5. The cytochrome | 0.42 |

| | | | |
|---|---|---|---|
| | | b5/NADH cytochrome b5 reductase electron transfer system supports the catalytic activity of several sterol biosynthetic enzymes (By similarity) | |
| cyc1 | DDB0238603 | Cytochrome c1, heme protein, mitochondrial; This is the heme-containing component of the cytochrome b-c1 complex, which accepts electrons from Rieske protein and transfers electrons to cytochrome c in the mitochondrial respiratory chain | 0.78 |
| cyp508A4 | DDB0232355 | Probable cytochrome P450 508A4 | 0.07 |
| cysA | DDB0191318 | Cystathionine gamma-lyase; Belongs to the trans-sulfuration enzymes family | 0.79 |
| ddost | DDB0233148 | Dolichyl-diphosphooligosaccharide--protein glycosyltransferase 48 kDa subunit; Essential subunit of the N-oligosaccharyl transferase (OST) complex which catalyzes the transfer of a high mannose oligosaccharide from a lipid-linked oligosaccharide donor to an asparagine residue within an Asn-X-Ser/Thr consensus motif in nascent polypeptide chains | 0.58 |
| eapA | DDB0191146 | Alkyldihydroxyacetonephosphate synthase; Catalyzes the exchange of an acyl for a long-chain alkyl group and the formation of the ether bond in the biosynthesis of ether phospholipids | 0.54 |
| enoA | DDB0231355 | Enolase A | 0.84 |
| erg2 | DDB0267016 | Protein erg2 homolog; May function in lipid transport from the endoplasmic reticulum and be involved in a wide array of cellular functions probably through regulation of the biogenesis of lipid microdomains at the plasma membrane. May regulate calcium efflux at the endoplasmic reticulum (By similarity) | 0.47 |
| erg24 | DDB0232079 | Delta(14)-sterol reductase; Reduces the C14=C15 double bond of 4,4-dimethyl- cholesta-8,14,24- | 0.53 |

| | | | |
|---|---|---|---|
| | | trienol to produce 4,4-dimethyl-cholesta-8,24- dienol; Belongs to the ERG4/ERG24 family | |
| fah | DDB0231609 | Fumarylacetoacetase; Belongs to the FAH family | 0.66 |
| fimA | DDB0214994 | Fimbrin; Binds to actin | 0.57 |
| fkbp1 | DDB0233549 | FK506-binding protein 1; PPIases accelerate the folding of proteins by catalyzing the cis-trans isomerization of proline imidic peptide bonds in oligopeptides | 0.70 |
| gabT | DDB0231448 | 4-aminobutyrate aminotransferase | 0.76 |
| gar1 | DDB0235390 | Probable H/ACA ribonucleoprotein complex subunit 1; Required for ribosome biogenesis. Part of a complex which catalyzes pseudouridylation of rRNA. This involves the isomerization of uridine such that the ribose is subsequently attached to C5, instead of the normal N1. Pseudouridine ("psi") residues may serve to stabilize the conformation of rRNAs (By similarity) | 0.73 |
| glud2 | DDB0233691 | Glutamate dehydrogenase 2; Belongs to the Glu/Leu/Phe/Val dehydrogenases family | 0.57 |
| gnd | DDB0215011 | 6-phosphogluconate dehydrogenase, decarboxylating; Catalyzes the oxidative decarboxylation of 6- phosphogluconate to ribulose 5-phosphate and CO(2), with concomitant reduction of NADP to NADPH; Belongs to the 6-phosphogluconate dehydrogenase family | 0.72 |
| gpaG | DDB0185045 | Guanine nucleotide-binding protein alpha-7 subunit; Guanine nucleotide-binding proteins (G proteins) are involved as modulators or transducers in various transmembrane signaling systems | 0.66 |
| gpbB | DDB0185122 | Guanine nucleotide-binding protein subunit beta-like protein; Belongs to the WD repeat G protein beta family. Ribosomal protein RACK1 subfamily | 0.87 |

| | | | |
|---|---|---|---|
| gpt | DDB0232139 | Probable alanine aminotransferase, mitochondrial | 0.42 |
| grxB | DDB0183791 | Glutaredoxin-like protein; Belongs to the glutaredoxin family | 0.45 |
| gsta1 | DDB0231431 | Putative glutathione S-transferase alpha-1; Conjugation of reduced glutathione to a wide number of exogenous and endogenous hydrophobic electrophiles | 0.63 |
| hexa1 | DDB0191256 | Beta-hexosaminidase subunit A1; Responsible for the degradation of GM2 gangliosides, and a variety of other molecules containing terminal N-acetyl hexosamines. This enzyme plays a role during the slug stage of development in the maintenance of pseudoplasmodia of normal size; Belongs to the glycosyl hydrolase 20 family | 0.28 |
| hgsA | DDB0219924 | Hydroxymethylglutaryl-CoA synthase A; Condenses acetyl-CoA with acetoacetyl-CoA to form HMG-CoA, which is the substrate for HMG-CoA reductase | 0.15 |
| hpd | DDB0231603 | 4-hydroxyphenylpyruvate dioxygenase; Key enzyme in the degradation of tyrosine | 0.69 |
| hydA | DDB0201650 | Aldehyde dehydrogenase; Belongs to the aldehyde dehydrogenase family | 0.59 |
| idhC | DDB0231401 | Isocitrate dehydrogenase [NADP] cytoplasmic; Belongs to the isocitrate and isopropylmalate dehydrogenases family | 0.76 |
| impdh | DDB0230098 | Inosine-5'-monophosphate dehydrogenase; Catalyzes the conversion of inosine 5'-phosphate (IMP) to xanthosine 5'-phosphate (XMP), the first committed and rate- limiting step in the de novo synthesis of guanine nucleotides, and therefore plays an important role in the regulation of cell growth; Belongs to the IMPDH/GMPR family | 0.69 |
| mai | DDB0231608 | Maleylacetoacetate isomerase | 0.44 |

| | | | |
|---|---|---|---|
| manA | DDB0201569 | Lysosomal alpha-mannosidaseAlpha-mannosidase 60 kDa subunitAlpha-mannosidase 58 kDa subunit | 0.30 |
| maoA | DDB0231707 | Probable flavin-containing monoamine oxidase A; Belongs to the flavin monoamine oxidase family | 0.36 |
| metE | DDB0230069 | 5-methyltetrahydropteroyltriglutamate--homocysteine methyltransferase; Catalyzes the transfer of a methyl group from 5-methyltetrahydrofolate to homocysteine resulting in methionine formation; Belongs to the vitamin-B12 independent methionine synthase family | 0.37 |
| mfeA | DDB0201628 | Peroxisomal multifunctional enzyme A; Enzyme acting on the peroxisomal beta-oxidation pathway for fatty acids. Protects the cells from the increase of the harmful xenobiotic fatty acids incorporated from their diets and optimizes cellular lipid composition for proper development; Belongs to the short-chain dehydrogenases/reductases (SDR) family | 0.77 |
| mhcA | DDB0191444 | Myosin-2 heavy chain; Myosin is a protein that binds to actin and has ATPase activity that is activated by actin; Belongs to the TRAFAC class myosin-kinesin ATPase superfamily. Myosin family | 0.76 |
| mppB | DDB0231799 | Mitochondrial-processing peptidase subunit beta; The mitochondrial processing protease (MPP-I) cleaves presequences from mitochondrial protein precursors. Most MPP-I cleavage sites follow an arginine at position -2. mppB is the catalytic subunit of the heterodimeric metallo-endopeptidase. Mitochondrial processing peptidase plays an essential role in mitochondrial biogenesis | 0.81 |
| mroh1 | DDB0189282 | Maestro heat-like repeat-containing protein family member 1; HEAT repeat-containing protein 7A homolog | 0.78 |

| | | | |
|---|---|---|---|
| myoE | DDB0216200 | Myosin IE heavy chain; Myosin is a protein that binds to actin and has ATPase activity that is activated by actin. May play a role in moving membranes relative to actin | 0.61 |
| napA | DDB0231423 | Nck-associated protein 1 homolog; Involved in regulation of actin and microtubule organization. Involved in cell adhesion | 0.46 |
| nxnA | DDB0232009 | Annexin A7; Calcium/phospholipid-binding protein which promotes membrane fusion and is involved in exocytosis | 0.60 |
| omt9 | DDB0266734 | O-methyltransferase 9 | 0.20 |
| osbH | DDB0237794 | Oxysterol-binding protein 8; Belongs to the OSBP family | 0.80 |
| ost1 | DDB0233146 | Dolichyl-diphosphooligosaccharide--protein glycosyltransferase subunit 1; Essential subunit of the N-oligosaccharyl transferase (OST) complex which catalyzes the transfer of a high mannose oligosaccharide from a lipid-linked oligosaccharide donor to an asparagine residue within an Asn-X-Ser/Thr consensus motif in nascent polypeptide chains; Belongs to the OST1 family | 0.64 |
| pakC | DDB0267078 | Serine/threonine-protein kinase pakC; Has role in the regulation of chemotaxis; Belongs to the protein kinase superfamily. STE Ser/Thr protein kinase family. STE20 subfamily | 0.32 |
| pckA | DDB0231108 | Phosphoenolpyruvate carboxykinase [ATP]; Belongs to the phosphoenolpyruvate carboxykinase (ATP) family | 0.67 |
| pdi2 | DDB0231409 | Protein disulfide-isomerase 2; Participates in the folding of proteins containing disulfide bonds, may be involved in glycosylation, prolyl hydroxylation and triglyceride transfer | 0.70 |

| | | | |
|---|---|---|---|
| pefA | DDB0191092 | Penta-EF hand domain-containing protein 1; Belongs to the Peflin/Sorcin family | 0.44 |
| pepd | DDB0266378 | Xaa-Pro dipeptidase; Splits dipeptides with a prolyl or hydroxyprolyl residue in the C-terminal position; Belongs to the peptidase M24B family. Eukaryotic-type prolidase subfamily | 0.59 |
| pgl | DDB0231287 | Probable 6-phosphogluconolactonase; Hydrolysis of 6-phosphogluconolactone to 6- phosphogluconate | 0.31 |
| pirA | DDB0216270 | Protein pirA; Involved in regulation of actin and microtubule organization | 0.57 |
| pkiA | DDB0216234 | Protein pkiA | 0.54 |
| pksB | DDB0214951 | PksBShort-chain dehydrogenase/reductase family protein; Belongs to the short-chain dehydrogenases/reductases (SDR) family | 0.59 |
| plbA | DDB0185225 | Phospholipase B-like protein A; Phospholipase that removes both fatty-acid chains from phosphatidylcholine and produces the water-soluble glycerophosphorylcholine. In addition to phosphatidylcholine deacylation, it also hydrolyzes phosphatidylinositol and phosphatidylethanolamine | 0.48 |
| ponA | DDB0215380 | Ponticulin; Binds F-actin and nucleates actin assembly. Major high affinity link between the plasma membrane and the cortical actin network | 0.26 |
| prep | DDB0185041 | Prolyl endopeptidase; Cleaves peptide bonds on the C-terminal side of prolyl residues within peptides that are up to approximately 30 amino acids long; Belongs to the peptidase S9A family | 0.37 |
| proA | DDB0191178 | Profilin-1; Binds to actin and affects the structure of the cytoskeleton. At high concentrations, profilin prevents the polymerization of actin, whereas it enhances it at low concentrations. By binding to PIP2, it inhibits the formation of IP3 and DG | 0.77 |

| | | | |
|---|---|---|---|
| proB | DDB0191249 | Profilin-2; Binds to actin and affects the structure of the cytoskeleton. At high concentrations, profilin prevents the polymerization of actin, whereas it enhances it at low concentrations. By binding to PIP2, it inhibits the formation of IP3 and DG | 0.61 |
| prsA | DDB0237882 | Ribose-phosphate pyrophosphokinase A | 0.79 |
| purD | DDB0230084 | Bifunctional purine biosynthetic protein purDPhosphoribosylamine--glycine ligasePhosphoribosylformylglycinamidine cyclo-ligase; In the N-terminal section; belongs to the GARS family | 0.56 |
| pyd3 | DDB0185221 | Beta-ureidopropionase; Converts N-carbamoyl-beta-aminoisobutyrate and N- carbamoyl-beta-alanine (3-ureidopropanoate) to, respectively, beta-aminoisobutyrate and beta-alanine, ammonia and carbon dioxide | 0.72 |
| pyr1-3 | DDB0201646 | Protein PYR1-3; This protein is a "fusion" protein encoding four enzymatic activities of the pyrimidine pathway (GATase, CPSase, ATCase and DHOase) | 0.68 |
| rac1A | DDB0214822 | Rho-related protein rac1A; Overexpression promotes the formation of filopodia and membrane ruffles; Belongs to the small GTPase superfamily. Rho family | 0.63 |
| racC | DDB0201659 | Rho-related protein racC; Belongs to the small GTPase superfamily. Rho family | 0.64 |
| ranA | DDB0215409 | GTP-binding nuclear protein Ran; GTP-binding protein involved in nucleocytoplasmic transport. Required for the import of protein into the nucleus and also for RNA export. Involved in chromatin condensation and control of cell cycle (By similarity) | 0.83 |
| rasG | DDB0201663 | Ras-like protein rasG; Ras proteins bind GDP/GTP and possess intrinsic GTPase activity; Belongs to the small GTPase superfamily. Ras family | 0.75 |

| | | | |
|---|---|---|---|
| sahA | DDB0191108 | Adenosylhomocysteinase; Adenosylhomocysteine is a competitive inhibitor of S- adenosyl-L-methionine-dependent methyl transferase reactions; therefore adenosylhomocysteinase may play a key role in the control of methylations via regulation of the intracellular concentration of adenosylhomocysteine | 0.79 |
| sarA | DDB0229965 | GTP-binding protein Sar1A; Component of the coat protein complex II (COPII) which promotes the formation of transport vesicles from the endoplasmic reticulum (ER). The coat has two main functions, the physical deformation of the endoplasmic reticulum membrane into vesicles and the selection of cargo molecules (By similarity) | 0.68 |
| sasA | DDB0214885 | Ras-related protein Rab-8A; Protein transport. Probably involved in vesicular traffic (By similarity) | 0.80 |
| sec31 | DDB0235185 | Protein transport protein SEC31; Component of the coat protein complex II (COPII) which promotes the formation of transport vesicles from the endoplasmic reticulum (ER). The coat has two main functions, the physical deformation of the endoplasmic reticulum membrane into vesicles and the selection of cargo molecules (By similarity) | 0.56 |
| serA | DDB0230052 | D-3-phosphoglycerate dehydrogenase; Catalyzes the reversible oxidation of 3-phospho-D- glycerate to 3-phosphonooxypyruvate, the first step of the phosphorylated L-serine biosynthesis pathway. Also catalyzes the reversible oxidation of 2-hydroxyglutarate to 2-oxoglutarate; Belongs to the D-isomer specific 2-hydroxyacid dehydrogenase family | 0.68 |
| sevA | DDB0232954 | Severin; Severin blocks the ends of F-actin and causes the fragmentation and depolymerization of actin filaments in a Ca(2+) dependent manner | 0.59 |
| smt1 | DDB0237965 | Probable cycloartenol-C-24-methyltransferase 1; Catalyzes the methyl transfer from S-adenosyl- | 0.39 |

| | | | |
|---|---|---|---|
| | | methionine to the C-24 of cycloartenol to form 24-methylene cycloartenol | |
| snpA | DDB0231538 | Alpha-soluble NSF attachment protein; May be required for vesicular transport between the endoplasmic reticulum and the Golgi apparatus (By similarity). Involved in vesicle fusion with nsfA and probably SNARE proteins; Belongs to the SNAP family | 0.61 |
| sodC | DDB0232186 | Extracellular superoxide dismutase [Cu-Zn] 3; Protect the extracellular space from toxic effect of reactive oxygen intermediates by converting superoxyde radicals into hydrogen peroxyde and oxygen | 0.48 |
| ssr1 | DDB0266492 | Translocon-associated protein subunit alpha; TRAP proteins are part of a complex whose function is to bind calcium to the ER membrane and thereby regulate the retention of ER resident proteins; Belongs to the TRAP-alpha family | 0.49 |
| swp1 | DDB0233147 | Dolichyl-diphosphooligosaccharide--protein glycosyltransferase subunit swp1; Essential subunit of the N-oligosaccharyl transferase (OST) complex which catalyzes the transfer of a high mannose oligosaccharide from a lipid-linked oligosaccharide donor to an asparagine residue within an Asn-X-Ser/Thr consensus motif in nascent polypeptide chains | 0.60 |
| thfA | DDB0230118 | Methylenetetrahydrofolate dehydrogenase [NAD(+)]; Catalyzes oxidation of cytoplasmic one-carbon units for purine biosynthesis | 0.68 |
| trrA | DDB0231235 | Thioredoxin reductase; Belongs to the class-II pyridine nucleotide-disulfide oxidoreductase family | 0.80 |
| trxE | DDB0237674 | Putative thioredoxin-5; Participates in various redox reactions through the reversible oxidation of its active | 0.69 |

| | | | |
|---|---|---|---|
| | | center dithiol to a disulfide and catalyzes dithiol-disulfide exchange reactions | |
| vasp | DDB0229340 | Protein VASP homolog; Ena/VASP proteins are actin-associated proteins involved in a range of processes dependent on cytoskeleton remodeling and cell polarity such as lamellipodial and filopodial dynamics in migrating cells. Plays a crucial role in filopodia formation, cell-substratum adhesion, and proper chemotaxis. Nucleates and bundles actin filaments. When complexed with fotH in filopodial tips, may support formin-mediated filament elongation by bundling nascent actin filaments; Belongs to the Ena/VASP family | 0.52 |

## APPENDIX 8 BOOK CHAPTER

CHAPTER28

# Tau and its interactions with other proteins in neurodegenerative diseases

Katelyn H. Mroczek, Sarah J. Annesley, Paul R. Fisher

Discipline of Microbiology, Department of Physiology, Anatomy and Microbiology, La Trobe University, Bundoora, VIC, Australia

### List of abbreviations

AD Alzheimer's disease
APP amyloid precursor protein
Ab amyloid beta
CBD corticobasal degeneration
DLBD dementia with Lewy body disease
DS Down's syndrome
FTDP-17 frontotemporal dementia with parkinsonism linked to chromosome 17
GSK-3b glycogen synthase kinase 3 beta
GSS GertsmanneStrausslereScheinker
KO knockout
LB Lewy body
MT microtubules
NFT neurofibrillary tangles PD Parkinson's disease
PHF paired helical filament
PiD Pick's disease PrP prion protein
PSP progressive supranuclear palsy a-syn alpha synuclein

### Minidictionary of terms

Contursi kindred A family with an autosomal dominant form of Parkinson's disease from the village of Contursi Terme, Italy
Lewy body Abnormal protein deposits in the brain predominantly made up of alpha-synuclein
Neurofibrillary tangles Aggregates of hyperphosphorylated tau protein found in some neurodegenerative diseases
Synucleinopathies A group of neurodegenerative diseases in which the hallmark is aggregated a-synuclein protein
Tauopathies A group of neurodegenerative diseases in which the hallmark is aggregated tau protein

Genetics, Neurology, Behavior, and Diet in Parkinson's Disease
ISBN 978-0-12-815950-7, https://doi.org/10.1016/B978-0-12-815950-7.00028-X

## Introduction

Deposits of aggregated protein are a prominent feature of many neurodegenerative diseases. Tau is an abundant protein found in the brain and produces neurofibrillary tangles and other aggregates predominantly found in a group of diseases known as tauopathies (Table 28.1) (Goedert & Spillantini, 2011; Lee, Goedert, & Trojanowski, 2001; Spillantini & Goedert, 1998). Other proteins implicated in neurodegeneration include alphasynuclein, the hallmark of synucleinopathies (Galpern & Lang, 2006), amyloid beta, one of the main proteins involved in Alzheimer's disease (AD) (Glenner & Wong, 1984) and the abnormal isoform of prion protein involved in disorders known as prion diseases (Prusiner, 1991). Tau is a major protein involved in many disorders and has been associated with these proteins in different diseases (Fig. 28.1). In many of these disorders more than one of these proteins are detected with an overlap of symptoms and pathologies. This may indicate an interaction and a possible synergistic relationship of these proteins leading to neurodegeneration. Therefore, this review will focus on the interactions between pathological proteins and tau in neurodegenerative diseases.

## Tau

Tau is encoded by the MAPT gene, which is located on chromosome 17q21, contains 16 exons, and is 100 kb in size. The protein binds to tubulin, promoting the assembly and stability of microtubules (MTs) thus aiding in axonal transport and supporting the structure of neurons (Cleveland, Hwo, & Kirschner, 1977; Kosik, 1993). Tau is predominantly located within the neurons (Drubin & Kirschner, 1986) where it may work synergistically with other microtubule-associated proteins (De Vos, Grierson, Ackerley, & Miller, 2008). The protein contains an acidic N-terminal region, thought to maintain

Table 28.1 Neurodegenerative tauopathies. Neurodegenerative diseases with predominant tau pathology are classified as tauopathies.

| |
|---|
| Alzheimer's disease |
| Down's syndrome |
| Dementia pugilistica |
| Corticobasal degeneration |
| Frontotemporal dementia with parkinsonism linked to chromosome 17 |
| Progressive supranuclear palsy |
| Argyrophilic grain disease |
| Pick's disease |
| Dementia with tangles |
| Diffuse neurofibrillary tangles with calcification |
| Myotonic dystrophy |

Tau accumulates into aggregates that are the hallmarks of these diseases (Goedert & Spillantini, 2011; Iqbal et al., 2005; Lee et al., 2001; Spillantini & Goedert, 1998).

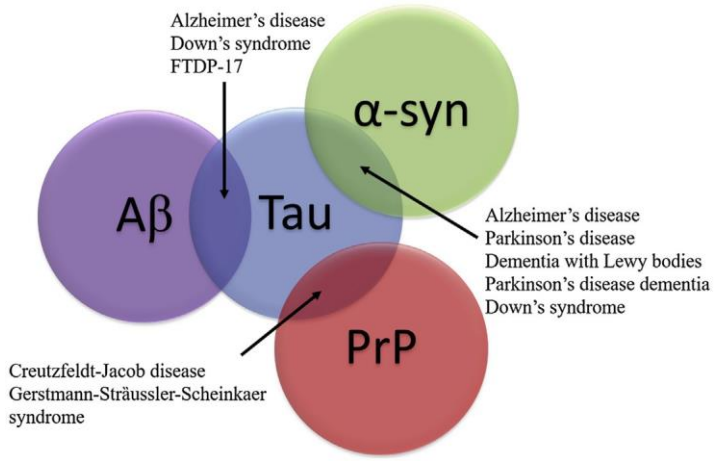


Figure 28.1 Protein deposits in neurodegenerative diseases. Illustrating the disorders in which neurotoxic protein aggregates of amyloid beta (Ab), a-synuclein (a-syn), and prion protein (PrP) are found together with tau protein aggregates.

spacing between MT and promote interactions with other cytoskeletal proteins (Avila, Lucas, Perez, & Hernandaz, 2004; Mandelkow, Von Bergen, Biernat, & Mandelkow, 2007). The middle region consists of a proline-rich domain that binds proteins and the C-terminal portion is known as the assembly domain, which contains a tubulinbinding domain to promote MT assembly (Mandelkow et al., 2007).

There are six tau protein isoforms that are expressed in the brain due to alternative splicing of the RNA transcript (Andreadis, Brown, & Kosik, 1992) (Fig. 28.2). These range from 352 to 441 amino acids in length and contain either three (3R) or four (4R) microtubule-binding repeat sequences that are in the C-terminus of the protein (Goedert, Spillantini, Jakes, Rutherford, & Crowther, 1989, Goedert, Spillantini, Potier, Ulrich, & Crowther, 1989; Himmler, Drechsel, Kirschner, & Martin, 1989). The MT repeats are encoded by exons 9e12 and contain either three or four repeats dependent on the presence or absence of exon 10. The affinity for MT binding increases with the number of repeats (Spires-Jones, Stoothoff, de Calignon, Jones, & Hyman, 2009). The isoforms also differ in N-terminal inserts due to the alternative splicing of exons 2 and 3. This results in isoforms containing both exons (2N), only exon 2 (1N) or neither exon 2 or 3 (0N). The shortest of the isoforms (0N3R) is known as fetal tau as it is present at birth, while the other isoforms are developmentally regulated such that all six isoforms are expressed in the adult brain (Goedert et al., 1989).

Normally tau binds to and is released from MT dependent on the phosphorylation state of the protein. Phosphorylation of tau negatively affects its ability to bind, while tau dephosphorylation increases the affinity to bind and stabilize MT (Cleveland et al., 1977; Lindwall & Cole, 1984). There are over 80 phosphorylation sites on the longest

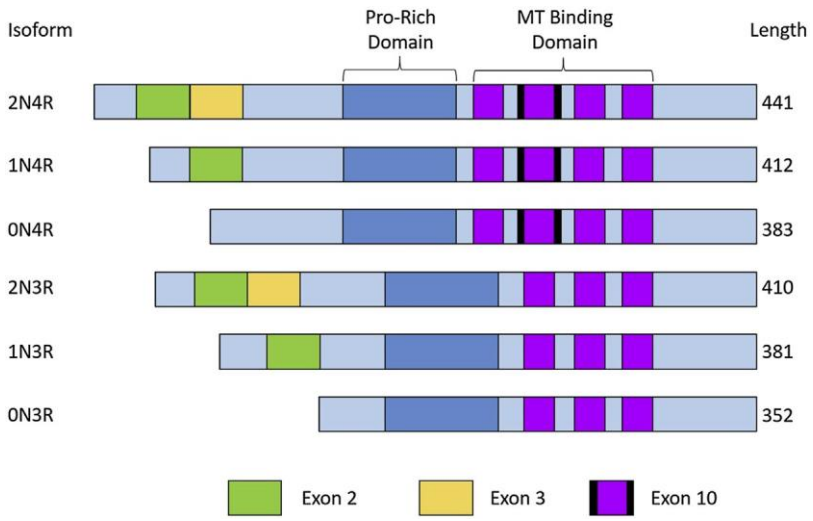


Figure 28.2 Tau protein isoforms. Alternative splicing of MAPT produces six isoforms differing in sequences from exons 2 and 3 and the presence or absence of exon 10. The shortest isoform (0N3R) is the fetal form, and the other isoforms are developmentally regulated to express all six isoforms in the adult brain. (Information from Spillantini, M. G., & Goedert, M. (1998). Tau protein pathology in neurodegenerative diseases. Trends in Neurosciences, 21, 428e433; Lee, V. M. Y., Goedert, M., & Trojanowski, J. Q. (2001). Neurodegenerative tauopathies. Annual Review of Neuroscience, 24, 1121e1159; Guo, T., Noble, W., & Hanger, D. P. (2017). Roles of tau protein in health and disease. Acta Neuropathologica, 133,

665e704.)

tau isoform, 71 of which have been implicated in either physiological or pathological conditions (Buee, Bussiere, Buee-Scherrer, Delacourte, & Hof, 2000; Hanger et al., 2007), with over 20 kinases that phosphorylate at these sites. One of the major tau kinases found to employ significant roles in the regulation of tau phosphorylation during normal and pathological circumstances is GSK-3b (Lee, Lau, Miller, & Shaw, 2002). In pathological conditions further hyperphosphorylation of tau is the main contributing factor in the formation of tau aggregates (Fig. 28.3). These aggregates can adopt many conformations, but the most commonly found is neurofibrillary tangles (NFTs) composed of paired helical filaments (PHFs) of tau (Grundke-Iqbal et al., 1986). In 1987 antibodies detected tangles composed of tau in the normal brain and in many neurodegenerative diseases such as AD, Down's syndrome (DS), Parkinson's disease (PD), progressive supranuclear palsy (PSP), and parkinsonism-dementia complex of Guam (Joachim, Morris, Kosik, & Selkoe, 1987). These diseases, characterized by the accumulation of abnormally phosphorylated and aggregated tau, are collectively known as tauopathies. Although tau is the main neurotoxic protein found in these diseases, other proteins have been found to colocalize and interact with tau (also within other disorders), suggesting possible synergistic relationships between neurodegenerative proteins (Table 28.2).

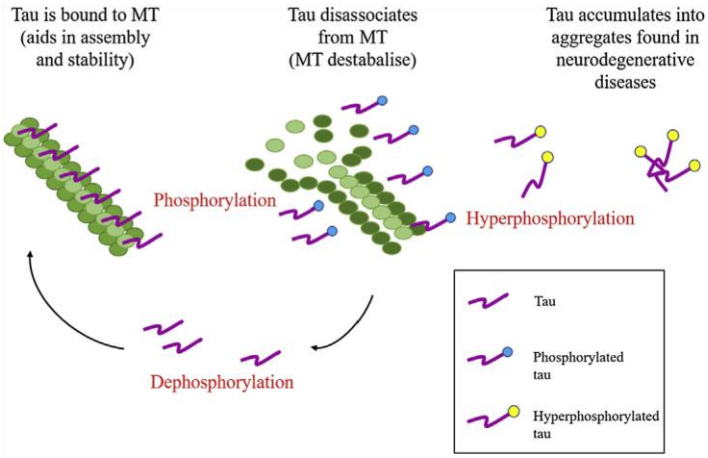


Figure 28.3 Tau phosphorylation and accumulation into aggregates. Tau binds on and off microtubules (MTs) depending on its phosphorylation state. Phosphorylation causes tau to dissociate from the microtubules leading to their destabilization. Dephosphorylated tau regains its affinity for and binds to MT. Further hyperphosphorylation leads to the accumulation of tau protein into the aggregates found in tauopathies and other neurodegenerative diseases.

Table 28.2 Tau-associated proteins in neurodegenerative disease.

| Disease | Tau aggregate | Associated proteins |
|---|---|---|
| Alzheimer's disease | NFT | Ab<br>a-syn<br>Filamin<br>Myosin |
| Parkinson's disease | Neurites | a-syn |
| Pick's disease | Pick bodies<br>Neurites | DJ-1 |
| Corticobasal degeneration | NFT | DJ-1 |
| Prion disease | NFT | PrP |
| FTDP-17 | NFT<br>Neuropil threads | Ab<br>a-syn<br>Filamin<br>Myosin |

In tauopathies and other neurological diseases, tau is observed in addition to other proteins implicated in neurodegeneration. Tau aggregates and associated proteins can differ between diseases.

### Alzheimer's disease

The most common tauopathy is Alzheimer's disease. The classical hallmarks of AD, namely NFT and amyloid plaques, were first discovered in 1906 by Alois Alzheimer (Stelzmann, Schnitzlein, & Murtagh, 1995). In 1984, Glenner and Wong purified the short amyloid protein from AD brains, which showed a beta sheet structure, and named it the amyloid beta (Ab) protein. Ab is generated from the amyloid-b precursor protein (APP), which, when cleaved by b and g secretases releases the major Ab isoforms, Ab40 and Ab42 (Selkoe, 1999). In sporadic forms of AD, Ab40 has been found at a 10-fold higher concentration than the other predominant isoform (N€aslund et al., 1994), although Ab42 is thought to be the more toxic form.

In familial AD, there is genetic evidence to link Ab aggregation leading to events inducing tau hyperphosphorylation and aggregation (Haass & Selkoe, 2007) with Ab correlating with synaptic dysfunction and cognitive decline. This corresponds with the amyloid cascade hypothesis (Fig. 28.4) originally proposed in the early 1990s (Hardy & Higgins, 1992). The consensus was that toxic Ab deposits are an early event and the main cause of AD pathology, leading to the formation of tau NFT and the death of neurons. Thus commenced many investigations into the brain pathology of AD patients using numerous cell and animal models of AD to elucidate the roles of tau and Ab and their possible interaction.

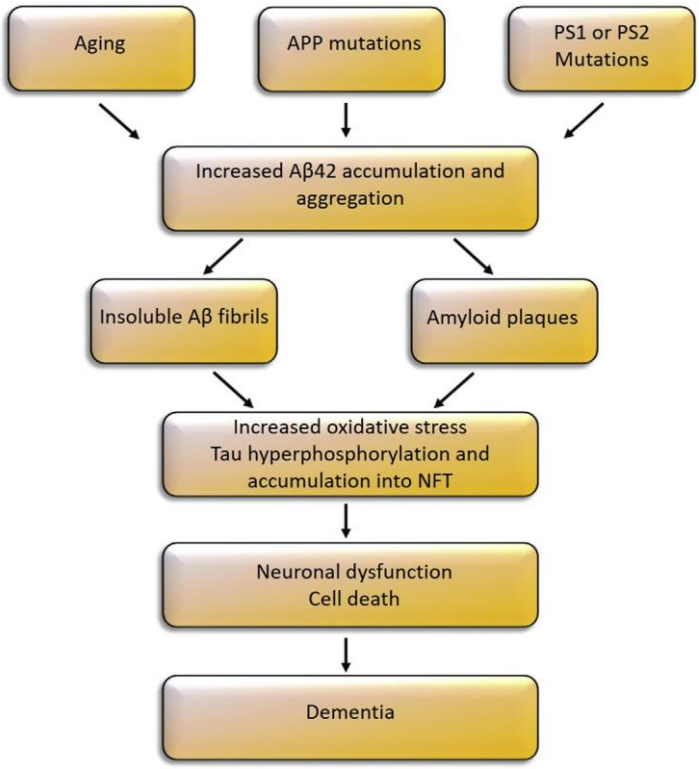


Figure 28.4 The amyloid cascade hypothesis. Originally suggested by Hardy and Higgins (1992), this proposes the sequence of pathological events leading to AD and dementia. In this hypothesis, Ab neurotoxicity is an early event preceding tau filament formation and aggregation to neurofibrillary tangles (NFTs).

Oddo et al. (2003) created a triple transgenic mouse model with mutations in presenilin-1 (a subunit of g secretase), APP, and Tau. In this model, mice progressively develop plaque and tangle pathology, with Ab deposits occurring at an earlier age (6 months), while extensive tau pathology did not occur until 12 months. This is consistent with the amyloid cascade hypothesis as Ab deposits develop much earlier than tau. Another study using transgenic mice showed that NFT pathology was elevated in mice harboring the tau point mutation P301L as well as a mutation in APP (Tau/APP), when compared to mice carrying only the mutant tau (Lewis et al., 2001). This provides some evidence that APP or Ab may influence NFT formation. However, the double mutant, tau/APP mice developed amyloid deposits

at the same time as mice with only the APP mutation. This suggests that the tau mutation did not exacerbate the development of Ab pathology.

Nevertheless, there is also evidence that tau is a toxic protein that contributes to Ab pathology. Rapoport, Dawson, Binder, Vitek, and Ferreira (2002) used cultured hippocampal neurons that were taken from tau knockout (KO) mice or mice expressing either the wild-type mouse or human tau gene. When these neurons were treated with fibrillar Ab, neurons that contained either mouse or human tau displayed degeneration, while the tau KO neurons did not exhibit this degeneration. This suggests that tau is necessary for the development of the downstream cytopathology caused by Abfibrils. It has also been reported that tau knockdown can lead to a reduction in Ab40 and Ab42 levels in vitro in primary human cortical neurons (Bright et al., 2015). Exogenous addition of extracellular tau to the cultured neurons increased Ab levels, suggesting tau to be a driver of Ab accumulation.

Ab is not the only protein seen to be present with tau in AD. Another protein profoundly involved in neurodegenerative disease is alpha-synuclein (a-syn). This protein is the foremost component of Lewy bodies (LBs) found in neurodegenerative diseases and has also been found to coexist with tau. In two studies of sporadic cases of AD, LBs were found to exist in 60% of affected brains (Hamilton, 2000), and a-syn positive structures were detected in 13/27 other AD cases (Arai et al., 2001). In both of these reports deposits were mainly confined to the amygdala.

**Parkinson's disease**

Lewy bodies containing a-syn are the definitive feature of Parkinson's disease. However like tau, a-syn aggregates are found not only in PD but in other neurodegenerative diseases. Disorders known collectively as synucleinopathies exhibit a-syn aggregates as their defining feature. There is much overlap in the symptoms of tauopathies and synucleinopathies with the coexistence of the two proteins in many of these diseases. PD is the most common synucleinopathy.

Both idiopathic and familial forms of PD occur, with a-syn-containing LB the prominent pathological feature. As mentioned, tau is often seen to coexist with a-syn, and this is also evident in cases of PD. Mutations in SNCA, which encodes a-syn, cause a familial form of PD. However the question arises as to whether a genetic predisposition for idiopathic PD may also exist. A complete genome screen of PD conducted in 2001 aimed to determine genetic risk factors of genes associated with idiopathic PD (Scott et al., 2001). An observed linkage to a region on chromosome 17 that contains the tau gene was identified. This led the investigators to conduct a study of 235 families with 426 affected with PD and 579 nonaffected individuals. They implicated MAPT as a susceptibility gene for late-onset idiopathic PD as they found a MAPT haplotype that strongly correlated with an increased risk of inheriting PD

(Martin et al., 2001). There have been many studies on PD brains and model systems used to determine whether there is an interaction between these two proteins, and there is much evidence to suggest this.

The first familial form of PD was discovered and subsequently found to be caused by an autosomal dominant a-syn mutation (A53T) in the Contursi kindred, a large extended family from the Italian village of Contursi. Within brain tissues from the family, there has been a notable coexistence of a-syn and tau. One study found rare LB pathology and previously unrecognized a-syn pathology (Duda et al., 2002). Within these neurites, tau inclusions were also unexpectedly found, and in some inclusions colocalized with a-syn. Another study conducted on an individual from the Contursi kindred indicated insoluble a-syn throughout the brain and significant accumulation of filamentous tau in specific areas of the brain (Kotzbauer et al., 2004). Large spheroids reacted positively to tau immunoreactivity, and tau and a-syn were sometimes stained in the same inclusion. The authors speculated the A53T mutation may play a role in the fibrillization of tau. Therefore, they performed in vitro fibrillization assays using WT a-syn, a-syn with the A53T mutation and tau. The results indicated that the A53T mutation promotes faster fibrillization of a-syn and tau filament formation as well as synergistically enhancing tau and a-syn cofibrillization (Kotzbauer et al., 2004).

As directly studying the interaction of a-syn and tau in PD patients was limited to investigating postmortem brains, many models have been used to gain insights to the possible mechanisms and toxicity that coexpression of these proteins may cause. The A30P missense mutation in SNCA causes an autosomal dominant form of PD, and mice expressing A30P a-syn were found to develop a four-fold increase in tau phosphorylated at serine 396/404 (a pathological residue) when compared to controls (Frasier et al., 2005). Although a strong colocalization of a-syn and tau was not seen in this study, it has been known to occur. When tau and a-syn were expressed in Chinese hamster ovary (CHO) cells, tau and a-syn were seen to largely colocalize except in the nucleus (Esposito, Dohm, Kermer, B€ahr, & Wouters, 2007). However the authors acknowledged that this was not indicative of an interaction of these two proteins. Waxman & Giasson (2011) made similar findings when expressing two plasmids containing tau and a-syn in cells derived from human embryonic kidney cells. Again, colocalization seemed coincidental. However, when these cells were treated with recombinant prefibrillized a-syn protein, large intracellular aggregates were formed containing both a-syn and tau.

Two studies have used the $MMP^{þ}$/MPTP model of PD to study the interaction of tau and a-syn. 1-methyl-4-phenyl-1,2,3,6-tetrahydropyridine (MPTP) is metabolized into 1-methyl-4-phenylpyridinium ($MMP^{þ}$), a neurotoxin that produces severe PD (Tieu, 2011). $MMP^{þ}$/MPTP-induced PD models have been created in cell lines and transgenic mice (Duka, Duka, Joyce, & Sidhu, 2009; Qureshi & Paudel,

2011). In some models, GSK-3b is heavily activated as seen in transgenic mice overexpressing a-syn and in the postmortem striatum of PD patients (Duka et al., 2009). MPTP activated tau phosphorylation by GSK-3b in the transgenic mouse model, and this was dependent on the presence of a-syn. A physical interaction between a-syn, GSK-3b, and tau was confirmed by coimmunoprecipitation, indicating that these proteins form a complex.

MPTP has also been used in models with mutations in a-syn. In human neuroblastoma M17 cells treated with MPTP, a-syn bound to Ser214 of tau and induced the phosphorylation of tau at serine 262 (Qureshi & Paudel, 2011). MPTP-induced tau phosphorylation at this site was suppressed in KO a-syn mice, suggesting that MPTP enhances the ability of intracellular a-syn to stimulate the increased phosphorylation of tau (Qureshi & Paudel, 2011). In a similar vein, in MPTP-treated HEK-293 cells, a-syn mutants (A30P, E4KR, and A53T) contributed to destabilization of the cytoskeleton (Qureshi & Paudel, 2011). When these mutant forms of a-syn were coexpressed with tau, MT destabilization was significantly more pronounced compared to coexpression with wildtype a-syn. This indicates that point mutations in SNCA may contribute to tau pathology in neurodegeneration.

A similar suggestion that these proteins enhance neurodegenerative pathology when combined comes from a study of neurotoxicity using a Drosophila model of PD. Roy and Jackson (2014) misexpressed a-syn and tau singly and in combination in Drosophila and used three different tissues to gain insights into interactions between these two proteins. Misexpression of a-syn alone caused no phenotype in the retina, while tau caused a rough eye phenotype and produced smaller eyes, a phenotype that was enhanced when both tau and a-syn were expressed together. Likewise, the ectopic expression of a-syn enhanced tau-induced motor dysfunction, and coexpression resulted in abnormal MT organization and actin cytoskeletal disorganization. These results suggest a synergistic interaction between tau and a-syn in producing cytoskeletal cytopathologies.

**Synucleinopathies**

As described in the preceding section, there is evidence that tau and a-syn work together in PD to produce neurodegeneration. However, this is not the only neurological disorder in which a-syn is a pathological protein. More examples of cooperative tau and a-syn pathology are found in other synucleinopathies. Badiola et al. (2011) used different cellular models of synucleinopathies to investigate the effects of tau on a-syn aggregation. In both human cell lines and primary neuronal cultures tau and a-syn colocalized in aggregates and in other parts of the cell, where tau phosphorylated and dephosphorylated forms were detected. The overexpression of tau in these cells

led to an increased number and decreased size of a-syn aggregates. Overall the study concluded that tau enhanced a-syn cytotoxicity.

Postmortem brains of patients with dementia with Lewy bodies disease (DLBD) were examined to determine the frequency of neurons that contained both LB and NFT (Iseki, Marui, Kosaka, & Ueda, 1999). Neurons positive for both inclusions were frequently seen in the limbic areas. Generally, a-syn-positive LBs were surrounded with small, randomly oriented paired helical filaments (PHF) (Iseki et al., 1999). Coaggregation of tau and a-syn was also seen in LBs taken from patients with LB disease. Double immunostaining in LB cases found tau-containing LB in 80% of cases where LBs were present in the medulla (Ishizawa, Mattila, Davies, Wang, & Dickson, 2003). Colocalization of a-syn with tau has also been implicated in some of the tauopathies where tau forms the prominent pathological aggregate.

**Tauopathies**

Protein aggregates including a-syn have been found within postmortem brains of patients with tauopathy diseases. Immunohistochemical examination with a-syn antibodies detected LBs in 50% of cases of Down's syndrome with AD (Lippa, Schmidt, Lee, & Trojanowski, 1999). These were more frequent in the amygdala and the LBs sometimes colocalized with NFT.

LBs have also been detected in a small number of PSP cases (Jellinger, 2004; Mori et al., 2002). Mori et al. (2002) found with LB pathology and colocalization of tau and a-syn in some neurons in 5 out of 16 patients with PSP.

Another protein seen to colocalize with tau in some of the tauopathies is DJ-1. Patrizia et al. (2004) detected immunopositively labeled DJ-1 in NFT and neuropil threads in several cases of DLBD. They also observed DJ-1 reactivity in Pick bodies in Pick's disease (PiD). Up to 50% of tau-positive inclusions stained positive for DJ-1 in the hippocampus in the PiD cases. Antibodies against DJ-1 have also been used to test its prevalence in a range of synucleinopathies and tauopathies. In tauopathies, neuronal tau deposits reacted positively to DJ-1 in PiD, corticobasal degeneration (CBD), PSP, and AD. Conversely, DJ-1 was not detected in human LB containing a-syn (Neumann et al., 2004).

**Prion diseases**

Other than disease hallmarked by either tau or a-syn deposits, other proteinopathies exists, such as prion diseases where tau has also been found to localize in protein aggregates. Prion diseases are a group of neurodegenerative disorders that are transmissible and contain genetic familial forms caused by abnormal isoforms of the prion protein (PrP) (Prusiner, 1991). In 1992, the familial GertsmanneStrausslereScheinker (GSS) disease, associated with mutations in prion proteins, was

discovered for the first time to contain both the PrP amyloid plaques and NFT (Hsiao et al., 1992). NFT with amyloid plaques reacting to PrP antibodies were detected in the neocortex, together with the accumulation of protease-resistant PrP. Two families with GSS have been studied and found to contain NFT composed of PHF of abnormally phosphorylated tau and the accumulation of PrP (Ghetti et al., 1994).

The interaction of tau and PrP has been investigated in cellular and mouse models. CHO cells transfected with constructs to express both tau and PrP showed colocalization of the two proteins using immunofluorescence microscopy (Han et al., 2006). Tau interacted with both the native PrP and protease-resistant (toxic) PrP isoforms. This interaction occurred on the N-terminal residues of PrP. More recently phosphorylated tau and PrP were studied in mouse models that were inoculated with prion agents and developed PrP amyloid without any indication of prion disease (Piccardo, King, Brown, & Barron, 2017). Replication and transmissibility of the PrP was confirmed by serially infecting subsequent passages of mice, and phosphorylated tau was consistently present. However, tau phosphorylation was hardly seen in mice harboring the PrP amyloid plaques without the replication of PrP (Piccardo et al., 2017). Therefore, the authors suggested that toxicity or replication of the prion protein, not conformation of PrP, may contribute to tau phosphorylation and fibril formation.

**FTDP-17**

Tauopathies are generally sporadic neurodegenerative diseases, however, mutation in MAPT does cause a major neurodegenerative tauopathy known as frontotemporal dementia with parkinsonism linked to chromosome 17 (FTDP-17). More than 35 MAPT mutations have been identified from over 150 families affecting all six isoforms (Shiarli et al., 2006). As these mutations cause a genetic form of a tauopathy, many studies using the most commonly found mutation (P301L) have been directed at assessing the different protein interactions with tau.

The P301L transgenic mouse model has been extensively used. Injections of Abfibrils directly into the brain of P301L mice cause a fourfold increase in NFT around the site of injection (Gotz, Chen, van Dorpe, & Nitsch, 2001). The NFT formed contained tau phosphorylated at serine 212/threonine 214 and serine 422. Oligomeric and fibrillar species of Ab have also been shown to decrease mitochondrial membrane potential and impair mitochondrial function in tau mutant mice (Eckert et al., 2008). The P301L mutation also increases the propensity of tau to form NFT when cross-seeded with preformed a-syn fibrils. A wild-type tau cellular model generated a small number of NFT when cross-seeded with a-syn, whereas cells with the P301L mutation converted over 50% of total tau to NFT (Waxman & Giasson, 2011).

FTDP-17 brains have also been found to contain tau colocalizing with the cytoskeletal proteins Filamin-A and Myosin-VI (Feuillette et al., 2010). Filamin A was a component in NFT, neuropil threads and in coiled bodies with myosin VI-positive "ghost tangles." The accumulation of these two proteins was also seen in AD brains, but not those of PiD or PSP. Since these proteins are involved in the cytoskeletal network, the authors proposed that tau toxicity may be compounded by the breakdown of the actin network.

**Conclusion**

Although tau appears to interact with many of the proteins associated with pathological conditions in neurodegeneration, the mechanism of many of these interactions is still unclear. Animal and cellular models have aided in understanding the possible interactions and how these proteins coactively may cause disease. However, ongoing research is needed to further elucidate the pathways in which these proteins contribute to neurodegenerative disorders.

**Key points about tauopathies**

- Tauopathies are a group of neurodegenerative disease in which the hallmark is the accumulation of the tau protein into aggregates
- Alzheimer's disease is the most common tauopathy and the most prevalent neurodegenerative disease
- Tauopathies are mainly sporadic and include: progressive supranuclear palsy, corticobasal degeneration, Pick's disease, and Down's syndrome
- Mutations of tau cause a familial tauopathy known as frontotemporal dementia with parkinsonism linked to chromosome 17 (FTDP-17); this is the only tauopathy caused by tau mutations
- In the healthy human brain and also in Alzheimer's disease, the ratio of three repeat (3R) to four repeat (4R) tau is approximately equal

- In tauopathies, the ratio of 3e4R tau differs and is dependent on the disorder
- Tau filament and aggregate formation also differs between tauopathies
- There is an overlap in the pathological symptoms of tauopathies and other proteinopathies with the coexistence of many proteins in protein aggregates in these diseases

**Summary points**

- Tau is a microtubule-associated protein that dynamically binds on and off microtubules dependent on the protein's phosphorylation state
- Hyperphosphorylated tau accumulates into aggregates associated with neurodegenerative diseases
- Tau aggregates have been detected in many neurodegenerative diseases (called tauopathies) in which it may interact with other pathological proteins
- Mutations in tau cause frontotemporal dementia with parkinsonism linked to chromosome 17, a disease in which other neurodegenerative proteins have been associated

- Animal and cellular models have been useful in researching the interactions of these proteins
- Research needs to continue to determine whether these associations contribute to disease

## References


Andreadis, A., Brown, W. M., & Kosik, K. S. (1992). Structure and novel exons of the human-tau gene. Biochemistry, 31, 10626e10633.

Arai, Y., Yamazaki, M., Mori, O., Muramatsu, H., Asano, G., & Katayama, Y. (2001). a-Synuclein-positive structures in cases with sporadic Alzheimer's disease: morphology and its relationship to tau aggregation. Brain research, 888, 287e296.

Avila, J., Lucas, J. J., Perez, M., & Hernandaz, F. (2004). Role of tau protein in both physiological and pathological conditions. Physiological Reviews, 84, 361e384.

Badiola, N., de Oliveira, R. M., Herrera, F., et al. (2011). Tau enhances alpha-synuclein aggregation and toxicity in cellular models of synucleinopathy. PLoS One, 6(10), e26609.

Bright, J., Hussain, S., Dang, V., et al. (2015). Human secreted tau increases amyloid-beta production. Neurobiology of Aging, 36, 693e709.

Buee, L., Bussiere, T., Buee-Scherrer, V., Delacourte, A., & Hof, P. R. (2000). Tau protein isoforms, phosphorylation and role in neurodegenerative disorders. Brain Research Reviews, 33, 95e130.

Cleveland, D. W., Hwo, S.-Y., & Kirschner, M. W. (1977). Physical and chemical properties of purified tau factor and the role of tau in microtubule assembly. Journal of Molecular Biology, 116, 227e247.

De Vos, K. J., Grierson, A. J., Ackerley, S., & Miller, C. C. J. (2008). Role of axonal transport in neurodegenerative diseases. Annual Review of Neuroscience, 31, 151e173.

Drubin, D. G., & Kirschner, M. W. (1986). Tau protein function in living cells. The Journal of Cell Biology, 103, 2739e2746.

Duda, J. E., Giasson, B. I., Mabon, M. E., Miller, D. C., Golbe, L. I., Lee, V. M.-Y., et al. (2002). Concurrence of alpha-synuclein and tau brain pathology in the contursi kindred. Acta Neuropathologica, 104, 7e11.

Duka, T., Duka, V., Joyce, J. N., & Sidhu, A. (2009). a-Synuclein contributes to GSK-3b-catalyzed Tau phosphorylation in Parkinson's disease models. The FASEB Journal, 23, 2820e2830.

Eckert, A., Hauptmann, S., Scherping, I., et al. (2008). Oligomeric and fibrillar species of betaamyloid (A beta 42) both impair mitochondrial function in P301L tau transgenic mice. Journal of Molecular Medicine, 86.

Esposito, A., Dohm, C. P., Kermer, P., B€ahr, M., & Wouters, F. S. (2007). a-Synuclein and its diseaserelated mutants interact differentially with the microtubule protein tau and associate with the actin cytoskeleton. Neurobiology of Disease, 26, 521e531.

Feuillette, S., Deramecourt, V., Laquerriere, A., et al. (2010). Filamin-A and Myosin VI colocalize with fibrillary Tau protein in Alzheimer's disease and FTDP-17 brains. Brain Research, 1345, 182e189.

Frasier, M., Walzer, M., McCarthy, L., Magnuson, D., Lee, J. M., Haas, C., et al. (2005). Tau phosphorylation increases in symptomatic mice overexpressing A30P a-synuclein. Experimental Neurology, 192, 274e287.

Galpern, W. R., & Lang, A. E. (2006). Interface between tauopathies and synucleinopathies: A tale of two proteins. Annals of Neurology, 59, 449e458.

Ghetti, B., Tagliavini, F., Giaccone, G., Bugiani, O., Frangione, B., Farlow, M. R., et al. (1994). Familial Gerstmann-Str€aussler-Scheinker disease with neurofibrillary tangles. Molecular Neurobiology, 8, 41e48.

Glenner, G. G., & Wong, C. W. (1984). Alzheimer's disease: Initial report of the purification and characterization of a novel cerebrovascular amyloid protein. Biochemical and Biophysical Research Communications, 120, 885e890.

Goedert, M., & Spillantini, M. (2011). Pathogenesis of the tauopathies. Journal of Molecular Neuroscience, 45, 425e431.

Goedert, M., Spillantini, M. G., Jakes, R., Rutherford, D., & Crowther, R. A. (1989). Multiple isoforms of human microtubule-associated protein tau: Sequences and localization in neurofibrillary tangles of Alzheimer's disease. Neuron, 3, 519e526.

Goedert, M., Spillantini, M. G., Potier, M. C., Ulrich, J., & Crowther, R. A. (1989). Cloning and sequencing of the cDNA encoding an isoform of microtubule-associated protein tau containing four tandem repeats: Differential expression of tau protein mRNAs in human brain. The EMBO Journal, 8, 393e399.

Gotz, J., Chen, F., van Dorpe, J., & Nitsch, R. M. (2001). Formation of neurofibrillary tangles in P301l tau transgenic mice induced by Abeta 42 fibrils. Science, 293, 1491e1495.

Grundke-Iqbal, I., Iqbal, K., Quinlan, M., Tung, Y. C., Zaidi, M. S., & Wisniewski, H. M. (1986). Microtubule-associated protein tau. A component of Alzheimer paired helical filaments. Journal of Biological Chemistry, 261, 6084e6089.

Haass, C., & Selkoe, D. (2007). Soluble protein oligomers in neurodegeneration: Lessons from the Alzheimer's amyloid beta-peptide. Nature Reviews Molecular Cell Biology, 8, 101e112.

Hamilton, R. L. (2000). Lewy Bodies in Alzheimer's Disease: A Neuropathological Review of 145 Cases Using a-Synuclein Immunohistochemistry. Brain Pathology, 10, 378e384.

Hanger, D. P., Byers, H. L., Wray, S., Leung, K.-Y., Saxton, M. J., Seereeram, A., et al. (2007). Novel phosphorylation sites in tau from Alzheimer brain support a role for casein kinase 1 in disease pathogenesis. Journal of Biological Chemistry, 282, 23645e23654.

Han, J., Zhang, J., Hailan, Y., et al. (2006). Study on interaction between microtubule associated protein tau and prion protein. Science in China - Series C: Life Sciences, 49, 1e7.

Hardy, J. A., & Higgins, G. A. (1992). Alzheimer's disease: The amyloid cascade hypothesis. Science, 256, 184þ.

Himmler, A., Drechsel, D., Kirschner, M. W., & Martin, D. W. (1989). Tau consists of a set of proteins with repeated C-terminal microtubule-binding domains and variable N-terminal domains. Molecular and Cellular Biology, 9, 1381e1388.

Hsiao, K., Dlouhy, S. R., Farlow, M. R., Cass, C., Da Costa, M., Conneally, M.,P., et al. (1992). Mutant prion proteins in Gerstmann-Straussler-Scheinker disease with neurofibrillary tangles. Nature Genetics, 1, 68e71.

Iqbal, K., Alonso Adel, C., Chen, S., et al. (2005). Tau pathology in Alzheimer disease and other tauopathies. Biochimica et Biophysica Acta, 1739, 198e210.

Iseki, E., Marui, W., Kosaka, K., & Ueda, K. (1999). Frequent coexistence of Lewy bodies and neurofibrillary tangles in the same neurons of patients with diffuse Lewy body disease. Neuroscience Letters, 265, 9e12.

Ishizawa, T., Mattila, P., Davies, P., Wang, D., & Dickson, D. W. (2003). Colocalization of tau and alphasynuclein epitopes in Lewy bodies. Journal of Neuropathology and Experimental Neurology, 62, 389e397.

Jellinger, K. A. (2004). Lewy body-related a-synucleinopathy in the aged human brain. Journal of Neural Transmission, 111, 1219e1235.

Joachim, C. L., Morris, J. H., Kosik, K. S., & Selkoe, D. J. (1987). Tau antisera recognize neurofibrillary tangles in a range of neurodegenerative disorders. Annals of Neurology, 22, 514e520.

Kosik, K. S. (1993). The molecular and cellular biology of tau. Brain Pathology, 3, 39e43.

Kotzbauer, P. T., Giasson, B. I., Kravitz, A. V., Golbe, L. I., Mark, M. H., Trojanowski, J. Q., et al. (2004). Fibrillization of a-synuclein and tau in familial Parkinson's disease caused by the A53T a-synuclein mutation. Experimental Neurology, 187, 279e288.

Lee, V., Goedert, M., & Trojanowski, J. (2001). Neurodegenerative tauopathies. Annual Review of Neuroscience, 24, 1121e1159.

Lee, C. W. C., Lau, K. F., Miller, C. C. J., & Shaw, P. C. (2002). Glycogen synthase kinase-3b-mediated tau phosphorylation in cultured cell lines. Molecular Neuroscience, 14, 257e260.

Lewis, J., Dickson, D. W., Lin, W.-L., et al. (2001). Enhanced neurofibrillary degeneration in transgenic mice expressing mutant tau and APP. Science, 293, 1487.

Lindwall, G., & Cole, R. D. (1984). Phosphorylation affects the ability of tau protein to promote microtubule assembly. Journal of Biological Chemistry, 259, 5301e5305.

Lippa, C. F., Schmidt, M. L., Lee, V. M. Y., & Trojanowski, J. Q. (1999). Antibodies to a-synuclein detect Lewy bodies in many Down's syndrome brains with Alzheimer's disease. Annals of Neurology, 45, 353e357.

Mandelkow, E., Von Bergen, M., Biernat, J., & Mandelkow, E.-M. (2007). Structural principles of tau and the paired helical filaments of Alzheimer's disease. Brain Pathology, 17, 83e90.

Martin, E. R., Scott, W. K., Nance, M. A., et al. (2001). Association of single-nucleotide polymorphisms of the tau gene with late-onset Parkinson disease. Journal of the American Medical Association, 286, 2245e2250.

Mori, H., Oda, M., Komori, T., Arai, N., Takanashi, M., Mizutani, T., et al. (2002). Lewy bodies in progressive supranuclear palsy. Acta Neuropathologica, 104, 273e278.

N€aslund, J., Schierhorn, A., Hellman, U., et al. (1994). Relative abundance of Alzheimer A beta amyloid peptide variants in Alzheimer disease and normal aging. Proceedings of the National Academy of Sciences, 91, 8378e8382.

Neumann, M., Muller, V., G€ orner, K., Kretzschmar, H. A., Haass, C., & Kahle, P. J. (2004). Pathological€ properties of the Parkinson's disease-associated protein DJ-1 in a-synucleinopathies and tauopathies: Relevance for multiple system atrophy and Pick's disease. Acta Neuropathologica, 107, 489e496.

Oddo, S., Caccamo, A., Shepherd, J. D., et al. (2003). Triple-transgenic model of Alzheimer's disease with plaques and tangles: Intracellular abeta and synaptic dysfunction. Neuron, 39.

Piccardo, P., King, D., Brown, D., & Barron, R. M. (2017). Variable tau accumulation in murine models with abnormal prion protein deposits. Journal of the Neurological Sciences, 383, 142e150.

Prusiner, S. B. (1991). Molecular biology of prion diseases. Science, 252, 1515þ.

Qureshi, H. Y., & Paudel, H. K. (2011). Parkinsonian neurotoxin 1-Methyl-4-phenyl-1,2,3,6tetrahydropyridine (MPTP) and a-synuclein mutations promote tau protein phosphorylation at Ser262 and destabilize microtubule cytoskeleton in vitro. Journal of Biological Chemistry, 286, 5055e5068.

Rapoport, M., Dawson, H. N., Binder, L. I., Vitek, M. P., & Ferreira, A. (2002). Tau is essential to b-amyloid-induced neurotoxicity. Proceedings of the National Academy of Sciences, 99, 6364e6369.

Roy, B., & Jackson, G. R. (2014). Interactions between Tau and a-synuclein augment neurotoxicity in a Drosophila model of Parkinson's disease. Human Molecular Genetics, 23, 3008e3023.

Patrizia, R., Hinkley, H. D., Victoria, Z., et al. (2004). DJ-1 colocalizes with tau inclusions: A link between parkinsonism and dementia. Annals of Neurology, 55, 113e118.

Scott, W. K., Nance, M. A., Watts, R. L., et al. (2001). Complete genomic screen in Parkinson disease: Evidence for multiple genes. Journal of the American Medical Association, 286, 2239e2244.

Selkoe, D. J. (1999). Translating cell biology into therapeutic advances in Alzheimer's disease. Nature, 399, A23eA31.

Shiarli, A. M., Jennings, R., Shi, J., et al. (2006). Comparison of extent of tau pathology in patients with frontotemporal dementia with Parkinsonism linked to chromosome 17 (FTDP-17), frontotemporal lobar degeneration with Pick bodies and early onset Alzheimer's disease. Neuropathology and Applied Neurobiology, 32, 374e387.

Spillantini, M. G., & Goedert, M. (1998). Tau protein pathology in neurodegenerative diseases. Trends in Neurosciences, 21, 428e433.

Spires-Jones, T. L., Stoothoff, W. H., de Calignon, A., Jones, P. B., & Hyman, B. T. (2009). Tau pathophysiology in neurodegeneration: A tangled issue. Trends in Neurosciences, 32, 150e159.

Stelzmann, R. A., Schnitzlein, N. H., & Murtagh, R. F. (1995). An English translation of Alzheimer's 1907 paper, "uber eine eigenartige erkankung der hirnrinde€ ". Clinical Anatomy, 8, 429e431.

Tieu, K. (2011). A guide to neurotoxic animal models of Parkinson's disease. Cold Spring Harbor Perspectives in Medicine, 1.

Waxman, E. A., & Giasson, B. I. (2011). Induction of intracellular tau aggregation is promoted by alphasynuclein seeds and provides novel insights into the hyperphosphorylation of tau. Journal of Neuroscience, 31, 7604e7618.

# APPENDIX 9 JOURNAL PUBLICATION

frontiers in Cell and Developmental Biology

ORIGINAL RESEARCH
published: 06 September 2021doi: 10.3389/fcell.2021.741662

# Interactions and Cytotoxicity ofHuman Neurodegeneration-Associated Proteins Tau and α-Synuclein in the Simple Model *Dictyostelium discoideum*

*Katelyn Mroczek, Sanjanie Fernando, Paul R. Fisher and Sarah J. Annesley**

*Department of Physiology, Anatomy and Microbiology, La Trobe University, Bundoora, VIC, Australia*

OPEN ACCESS

*Edited by:*
*Robin S. B. Williams,University of London, United Kingdom*

*Reviewed by:*
*Xuehua Xu, National Institute of Allergyand Infectious Diseases, NationalInstitutes of Health (NIH), United StatesRichard H. Gomer, Texas A&M University, United States*

**Correspondence: Sarah J. Annesley S.Annesley@latrobe.edu.au*

*Specialty section: This article was submitted to Molecular and Cellular Pathology, a section of the journalFrontiers in Cell and Developmental Biology*

*Received: 15 July 2021*
*Accepted: 19 August 2021*
*Published: 06 September 2021*

*Citation:*
*Mroczek K, Fernando S,Fisher PR and Annesley SJ (2021)Interactions and Cytotoxicity of Human Neurodegeneration-Associated Proteins Tauand α-Synuclein in the Simple ModelDictyostelium discoideum. Front. Cell Dev. Biol. 9:741662.doi: 10.3389/fcell.2021.741662*

The abnormal accumulation of the tau protein into aggregates is a hallmark in neurodegenerative diseases collectively known as tauopathies. In normal conditions, tau binds off and on microtubules aiding in their assembly and stability dependent on the phosphorylation state of the protein. In disease-affected neurons, hyperphosphorylation leads to the accumulation of the tau protein into aggregates, mainly neurofibrillary tangles (NFT) which have been seen to colocalise with other protein aggregates in neurodegeneration. One such protein is $\alpha$-synuclein, the main constituent of Lewy bodies (LB), a hallmark of Parkinson's disease (PD). In many neurodegenerative diseases, including PD, the colocalisation of tau and $\alpha$-synuclein has been observed, suggesting possible interactions between the two proteins. To explore the cytotoxicity and interactions between these two proteins, we expressed full length human tau and$\alpha$-synuclein in *Dictyostelium discoideum* alone, and in combination. We show that tau is phosphorylated in *D. discoideum* and colocalises closely (within 40 nm) with tubulin throughout the cytoplasm of the cell as well as with $\alpha$-synuclein at the cortex. Expressing wild type $\alpha$-synuclein alone caused inhibited growth on bacterial lawns, phagocytosis and intracellular *Legionella* proliferation rates, but activated mitochondrial respiration and non-mitochondrial oxygen consumption. The expression of tau alone impaired multicellular morphogenesis, axenic growth and phototaxis, while enhancing intracellular *Legionella* proliferation. Direct respirometric assays showed that tau impairs mitochondrial ATP synthesis and increased the "proton leak," while having no impact on respiratory complex I or II function. In most cases depending on the phenotype, the coexpression of tau and $\alpha$-synuclein exacerbated (phototaxis, fruiting body morphology), or reversed (phagocytosis, growth on plates, mitochondrial respiratory function, *Legionella* proliferation) the defects caused by either tau or $\alpha$-synuclein expressed individually. Proteomics data revealed distinct patterns of dysregulationin strains ectopically expressing tau or $\alpha$-synuclein or both, but down regulation of expression of cytoskeletal proteins was apparent in all three groups and most evidentin the strain expressing both proteins. These results indicate that tau and $\alpha$-synuclein exhibit different but overlapping patterns of intracellular localisation, that they individually

exert distinct but overlapping patterns of cytotoxic effects and that they interact, probably physically in the cell cortex as well as directly or indirectly in affecting somephenotypes. The results show the efficacy of using *D. discoideum* as a model to studythe interaction of proteins involved in neurodegeneration.

Keywords: tau, ***α***-synuclein, *Dictyostelium*, tauopathies, Alzheimer's disease

## INTRODUCTION

Neurodegenerative diseases are the leading cause of disability worldwide and as the population ages they are expected to increase in their prevalence. The WHO estimate that collectively neurological disorders will eclipse cancer as the second leading cause of death worldwide by 2040 (Gammon, 2014). The most common neurodegenerative disease is Alzheimer's disease (AD) in which the hallmarks like other neurodegenerativediseases are the accumulation of aggregated proteins. In AD, first described by Alois Alzheimer in 1906, the most abundant aggregated proteins are tau and amyloid beta (Stelzmann et al., 1995). The accumulation of the tau protein is present as the dominant aggregate in a group of neurodegenerative diseases known as tauopathies with AD being the most common tauopathy. However, tau aggregation is also implicated in other diseases including Pick's disease, Cortico-basal degeneration, Progressive supranuclear palsy and Fronto-temporal dementia with Parkinsonism linked to chromosome 17 (Spillantini and Goedert, 1998; Lee et al., 2001; Goedert and Spillantini, 2011).

Tau is a major mammalian microtubule associated protein (MAP), and in humans it is predominantly found in the neurons (Drubin and Kirschner, 1986). The protein binds to tubulin promoting the assembly and stability of microtubules, supporting axonal transport and structure of neurons (Cleveland et al., 1977; Kosik, 1993). Tau is encoded by the MAPT gene, is 100 kb in size containing 16 exons. Alternative splicing of the RNA transcript at exons 2, 3, and 10 produces six isoforms (Andreadis et al., 1992), which range from 352 to 441 amino acids in length containing either 3 or 4 microtubule binding repeat sequences (Goedert et al., 1989a,b; Himmler et al., 1989). The tau protein contains an acidic N terminal region known as the projection domain, thought to maintain space between microtubules as wellas interacting with other cytoskeletal proteins (Avila et al., 2004; Mandelkow et al., 2007). The proline rich middle of the protein binds other proteins and the C terminal contains the microtubule binding domain (MTBD), with either 3 or 4 repeats dependent on the presence or absence of exon 10 (Mandelkow et al., 2007). Four-repeat (4R) tau binds with a higher affinity to microtubules than 3R tau. The longest tau isoform (2N4R) contains both exons 2 and 3 in the N terminus and 4 repeats in the MTBD.

In normal conditions tau binds on and off microtubules depending on the phosphorylation state of the protein. On the 2N4R isoform there have been over 80 phosphorylation sites detected with the majority of these implicated in pathological conditions (Buée et al., 2000; Hanger et al., 2007). Dephosphorylation of tau induces the affinity to bind to MT while phosphorylation leads to a disassociation with MT (Cleveland et al., 1977; Lindwall and Cole, 1984).

The further hyperphosphorylation of tau stimulates the accumulation of the protein into aggregates. There are many tau aggregate conformations but the most commonly observed is neurofibrillary tangles (NFT) composed of paired helical filaments (Grundke-Iqbal et al., 1986). Tangles of tau have been pathologically implicated in Alzheimer's disease, Parkinson's disease (PD), Down's syndrome, Parkinsonism– dementia complex of Guam, and progressive supranuclear palsy (Joachim et al., 1987).

The toxic aggregation of tau in diseases like AD, PD, and other tauopathies seems to coincide with mitochondrial impairment associated with transport, dynamics and bioenergetics of the mitochondria (reviewed by Gibson et al., 2010; Eckert et al., 2011; Cabezas-Opazo et al., 2015; Pérez et al., 2018a). Mitochondrial abnormalities include impaired oxidative phosphorylation ina mouse model of AD (Rhein et al., 2009) and impaired mitochondrial dynamics by truncated tau in immortalised cortical neurons and primary cortical neurons from tau knockout mice (Pérez et al., 2018b). The overexpression of tau in neuronal cultures decreased ATP production, the ratio of ATP/ADP and inhibited Complex I activity (Li et al., 2016) and ithas been suggested that tau impairs mitochondrial function while simultaneously inhibiting the degradation of damaged mitochondria leading to a cycle of mitochondrial dysfunction (Cummins et al., 2019).

Aggregation and mitochondrial dysfunction are hallmarks of many neurodegenerative diseases. Within the large group of tauopathies the accumulation of proteins other than tau is evident. One such protein is $\alpha$-synuclein. $\alpha$-synuclein is encoded by the *SNCA* gene, is 140 amino acids in length and like tauis richly expressed in neurons. Aggregation of $\alpha$-synuclein andits presence as the dominant protein in Lewy bodies (LB) is a hallmark of a group of neurodegenerative diseases classified as the synucleinopathies. PD is the most common synucleinopathy but other diseases include Lewy Body Dementia, multiple system atrophy, and Parkinsonism with dementia (Galpern and Lang, 2006; Savica et al., 2013). $\alpha$-Synuclein is the most abundant aggregated protein in these disorders although other proteins like tau have been seen to colocalise within these aggregates as well suggesting an overlap of the tau- and synuclein-opathies.

There have been many neurodegenerative diseases in which tau and $\alpha$-synuclein have been found to coexist, and several lines of evidence suggest an interaction between the two proteins. Colocalisation of tau and $\alpha$-synuclein has been seen in both NFT and LB (Arima et al., 2000; Ishizawa et al., 2003). $\alpha$-synuclein containing LB were seen to be present in AD brains over 50% of the time (Hamilton, 2000), in Down's syndrome brains withAD 50% of the time (Lippa et al., 1999) and found with PHFof tau in the same neurons (Iseki et al., 1999). The C-terminus

of $\alpha$-synuclein has been seen to bind to the MT Binding Domain of tau promoting phosphorylation by protein-kinase A (Jensen et al., 1999). *In vitro* experiments using human cell lines have shown that tau and $\alpha$-synuclein can promote the aggregation of each other and increase cytotoxicity (Badiolaet al., 2011; Castillo-Carranza et al., 2018). The application of models to study the interaction of the proteins has proved useful and support an interaction. A transgenic mouse model of PD overexpressing $\alpha$-synuclein increased tau phosphorylation and hyperphosphorylation and aggregates similar to LB were formed containing both tau and $\alpha$-synuclein (Haggerty et al., 2011). In *Drosophila*, neurotoxic symptoms were enhanced with the coexpression of both proteins compared to when tau or $\alpha$-synuclein were expressed individually (Roy and Jackson, 2014).In yeast models, the coexpression enhanced aggregation of the proteins, increased phosphorylation of tau and produced toxic effects (Zabrocki et al., 2005; Ciaccioli et al., 2013).

There are many models of tauopathies and using simple models to study complex disease mechanisms has its advantages. *Dictyostelium discoideum* is a novel eukaryotic model organism recognised by the National Institute of Health (NIH) in the United States for its importance in biomedical research. It has been used as a biomedical model for studying human diseases including neurodegeneration, lysosomal trafficking disorders and mitochondrial disease (Annesley and Fisher, 2009a; Francione et al., 2011; Maniak, 2011; Martín-González et al., 2021). The complete nuclear (Eichinger et al., 2005) and also mitochondrial (Ogawa et al., 2000) genomes have been sequenced, allowing for orthologues of human genes to be studied. Of interest is the distinctive life cycle of *D. discoideum*in which there are both unicellular and multicellular stages with numerous cell types. This allows diverse, reproducible phenotypic traits to serve as "readouts" of disease gene-related disturbances in cellular processes and the signalling pathways that control them (Annesley and Fisher, 2009a). Additionally, *D. discoideum* is greatly accessible for use in biomedical research, genetically manipulable and easily grown clonally. Mitochondrial disease has been created and well characterisedin *D. discoideum*. Through the knockdown of nuclear encoded mitochondrial proteins or disrupting mitochondrial genes, a clear set of phenotypes was exhibited in each case (reviewed by Francione and Fisher, 2011). Among these phenotypes were: decreased growth on bacterial lawns and in axenic medium, aberrant fruiting body with shorter and thicker stalks, defective slug phototaxis and increased susceptibility to *Legionella* proliferation. These mitochondrially diseased *D. discoideum* phenotypes were attributed to the chronic activation of the energy sensing protein AMP-activated protein kinase (AMPK) by Bokko et al. (2007) and Francione et al. (2009) that showed when AMPK was knocked down by antisense inhibition, the defective phenotypes returned to wildtype levels, and chronic activation of AMPK mimicked the disease phenotypes.

Previously we showed that human $\alpha$-synuclein can be expressed in *D. discoideum* and has effects on plaque expansion rates, phagocytosis, and PD associated mutations impaired phototaxis. These impaired phenotypes were rescued or partially rescued with the coexpression of an AMPK antisense construct. Suggesting that mitochondrial dysfunction may be attributingto at least some of the defective phenotypes. However, when mitochondrial function was directly measured, $\alpha$-synuclein displayed an increased mitochondrial respiration rather than a dysfunction (Fernando et al., 2020). This was in line with other PD models in which mitochondrial respiration was seen to be increased including $\alpha$-synuclein fibrils in neuroblastoma cells (Ugalde et al., 2020), lymphoblast cell lines made from idiopathic PD patients (iPD) (Annesley et al., 2016) and fibroblasts from iPD patients (Haylett et al., 2016). Here we expressed thelongest human tau isoform to create a *D. discoideum* model of tauopathies. *D. discoideum* has already been used as a model to study elements involved in AD. Orthologues of the presenilin proteins and other $\gamma$ secretase subunits that cause the cleavageof amyloid precursor protein (APP) to A$\beta$ have been identified in *D. discoideum* and have similar functionality to the mammalian complex (McMains et al., 2010; Ludtmann et al., 2014). Mutationsin the presenilin genes have been known to cause early-onset familial AD (De Strooper and Annaert, 2010). In *D. discoideum*, the knockout of the presenilin genes resulted in a developmental block in aggregation, which was restored with the expression of human presenilin 1 (Ludtmann et al., 2014). Also importantly, *D. discoideum* was seen to process ectopically expressed human APP to the amyloid-$\beta$ peptides A$\beta_{40}$ and A$\beta_{42}$, while in strains that were deficient in $\gamma$ secretase this APP processing was blocked (McMains et al., 2010). As is the case with APP, there are no homologues of tau in *D. discoideum*, but many of the proteins that interact with tau have been evolutionarily conserved such as the kinases AMPK and glycogen synthase kinase 3 (GSK3) as well as cytoskeletal proteins tubulin and filamin. This allows the study of the cytotoxic effects of tau directly without the complication of the endogenously expressed protein or homologue.

As there is evidence of an interaction of tau and $\alpha$-synucleinin neurodegeneration, we also coexpressed human tau and human $\alpha$-synuclein together to compare to the phenotypes displayed by expressing tau and $\alpha$-synuclein alone. Tau caused phenotypes similar to those of mitochondrially diseased strains and direct measurements of mitochondrial activity showed a decrease in ATP synthesis. We show here that *D. discoideum*is a viable model to study tauopathies as tau is cytotoxic, can be phosphorylated and is readily coexpressed with other neurodegenerative proteins. The coexpression of human tau and human $\alpha$-synuclein in this work revealed physical and functional interactions between the two proteins that enhance or reverse their individual cytotoxic effects.

## MATERIALS AND METHODS

### *Dictyostelium* Strains and CultureConditions

Wildtype (AX2) and transformed *D. discoideum* strains were grown both axenically and on SM agar plates. Axenically, strains were shaken at 150 rpm at 21°C in HL5 medium containing glucose (Formedium, Hunstanton, Norfolk, United Kingdom),

with the addition of 20 $\mu$g mL$^{-1}$ geneticin (G418—Thermo Fisher Scientific, Waltham, MA, United States) for transformed strains. They were also grown on SM agar plates (Formedium, Hunstanton, Norfolk, United Kingdom), with *Enterobacter aerogenes* as a food source and supplemented with G418 for transformants. The transformants expressed either human tau (containing plasmid construct pPROF665), human $\alpha$-synuclein (containing plasmid pPROF629) or were cotransformants expressing both tau and $\alpha$-synuclein.

## Plasmid Construction

The human tau gene was PCR amplified using a commercially purchased plasmid template tau/pET29b (Addgene plasmid # 16316) containing a cloned copy of the full-length humantau gene (2N4R). Primers Tau2F (CG**A TCG ATA** TGG CTG AGC CCC GC) and Tau2R (CG**C TCG AG**T CAC AAA CCC TGC TTG GC) synthesised by Gene Works Ltd., incorporated *Xho*I (Promega, Madison, WI, United States) and *Cla*I (Promega, Madison, WI, United States) restriction sites and was initially cloned into the *Escherichia coli* vector pCR® 2.1-TOPO (Thermo Fisher, Waltham, MA, United States, A32728) to produce pPROF664. Subsequently, the Tau insert was subcloned into a *D. discoideum* expression vector by replacing the existing tetracycline cassette in pPROF267. The resultant clone was called pPROF665. The construction of the $\alpha$-synuclein construct (pPROF629) has been described previously (Fernando et al., 2020).

## Transformation

The transformation of AX2 cells was performed using the calcium phosphate DNA coprecipitation method (Nellen et al., 1984) with20 $\mu$g of construct DNA. Transformants were selected for on SM agar plates containing 20 $\mu$g mL$^{-1}$ G418 and a lawn of *Micrococcus luteus* (Wilczynska and Fisher, 1994), the purified transformants were maintained by subculturing in HL5 medium and onto lawns of *E. aerogenes*.

## Quantitative PCR

To quantify the construct copy number in the transformants, quantitative PCR was performed using iQ SYBR Green supermix and an iCycler IQ Multicolor Real-Time PCR Detection system according to manufacturer's instructions (Bio-Rad, Hercules, CA, United States). The primers used for amplification of a portion of each gene were RTTauF (AAGAGCACTCCAACAGCGGAAGAT) and RTTauR (GTGTCTCCAATGCCTGCTTCTTCA) for tau, and for the $\alpha$-synuclein gene RTsynF (GCGCTCTAGAATCGATATGGATGTATTCATGAAAGGACT TTCAAAGGCC) and RTsynR (GCGCTCTAGACTCGAGTT AAGGATCCACAGGCATATCTTCCAGAATTCC). The filamin gene was amplified and used as loading control, as it is a single copy gene, and amplified using the primers Fil443For (CCACAGAGATATTGGAGTTGCGTACC) and Fil552Rev (CAACTCAACCAATGTGCCTGCCAA). Two calibration curves were prepared, one to estimate loading using genomic DNA of the wildtype AX2 and the filamin primers to estimate the total quantity of genomic DNA, and the second using purified plasmids to determine the quantity of inserted plasmid constructs. Copy numbers of the inserted constructs for each strain were calculated based on the quantity of the construct, the quantity of gDNA and the sizes (in base pairs) of the amplified fragment and the *Dictyostelium* genome. The copy numbers were then normalised against the copy number of the control AX2 parental strain.

## Western Blotting

An aliquot of 1 $10^7$ cells of either tau or cotransformant strains as well as the WT were pelleted, supernatant removed andthe pellet resuspended in 75 $\mu$L of Laemmli 2 sample buffer (4% SDS, 20% glycerol, 0.004% bromophenol blue and 0.125M Tris-Cl, pH 6.8). Samples were boiled for 10 min and 15 $\mu$L loaded to a 10–15% SDS-PAGE gel and transferred to a PVDF membrane (Bio-Rad, Hercules, CA, United States). To detect tau, membranes were incubated with mouse monoclonal anti- tau antibody [Tau-5] (Abcam, Cambridge, United Kingdom, ab80579) (1:2,000), to detect $\alpha$-synuclein membranes were incubated with mouse monoclonal anti-alpha-synuclein antibody [syn211] (Abcam, Cambridge, United Kingdom, ab80627) (1:2,000) and to detect phosphorylated tau membranes were incubated with rabbit monoclonal recombinant anti-tau (phosphor S404) antibody [EPR2605] (Abcam, Cambridge, United Kingdom, ab92676) (1:500). This was followed by incubation with (goat) anti-mouse or anti-rabbit Cross-Adsorbed Secondary antibody Alexa-Fluor™ 647 (Thermo Fisher Scientific, Waltham, MA, United States, A32728) (1:1,000). Proteins were visualised using the STORM image analyser.

## Multicellular Development

*Dictyostelium discoideum* wildtype and transformant cells were grown on SM plates containing a lawn of *E. aerogenes* at 21°C until multicellular fruiting bodies were observed. The fruiting bodies were examined using an Olympus S761TM dissecting microscope and images were captured using a digital Moticam 2300TM camera. Photographs were taken from above the plates to gain an overall view of the population as well as pictures of singular fruiting bodies. This was obtained by slicing out a thin section of agar and placing it on its side so that the entire fruiting body could be seen.

## Growth on Bacterial Lawns

A scraping of wildtype and transformed amoebae were inoculated into the centre of four normal agar [20 g L$^{-1}$ agar (Difco, Detroit, MI, United States); 1 g L$^{-1}$ peptone (Oxoid, Basingstoke, United Kingdom), 1.1 g L$^{-1}$ anhydrous glucose, 1.9972 g L$^{-1}$ $KH_2PO_4$, and 0.356 g L$^{-1}$ $Na_2HPO_4$_$2H_2O$, pH 6.0] plates containing a lawn of *E. coli* B2 as previously described (Bokkoet al., 2007). Plates were incubated at 21°C, the diameter of plaque expansion was measured in mm twice daily over a period of approximately 100 h. The plaque expansion rates for each strain was calculated using the statistical computing and graphicssoftware program "R" by linear regression.

## Growth in Axenic Medium

*Dictyostelium discoideum* cells were axenically grown in HL5 until exponential phase was reached, then inoculated into 50 mL of HL5 in 150 mL flasks to a final density of $1 \times 10^4$ cells $mL^{-1}$. Cells were incubated at 21°C on an orbital shaker (Ratek, Boronia, VIC, Australia) at 150 rpm over a period of 100 h. Cells were counted twice daily using a haemocytometer (Bright Line, 0.1 mm deep) and the generation times of each strain was calculated in R by log linear regression during exponential growth phase.

## Phagocytosis Assay

The *E. coli* strain expressing the fluorescent protein DsRed (Maselli et al., 2002) was used to measure bacterial uptake of wildtype and transformed cells using the previously described method (Bokko et al., 2007). Cells were grown axenically in HL5, $5 \times 10^6$ cells were harvested, washed, and resuspended in 1 mL of phosphate buffer. Cells were starved for 30 min at 21°C with shaking at 150 rpm, then 1 mL of *E. coli* DsRed suspension was added to each sample, and 400 $\mu$L of cells were taken in duplicate at time points T = 0 min and T = 30 min. Cells were washed by centrifugation to remove surface bound *E. coli* using 5 mM sodium azide (Sigma-Aldrich, St. Louis, MI, United States) and lysed using 2 mL of 0.25% (v/v) Triton-X-100 in 100 mM $Na_2HPO_4$, pH 9.2. The hourly rate of bacterial consumption was determined by taking fluorescence measurements at both time points using a Special Module (530 nm excitation and 580 nm emission) in a Modulus Fluorometer (Turner Biosystems, Sunnyvale, CA, United States). The increase in fluorescence over 30 min, the amoebal density and the fluorescence signal per million bacteria (separately determined) were used to calculate the rates of bacterial consumption.

## Pinocytosis Assay

The Fluorescein Isothiocyanate (FITC)-dextran (Sigma-Aldrich, St. Louis, MI, United States, average mol. mass 70 kDa) method was used for measuring liquid uptake as previously described (Klein and Satre, 1986). Vegetative cells were harvested to a density of $1 \times 10^7$ cells, resuspended in 1 mL of HL5 and starved for 30 min at 21° shaking. FITC-dextran was added to a concentration of 2 $\mu$g $mL^{-1}$ and incubated for 70 min. Cell samples (200 $\mu$L) were taken in duplicate at T = 0 min and T = 70 min, pelleted by centrifugation, washed twice in Sorenson buffer and lysed in 2 mL of 0.25% (v/v) Triton-X-100 in 100 mM $Na_2HPO_4$, pH 9.2. Fluorescence was measured in the Modulus Fluorometer using the Green Module (525 nm excitation and 580–640 nm emission). The hourly rate of uptake of the medium was calculated using a calibration curve relating to fluorescence signal to volume of fluorescence medium, the cell density and the increase in fluorescence over 70 min.

## Legionella Infection Assay

*Legionella pneumophila* infection and proliferation rates in *D. discoideum* was measured as previously described (Francione et al., 2009) and was adapted from Hagele et al. (2000) and Ottoet al. (2004). Wildtype and transformant strains were grown to exponential phase axenically in HL5 at 25°C with shaking. Cells were pelleted, washed twice in Sorensen 1× C buffer (17 mM $KH_2PO_4/Na_2PO_4$, 50 $\mu$M $CaCl_2$, pH 6.0) at 600 *g* for 3 min and resuspended in modified broth (MB) medium (0.7% yeastextract, 1.4% proteose peptone, 0.062% $Na_2HPO_4.2H_2O$, 0.049% $KH_2PO_4$, pH 6.9) at $5 \times 10^5$ cells $mL^{-1}$. Each suspension was aliquoted into 5 wells of a 96 well tissue culture plate to a final density of $1 \times 10^5$ cells to be used at a series of time points (0, 24, 48, 72, and 96 h) along with a negative control of only MB, and allowed to adhere for 30 min at 21°C.

The *L. pneumophila* strains used were derivatives of the pathogenic Corby strain (Mampel et al., 2006) and grown on buffered charcoal yeast extract (BCYE) agar containing 5 $\mu$g $mL^{-1}$ chloramphenicol at 37°C with 5% $CO_2$ atmosphere for 3 days. After this time, the bacteria were harvested and resuspended in distilled water and used to infect the *D. discoideum* strains at a multiplicity of infection (MOI) of 1:1. This was achieved by reading the OD of the bacterial suspension, assuming that an $OD_{600}$ of 1 equates to $10^9$ bacteria $mL^{-1}$. Initial adherence of the *L. pneumophila* to *D. discoideum* cells was performed by centrifugation at 1,370 *g* for 10 min. At each time point 50 $\mu$g $mL^{-1}$ gentamycin sulphate was added to each well for 30 min to kill the extracellular *L. pneumophila*. Then cells were resuspended and pelleted at 13,000 *g* for 12 min in a microcentrifuge, washed twice and resuspended in Sorenson 1 C× buffer. The cells were lysed with 0.02% (w/v) Saponin and vortexed vigorously to release the intracellular *L. pneumophila*. A 10-fold dilution series of the harvested bacteria was prepared up to 1,000-fold for the first two time points and from $10^{-1}$ to $10^{-5}$ for time points 48 h and over. This was plated onto BCYE agar plates and incubated at 25–26°C with 5% $CO_2$ for 7 days in order to determine the colony-forming units (c.f.u.).

## Phototaxis and Thermotaxis Assays

Qualitative phototaxis and quantitative photo-and-thermotaxis were performed as previously described (Annesley and Fisher, 2009b). Qualitative phototaxis involved scraping the edge of *D. discoideum* plaques growing on *E. aerogenes* lawns and inoculating onto the centre of charcoal agar plates [5% activated charcoal (Sigma-Aldrich, St. Louis, MI, United States), 1.0% agar technical (Thermo Fisher, Waltham, MA, United States)].

For quantitative phototaxis and thermotaxis amoebae were harvested from mass plates and repeatedly washed in cold sterile saline, followed by centrifugation (600 *g* for 5 min) to remove any bacterial cells. Quantitative phototaxis involved creating dilutions of the cell pellet with cell densities ranging from $6 \times 10^4$ to $1.5 \times 10^6$. Twenty microlitre of each dilution was plated in duplicate onto charcoal agar plates in a 1 $cm^2$ area in the middle of the plate. Both qualitative and quantitative phototaxis plates were incubated at 21°C for 48 h with a single lateral light source to allow slug trails to form. Cell pellets were diluted to 20% (approximately $3 \times 10^6$ cells) for quantitative thermotaxis. A 20 $\mu$L aliquot was placed in a 1 $cm^2$ area onto the centre of water agar plates (1% agar) and incubated in PVC boxes with no light source on a heat bar producing a 0.2°C $cm^{-1}$ temperature gradient at the agar surface. Plates were placed in duplicate at arbitrary temperature points from 1 to 8 with T1

corresponding to 14°C and increasing in 2°C increments to reach 28°C at T8.

All slug trails were transferred to PVC discs and stained with Coomassie blue (Sigma-Aldrich, St. Louis, MI, United States) before being digitised. Qualitative digitising was performed by tracing entire slug trails with a light source at 0°. For quantitative phototaxis and thermotaxis only the beginning and end of the slug trails were digitised and orientation analysed using directional statistics.

## Immunofluorescence

*Dictyostelium discoideum* transformed and wildtype cells were grown axenically to a density of 2 $10^6$ cells $mL^{-1}$ and then transferred onto sterile coverslips in six-well Costar plates (Nunc™). The cells were allowed to settle for 30 min before the media was replaced with Lo-Flo HL5 (3.85 g $L^{-1}$ glucose, 1.78 g $L^{-1}$ proteose peptone, 0.45 g $L^{-1}$ yeast extract, 0.485 g $L^{-1}$ $KH_2PO_4$, and 1.2 g $L^{-1}$ $Na_2HPO_4$ $12H_2O$; filter sterilised) for1 h to equilibrate the cells. The media was aspirated off and the coverslips rinsed in PBS [12 mM $Na_2HPO_4$, 12 mM $NaH_2PO_4$ (pH 6.5)] then cells were fixed with the addition of prechilled (-20°C) methanol/acetone solution (1:1) and left at 20°C for 10 min and again rinsed in PBS.

The coverslips were then incubated with mouse monoclonal anti-tau antibody [Tau-5] (Abcam, Cambridge, United Kingdom, ab80579) or a combination of Tau-5 and rabbit monoclonal anti-alpha beta synuclein antibody [EP1646Y] (Abcam, Cambridge, United Kingdom, ab51252) diluted (1:100) in blocking buffer [1% (w/v) bovine serum albumin (BSA) and 1% (v/v) cold-water fish skin gelatin in PBS] for 1 h. Coverslips were rinsed in PBS with 0.1% (w/v) BSA twice and incubated with secondary antibody [goat anti-mouse Alexa-Fluor594 (Molecular Probes™ Invitrogen™) or a combination of Alexa-Fluor 594 (goat) and anti-rabbit Alexa-Fluor−488 conjugated IgG antibody (Thermo Fisher Scientific, Waltham, MA, United States, A11034) for cotransformants], diluted (1:500) in PBS with 1% (w/v) BSA and incubated for 45 min in the dark. The coverslips were rinsed in PBS, then DAPI diluted (1:1,000) in PBS was added and incubated for 5 min. The cells were rinsed in PBS then MilliQ $H_2O$ drained and mounted onto a microscope slide with Ultramount No. 4 (Fronine Laboratory Supplies) and left to dry for 4 h or overnight before visualisation. The cells were detected on an Olympus (Shinjuku City, Tokyo, Japan) BX61T fluorescent microscope and images were digitally captured with the use of an Olympus DP80 camera.

## Duolink®

*Dictyostelium discoideum* transformed and wildtype cells were axenically grown to a density of $2\times10^6$ cells $mL^{-1}$. Coverslips were lined with a Mini PAP pen (Invitrogen™) to create a1 $cm^2$ area then cells were adhered and fixed to the coverslips as described in the previous section. To detect protein interactions using IF techniques, the Duolink® system was used as per manufacturer's instructions.

Cells were stained in combinations using mouse monoclonal anti-tau antibody Tau-5, rabbit monoclonal anti-tau antibody (E178) (Abcam, Cambridge, United Kingdom, ab32057), rabbit monoclonal anti-alpha beta synuclein antibody [EP1646Y] and mouse monoclonal anti-alpha-tubulin antibody [12G10] (developed by Frankel & Nelsen, Developmental Studies Hybridoma Bank, created by the NICHD of the NIH and maintained at The University of Iowa, Department of Biology, Iowa City, IA, United States, 52242). The protein-protein interaction was observed (as red dots) using secondary proximity probes, anti-Rabbit MINUS and anti-Mouse PLUS Duolink™ *in situ* detection kit (Sigma-Aldrich Co. LLC) according tothe manufacturer's instructions. An additional Alexa-Fluor 488 conjugated secondary antibody was added in with the proximity probes at times to visualise tubulin.

## Seahorse Respirometry

Mitochondrial respiration of *D. discoideum* wildtype and transformed strains were measured using the Seahorse Extracellular Flux Analyser (Seahorse Biosciences, North Billerica, MA, United States) as described previously (Layet al., 2016). A combination of drugs were used in sequential order to measure the Oxygen Consumption Rate (OCR)of specific elements of mitochondrial respiration [10 $\mu$M DCCD (N,N0-dicyclohexylcarbodimide, an ATP synthase inhibitor (Sigma-Aldrich, St. Louis, MI, United States), 10 $\mu$M CCCP (carbonyl cyanide 3-chlorophenol hydrazone, a protonophore (Sigma-Aldrich, St. Louis, MI, United States)], 20 $\mu$M rotenone [Complex I inhibitor (Sigma-Aldrich, St. Louis, MI, United States)] and either 10 $\mu$M antimycin A [Complex III inhibitor (Sigma-Aldrich, St. Louis, MI, United States)] or 1.5 mM BHAM [benzohydroxamic acid, alternative oxidase (AOX) inhibitor (Sigma-Aldrich, St. Louis, MI, United States)]. Axenically grown *D. discoideum* were harvested, washed, then resuspended in SIH medium (Formedium, Hunstanton, Norfolk, United Kingdom) and supplemented with 20 mM sodium pyruvate and 5 mM sodium malate (pH 7.4). Each strain was plated into eight wells of an assay plate precoated in Matrigel, and the cells were left to settle for 30 min. Measurement cycles consisting of 3 min of mixing, 2 min wait and 3 min measurement time were completed before and after each sequentially added drug, at least three cycles per condition. There were eight replicates of a strain for each condition, except for the last in which either BHAM or Antimycin A were addedto four replicate wells. The wildtype AX2 was included as a control in every experiment in four replicate wells, and two each for the final condition. From the measurements taken before and after the addition of the pharmacological agents averagesof specific components of mitochondrial respiration were able to be calculated.

## Whole Cell Proteomics

For proteomic analysis each sample ($5\times10^6$ cells in 100 $\mu$L of PBS) was prepared for analysis by the La Trobe University Comprehensive Proteomics Platform according to the following protocol: Cell pellets were dissolved in digestion buffer (8 M urea,50 mM $NH_4HCO_3$, 10 mM dithiothreitol) and incubated at 25°C for 5 h. Iodoacetamide (IAA) was added to a final concentration of 55 mM and incubated for 35 min at 20°C in the dark to alkylatethiol groups. The preparation was then diluted to 1 M urea in

25 mM ammonium bicarbonate (pH 8.5) and sequencing-grade trypsin (Promega) was added to a ratio of 1:50 (wt/wt) to the sample and incubated for 16 h at 37°C. The digests were acidified with 1% (v/v) trifluoroacetic acid (TFA), dried in a SpeedVac centrifuge followed by a desalting step on SDB-XC StageTips (Empore, SDB-XC reversed-phase material, 3M, St. Paul, MN, United States). Briefly: digested proteins were resuspended in 100 $\mu$L of 1% (v/v) formic acid and centrifuged at 14,000 rpm for 2 min. The solid-phase extraction was performed according to Rappsilber et al. (2007) with the following modifications: the membrane was conditioned with 50 $\mu$L of 80% (v/v) acetonitrile, 0.1% (w/v) trifluoroacetic acid, and then washed with 50 $\mu$L of 0.1% trifluoroacetic acid before the tryptic peptides were bound to the membrane. The bound peptides were eluted by 50 $\mu$L 80% (v/v) acetonitrile, 0.1% (w/v) trifluoroacetic acid, and dried in a SpeedVac centrifuge.

Peptides reconstituted in 0.1% TFA and 2% acetonitrile (ACN) were loaded using a Thermo Fisher Scientific™ UltiMate™ 3000 RSLCnano system onto a trap column (C18 PepMap 300 $\mu$m ID 2 cm×trapping column, Thermo Fisher Scientific) at15 $\mu$L $min^{-1}$ for 6 min. The valve was then switched to allow the precolumn to be in line with the analytical column (Vydac MS C18, 3 $\mu$m, 300 Å, and 75 $\mu$m ID ×25 cm, Grace Pty. Ltd.). The separation of peptides was performed at 300 nL $min^{-1}$ at 45°C using a linear ACN gradient of buffer A (water with 0.1% formic acid, 2% ACN) and buffer B (water with 0.1% formic acid, 80% ACN), starting at 5% buffer B to 45% over 105 min, then 95% B for 5 min followed by an equilibration step of 15 min (water with 0.1% formic acid, 2% ACN). Data were collected on an Orbitrap Elite (Thermo Fisher Scientific) in Data Dependent Acquisition mode using m/z 300–1,500 as MS scan range, CID MS/MS spectra were collected for the 10 most intense ions at performed at a normalised collision energy of 35% and an isolation width of 2.0 m/z. Dynamic exclusion parameters were set as follows: repeat count 1, duration 90 s, the exclusion list size was set at 500 with early expiration disabled. Other instrument parameters for the Orbitrap were the following: MS scan at 120,000 resolution, maximum injection time 150 ms, AGC target 1 × $10^6$ for a maximum injection time of 75 ms with AGT target of 5000.

The spectra obtained from the instrument were usedto search against *Dictyostelium* database (February 2018), together with common contaminants using the Mascot search engine (Matrix Science Ltd., London, United Kingdom). Briefly, carbamidomethylation of cysteines was set as a fixed modification, acetylation of protein N-termini, methionine oxidation was included as variable modifications. Precursor mass tolerance was 10 ppm, product ions were searched at 0.5 Da tolerances, minimum peptide length defined at 6, maximum peptide length 144, and peptide spectral matches (PSM) were validated using Percolator based on q-values at a 1% false discovery rate (FDR).

## Quantification and Statistical Analysis

Proteomics data was analysed using Scaffold (Proteome Software) before exporting data to Excel for further analysis. Proteins detected in fewer than five samples were excluded from analysis. Intensity-Based Absolute Quantitation abundance values were normalised for each set of transformants to the mean total abundance of the parental strain AX2. Data was exported to Excel in which genes/proteins were assigned to one of either two groups on the basis of whether they were significantly upor significantly down compared to the WT using the *p*-values of a two sample *t*-test. Gene enrichment in biological functionsand cellular components associated with these resultant genelists were determined in FunRich software using hypergeometricanalysis and Bonferroni method to gain *p*-values. Lists were also entered into the STRING database for a visual representation andfalse discovery rates of biological processes.

# RESULTS

## Human Tau Can Be Expressed in *D. discoideum* Alone and in CombinationWith Human *α*-Synuclein and Is Phosphorylated

The longest human tau isoform (2N4R) was expressed in *D. discoideum* singly and in combination with human *α*-synuclein. The plasmid expression constructs enter the *D. discoideum* genome through rolling circle replication and recombination, this results in strains with a varying number of the construct and therefore different expression levels. Tau phosphorylation plays a major role in the aggregation of the tau protein found in neurodegenerative diseases. In normal circumstances tau binds on and off MT depending on the phosphorylation state of the protein. Phosphorylation causes tau to disassociate from MT while regained affinity to bindto MT occurs with dephosphorylation (Cleveland et al., 1977; Lindwall and Cole, 1984). Further hyperphosphorylation of the protein leads to aggregation and the pathological conformations of tau seen in the tauopathies (Grundke-Iqbal et al., 1986).

*D. discoideum* has homologues of many of the kinases that phosphorylate tau in the human brain and as evident in **Figure 1**, human tau is phosphorylated at least at residue S404 in *D. discoideum.*

## Tau Is Localised Throughout the Cytoplasm in *D. discoideum* Whereas *α*-Synuclein Is Localised to the Cortex

To visualise the localisation of tau in *D. discoideum* immunofluorescence microscopy was performed. Tau was detected using an anti-tau antibody coupled with Alexa-Fluor 594-conjugated secondary antibody and was seen throughout the cytoplasm of the cell. *α*-synuclein had previously been seento localise to the cortex of the cell in *D. discoideum* (Fernando et al., 2020). To detect *α*-synuclein and tau in the cotranformants anti-tau and anti-*α*-synuclein antibodies were coupled with Alexa-Fluor 594 and 488-conjugated secondary antibodies respectively. In the cotransformants tau was again locatedthroughout the cytoplasm and *α*-synuclein primarily at the cortex. Tau and *α*-synuclein have been found to colocalise in many neurodegenerative diseases where they may enhance the pathological process of the other protein. To investigate whether

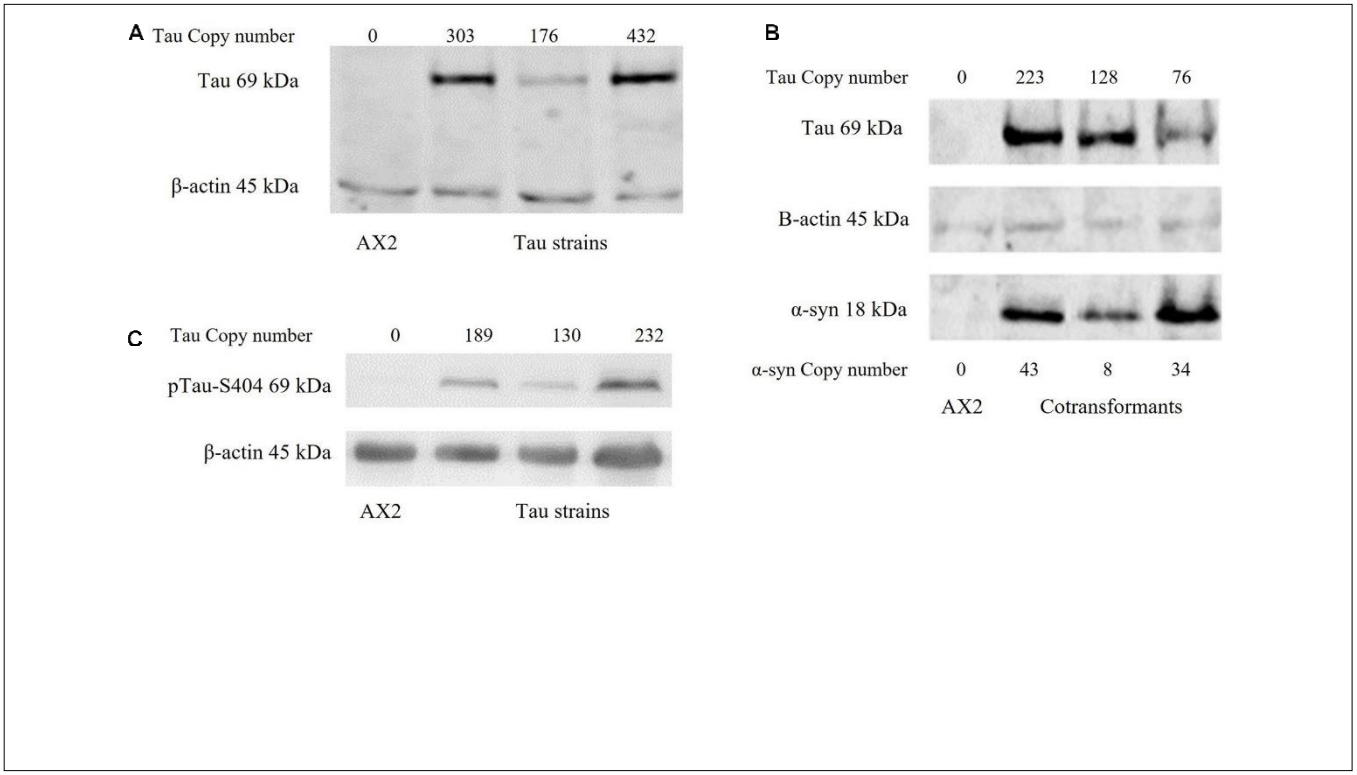


tau and *α*-synuclein colocalise within *D. discoideum*, proximity ligation assays (PLA) were performed using the Duolink™ *in situ* protein-protein interaction detection assay. Tau and *α*-synuclein were found to colocalise at the cortex of the cell where *α*-synuclein is primarily concentrated (**Figures 2A–C**).

## Human Tau and *α*-Synuclein Can Interact With *D. discoideum* Tubulin

In humans, tau binds to microtubules aiding in their assembly and stability and supporting axonal transport. To determine whether tau interacts with tubulin in *D. discoideum* the Duolink™ detection assay was again used. Tau was seen to localise with tubulin throughout the cytoplasm of the cell (**Figure 2D**). Tubulin and *α*-synuclein were also seen to colocalise, however, this interaction was seen at the cortex of the cell where *α*-synuclein is primarily located (**Figure 2E**).

## Tau Negatively Affects Fruiting Body Morphology

Loss of a food source induces chemotaxis among unicellular *D. discoideum* leading to aggregation and multicellular development culminating in the development of a fruiting body consisting of a sorus of spores atop a slender stalk.Fruiting body morphology previously seen in *α*-synucleinexpressing strains resembles that of the parental strain AX2 (Fernando et al., 2020). The expression of tau, however, producesan abnormal stalk with enlarged basal disk when compared to the parental strain (**Figure 3A**). Cells in the basal disk have undergone a programmed cell death and the result suggests that expression of tau increases the number of cells entering this pathway. This phenotype was observed in *D. discoideum* strains characterised as mitochondrially diseased. The strains expressing both tau and *α*-synuclein have a larger sorus and thicker stalk, suggesting that they form larger aggregates (**Figure 3A**).

## Tau Causes an Impairment in Phototaxis and Thermotaxis, Which Is Enhanced by the Coexpression With *α*-Synuclein

Qualitative and quantitative phototaxis experiments were performed with tau strains and cotransformants (**Figures 3B,C**). In agreement with previous studies WT *α*-synuclein expressing strains exhibited no phototaxis defect when compared with the wildtype (Fernando et al., 2020). The tau strains displayeda mild defect in accuracy of phototaxis which was more severe in the strains expressing both tau and *α*-synuclein.The increased severity of the phototaxis defect when both tau and *α*-synuclein were expressed together hints at an interaction between the two proteins. This is consistent with yeast models of a synergistic relationship between the two proteins, with enhanced defects when both proteins are expressed (Zabrocki et al., 2005; Ciaccioli et al., 2013). In *D. discoideum*, phototaxis and thermotaxis pathways share many downstream genes (Darcy et al., 1994), so that when a phototaxis defect is detected, a thermotaxis defect is usually also present. In support of this, strains expressing *α*-synuclein displayed no defect in thermotaxis with accuracies similar to AX2 and strains expressing tau displayed reduced accuracies of thermotaxis (**Figure 3D**). However, cotransformants expressing

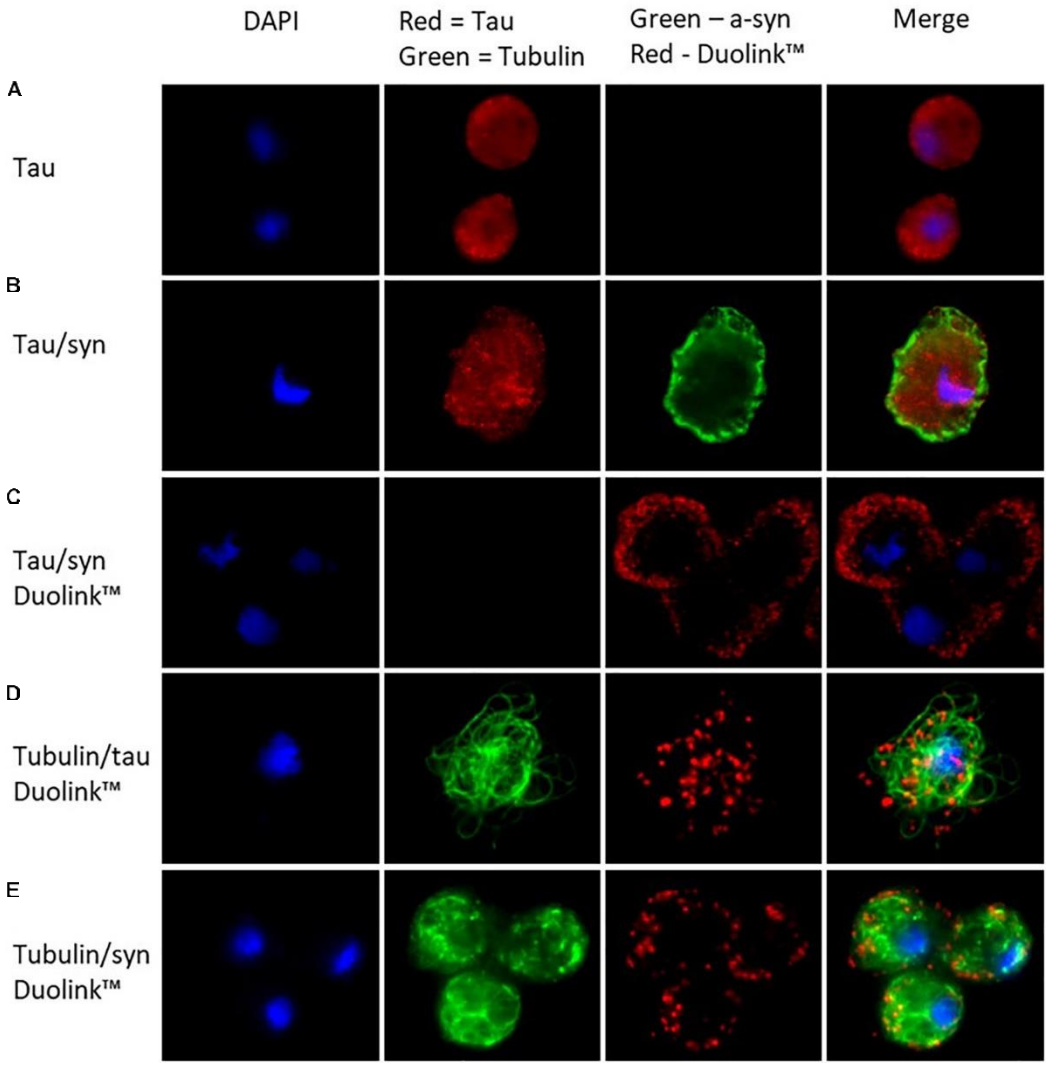


FIGURE 2 | In *D. discoideum* tau localises throughout the cytoplasm of the cell while $\alpha$-synuclein concentrates at the cortex. The colocalisation of the two proteinstakes place at the cortex of the cell where $\alpha$-synuclein is most concentrated. (A) Tau was detected in the tau transformant using an anti-tau primary antibody and observed using Alexa-Fluor 594 conjugated secondary antibody. (B) $\alpha$-synuclein was detected using an anti-$\alpha$-synuclein antibody and visualised using Alexa Fluor 488 conjugated secondary antibody along with tau in the cotransformant. (C) To view colocalisation of tau and $\alpha$-synuclein the cotransformants were stained with mouse anti-tau antibody and rabbit anti-$\alpha$-synuclein antibody, the protein–protein interaction was observed (as red dots) using secondary proximity probes, anti-rabbit MINUS and anti-mouse PLUS in the Duolink$^{textrmTM}$ in situ detection kit (Sigma-Aldrich). To visualise colocalisation of tau or $\alpha$-synuclein with tubulin Duolink$^{textrmTM}$ was again used, this time using a mouse-anti-tubulin primary antibody and rabbit-anti-tau or anti-$\alpha$-synuclein antibodies. An additional Alexa-Fluor 488 conjugated secondary antibody was added in with the proximity probes in order to visualise tubulin. (D) Tau colocalised with tubulin throughout the cytoplasm ofthe cell. (E) The colocalisation of tubulin and $\alpha$-synuclein occurred at the cortex of the cell where $\alpha$-synuclein is most abundant.

both tau and $\alpha$-synuclein showed reduced accuracies of thermotaxis at a similar magnitude to the tau expressing strains suggesting that $\alpha$-synuclein imparts no additional defect as was seen in phototaxis.

## Coexpression of Tau and *α*-Synuclein Positively Affects Growth on Plates but Negatively Affects Axenic Growth

*Dictyostelium discoideum* strains expressing tau and $\alpha$-synuclein alone and in combination were grown on lawns of *E.coli* B2 to measure plaque expansion rates. Previous experiments showed a decrease in plaque expansion rates and no affect on axenic growthby $\alpha$-synuclein expressing strains (Fernando et al., 2020). Tau strains produced plaque expansion rates similar to AX2, while the cotransformant had slightly faster plaque expansion rates (**Figure 4A**). This could indicate an interaction between tau and $\alpha$-synuclein that rescues the $\alpha$-synuclein defect. Axenic growth was slightly impaired in both tau and cotransformant strains with slightly longer generation times (**Figure 4B**). These results differ from those seen with mitochondrially diseased strains which displayed decreased growth on both solid and in liquid media.

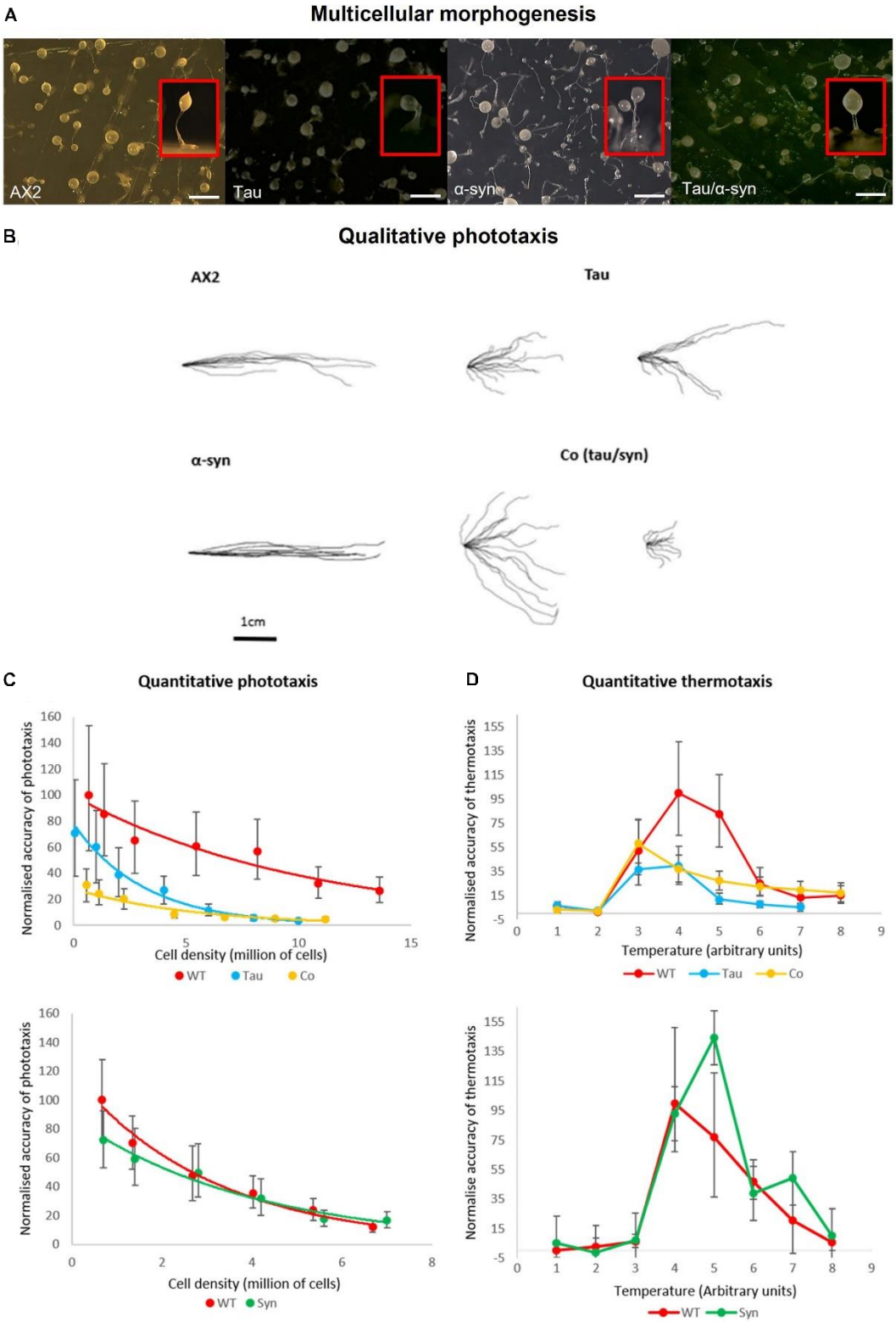


FIGURE 3 | Multicellular morphogenesis, phototaxis and thermotaxis. (A) Fruiting body morphology by AX2, strains expressing tau and $\alpha$-synuclein singularly and coexpression of the two proteins. Tau strains produce an abnormal stalk with enlarged basal disk when compared to the parental strain. The $\alpha$-synuclein strains resemble that of the parental strain AX2 (Fernando et al., 2020). The strains expressing both tau and $\alpha$-synuclein have a thicker stalk and larger sorus indicating that these strains produce larger aggregates than AX2. Top view of plates with insets showing the side view of a single representative fruiting body of each strain. Scale *(Continued)*

FIGURE 3 | Continued

bar indicates 1 mm. (B) Qualitative phototaxis. Slug trails of WT AX2, tau, $\alpha$-synuclein, and cotransformants were traced and digitised. Strains expressing

$\alpha$-synuclein showed no defect in phototaxis when compared to WT. Tau strains exhibited a reduced accuracy of phototaxis which was enhanced by the coexpression with $\alpha$-synuclein. (C) Quantitative Phototaxis. WT AX2, tau, $\alpha$-synuclein, and cotransformant strains were statistically analysed to measure the accuracy of phototaxis ($\kappa$), normalised, and were plotted againt cell density. Tau expressing strains displayed an impaired accuracy of phototaxis when compared with the WT AX2. This defect was more severe in the strains expressing tau and $\alpha$-synuclein in combination. Error bars represent standard errors (D) Thermotaxis.AX2, tau strain, $\alpha$-synuclein [HPF885—data taken from previous experiments (Fernando et al., 2020)], and cotransformants were measured for accuracy of thermotaxis ($\kappa$), normalised and plotted against temperature. Temperature is expressed in arbitrary units (1–8) corresponding to agar surface temperatures of 14–28°C. $\alpha$-synuclein caused no

## Combined Expression of Tau and ***α***-Synuclein Positively Affects Phagocytosis Rates While Macropinocytosis Is Not Affected

*Dictyostelium discoideum* consume nutrients through endocytosis. When feeding on bacterial lawns, bacteria are ingested through phagocytosis, and in liquid media nutrientsare taken up through macropinocytosis (pinocytosis). The normalised rates of endocytosis can be seen in **Figures 4C,D**. Tau did not affect phagocytosis or pinocytosis rates, which resembles the phenotypes of mitochondrially diseased cells (Bokko et al., 2007). Phagocytosis but not pinocytosis was affected in $\alpha$-synuclein strains, indicating the impaired growth on bacterial lawns was due at least partly to a phagocytosis defect. The cotransformants had an increased phagocytosis rate suggesting that the increased growth rate on bacterial lawns was also due to elevated rates of phagocytosis. Pinocytosis was not affected in these strains and therefore not the cause of the impaired axenic growth of the tau and cotransformant strains.

## *Legionella* Proliferation Is Increased in Tau and Cotransformant Strains

*Dictyostelium discoideum* is naturally found in soil environments where it consumes bacteria as a food source. *Legionella* also reside in moist soil environments where they can infect and proliferate within amoebae by exploiting phagocytosis. In healthy *D. discoideum* cells, *Legionella* is taken up and proliferates, but in mitochondrially diseased cells, *Legionella* proliferation is enhanced by up to two-fold when compared to wildtype (Francione et al., 2009). To measure *Legionella* infection and intracellular proliferation rates, *D. discoideum* amoebae were plated in a monolayer in a tissue culture plate and infected with *L. pneumophila* Corby. Viable counts of *L. pneumophila* were determined over 5 days at time points 0–96 h. Tau strains and cotransformants exhibited increased *L. pneumophila*proliferation compared to the parental strain AX2 (**Figure 5**), which corresponds to previous results seen in mitochondrially diseased cells. *D. discoideum* strains expressing $\alpha$-synuclein showed a decrease in *L. pneumophila* proliferation.

## Phototaxis Defect Is Mediated by AMPK

Some of the phenotypes with tau-expressing stains resemble phenotypes attributed to mitochondrial dysfunction in *D. discoideum*. These phenotypes have previously been attributed to the chronic activation of AMPK, an energy- sensing enzyme important in cellular homeostasis. One of the main phenotypes associated with mitochondrial dysfunction and chronic activation of AMPK is a defective slug phototaxis. This was observed in strains in which Cpn60 had been antisense inhibited (Bokko et al., 2007), the mitochondrial protein MidA was knocked out (Carilla-Latorre et al., 2010) and mitochondrial genes were disrupted in a subset of mitochondrial genomes (Francione and Fisher, 2011; Francione et al., 2011). The phototaxis defect in mitochondrially diseased strains is rescued by antisense inhibition of AMPK. Furthermore AMPK has been shown to interact in a photosensory signalling complex with filamin (Bandala-Sanchez et al., 2006) and other proteins implicated in this pathway including RasD (Wilkins et al., 2000), FIP (Knuth et al., 2004), the protein kinases PKB, and ErkB (Bandala-Sanchez et al., 2006). Knockdown of AMPK has also rescued the defective phototaxis seen in strains expressing PD associated mutations of $\alpha$-synuclein (Fernando et al., 2020). Because of this, we decided to investigate whether the phototaxis defect caused by the expression of tau and the more severe defectof the cotransformant was mediated by increased AMPK activity.To do this, cotransformants were created expressing tau and an AMPK antisense construct. As the expression of tau and $\alpha$-synuclein combined yielded a more severe phototaxis defect, strains expressing tau, $\alpha$-synuclein and AMPK knockdown were also produced. Copy numbers of the tau, AMPK antisense and $\alpha$-synuclein expression constructs were determined by qPCR.AMPK antisense inhibition rescued the phototaxis defect caused by both the expression of tau and the more severe impairmentobserved in the $\alpha$-synuclein/tau cotransformants (**Figure 6**). The slug trails resemble the parental strain in accuracies toward the light source, suggesting that the phototaxis defect in thesestrains is mediated by chronic AMPK hyperactivity as is known to be the case for mitochondrially diseased strains. It would be of interest in future work to determine if the phenotypes produced by tau that mimic those of mitochondrial disease are also mediated by AMPK. These include the defective fruiting body morphology, axenic growth, thermotaxis, and enhanced *L. pneumophila* proliferation.

## Tau Impairs ATP Synthesis While the Coexpression With ***α***-Synuclein Leads to Normally Functioning Mitochondria

The phenotypes caused by ectopic tau expression suggest a possible mitochondrial defect producing at least some AMPK-dependent cytopathological outcomes. Therefore we measured the function of the mitochondria using the Seahorse ExtracellularFlux Analyser in combination with a series of inhibiting

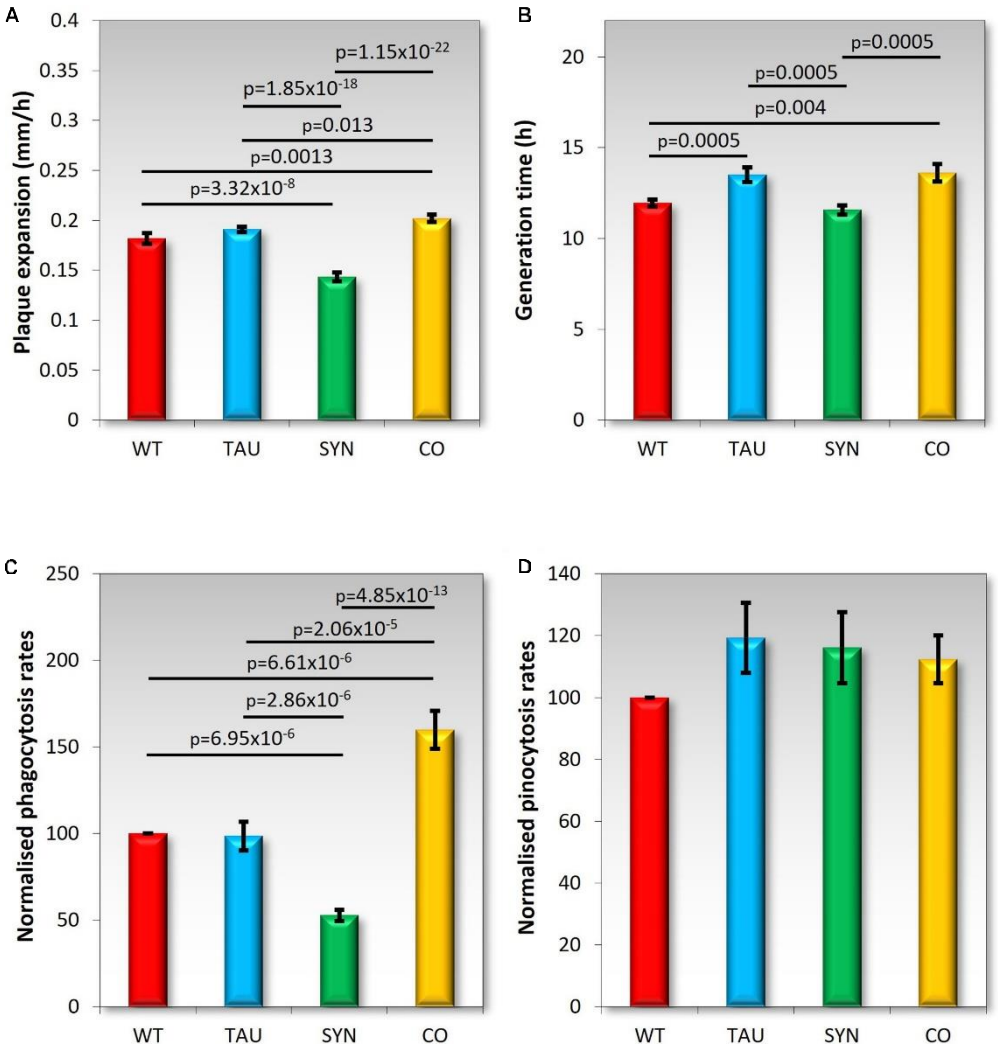


FIGURE 4 | Growth and endocytosis Wild type AX2 (WT) and strains expressing tau (TAU), $\alpha$-synuclein (SYN), or both tau and $\alpha$-synuclein (CO) were tested. (A) Plaque expansion rates were measured during growth on bacterial lawns of *E. coli* B2. Plaques were measured twice daily over one hundred hours. Experiments were performed in triplicate in four different experiments. As previously seen (Fernando et al., 2020) $\alpha$-synuclein-expressing strains display slower growth on bacterial lawns when compared to the WT AX2. Tau does not affect growth on plates, but strains expressing both tau and $\alpha$-synuclein grew slightly but significantly faster. (B) Axenic growth rates were measured by determining the generation time of strains (doubling in exponential growth phase). Strains were grown in HL5 liquid medium on a shaker at 21°C for 100 h. Experiments were performed on tau and cotransformant strains over four separate experiments. As previously shown, $\alpha$-synuclein did not affect axenic growth (Fernando et al., 2020). Strains expressing tau displayed significantly longer generation times during growth in liquid medium. Strains expressing both tau and $\alpha$-synuclein also showed significantly longer generation times than AX2. Error bars are standard errors of the mean, p-values represent statistically significant values using a two sample *t*-test. (C) Phagocytosis rates were measured by feeding *D. discoideum* amoeba *E. coli* DS-Redand taking fluorescent measurements directly after addition of the bacteria, then again after 30 min of incubation at 21°C on a shaker. The uptake rates of bacteria were normalised to the rate of uptake of AX2 (WT). Tau did not affect phagocytosis rates and shows a similar uptake rate to AX2. Previously, $\alpha$-synuclein expression caused a significant decrease in phagocytosis rates (two-sample *t*-test pictured). The coexpression of tau and $\alpha$-synuclein significantly increased the rate of phagocytosis (two-sample *t*-test). Cell lines were assayed in at least three separate experiments (D) Pinocytosis rates were measured by feeding *D. discoideum* amoeba with HL5 that contained FITC-dextran. Fluorescent measurements were taken directly after the addition of the FITC-dextran and again after an incubation period of 70 min at 21°C on a shaker. Cell lines were assayed in at least three separate experiments. Pinocytosis rates were not significantly affected by the expression of tau, $\alpha$-synuclein (Fernando et al., 2020), or the combined expression of these two proteins.

drugs added in sequential order. This allows the analysis of various components of mitochondrial respiration using the Oxygen Consumption Rate (OCR) as a readout of mitochondrial activity (**Figure 7**).

**Figure 7A** shows a typical example of a Seahorse experiment and indicates how each of the components are measured.

In agreement with previously conducted experiments, the $\alpha$-synuclein-expressing strains showed significant increases in mitochondrial respiration and also an increase in the OCR by non-mitochondrial processes. There was no significant differencein the contribution of each component to basal respirationor maximum respiration rates suggesting that all complexes

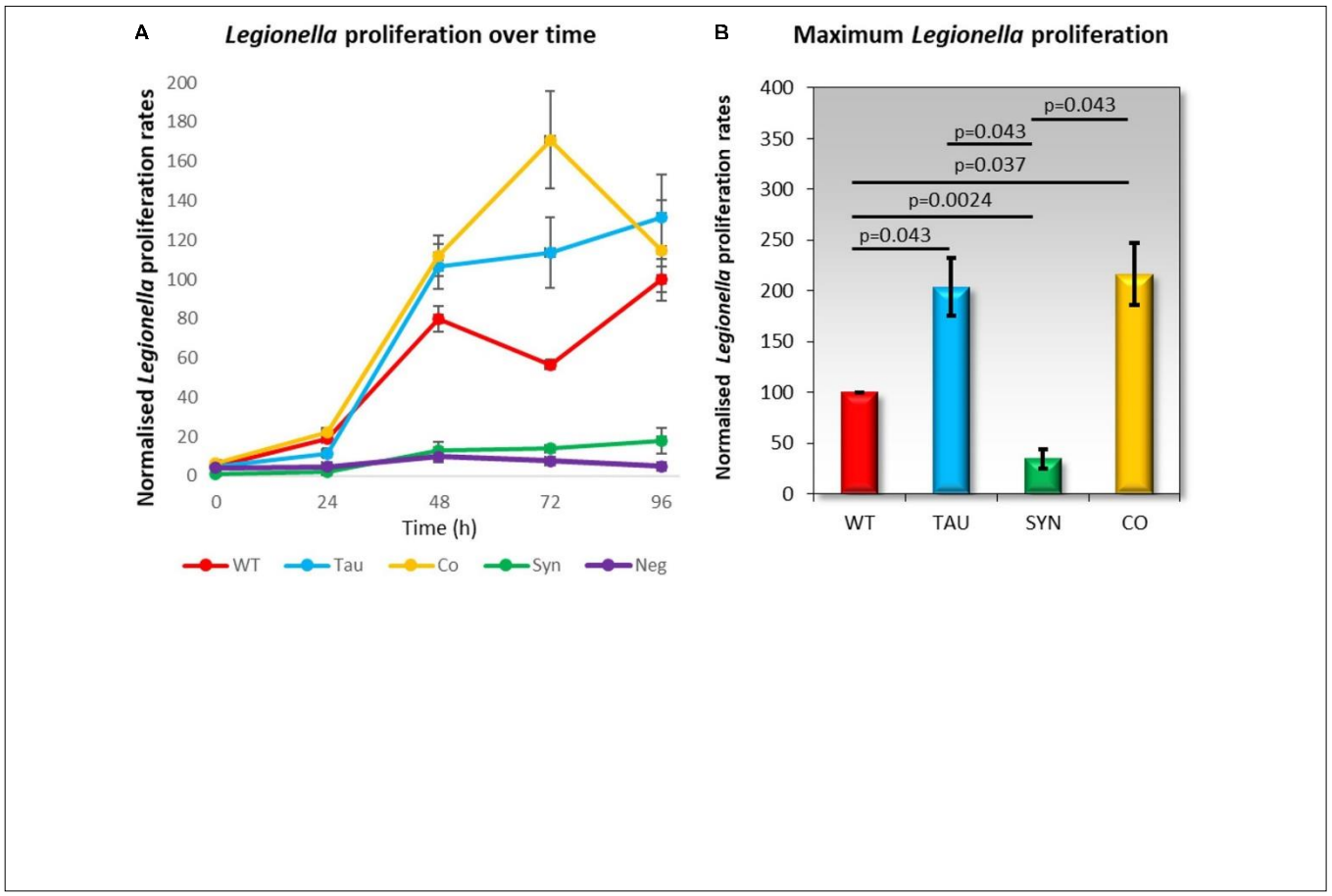


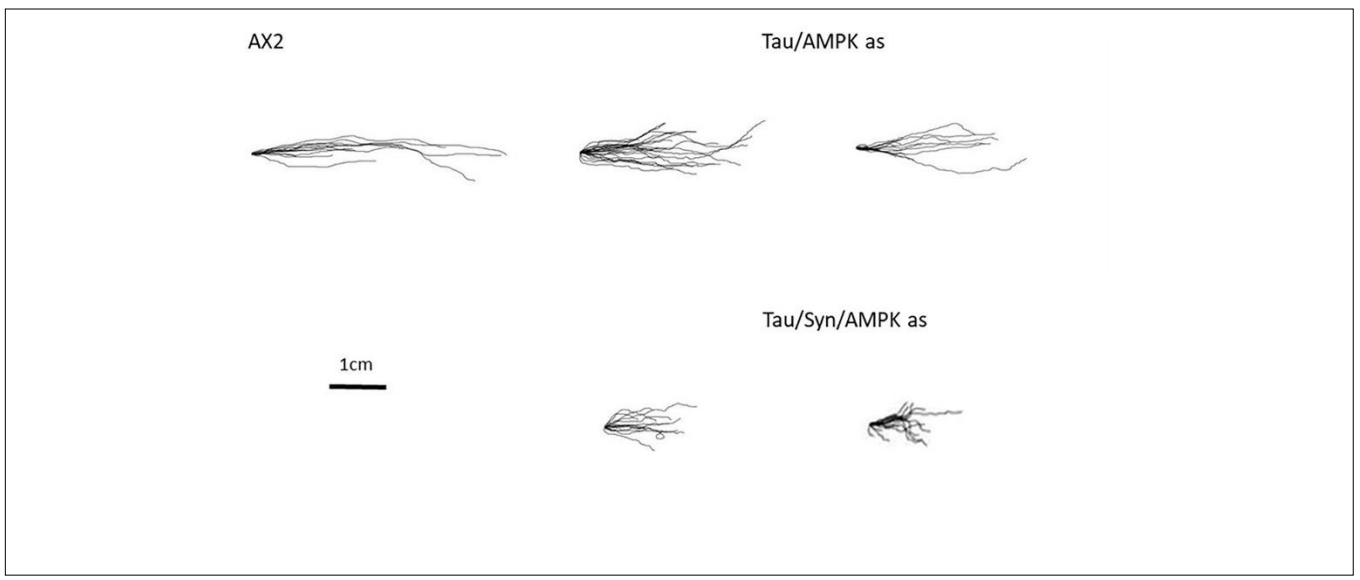


and components are functionally normal but hyperactive, as previously reported. The expression of tau did not affect total mitochondrial respiration but there was a significant decreasein OCR dedicated to ATP synthesis both in absolute terms (pmol $min^{-1}$) and relative to the basal mitochondrial respiration rate. Tau did not affect the maximum uncoupled $O_2$ consumption rate, or the contributions to this of Complex I and Complex II. These results suggest a specific defect in Complex V, the mitochondrial ATP synthase. It was accompanied by a significant increase in the $O_2$ consumption rate attributableto "proton leak," both the absolute rate and the proportion it contributed to basal respiration. This could reflect compensatory

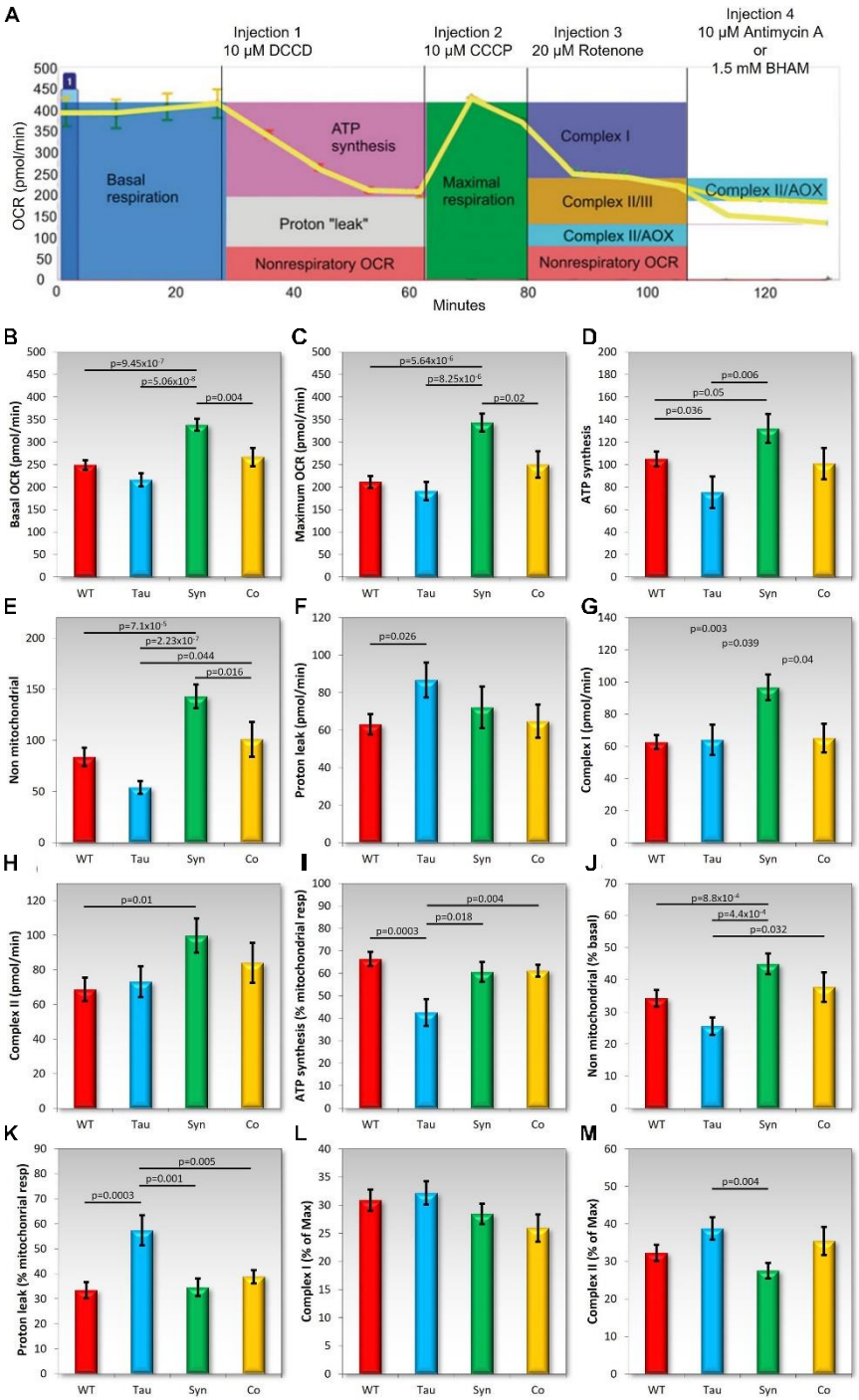


FIGURE 7 | Tau impairs mitochondrial ATP synthesis and coexpression with $\alpha$-synuclein rescues the defect. In each experiment, cells of the *D. discoideum* parental strain (AX2), and strains expressing tau or $\alpha$-synuclein alone or in combination were plated in four wells per sample of a Seahorse XFe24 plate. Mitochondrial respiration was measured as the oxygen consumption rate (OCR) using the Seahorse XFe24 Analyzer following the addition of pharmacological agents. The following agents were added sequentially [as seen in panel (A) and into all wells: DCCD (dicyclohexylcarbodimide), CCCP (carbonyl cyanide m-chlorophenyl hydrazone), and rotenone]. Then either Antimycin A or BHAM (benzohydroxamic acid) was added to the wells. The coloured boxes in panel (A) indicate how each component of the respiratory chain was measured (Lay et al., 2016). Total activity for Complex II was calculated by adding the effects of Antimycin A and BHAM. Panels (B–H) represent each component of mitochondrial respiration measured by the OCR. Each strain was assayed as four replicates per experiment across an average of 3–6 experiments. Horizontal bars with *p* values represent statistically significant pairwise comparisons using the *t*-test. All other pairwise differences werenot statistically significant. Error bars are a standard error of the mean. The following components were measured: (B) Basal OCR, (C), maximum OCR, (D) ATP synthesis, (E) non-mitochondrial respiration, (F) proton leak, (G) Complex I activity, and (H) Complex II activity. As seen previously, *D. discoideum* expressing
*(Continued)*

FIGURE 7 | Continued

$\alpha$-synuclein showed an increase in mitochondrial respiration and also an increase in oxygen consumption rates as a result of non-mitochondrial processes. In contrast tau expressing strains displayed a reduced OCR dedicated to ATP synthesis (D) and an increased proton leak (F) and the two appeared to balance each other out as basal respiration was unchanged (A) The proportion of ATP synthesis and proton leak to basal respiration was also significantly affected suggesting functional defects in Complex V and proton leak. There were significant differences between tau and $\alpha$-synuclein expressing strains in the basal and maximum OCRs, ATP synthesis, non-mitochondrial respiration and Complex I activity. In all cases $\alpha$-synuclein displayed higher OCR measurements than tau strains. The effects on either of these strains seemed to be "balanced" out with the combination of the two proteins being expressed together. The cotransformants showed similar results to the parental strain and did not differ significantly in any component when compared to AX2. (I–M) The following were plotted as a proportion ofeither the Basal, maximum, or mitochondrial respiration dedicated OCR in order to determine the contribution of each component to the relative respiration rates. Shown in these panels are the OCR attributed to ATP synthesis as a % of mitochondrial OCR (I), non-mitochondrial OCR as a % of Basal OCR (J), the "proton leak"or the mitochondrial OCR rate not contributed to by ATP synthesis; as a % of mitochondrial respiration (K), relative contribution of Complex I activity as a % of Maximum OCR (L), and the relative contribution of Complex II activity as a % of Maximum OCR (M). Strains expressing $\alpha$-synuclein increase in non-mitochondrial OCR as a % of basal. Tau expressing strains displayed a decrease in OCR attributed to ATP synthesis relative to mitochondrial OCR but an increase in mitochondrialOCR attributed to by the "proton leak." Once again, the cotransformants expressing both tau and $\alpha$-synuclein did not differ from the parental strain indicating allcomplexes were functioning normally,

upregulation of mitochondrial transport processes responsiblefor provisioning the mitochondria with oxidizable substrates and other molecules. The coexpression of tau and $\alpha$-synuclein rescued all of these defects and these strains displayed normal mitochondrial function resembling the wild type AX2 strain. This again signifies a functional interaction between the two proteins.

## Conclusions of Proteomics

To investigate whether any of the phenotypes caused by the expression of tau, $\alpha$-synuclein or the cotransformant strains were caused by differentially regulated proteins, whole cell proteomics was performed and analysed to compare protein abundances between strains. The number of up- and down-regulated proteinsof each strain when compared to AX2 was determined using data exported to Excel from Scaffold and using the *p*-valuesof two sample *t*-tests. The number of proteins differentially expressed in the tau, $\alpha$-synuclein, and cotransformant strains canbe seen in **Figure 8**. There were more proteins down-regulated(tau $n = 99$, $\alpha$-synuclein $n = 53$, cotransformants $n = 144$) inall groups compared to proteins that were up-regulated (tau$n = 42$, $\alpha$-synuclein $n = 27$, cotransformants $n = 59$), and the cotransformants had more proteins differentially expressed than either the tau or $\alpha$-synuclein alone.

Enrichment analysis using FunRich software (**Figures 9A,B**) revealed that of the proteins up-regulated in the tau strains there were significantly more genes affecting protein catabolism ($p$ 0.0001), the proteasome ($p$ 0.0001), and translation($p$ = 0.0001) indicating that protein degradation and synthesis i.e., turnover are up-regulated. $\alpha$-synuclein did not have any effecton these processes while the cotransformants up-regulated fewer proteins involved in protein catabolism but more in the process of protein synthesis (translation, $p = 0.0001$). Thus, the biological processes up-regulated by $\alpha$-synuclein were unlike those up-regulated by tau. Tau induces protein catabolism, possibly as part of a spectrum of homeostatic compensatory processes that favour energy production by alternative catabolic processes in the face of defective mitochondrial ATP synthesis. By contrast,$\alpha$-synuclein expression enhances mitochondrial respiration and perhaps in support of this elevated activity, these strains exhibited higher levels of expression of enzymes involved in carbohydrate metabolism. This may provide the energy to support elevated rates of protein biosynthesis.

In $\alpha$-synuclein-expressing strains, proteins involvedin responding to bacteria were up-regulated as well as proteins associated with the pathogen-containing vacuole ($p = 0.0001$). This accords with the *L. pneumophila* infection and proliferation experiments in which $\alpha$-synuclein was significantly less susceptible to proliferation when compared with the parental strain AX2. These observations suggest that in $\alpha$-synuclein-expressing strains, *Legionella*-containing vacuoles may be up-regulated increasing the capacity of the cell to directly handle the pathogens through the endolysosomal *Legionella*-destroying pathway.

In accord with their different subcellular localisations, tau up-regulated proteins in the cytosol and cytoplasm where it was localised (as well as the nucleus), while $\alpha$-synuclein up-regulated proteins in the plasma membrane, extracellular matrix, and phagocytic vesicle which are all associated with the cell cortex (**Figure 9B**). STRING was used as a visual representation of the interacting protein groups up-regulated in the tau and cotransformant strains and the False Discovery Rates of each biological process affected (**Figure 9C**). There were too few up-regulated proteins in the $\alpha$-synuclein expressing strains for valid comparisons.

More biological process and cellular components were down- than up-regulated in all three strain groups (**Figure 10**). Proteins involved with the cytoskeleton were down-regulated in all strains($p$ 0.0001), with the highest number of proteins down- regulated in strains expressing both tau and $\alpha$-synuclein. This is another indication of functional interactions between these cytotoxic proteins and is not surprising as the cytoskeletonis involved in many processes that were affected in thesestrains, including phagocytosis, phototaxis and thermotaxis, differentiation, and development (Noegel and Schleicher, 2000). Of note, the biological processes of cell motility ($p = 0.012$), polarity ($p = 0.018$), morphogenesis ($p = 0.01$), and filopodiumassembly ($p = 0.005$) were only significantly down-regulated in the cotransformants. This corresponds with the more severe phototaxis defect in the cotransformants which also displayed a possible motility defect, as the slugs did not travel as far as other strains. It would be of interest to measure single cell motility andchemotaxis in these strains.

Several proteins involved in the response to bacteria are down-regulated in all strain groups, however, this is more significant

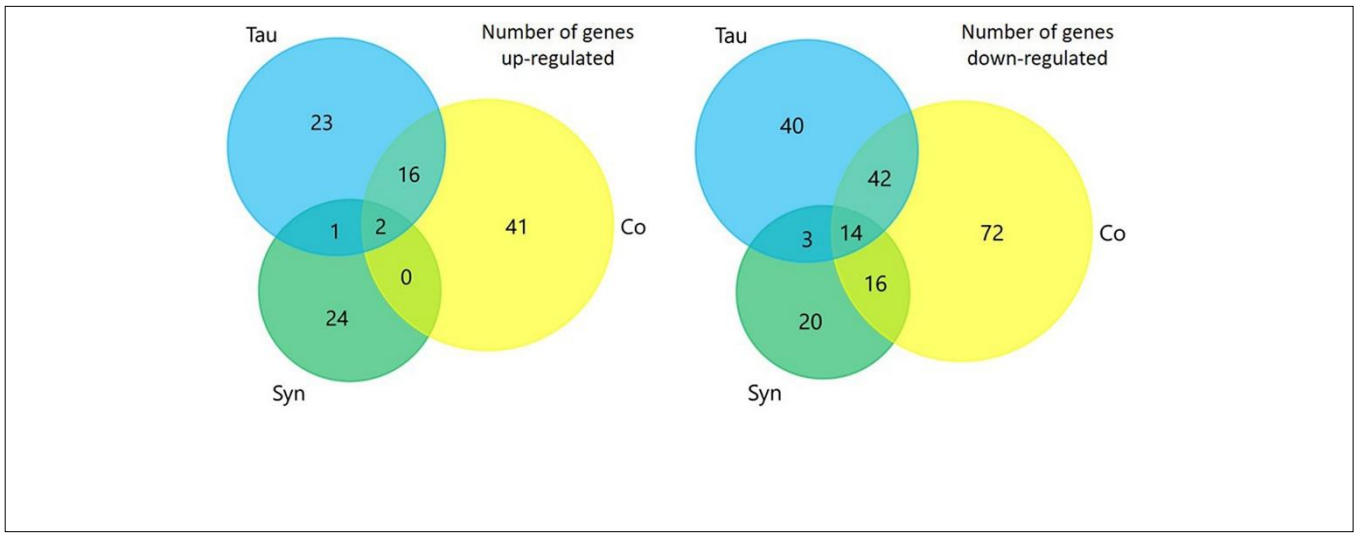


and there are more proteins affected in the tau-expressing and cotransformant strains ($p$ = 0.0001) when compared to those expressing $\alpha$-synuclein alone ($p$ = 0.005). Proteins upregulatedin this pathway in the $\alpha$-synuclein strains were downregulatedin the cotransformants. This again relates to the *L. pneumophila*results, wherein the tau and cotransformants both displayed an increased susceptibility to *L. pneumophila* proliferation when compared to the parental strain. Oxidation-reduction processes are significantly down regulated in the tau and cotransformant strains. Most of the proteins involved in these processes are involved in response to oxidative stress and the biosynthetic pathways of amino acid, fatty acid and lipid synthesis.

Lipid metabolism has been found to be dysregulated in association with tau pathology in AD and $\alpha$-synuclein in PD and synucleinopathies. For reviews see (Bok et al., 2021) and (Alecu and Bennett, 2019). Lewy bodies, the $\alpha$-synuclein-containing aggregates that are the pathological hallmark of PD, contain high lipid content and lipid membranes (Shahmoradian et al., 2019), while membrane lipids such as those associated with cholesterol have been associated with PHF in AD brains (Gellermannet al., 2006). Here tau and $\alpha$-synuclein when expressed alone significantly reduced lipid and sterol metabolic pathways, but when coexpressed, the down-regulation was rescued. This resembles the results of mitochondrial respiration where there were effects caused by the single expression of each protein and these were rescued to normal levels with coexpression. Again this signifies a functional interaction between tau and $\alpha$-synuclein. STRING was used as a visual representation of the protein groups down-regulated in three sets of strains and the False Discovery Rates of each biological process affected (**Figure 11**).

## DISCUSSION

Tauopathies are a diverse set of neurodegenerative diseases characterised by the accumulation of the tau protein into aggregates. Tau is important in the stabilisation of MT and axonal transport and binds to microtubules based on the phosphorylation state of the protein. Here we expressed the full-length human tau isoform (2N4R) in *D. discoideum* as a model to study tauopathies. As many neurodegenerative diseasesincluding the tauopathies suggest a synergistic relationship between pathological proteins, we also expressed tau in combination with $\alpha$-synuclein to investigate the interaction between these two proteins.

Phosphorylation of tau leads to disassociation of tau and MT, and further hyperphosphorylation causes the accumulation of tau into aggregates, while dephosphorylation restores tau/MT binding. Tau is regulated by many different kinases and phosphatases (Avila, 2008). Tau has over 80 different phosphorylation sites on the 2N4R isoform and many of these are involved in pathological conditions (Hanger et al., 1998; Buée et al., 2000). Over 20 kinases have been identified which are able to phosphorylate tau. These can be divided into two main groups—the proline directed protein kinases (PDPKs) and non-PDPKs. The PDPKs phosphorylate tau at Serine/Threonine residues and have been linked to the process of neurodegeneration (Sergeant et al., 2008; De Vos et al.,2011). Some common PDPKs are GSK-3$\beta$, mitogen activated protein kinase and cyclin dependent kinases which all have homologues in *D. discoideum* (Goldberg et al., 2006). These kinases phosphorylate tau at multiple Serine/Threonine sites on the 2N4R isoform (Augustinack et al., 2002). Phosphatases of tau have also been defined and include protein phosphatase 1 (PP1), 2A (PP2A), 2B (PP2B), and 5 (PP5), all of which have homologues in *D. discoideum.* Tau was phosphorylated in *D. discoideum* at S404 which is an important residue in the process of aggregation of the tau protein. Mondragón-Rodríguez et al. (2014) found that the double phosphorylationof Ser396 and Ser404 was an early event in AD and Down's syndrome. They saw early pathological tau structures (not yet defined NFT) correlating with phosphorylation at Ser396/404, while other phosphorylation sites corresponded with mature NFT. Pseudophosphorylation of tau (achieved by mutating the serine to glutamic acid to mimic phosphorylation) at this epitope has also been found to be an early event in the

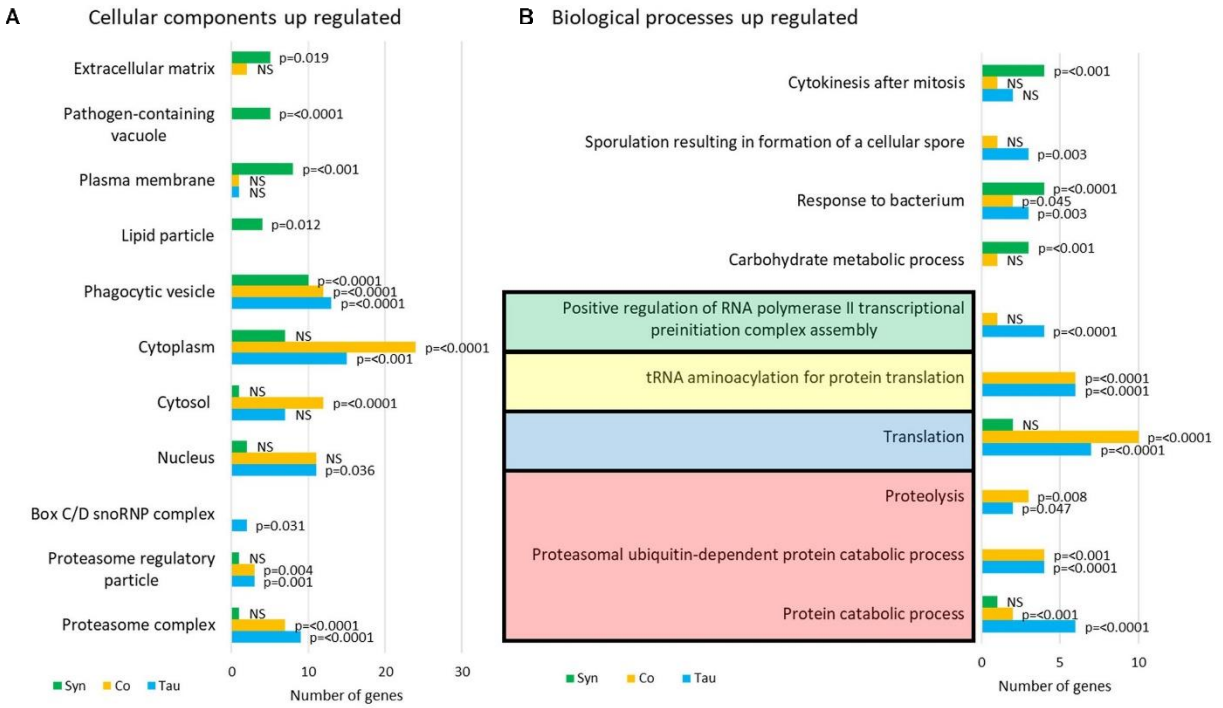


C

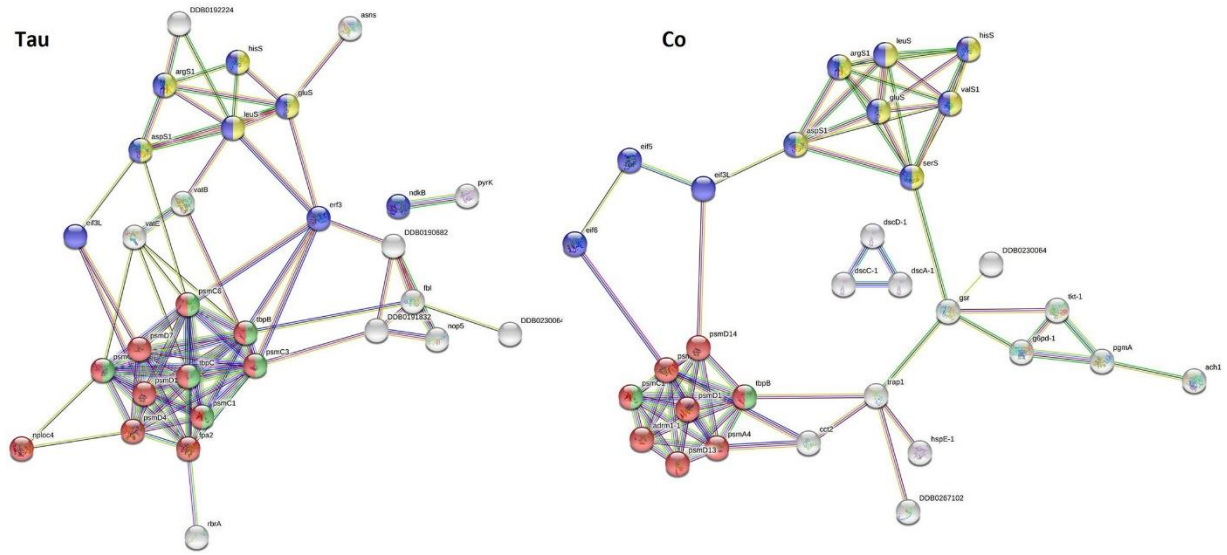


| Biological process | Colour | Tau (FDR) | Co (FDR) |
|---|---|---|---|
| Proteolysis | Red | $p=5.89\times10^{-11}$ | $p=1.18\times10^{-6}$ |
| Positive regulation of RNA polymerase II transcriptional preinitiation complex | Green | $p=1.15\times10^{-11}$ | NS |
| Translation | Blue | $p=4.09\times10^{-7}$ | $p=1.15\times10^{-8}$ |
| tRNA aminoacylation for protein translation | Yellow | $p=5.97\times10^{-7}$ | $p=1.18\times10^{-8}$ |

FIGURE 9 | Cellular components and biological processes up-regulated in strains expressing tau and/or $\alpha$-synuclein. Funrich enrichment analysis of cellular components (A) and biological processes (B) indicate that tau affects the proteasome and proteolytic processes as well as translation. The expression of $\alpha$-synucleinresulted in different biological processes and therefore different cellular components being affected. The cotransformants displayed patterns of up-regulated expression similar to those in strains expressing tau alone. The reported *p*-values are based on hypergeometric tests (A) and corrected using the Bonferroni method
*(Continued)*

FIGURE 9 | Continued

(B) calculated in FunRich software. This is based on the number of genes up-regulated within each strain divided by the total number of genes generated for each process/component using the Gene Ontology database for *D. discoideum.* To give a visual representation of protein groups, STRING was used to view the groups of interacting proteins involved in the major up-regulated processes in the tau-expressing strains and cotransformants and calculate False Discovery Rates (FDR) (C) which indicate statistical significance of the overrepresentation of these biological processes in the list of interacting up-regulated proteins. There was insufficient data to provide a network of interacting up-regulated proteins in the $\alpha$-synuclein expressing strains using STRING (Not pictured). Proteins and STRING protein annotations can be found in Supplementary Tables 1–3, 5.

hyperphosphorylation and aggregation of tau *in vitro* (Abrahaet al., 2000; Haase et al., 2004). Phosphorylation specificallyat Ser404 has been shown by kinases including GSK-3$\beta$ and the mitogen activating protein kinase ERK2 (Reynolds et al., 2000). Phosphopeptide mapping and sequencing shows that GSK-3$\beta$ displays the most pronounced phosphorylation at S404 (Augustinack et al., 2002). Phosphorylation of tau was also seen in other simple models including the yeast modelof tauopathy, in which human tau was phosphorylated and dephosphorylated by yeast kinases and phosphatases (De Voset al., 2011), and site specific phosphorylation resulted in tau aggregates and damage to MT (Vanhelmont et al., 2010). As tau is phosphorylated at S404 in *D. discoideum*, it is likely that it is also phosphorylated at other residues and this could be further investigated. Despite there being no tau orthologuein *D. discoideum*, the presence of homologous kinases that phosphorylate tau and the demonstration that at least one of them does act on tau suggest that the cellular machinery that regulates tau is ancient and could act on it in a similar way in
*D. discoideum* as it is in mammals. This is not unlike the case of APP which has no orthologue in *D. discoideum,* but which has been shown to be processed by $\gamma$-secretase in *D. discoideum* as in mammalian cells (McMains et al., 2010). As phosphorylation is the first step in the eventual pathological accumulation of tau, the next steps could be to investigate tau aggregation as well as other posttranslational modifications and structural conformations of the protein in *D. discoideum.*

In normal healthy cells, tau binds on and off MT dependingon the phosphorylation state of the protein. The longest tau isoform has a high affinity for MT as it has 4 MTBR. Here, tau was localised in the cytoplasm of the cell where it interacted with tubulin, although not necessarily on the MT. As tau was phosphorylated, this could have caused MT disassembly as it does in human neurons. However, as tau is not endogenously expressed in *D. discoideum* it is not necessary for MT stability. In agreement with this, our results provided no evidence of MT disassembly when tau was ectopically expressed in *D. discoideum,* although this was not directly measured.

Ectopic expression of human tau in *Drosophila* revealed that, unlike the endogenous *Drosophila* orthologue, it interacted poorly with *Drosophila* microtubules but was nonetheless cytotoxic (Feuillette et al., 2010). These findings would suggest that tau can exert cytopathological effects that are not related to dysregulated MT assembly/disassembly. What might those processes be? The proteomics results suggested that ectopic tau expression had a major impact on protein turnover with both protein degradation (proteasomal) and protein biosynthesis (transcription and translation) being up-regulated. The phosphorylation state of tau could impact the proteins involved in the proteasome as seen by Ren et al. (2007). Here, tau was expressed in embryonic kidney cells and phosphorylation of tau increased proteasome activity while further hyperphosphorylation decreased activity by the proteasome.

Like tau, $\alpha$-synuclein has been reported to interact with tubulin heterodimers in the cytosol (Payton et al., 2001) but also with MT, where it altered the cell surface recruitment of the dopamine transporter (Wersinger and Sidhu, 2005). A study by Alim et al. (2002) found that tubulin was a binding partner of $\alpha$-synuclein and colocalised in LB in a case of PD. However, colocalisation of proteins in the aggregates of Lewy Bodies does not necessarily reflect their normal interactions in the absence of such aggregates. We found that both tubulin and tau colocalise with $\alpha$-synuclein in *D. discoideum* in the cortex of the cell where $\alpha$-synuclein is concentrated. It is also here in the cortical regions of the cell that the cytopathological effects of ectopically expressed $\alpha$-synuclein are exercised—in the inhibition of phagocytosis and *L. pneumophila* proliferation. Furthermore the proteomics revealed significant dysregulation of proteins involved in these processes with $\alpha$-synuclein-expressing cells having lower levels of proteins involved in phagocytosis, but elevated levels of proteins involved in the response to and uptake of bacteria into pathogen-containing vesicles. The phagocytic vesicle associated proteins that were upregulated were mainly related to membrane fusion and protein transport. While the down regulated proteins were associated mainly with actin binding and the cytoskeleton. In relation to response to bacterium, proteins involved in vesicle transport were upregulated (rab1A, rab5A, rasG, sasA, and vatC). The interaction of tau with $\alpha$-synuclein in these same cortical regions can explain the ability of tau to reverse the inhibition of phagocytosis by $\alpha$-synuclein, when tau on its own has no effect on this phenotype, despite also downregulating expression of proteins involved in this pathway.

The colocalisation of tau and $\alpha$-synuclein at the cortex has been observed in cellular models where tau and $\alpha$-synuclein have both been found to interact with the plasma membrane (Brandt et al., 1995; Nakamura et al., 2001) and $\alpha$-synuclein stimulated phosphorylation of tau has been seen to occur here
too (Jensen et al., 1999). Esposito et al. (2007) proposed a membrane-bound functional complex with tau and $\alpha$-synuclein that may involve the actin cytoskeleton. In a Chinese hamster ovary cell line, $\alpha$-synuclein was found interacting with actin at the plasma membrane and the colocalisation of tau and $\alpha$-synuclein was highest at the cell periphery. The colocalisation of tau and $\alpha$-synuclein has been seen in autopsied brain sections of patients with AD (Hamilton, 2000; Arai et al., 2001), cellular

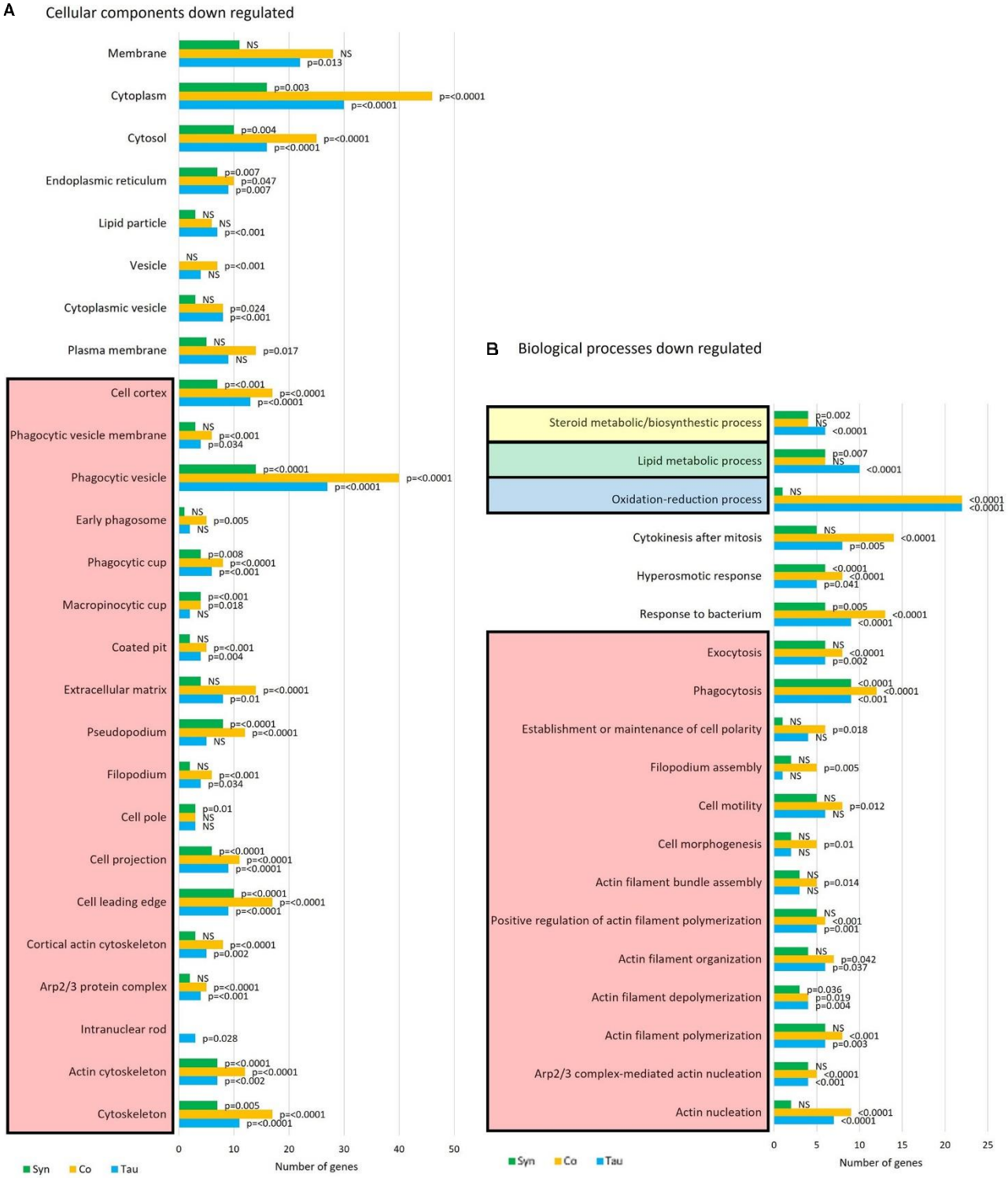


FIGURE 10 | Cellular components and biological processes down-regulated in strains expressing tau and/or $\alpha$-synuclein. Funrich enrichment analysis of cellular components (A) and biological processes (B) indicate that the cytoskeleton is significantly down-regulated in all strains. The coexpression of tau and $\alpha$-synuclein compounded the effect. The reported *p*-values are based on hypergeometric tests using the Bonferroni method of correction calculated in FunRich software. This isbased on the number of proteins down-regulated within each strain divided by the total number of proteins generated for each process/component using the GeneOntology database for *D. discoideum*.

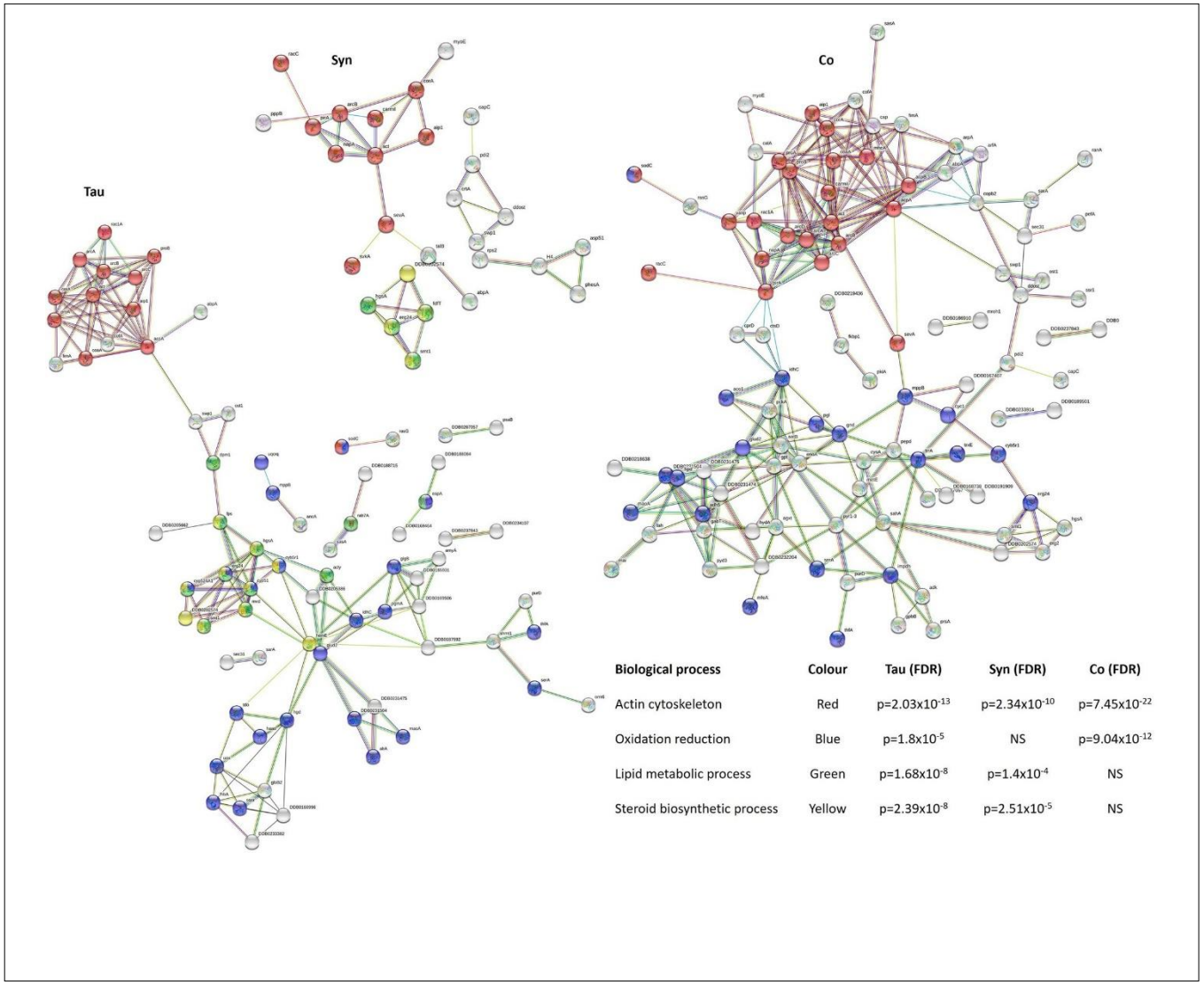


models (Badiola et al., 2011) and in LB from patients with LBD (Ishizawa et al., 2003). *D. discoideum* is an accepted model for investigating microtubule dynamics and interactions with microtubule associated proteins (MAPs) and is the best understood model for actin dynamics and function in eukaryotic cells (Eichinger et al., 1999; Noegel and Schleicher, 2000; Gerisch, 2009). An interaction between actin and MTs at the cell cortex has been established (Hestermann et al., 2002) and *D. discoideum* has many homologues of the mammalian MAPs (Graf et al., 2000; Rehberg and Gräf, 2002; Rehberg et al., 2005; Koch et al.,2006). The results presented here indicate an interaction of tau,tubulin and $\alpha$-synuclein which could be further investigated in the future exploiting the well-established cytoskeletal genetics and molecular biology of the *D. discoideum* model.

There has been much evidence to suggest that mitochondrial dysfunction is involved in neurodegenerative diseases (Lin and Beal, 2006) and both tau and $\alpha$-synuclein have been implicated. As *D. discoideum* has been well characterised asa model for mitochondrial disease exhibiting a clear set of phenotypes, we analysed the phenotypes of strains expressing tau or $\alpha$-synuclein or both to determine which might be sharedwith mitochondrially diseased strains. The $\alpha$-synuclein-mediated phenotypes and those caused by mitochondrial dysfunction have been compared previously and shown to be distinct (Fernandoet al., 2020). Whereas impaired mitochondrial function caused greater intracellular *L. pneumophila* proliferation as well as defects in phototaxis, thermotaxis, growth and development, but did not impair phagocytosis or pinocytosis. Despite similaritiesin some of these phenotypes, the expression of wild type $\alpha$-synuclein differed in that it impaired phagocytosis and *L. pneumophila* proliferation, while having no significant effect on growth in liquid, phototaxis, thermotaxis, or fruiting body morphology. In fact, direct assay of mitochondrial function showed that $\alpha$-synuclein expression did not impair but enhanced mitochondrial respiration. The overall pattern of phenotypes suggested that $\alpha$-synuclein cytotoxicity lies not in mitochondrial defects but in its impairment of specific endocytic pathways (Fernando et al., 2020).

In this work we report for the first time that tau expression increases *L. pneumophila* susceptibility, has no significant effect on phagocytosis or pinocytosis, impairs growth in liquid but not on bacterial lawns, and causes moderate phototaxis and thermotaxis defects as well as aberrant fruiting bodies with shorter, thicker stalks. This pattern of phenotypic outcomes is very distinct to those caused by α-synuclein expression and indicates that tau and α-synuclein cause different cytotoxic effects in *D. discoideum*. In fact the phenotypic consequences of tau expression are reminiscent of mitochondrial disease phenotypes, with the exception of the normal plaque expansion rates in tau-expressing strains. When mitochondrial respiratory function was measured using Seahorse respirometry, we found an isolated defect in ATP synthesis by complex V, accompanied by an elevation of the mitochondrial "proton leak" (the use of the mitochondrial proton gradient to drive diverse mitochondrial transport processes other than ATP synthesis). Were it not for the normal growth on bacterial lawns, the cytopathological effects of tau expression in *D. discoideum* could thus be attributed entirely to this mitochondrial defect. This raises the question of what other mechanisms might be involved.

The phenotypic abnormalities caused by tau all involved the cytoskeleton and this corresponds with the downregulation of actin cytoskeletal proteins found in the proteomic analysis. Tau impaired axenic growth with a slower generation time in liquid compared to the WT, but this was not mediated by a pinocytosis defect and there was no significant downregulation of proteins associated with the macropinocytic cup. This suggests that other pathways mediating cell proliferation could be causing the defect. This could be a defect in cytokinesis as proteins involved in this process were down-regulated. *Dictyostelium* cytokinesis during growth in suspension in liquid medium depends entirely on the actomyosin cytoskeleton (Zang et al., 1997; Bosgraaf and van Haastert, 2006), whereas on surfaces it can take place by a different mechanism (De Lozanne and Spudich, 1987; Knecht and Loomis, 1987). In the tau transformant the Rho-related protein racE was downregulated. Larochelle et al. (1996) showed that racE was necessary for cytokinesis as *D. discoideum* mutants that did not express racE did not grow in suspension due to a cytokinesis defect. The same group found that racE cells containing an expression vector for racE were able to produce racE to wildtype levels and had no defect in cytokinesis and growth rates in suspension (Larochelle et al., 1997). A study detailing the effect of an *abiA* null mutant (part of the SCAR/WAVE complex that drives actin polymerisation) in *D. discoideum* showed that the axenic growth defect was due to a defect in cytokinesis (Pollitt and Insall, 2008). Tau-expressing strains also exhibited an increased susceptibility to intracellular *L. pneumophila* proliferation, which again corresponded with proteomics data that indicated proteins responsible for the cellular response to bacteria were down-regulated.

In view of the distinctive and sometimes opposite phenotypic outcomes of expressing tau and α-synuclein in *D. discoideum*, the question arises as to what happens in cotransformants expressing both proteins. We showed here that the cotransformants displayed a third distinct pattern of phenotypes, with the presence of the second protein either exacerbating (phototaxis, fruiting body morphology), reversing (phagocytosis, growth on plates, mitochondrial respiratory function, *L. pneumophila* proliferation), or having no significant impact (growth in liquid) on defects caused by the other. This indicates clear functional interactions of the two proteins in several phenotypic pathways and in some cases a synergistic effect. There is similar evidence to suggest an interaction and synergistic cytotoxicity of these two proteins in other model systems coexpressing tau and α-synuclein. In cellular models Badiola et al. (2011) found that tau and α-synuclein colocalised in primary neuronal cultures and the overexpression of tau lead to enhanced α-synuclein cytotoxicity. In a *Drosophila* model of PD, Roy and Jackson (2014) misexpressed tau and α-synuclein singly and in combination. They found that the expression of α-synuclein produced no phenotype associated with the eye, while the expression of tau caused the rough eye phenotype with smaller eyes and the combined expression of the two proteins resulted in a more severe phenotype. This accords with our finding that α-synuclein exacerbates tau-mediated defects in phototaxis and fruiting body morphology. Similarly in yeast, tau exacerbated the growth defects caused by α-synuclein (tau alone produced no defect) (Ciaccioli et al., 2013).

Although our results support a cytotoxic interaction between the two proteins in some phenotypes, we also found that in relation to other phenotypes the two proteins exerted opposing actions. Thus the significantly impaired growth on bacterial lawns and the phagocytosis defect observed in the α-synuclein strains were reversed in the cotransformants. In the case of intracellular *L. pneumophila* proliferation, tau not only reversed the reduction caused by α-synuclein, but increased the proliferation of the pathogen to the same elevated levels as observed when tau was expressed singly. There is evidence that tau affects neuronal phagocytosis (Xie et al., 2019) and α-synuclein affects synaptic endocytosis (Lautenschläger et al., 2017), but the effect of combined expression on endocytic pathways has not been previously reported.

Another of the phenotypes in which coexpression of tau and α-synuclein had opposing effects was in mitochondrial respiratory function. Previously we showed that α-synuclein did not cause an impairment in mitochondrial function but instead it increased respiratory activity coordinately in all components measured (Fernando et al., 2020). This result was consistent with increases in mitochondrial respiration seen in lymphoblast cell lines made from iPD patients (Annesley et al., 2016), fibroblasts from iPD patients (Haylett et al., 2016) and when neuroblastoma cells were seeded with α-synuclein fibrils (Ugalde et al., 2020). In this work we found that tau expression caused a significant decrease in the OCR dedicated to ATP synthesis thereby revealing a specific defect in Complex V. A decrease in ATP production has been seen in neuronal cultures overexpressing tau (Li et al., 2016) and this was accompanied by decreases in Complex I activity and in the ratio of ATP/ADP. Here we found no Complex I defect caused by tau in *D. discoideum*. The combined expression of tau and α-synuclein returned mitochondrial respiration to normal, reversing the elevated mitochondrial respiration caused by α-synuclein as well as the Complex V defect and elevated proton leak caused by tau. Altered mitochondrial function is associated

with many neurodegenerative diseases and this result highlights that it may occur through different mechanisms and the importance of looking at neuronal protein-protein interactionsto advance our understanding of the part played by mitochondriain neurodegeneration. This emphasises the usefulness of using a simple model to study complex interactions and processes.

Many of the defective phenotypes observed in the tau-expressing strains were in line with mitochondrial dysfunction and previously this has been shown to be due to the chronic activation of AMPK (Bokko et al., 2007; Francione et al., 2009). To determine if there was a functional relationship between tau and AMPK in *D. discoideum,* we created cotransformants which expressed tau or tau and $\alpha$-synuclein and antisense inhibited AMPK. As phototaxis is a signature defect of impaired mitochondrial function we investigated whether this phenotype was mediated by increased AMPK activity. The antisense inhibition of AMPK in tau strains and strains expressing both tau and $\alpha$-synuclein resulted in a rescue of the phototaxis defect, suggesting that AMPK mediates the phototaxis defectcaused by tau and exacerbated by $\alpha$-synuclein coexpression. This suggests that AMPK may have been upregulated in the transformants, however, we could not measure this directlyas AMPK could not be detected in any of the transformantsor wild type strains. In neurons containing tau pathology in AD and many other tauopathies, AMPK levels and degree of activation (phosphorylation) are elevated (Vingtdeux et al., 2011). In cell culture a physical interaction between AMPK and tau was established and overexpression of AMPK increased tau toxicity and phosphorylation (Galasso et al., 2017). Interestingly, the inhibition of AMPK might serve as neuronal protection in neurodegenerative diseases (McCullough et al., 2005). Modelsof motor neuron disease and amylotrophic lateral sclerosis found benefits of downregulating AMPK (Lim et al., 2012). In *Drosophila* expressing tau downregulation of the AMPK$\alpha$ subunit partially rescued the tau rough eye phenotype. In future studies, determining if AMPK knockdown can rescue the other tau-mediated phenotypes would be beneficial, as would investigating whether AMPK phosphorylates tau in *D. discoideum.*

Proteomics analysis revealed that there were a numberof proteins up- and down-regulated in these strains. In all strains more proteins were down-regulated than up- regulated, and the combined effect of tau and $\alpha$-synuclein coexpression dysregulated the expression of more proteins than did expression of either protein on its own. The pattern of dysregulation caused by tau and $\alpha$-synuclein expression were quite distinct from each other. Tau significantly up-regulated protein degradation and turnover, possibly in response to the defect in ATP synthesis, while $\alpha$-synuclein up-regulated proteins involved in the response to bacterium corresponding with decreased *Legionella* susceptibility possiblyas a result of a more efficient endolysosomal pathway. All strains exhibited a down-regulation of cytoskeletal proteins, which was exacerbated in the cotransformants. Interestingly here, the cotransformants displayed unique downregulation in some aspects of the cytoskeleton relating to cell motility, polarity, morphogenesis, and filopodium assembly corresponding with the more severe phototaxis defect. Both tau and $\alpha$-synuclein down-regulated proteins involved in lipid and steroid metabolism, which are dysregulated in diseases like AD and PD. However, these pathways were not affected in the cotransformants, again consistent with a functional interaction between these two proteins that is sometimes beneficial rather than cytotoxic.

## CONCLUSION

Our results show that *D. discoideum* can be a useful modelto study the biological functions of tau and the interactions with other neurodegeneration-associated proteins. Whilst neurodegenerative disease like Alzheimer's and Parkinson's is characterised by death or dysfunction of neurons research is accumulating to suggest that the underlying disease mechanisms are likely to be more systemic occurring in many more cell types and not just isolated to neurons. We believe that by understanding the underlying molecular pathology that is sharedby all cell types then we can understand why particular neurons or parts of the brain are selectively affected in these disorders.Here we used an organism which does not contain neurons, or a brain but it does contain many conserved pathways and proteins with humans and has been shown to be a good modelfor studying mitochondrial function, cell division, growth, endocytosis, autophagy and intracellular signalling all of which have been implicated in neurodegenerative disease. Here we expressed tau alone and in combination with $\alpha$-synuclein to investigate the cytotoxic effects and interactions between the proteins in this simple model system. The results showed that tau and $\alpha$-synuclein have different subcellular distributions but they colocalise in the cortical regions of the cell. They affect different pathways and phenotypes when expressed singly and, depending on the pathway and phenotype, these effects can be enhanced or reversed by the expression of both proteinsat once. Thus, the *D. discoideum* model has revealed that the $\alpha$-synuclein/tau interaction is clear but more complex than a simple synergistic cytotoxicity. These complexities are worthy of further investigation in models like *D. discoideum* in which they can be studied without concerns about the possible effects of endogenous orthologues.

## DATA AVAILABILITY STATEMENT

The datasets presented in this study can be found in online repositories. The name of the repository and accession number can be found below: MassIVE, https://massive.ucsd.edu/ProteoSAFe/static/massive.jsp, MSV000087848.

## AUTHOR CONTRIBUTIONS

KM made the tau construct and tau strains including cotransformants, performed all of the experiments for the

tau and cotransformant strains, analysed the data, and prepared, reviewed, and edited the original manuscript. SF made the $\alpha$-syn constructs and strains and performed most of the phenotypic experiments with these strains. PF and SA conceptualised the project, supervised KM, advised on data analysis, and reviewed/edited the manuscript. All authors have read and agreed to the published version of the manuscript.

## ACKNOWLEDGMENTS

KM was the recipient of a La Trobe University Postgraduate Scholarship and Australian Government Research Training Program Fees Offset.

## SUPPLEMENTARY MATERIAL

The Supplementary Material for this article can be found online at: https://www.frontiersin.org/articles/10.3389/fcell.2021.741662/full#supplementary-material

Supplementary Table 1 | Tau up-regulated proteins. Supplementary Table 2 | Tau down-regulated proteins. Supplementary Table 3 | $\alpha$-Synuclein up-regulated proteins. Supplementary Table 4 | $\alpha$-Synuclein down-regulated proteins. Supplementary Table 5 | Cotransformant up-regulated proteins. Supplementary Table 6 | Cotransformant down-regulated proteins.

## REFERENCES


Abraha, A., Ghoshal, N., Gamblin, T. C., Cryns, V., Berry, R. W., Kuret, J.,et al. (2000). C-terminal inhibition of tau assembly in vitro and in Alzheimer's disease. *J. Cell Sci.* 113, 3737–3745. doi: 10.1242/jcs.113.21.3737

Alecu, I., and Bennett, S. A. L. (2019). Dysregulated lipid metabolism and its role in $\alpha$-synucleinopathy in parkinson's disease. *Front. Neurosci.* 13:328. doi: 10.3389/fnins.2019.00328

Alim, M. A., Hossain, M. S., Arima, K., Takeda, K., Izumiyama, Y., Nakamura,M., et al. (2002). Tubulin seeds $\alpha$-synuclein fibril formation. *J. Biol. Chem.* 277,2112–2117. doi: 10.1074/jbc.M102981200

Andreadis, A., Brown, W. M., and Kosik, K. S. (1992). Structure and novel exonsof the Human-tau Gene. *Biochemistry* 31, 10626–10633. doi: 10.1021/bi001 58a027

Annesley, S. J., and Fisher, P. R. (2009a). Dictyostelium discoideum–a model for many reasons. *Mol. Cell. Biochem.* 329, 73–91. doi: 10.1007/s11010-009-0111-8

Annesley, S. J., and Fisher, P. R. (2009b). "Dictyostelium slug phototaxis," in *Chemotaxis: Methods and Protocols*, eds T. Jin and D. Hereld (Totowa, NJ: Humana Press), 67–76. doi: 10.1007/978-1-60761-198-1_4

Annesley, S. J., Lay, S. T., De Piazza, S. W., Sanislav, O., Hammersley, E., Allan, C. Y., et al. (2016). Immortalized Parkinson's disease lymphocytes have enhanced mitochondrial respiratory activity. *Dis. Models Mechan.* 9, 1295– 1305. doi: 10.1242/dmm.025684

Arai, Y., Yamazaki, M., Mori, O., Muramatsu, H., Asano, G., and Katayama, Y. (2001). $\alpha$-Synuclein-positive structures in cases with sporadic Alzheimer's disease: morphology and its relationship to tau aggregation. *Brain Res.* 888,287–296. doi: 10.1016/S0006-8993(00)03082-1

Arima, K., Mizutani, T., Alim, M. A., Tonozuka-Uehara, H., Izumiyama, Y., Hirai, S., et al. (2000). NACP/$\alpha$-synuclein and tau constitute two distinctive subsets of filaments in the same neuronal inclusions in brains from a familyof parkinsonism and dementia with Lewy bodies: double-immunolabeling fluorescence and electron microscopic studies. *Acta Neuropathol.* 100, 115–121. doi: 10.1007/s004010050002

Augustinack, J., Schneider, A., Mandelkow, E.-M., and Hyman, B. (2002). Specific tau phosphorylation sites correlate with severity of neuronal cytopathology in Alzheimer's disease. *Acta Neuropathol.* 103, 26–35. doi: 10.1007/s004010100423 Avila, J. (2008). Tau kinases and phosphatases. *J. Cell Mol. Med.* 12, 258–259. doi: 10.1111/j.1582-4934.2007.00214.x

Avila, J., Lucas, J. J., Perez, M., and Hernandaz, F. (2004). Role of Tau protein in both physiological and pathological conditions. *Physiol. Rev.* 84, 361–384.doi: 10.1152/physrev.00024.2003

Badiola, N., de Oliveira, R. M., Herrera, F., Guardia-Laguarta, C., Goncalves, S. A., Pera, M., et al. (2011). Tau enhances alpha-synuclein aggregation and toxicityin cellular models of synucleinopathy. *PLoS One* 6:e26609. doi: 10.1371/journal.pone.0026609

Bandala-Sanchez, E., Annesley, S. J., and Fisher, P. R. (2006). A phototaxis signalling complex in *Dictyostelium discoideum*. *Eur. J. Cell Biol.* 85, 1099–1106.doi: 10.1016/j.ejcb.2006.04.005

Bok, E., Leem, E., Lee, B.-R., Lee, J. M., Yoo, C. J., Lee, E. M., et al. (2021). Role ofthe lipid membrane and membrane proteins in Tau pathology. *Front. Cell Dev. Biol.* 9:2167. doi: 10.3389/fcell.2021.653815

Bokko, P. B., Francione, L., Bandala-Sanchez, E., Ahmed, A. U., Annesley, S. J., Huang, X., et al. (2007). Diverse cytopathologies in mitochondrial disease are caused by AMP-activated protein kinase signaling. *Mol. Biol. Cell.* 18, 1874–1886. doi: 10.1091/mbc.e06-09-0881

Bosgraaf, L., and van Haastert, P. J. M. (2006). The regulation of myosin II in *Dictyostelium*. *Eur. J. Cell Biol.* 85, 969–979. doi: 10.1016/j.ejcb.2006.04.004 Brandt, R., Léger, J., and Lee, G. (1995). Interaction of tau with the neural plasma membrane mediated by tau's amino-terminal projection domain. *J. Cell Biol.* 131, 1327–1340. doi: 10.1083/jcb.131.5.1327

Buée, L., Bussière, T., Buée-Scherrer, V., Delacourte, A., and Hof, P. R. (2000). Tau protein isoforms, phosphorylation and role in neurodegenerative disorders.*Brain Res. Rev.* 33, 95–130. doi: 10.1016/s0165-0173(00)00019-9

Cabezas-Opazo, F. A., Vergara-Pulgar, K., Pérez, M. J., Jara, C., Osorio-Fuentealba,C., and Quintanilla, R. A. (2015). Mitochondrial dysfunction contributes to the pathogenesis of Alzheimer's Disease. *Oxid. Med. Cell Longev.* 2015:509654. doi: 10.1155/2015/509654

Carilla-Latorre, S., Gallardo, M. E., Annesley, S. J., Calvo-Garrido, J., Graña, O., Accari, S. L., et al. (2010). MidA is a putative methyltransferase that is required for mitochondrial complex I function. *J. Cell Sci.* 123, 1674–1683. doi: 10.1242/ jcs.066076

Castillo-Carranza, D. L., Guerrero-Muñoz, M. J., Sengupta, U., Gerson, J. E., and Kayed, R. (2018). $\alpha$-Synuclein oligomers induce a unique toxic Tau strain. *Biol. Psychiatry* 84, 499–508. doi: 10.1016/j.biopsych.2017.12.018

Ciaccioli, G., Martins, A., Rodrigues, C., Vieira, H., and Calado, P. (2013). A powerful yeast model to investigate the synergistic interaction of $\alpha$-synuclein and Tau in neurodegeneration. *PLoS One* 8:e55848. doi: 10.1371/journal.pone. 0055848

Cleveland, D. W., Hwo, S.-Y., and Kirschner, M. W. (1977). Physical and chemical properties of purified tau factor and the role of tau in microtubule assembly.*J. Mol. Biol.* 116, 227–247. doi: 10.1016/0022-2836(77)90214-5

Cummins, N., Tweedie, A., Zuryn, S., Bertran-Gonzalez, J., and Götz, J. (2019). Disease-associated tau impairs mitophagy by inhibiting Parkin translocation to mitochondria. *EMBO J.* 38:e99360. doi: 10.15252/embj.201899360

Darcy, P. K., Wilczynska, Z., and Fisher, P. R. (1994). Genetic analysis of *Dictyostelium* slug phototaxis mutants. *Genetics* 137, 977–985.

De Lozanne, A., and Spudich, J. A. (1987). Disruption of the *Dictyostelium myosin* heavy chain gene by homologous recombination. *Science* 236, 1086–1091. doi: 10.1126/science.3576222

De Strooper, B., and Annaert, W. (2010). Novel research horizons for presenilins and $\gamma$-secretases in cell biology and disease. *Annu. Rev. Cell Dev. Biol.* 26, 235–260. doi: 10.1146/annurev-cellbio-100109-104117

De Vos, A., Anandhakumar, J., Van den Brande, J., Verduyckt, M., Franssens, V., Winderickx, J., et al. (2011). Yeast as a model system to study tau biology. *Int. J. Alzheimer's Dis.* 2011, 1–16. doi: 10.4061/2011/ 428970

Drubin, D. G., and Kirschner, M. W. (1986). Tau protein function in living cells. *J. Cell Biol.* 103, 2739–2746. doi: 10.1083/jcb.103.6.2739

Eckert, A., Schmitt, K., and Götz, J. (2011). Mitochondrial dysfunction - the beginning of the end in Alzheimer's disease? Separate and synergistic modes oftau and amyloid-$\beta$ toxicity. *Alzheimer's Res. Ther.* 3, 1–11. doi: 10.1186/alzrt74

Eichinger, L., Lee, S. S., and Schleicher, M. (1999). Dictyostelium as model system for studies of the actin cytoskeleton by molecular genetics. *Microsc. Res. Tech.*47, 124–134. doi: 10.1002/(sici)1097-0029(19991015)47:2<124::aid-jemt5>3.0.co;2-8

Eichinger, L., Pachebat, J. A., Glöckner, G., Rajandream, M. A., Sucgang, R., Berriman, M., et al. (2005). The genome of the social amoeba *Dictyostelium discoideum*. *Nature* 435, 43–57.

Esposito, A., Dohm, C. P., Kermer, P., Bähr, M., and Wouters, F. S. (2007). $\alpha$-Synuclein and its disease-related mutants interact differentially with the microtubule protein tau and associate with the actin cytoskeleton. *Neurobiol.Dis.* 26, 521–531. doi: 10.1016/j.nbd.2007.01.014

Fernando, S., Allan, C. Y., Mroczek, K., Pearce, X., Sanislav, O., Fisher, P. R., et al. (2020). Cytotoxicity and mitochondrial dysregulation caused by $\alpha$-synuclein in *Dictyostelium discoideum*. *Cells* 9:2289. doi: 10.3390/cells9102289

Feuillette, S., Miguel, L., Frébourg, T., Campion, D., and Lecourtois, M. (2010). Drosophila models of human tauopathies indicate that Tau protein toxicity in vivo is mediated by soluble cytosolic phosphorylated forms of the protein. *J. Neurochem.* 113, 895–903. doi: 10.1111/j.1471-4159.2010.06663.x

Francione, L. M., and Fisher, P. R. (2011). Heteroplasmic mitochondrial disease in *Dictyostelium discoideum*. *Biochem. Pharmacol.* 82, 1510–1520. doi: 10.1016/j.bcp.2011.07.071

Francione, L. M., Annesley, S. J., Carilla-Latorre, S., Escalante, R., and Fisher, P. R. (2011). The Dictyostelium model for mitochondrial disease. *Semin. Cell Dev.Biol.* 22, 120–130. doi: 10.1016/j.semcdb.2010.11.004

Francione, L., Smith, P. K., Accari, S. L., Taylor, P. E., Bokko, P. B., Bozzaro, S., et al. (2009). *Legionella pneumophila* multiplication is enhanced by chronic AMPK signalling in mitochondrially diseased *Dictyostelium* cells. *Dis. Models Mechan.*2, 479–489. doi: 10.1242/dmm.003319

Galasso, A., Cameron, C. S., Frenguelli, B. G., and Moffat, K. G. (2017). An AMPK-dependent regulatory pathway in tau-mediated toxicity. *Biol. Open* 6, 1434–1444. doi: 10.1242/bio.022863

Galpern, W. R., and Lang, A. E. (2006). Interface between tauopathies and synucleinopathies: a tale of two proteins. *Ann. Neurol.* 59, 449–458. doi: 10.1002/ana.20819

Gammon, K. (2014). Neurodegenerative disease: brain windfall. *Nature* 515, 299– 300. doi: 10.1038/nj7526-299a

Gellermann, G. P., Appel, T. R., Davies, P., and Diekmann, S. (2006). Paired helical filaments contain small amounts of cholesterol, phosphatidylcholine and sphingolipids. *Biol. Chem.* 387, 1267–1274. doi: 10.1515/BC.2006.157

Gerisch, G. (2009). Imaging actin cytoskeleton dynamics in *Dictyostelium chemotaxis*. *Methods Mol. Biol.* 571, 385–400. doi: 10.1007/978-1-60761-198- 1_26

Gibson, G. E., Shi, Q., Zhu, X., Beal, M. F., Wang, X., Perry, G., et al. (2010). A mitocentric view of Alzheimer's Disease suggests multi-faceted treatments. *J. Alzheimer's Dis.* 20, S591–S607. doi: 10.3233/JAD-2010-100336

Goedert, M., and Spillantini, M. G. (2011). Pathogenesis of the tauopathies. *J. Mol. Neurosci.* 45, 425–431. doi: 10.1007/s12031-011-9593-4

Goedert, M., Spillantini, M. G., Jakes, R., Rutherford, D., and Crowther, R. A. (1989a). Multiple isoforms of human microtubule-associated protein tau: sequences and localization in neurofibrillary tangles of Alzheimer's disease. *Neuron* 3, 519–526. doi: 10.1016/0896-6273(89)90210-9

Goedert, M., Spillantini, M. G., Potier, M. C., Ulrich, J., and Crowther, R. A. (1989b). Cloning and sequencing of the cDNA encoding an isoform of microtubule-associated protein tau containing four tandem repeats: differential expression of tau protein mRNAs in human brain. *EMBO J.* 8, 393–399. doi: 10.1002/j.1460-2075.1989.tb03390.x

Goldberg, J. M., Manning, G., Liu, A., Fey, P., Pilcher, K. E., Xu, Y., et al. (2006). The dictyostelium kinome—analysis of the protein kinases froma simple model organism. *PLoS Genet.* 2:e38. doi: 10.1371/journal.pgen. 0020038

Graf, R., Daunderer, C., and Schliwa, M. (2000). Dictyostelium DdCP224 is a microtubule-associated protein and a permanent centrosomal resident involved in centrosome duplication. *J. Cell Sci.* 113, 1747–1758. doi: 10.1242/jcs.113.10. 1747

Grundke-Iqbal, I., Iqbal, K., Quinlan, M., Tung, Y. C., Zaidi, M. S., and Wisniewski, H. M. (1986). Microtubule-associated protein tau. A component of Alzheimer paired helical filaments. *J. Biol. Chem.* 261, 6084–6089.

Haase, C., Stieler, J. T., Arendt, T., and Holzer, M. (2004). Pseudophosphorylation of tau protein alters its ability for self-aggregation. *J. Neurochem.* 88, 1509–1520. doi: 10.1046/j.1471-4159.2003.02287.x

Hagele, S., Kohler, R., Merkert, H., Schleicher, M., Hacker, J., and Steinert, M. (2000). Dictyostelium discoideum: a new host model system for intracellular pathogens of the genus Legionella. *Cell. Microbiol.* 2, 165–171. doi: 10.1046/j.1462-5822.2000.00044.x

Haggerty, T., Credle, J., Rodriguez, O., Wills, J., Oaks, A. W., Masliah, E., et al. (2011). Hyperphosphorylated Tau in an $\alpha$-synuclein-overexpressing transgenic model of Parkinson's disease. *Eur. J. Neurosci.* 33, 1598–1610. doi: 10.1111/j.1460-9568.2011.07660.x

Hamilton, R. L. (2000). Lewy bodies in alzheimer's disease: a neuropathological review of 145 cases using $\alpha$−synuclein immunohistochemistry. *Brain Pathol.*10, 378–384. doi: 10.1111/j.1750-3639.2000.tb00269.x

Hanger, D. P., Betts, J. C., Loviny, T. L. F., Blackstock, W. P., and Anderton, B. H. (1998). New phosphorylation sites identified in hyperphosphorylated tau (paired helical filament-tau) from Alzheimer's Disease brain using nanoelectrospray mass spectrometry. *J. Neurochem.* 71, 2465–2476. doi: 10.1046/j.1471-4159.1998.71062465.x

Hanger, D. P., Byers, H. L., Wray, S., Leung, K.-Y., Saxton, M. J., Seereeram, A., et al. (2007). Novel phosphorylation sites in tau from Alzheimer brain support a role for casein kinase 1 in disease pathogenesis. *J. Biol. Chem.* 282, 23645–23654. doi: 10.1074/jbc.M703269200

Haylett, W., Swart, C., van der Westhuizen, F., van Dyk, H., van der Merwe, L., van der Merwe, C., et al. (2016). Altered mitochondrial respiration and other features of mitochondrial function in parkin-mutant fibroblasts from Parkinson's Disease patients. *Parkinson's Dis.* 2016:1819209. doi: 10.1155/2016/ 1819209

Hestermann, A., Rehberg, M., and Gräf, R. (2002). Centrosomal microtubule plus end tracking proteins and their role in *Dictyostelium* cell dynamics. *J. MuscleRes. Cell Motility* 23, 621–630. doi: 10.1023/A:1024450922609

Himmler, A., Drechsel, D., Kirschner, M. W., and Martin, D. W. (1989). Tau consists of a set of proteins with repeated C-terminal microtubule-binding domains and variable N-terminal domains. *Mol. Cell. Biol.* 9, 1381–1388. doi: 10.1128/mcb.9.4.1381

Iseki, E., Marui, W., Kosaka, K., and Uéda, K. (1999). Frequent coexistence of Lewy bodies and neurofibrillary tangles in the same neurons of patients with diffuse Lewy body disease. *Neurosci. Lett.* 265, 9–12. doi: 10.1016/S0304-3940(99) 00178-0

Ishizawa, T., Mattila, P., Davies, P., Wang, D., and Dickson, D. W. (2003). Colocalization of Tau and alpha-synuclein epitopes in lewy bodies.*J. Neuropathol. Exp. Neurol.* 62, 389–397. doi: 10.1093/jnen/62.4.389

Jensen, P. H., Hager, H., Nielsen, M. S., Højrup, P., Gliemann, J., and Jakes, R. (1999). $\alpha$-Synuclein binds to tau and stimulates the protein kinase a-catalyzed tau phosphorylation of serine residues 262 and 356. *J. Biol. Chem.* 274, 25481–25489. doi: 10.1074/jbc.274.36.25481

Joachim, C. L., Morris, J. H., Kosik, K. S., and Selkoe, D. J. (1987). Tau antisera recognize neurofibrillary tangles in a range of neurodegenerative disorders. *Ann. Neurol.* 22, 514–520. doi: 10.1002/ana.410220411

Klein, G., and Satre, M. (1986). Kinetics of fluid-phase pinocytosis in *Dictyostelium discoideum* amoebae. *Biochem. Biophys. Res. Commun.* 138, 1146–1152. doi: 10.1016/S0006-291X(86)80402-8

Knecht, D. A., and Loomis, W. F. (1987). Antisense RNA inactivation of myosin heavy chain gene expression in *Dictyostelium discoideum*. *Science* 236, 1081– 1086. doi: 10.1126/science.3576221

Knuth, M., Khaire, N., Kuspa, A., Lu, S. J., Schleicher, M., and Noegel, A. A. (2004).A novel partner for *Dictyostelium filamin* is an alpha-helical developmentally regulated protein. *J. Cell Sci.* 117, 5013–5022. doi: 10.1242/jcs.01366

Koch, K. V., Reinders, Y., Ho, T.-H., Sickmann, A., and Gräf, R. (2006). Identification and isolation of *Dictyostelium* microtubule-associated protein interactors by tandem affinity purification. *Eur. J. Cell Biol.* 85, 1079–1090. doi: 10.1016/j.ejcb.2006.05.008

Kosik, K. S. (1993). The molecular and cellular biology of Tau. *Brain Pathol.* 3, 39–43. doi: 10.1111/j.1750-3639.1993.tb00724.x

Larochelle, D. A., Vithalani, K. K., and De Lozanne, A. (1996). A novel memberof the rho family of small GTP-binding proteins is specifically required for cytokinesis. *J. Cell Biol.* 133, 1321–1329. doi: 10.1083/jcb.133.6.1321

Larochelle, D. A., Vithalani, K. K., and De Lozanne, A. (1997). Role of *Dictyostelium* racE in cytokinesis: mutational analysis and localization studies by use of green fluorescent protein. *Mol. Biol. Cell* 8, 935–944. doi: 10.1091/mbc.8.5.935

Lautenschläger, J., Kaminski, C. F., and Kaminski Schierle, G. S. (2017). α-Synuclein – regulator of exocytosis, endocytosis, or both? *Trends Cell Biol.* 27,468–479. doi: 10.1016/j.tcb.2017.02.002

Lay, S. T., Sanislav, O., Annesley, S. J., and Fisher, P. R. (2016). "Mitochondrial stress test using Seahorse respirometry on intact cells," in *Methods in Molecular Biology*, eds D. Herald and T. Jin (Cham: Springer), 41–61. doi: 10.1007/978-1- 4939-3480-5_4

Lee, V., Goedert, M., and Trojanowski, J. (2001). Neurodegenerative tauopathies. *Annu. Rev. Neurosci.* 24, 1121–1159.

Li, X. C., Hu, Y., Wang, Z. H., Luo, Y., Zhang, Y., Liu, X. P., et al. (2016). Human wild-type full-length tau accumulation disrupts mitochondrial dynamics and the functions via increasing mitofusins. *Sci. Rep.* 6, 24756–24756. doi: 10.1038/ srep24756

Lim, M. A., Selak, M. A., Xiang, Z., Krainc, D., Neve, R. L., Kraemer, B. C.,et al. (2012). Reduced activity of AMP-activated protein kinase protects against genetic models of motor neuron disease. *J. Neurosci.* 32, 1123–1141. doi: 10.1523/JNEUROSCI.6554-10.2012

Lin, M. T., and Beal, M. F. (2006). Mitochondrial dysfunction and oxidative stressin neurodegenerative diseases. *Nature* 443, 787–795. doi: 10.1038/nature05292

Lindwall, G., and Cole, R. D. (1984). Phosphorylation affects the ability of tau protein to promote microtubule assembly. *J. Biol. Chem.* 259, 5301–5305. doi: 10.1016/s0021-9258(17)42989-9

Lippa, C. F., Schmidt, M. L., Lee, V. M. Y., and Trojanowski, J. Q. (1999). Antibodies to α−synuclein detect Lewy bodies in many Down's syndrome brains with Alzheimer's disease. *Ann. Neurol.* 45, 353–357. doi: 10.1002/1531-8249(199903)45:3<353::aid-ana11>3.0.co;2-4

Ludtmann, M. H. R., Otto, G. P., Schilde, C., Chen, Z.-H., Allan, C. Y., Brace,S., et al. (2014). An ancestral non-proteolytic role for presenilin proteins in multicellular development of the social amoeba *Dictyostelium discoideum*.*J. Cell Sci.* 127, 1576–1584. doi: 10.1242/jcs.140939

Mandelkow, E., Von Bergen, M., Biernat, J., and Mandelkow, E.-M. (2007). Structural principles of tau and the paired helical filaments of Alzheimer's Disease. *Brain Pathol.* 17, 83–90. doi: 10.1111/j.1750-3639.2007.00 053.x

Maniak, M. (2011). Dictyostelium as a model for human lysosomal and trafficking diseases. *Semin. Cell Dev. Biol.* 22, 114–119. doi: 10.1016/j.semcdb.2010.11.001

Mampel, J., Spirig, T., Weber, S. S., Haagensen, J. A. J., Molin, S., and Hilbi, H. (2006). Planktonic replication is essential for biofilm formation by *Legionella pneumophila* in a complex medium under static and dynamic flow conditions. *Appl. Environ. Microbiol.* 72, 2885–2895. doi: 10.1128/AEM.72.4.2885-2895.2006

Martín-González, J., Montero-Bullón, J.-F., and Lacal, J. (2021). Dictyostelium discoideum as a non-mammalian biomedical model. *Microb. Biotechnol.* 14, 111–125. doi: 10.1111/1751-7915.13692

Maselli, A., Laevsky, G., and Knecht, D. A. (2002). Kinetics of binding, uptake and degradation of live fluorescent (DsRed) bacteria by *Dictyostelium discoideum*. *Microbiology* 148, 413–420. doi: 10.1099/00221287-148-2-413

McCullough, L. D., Zeng, Z., Li, H., Landree, L. E., McFadden, J., and Ronnett, G. V. (2005). Pharmacological inhibition of AMP-activated protein kinase provides neuroprotection in stroke. *J. Biol. Chem.* 280, 20493–20502. doi: 10.1074/jbc.M409985200

McMains, V. C., Myre, M., Kreppel, L., and Kimmel, A. R. (2010). Dictyostelium possesses highly diverged presenilin/gamma-secretase that regulates growth and cell-fate specification and can accurately process human APP: a system for functional studies of the presenilin/gamma-secretase complex. *Dis. Model Mech.* 3, 581–594. doi: 10.1242/dmm.004457

Mondragón-Rodríguez, S., Perry, G., Luna-Muñoz, J., Acevedo-Aquino, M. C., and Williams, S. (2014). Phosphorylation of tau protein at sites Ser 396-404 is oneof the earliest events in Alzheimer's disease and Down syndrome. *Neuropathol. Appl. Neurobiol.* 40, 121–135. doi: 10.1111/nan.12084

Nakamura, T., Yamashita, H., Takahashi, T., and Nakamura, S. (2001). Activated Fyn phosphorylates α-synuclein at tyrosine residue 125. *Biochem. Biophys. Res. Commun.* 280, 1085–1092. doi: 10.1006/bbrc.2000.4253

Nellen, W., Silan, C., and Firtel, R. A. (1984). DNA-mediated transformation in Dictyostelium discoideum: regulated expression of an actin gene fusion. *Mol. Cell Biol.* 4, 2890–2898. doi: 10.1128/mcb.4.12.2890-2898.1984

Noegel, A. A., and Schleicher, M. (2000). The actin cytoskeleton of *Dictyostelium*: a story told by mutants. *J. Cell Sci.* 113, 759–766.

Ogawa, S., Yoshino, R., Angata, K., Iwamoto, M., Pi, M., Kuroe, K., et al. (2000). The mitochondrial DNA of *Dictyostelium discoideum*: complete sequence, gene content and genome organization. *Mol. Gen. Genet.* 263, 514–519. doi: 10.1007/ PL00008685

Otto, G. P., Wu, M. Y., Clarke, M., Lu, H., Anderson, O. R., Hilbi, H., et al. (2004). Macroautophagy is dispensable for intracellular replication of *Legionella pneumophila* in *Dictyostelium discoideum*. *Mol. Microbiol.* 51, 63–72. doi: 10.1046/j.1365-2958.2003.03826.x

Payton, J. E., Perrin, R. J., Clayton, D. F., and George, J. M. (2001). Protein–protein interactions of alpha-synuclein in brain homogenates and transfected cells. *Mol.Brain Res.* 95, 138–145. doi: 10.1016/S0169-328X(01)00257-1

Pérez, M. J., Jara, C., and Quintanilla, R. A. (2018a). Contribution of Tau pathology to mitochondrial impairment in neurodegeneration. *Front. Neurosci.* 12:441. doi: 10.3389/fnins.2018.00441

Pérez, M. J., Vergara-Pulgar, K., Jara, C., Cabezas-Opazo, F., and Quintanilla, R. A. (2018b). Caspase-cleaved tau impairs mitochondrial dynamics in Alzheimer's Disease. *Mol. Neurobiol.* 55, 1004–1018. doi: 10.1007/s12035-017-0385-x

Pollitt, A. Y., and Insall, R. H. (2008). Abi mutants in *Dictyostelium* reveal specific roles for the SCAR/WAVE complex in cytokinesis. *Curr. Biol.* 18, 203–210. doi: 10.1016/j.cub.2008.01.026

Rappsilber, J., Mann, M., and Ishihama, Y. (2007). Protocol for micro-purification, enrichment, pre-fractionation and storage of peptides for proteomics using StageTips. *Nat. Protocols* 2, 1896–1906. doi: 10.1038/nprot.2007.261

Rehberg, M., and Gräf, R. (2002). Dictyostelium EB1 Is a genuine centrosomal component required for proper spindle formation. *Mol. Biol. Cell.* 13, 2301– 2310. doi: 10.1091/mbc.e02-01-0054

Rehberg, M., Kleylein-Sohn, J., Faix, J., Ho, T.-H., Schulz, I., and Gräf, R. (2005). *Dictyostelium* LIS1 Is a centrosomal protein required for microtubule/cell cortex interactions, nucleus/centrosome linkage, and actin dynamics. *Mol. Biol.Cell.* 16, 2759–2771. doi: 10.1091/mbc.e05-01-0069

Ren, Q.-G., Liao, X.-M., Chen, X.-Q., Liu, G.-P., and Wang, J.-Z. (2007). Effects of tau phosphorylation on proteasome activity. *FEBS Lett.* 581, 1521–1528. doi: 10.1016/j.febslet.2007.02.065

Reynolds, C. H., Betts, J. C., Blackstock, W. P., Nebreda, A. R., and Anderton, B. H. (2000). Phosphorylation sites on tau identified by nanoelectrospray mass spectrometry. *J. Neurochem.* 74, 1587–1595. doi: 10.1046/j.1471-4159.2000.0741587.x

Rhein, V., Song, X., Wiesner, A., Ittner, L. M., Baysang, G., Meier, F., et al. (2009). Amyloid-beta and tau synergistically impair the oxidative phosphorylationsystem in triple transgenic Alzheimer's disease mice. *Proc. Natl. Acad. Sci. U.S.A.*106, 20057–20062. doi: 10.1073/pnas.0905529106

Roy, B., and Jackson, G. R. (2014). Interactions between Tau and α-synuclein augment neurotoxicity in a *Drosophila* model of Parkinson's disease. *Hum. Mol. Genet.* 23, 3008–3023. doi: 10.1093/hmg/ddu011

Savica, R., Grossardt, B. R., Bower, J. H., Ahlskog, J., and Rocca, W. A. (2013). INcidence and pathology of synucleinopathies and tauopathies related to parkinsonism. *JAMA Neurol.* 70, 859–866. doi: 10.1001/jamaneurol.2013.114

Sergeant, N., Bretteville, A., Hamdane, M., Caillet-Boudin, M.-L., Grognet, P., Bombois, S., et al. (2008). Biochemistry of tau in Alzheimer's disease and related neurological disorders. *Expert. Rev. Proteomic* 5, 207–224.

Shahmoradian, S. H., Lewis, A. J., Genoud, C., Hench, J., Moors, T. E., Navarro, P. P., et al. (2019). Lewy pathology in Parkinson's disease consists of crowded organelles and lipid membranes. *Nat. Neurosci.* 22, 1099–1109. doi: 10.1038/s41593-019-0423-2

Spillantini, M. G., and Goedert, M. (1998). Tau protein pathology in neurodegenerative diseases. *Trends Neurosci.* 21, 428–433. doi: 10.1016/s0166-2236(98)01337-x

Stelzmann, R. A., Schnitzlein, N. H., and Murtagh, R. F. (1995). An english translation of alzheimer's 1907 paper, "über eine eigenartige erkankung der hirnrinde". *Clin. Anatomy* 8, 429–431. doi: 10.1002/ca.980080612

Ugalde, C. L., Annesley, S. J., Gordon, S. E., Mroczek, K., Perugini, M. A., Lawson,
V. A., et al. (2020). Misfolded $\alpha$-synuclein causes hyperactive respiration without functional deficit in live neuroblastoma cells. *Dis. Models Mechan.* 13:dmm040899. doi: 10.1242/dmm.040899
Vanhelmont, T., Vandebroek, T., Vos, A. D., Terwel, D., Lamaire, K., Anandhakumar, J., et al. (2010). Serine-409 phosphorylation and oxidative damage define aggregation of human protein tau in yeast. *FEMS Yeast Res.* 10, 992–1005. doi: 10.1111/j.1567-1364.2010.00662.x
Vingtdeux, V., Davies, P., Dickson, D. W., and Marambaud, P. (2011). AMPK isabnormally activated in tangle- and pre-tangle-bearing neurons in Alzheimer's disease and other tauopathies. *Acta Neuropathol.* 121, 337–349. doi: 10.1007/s00401-010-0759-x
Wersinger, C., and Sidhu, A. (2005). Disruption of the interaction of $\alpha$-synuclein with microtubules enhances cell surface recruitment of the dopaminetransporter. *Biochemistry* 44, 13612–13624. doi: 10.1021/bi050402p
Wilczynska, Z., and Fisher, P. R. (1994). Analysis of a complex plasmid insertionin a phototaxis-deficient transformant of *Dictyostelium discoideum* selected ona *Micrococcus luteus* Lawn. *Plasmid* 32, 182–194. doi: 10.1006/plas.1994.1054
Wilkins, A., Khosla, M., Fraser, D. J., Spiegelman, G. B., Fisher, P. R., Weeks, G.,et al. (2000). Dictyostelium RasD is required for normal phototaxis, but not differentiation. *Genes Dev.* 14, 1407–1413.
Xie, A. J., Hou, T. Y., Xiong, W., Huang, H. Z., Zheng, J., Li, K., et al. (2019).Tau overexpression impairs neuronal endocytosis by decreasing the GTPase dynamin 1 through the miR-132/MeCP2 pathway. *Aging Cell* 18:e12929. doi: 10.1111/acel.12929
Zabrocki, P., Pellens, K., Vanhelmont, T., Vandebroek, T., Griffioen, G., Wera, S., et al. (2005). Characterization of $\alpha$-synuclein aggregation and synergistictoxicity with protein tau in yeast. *FEBS J.* 272, 1386–1400. doi: 10.1111/j.1742- 4658.2005.04571.x
Zang, J.-H., Cavet, G., Sabry, J. H., Wagner, P., Moores, S. L., and Spudich, J. A.(1997). On the role of myosin-II in cytokinesis: division of dictyostelium cellsunder adhesive and nonadhesive conditions. *Mol. Biol. Cell* 8, 2617–2629. doi: 10.1091/mbc.8.12.2617

**Conflict of Interest:** The authors declare that the research was conducted in theabsence of any commercial or financial relationships that could be construed as a potential conflict of interest.

**Publisher's Note:** All claims expressed in this article are solely those of the authors and do not necessarily represent those of their affiliated organizations, or those of the publisher, the editors and the reviewers. Any product that may be evaluated inthis article, or claim that may be made by its manufacturer, is not guaranteed orendorsed by the publisher.